The Molecular Genetic Investigation of Epilepsy of Infancy with Migrating Focal Seizures

by
Dr Amy McTague

A thesis submitted to University College London for the degree of DOCTOR OF PHILOSOPHY

I, Amy McTague, confirm that the work presented in this thesis is my own. Where information has been derived from other sources, I confirm that this has been indicated in the thesis.

Abstract

Epilepsy of infancy with migrating focal seizures (EIMFS) is characterised by the onset of frequent focal seizures in the first 6 months of life, a typical migratory EEG pattern and severe developmental delay. In this thesis, I report a cohort of patients with EIMFS, delineate clinical features and investigate the molecular genetic basis of this syndrome. In 2012, heterozygous mutations in the sodium-gated potassium channel *KCNT1,* were described in patients with EIMFS. Using a variety of genetic techniques, I have identified 12 patients with mutations in this gene. Four are novel, previously unreported mutations. Functional investigations, including protein homology modelling and electrophysiology in a xenopus oocyte model showed that all novel *KCNT1* variants were gain-of-function mutations. In addition, I describe a new genetic cause of EIMFS. Within my cohort, I identified a consanguineous family with two affected children. Autozygosity mapping and whole exome sequencing revealed a novel, homozygous mutation in *SLC12A5*. *SLC12A5* encodes KCC2, the neuronal potassium chloride co-transporter that determines the direction and polarity of GABA-mediated signalling. Through international collaboration, I found a second family with two affected children harbouring compound heterozygous *SLC12A5* mutations. All three *SLC12A5* variants were investigated using an overexpression HEK293 cell model. Immunoblotting and immunohistochemistry revealed decreased cell surface expression of mutant KCC2. Electrophysiology experiments showed a depolarization of the chloride reversal potential and a delayed response to chloride loading. Taken together, these results indicate that loss of KCC2 function is likely to result in abnormal neuronal inhibition in this form of EIMFS. The genetic heterogeneity in EIMFS is strong evidence that a wide variety of different pathogenic mechanisms can result in the severe epilepsy and abnormal neurodevelopment observed in this condition. Further elucidation of causative genes in both animal and cell models is needed to identify novel therapeutic targets for this devastating disorder.

Acknowledgements

Firstly, I would like to thank my supervisor, Dr Manju Kurian, who has been an unwavering source of support and encouragement. I have learnt an immense amount from Dr Kurian over the past five years, not only the laboratory skills and understanding of epilepsy genetics I have acquired, but also about how to be a clinician scientist. Dr Kurian's determination, critical thinking and clear scientific vision, coupled with her clinical acumen and compassion for her patients, are a source of great inspiration to me.

I would also like to express my gratitude to my two secondary supervisors, Professor Dimitri Kullmann and Professor Rod Scott. Professor Kullmann has provided invaluable scientific insights and practical suggestions at many points along this journey and has helped me to forge several important collaborations, as well as encouraging me in my development as a scientist. I have greatly enjoyed and benefitted from many rigorous scientific discussions with Professor Rod Scott over this period and I deeply appreciate the insights and overview he brought to this project.

Professor Helen Cross has been a highly important source of support and mentorship over the past four years. She has supported my research ambitions by allowing me to undertake protected research activities during my Epilepsy Fellow post and providing interim funding to support my write-up period. Professor Cross was also very helpful in reviewing EEGs and imaging for the EIMFS patients.

I would like to express my gratitude to those who have funded this research: the Medical Research Council for my Research Training Fellowship, the Medical Research Foundation for the training support grant, Child Brain Research and the Roald Dahl Marvellous Children's Charity for the pump-prime funding, and the MPSI Parents for their generous donation.

I had the great fortune to learn laboratory techniques from Dr Esther Meyer, whose attention to detail and ability to problem-solve has taught me a great deal. Dr Meyer was also kind enough to assist with proof-reading this thesis. I would also like to extend my

thanks to the members of the Kurian group, Dr Jo Ng, Dr Serena Barral, Dr Adeline Ngoh, Dr Apostolos Papandreou and Dr Karolin Kramer whose constructive input at lab meetings and support has been invaluable.

The work in this thesis would not have been possible without several important scientific and clinical collaborations. It has been a great pleasure to work with Dr Anna Wedell and Dr Tommy Stödberg on the discovery of *SLC12A5*. Dr Stephanie Schorge, Institute of Neurology was very supportive in the early stages of this project when I undertook the initial KCC2 mutagenesis experiments in her lab. I would like to thank her for her enthusiasm and support throughout this project. I would like to thank Professor Robert Harvey, UCL School of Pharmacy (SOP), for hosting me within the laboratory and providing the expression plasmid which I used in cloning and subsequent cell work for the electrophysiology experiments. My thanks to Dr Philip Long who was kind enough to supervise me in the SOP laboratory. I would also like to thank Dr Arnaud Ruiz who devoted a huge amount of time to teaching me at the electrophysiology rig. My gratitude also goes to Johanna Branco De Assis Manuel, who allowed me to shadow her and supported my electrophysiology training. I would like to express my gratitude to Dr Steve Petrou and Umesh Nair from the Florey Institute, Melbourne for the *KCNT1* electrophysiology experiments. My thanks go to Dr Juan Zhen and Professor Martin Reith, New York University for their help with biotinylation studies for KCC2. I would also like to extend my thanks to Dr Maya Topf, Dr Sony Malhotra and Dr Irene Farabella from Birkbeck, whose work on the modelling data was essential. This study relied on UK and international clinicians who referred their patients and I would like to thank them all for their interest and enthusiasm despite their busy clinical workloads.

I have been very fortunate to have had inspiring mentors who set me on this path. Dr Grace Vassallo encouraged me to apply for sub-specialty training in paediatric neurology and subsequently referred the two patients in whom I identified the *SLC12A5* mutations. Dr Rachel Kneen was my clinical supervisor during my training in Alder Hey and allowed me to undertake the BPNSU study which was the starting point for this project. I would also like to thank Dr Richard Appleton, who has been an important mentor and support during my epilepsy training.

The greatest privilege during this project has been to meet the children with EIMFS and their families. Their grace and forbearance in the face of great suffering is my continuing inspiration.

Lastly, my heartfelt thanks to my husband, Jon, and my daughter, Charlotte, for their patience and love. This is for you.

Table of Contents

List of Illustrations

List of Tables

Chapter 1 Introduction and Overview

1.1 Severe epilepsy in infancy and childhood

Since antiquity, epilepsy has formed an integral part of the human experience. The first written description of epilepsy was in 2000 B.C., with seizures in infancy and childhood described since Babylonian times (Magiorkinis et al. 2010). The term epilepsy comes from the Greek “epilambanein”, meaning to seize, possess or afflict (Magiorkinis et al. 2010). In the pre-Hippocratic era it became known as the “sacred disease” and was attributed to lunar influence or the displeasure of the Gods, but in his thesis “On the Sacred Disease”, Hippocrates asserted that epilepsy is due to natural causes and originates from the brain (Wolf 2014). Hippocrates also recognised that there were inherited forms of epilepsy and that earlier onset of epilepsy was associated with poorer prognosis (Magiorkinis et al. 2010). Although many further advances in seizure semiology and classification emerged over the following millennia, the first description of a severe childhood epilepsy syndrome was the account by Dr West of infantile spasms in his own child in 1841 (West 1841; Capovilla et al. 2013). The emergence of this concept is further discussed in 1.2.

Today, epilepsy is recognised as the commonest neurological condition of childhood, affecting 1 in 150 children (Aaberg et al. 2017). Onset of childhood epilepsy is commonest in the first two years of life and such early onset disease is commonly associated with reduced seizure freedom and cognitive impairment when compared to epilepsy with later onset in childhood (Eltze et al. 2013). The epilepsies of infancy and childhood include the epileptic encephalopathies, a devastating group of disorders characterised by multiple seizure types, florid epileptiform EEG abnormalities and developmental stagnation or regression (McTague et al. 2015). A number of age-related electroclinical syndromes with typical seizure types and EEG abnormalities are recognised **(Table 1.1).** Many of these syndromes can be caused by structural brain malformations as well as inborn errors of metabolism (Nordli 2012; Gaily et al. 2016) Both treatable metabolic disorders such as the Vitamin B6 responsive disorders and surgically treatable structural lesions should be excluded early in the investigative odyssey (Rahman 2012; Fridley et al. 2013) However, in

patients with normal brain imaging (or non-specific abnormalities) and negative metabolic investigations, a genetic cause is highly possible and should be pursued **(Figure 1-1**).

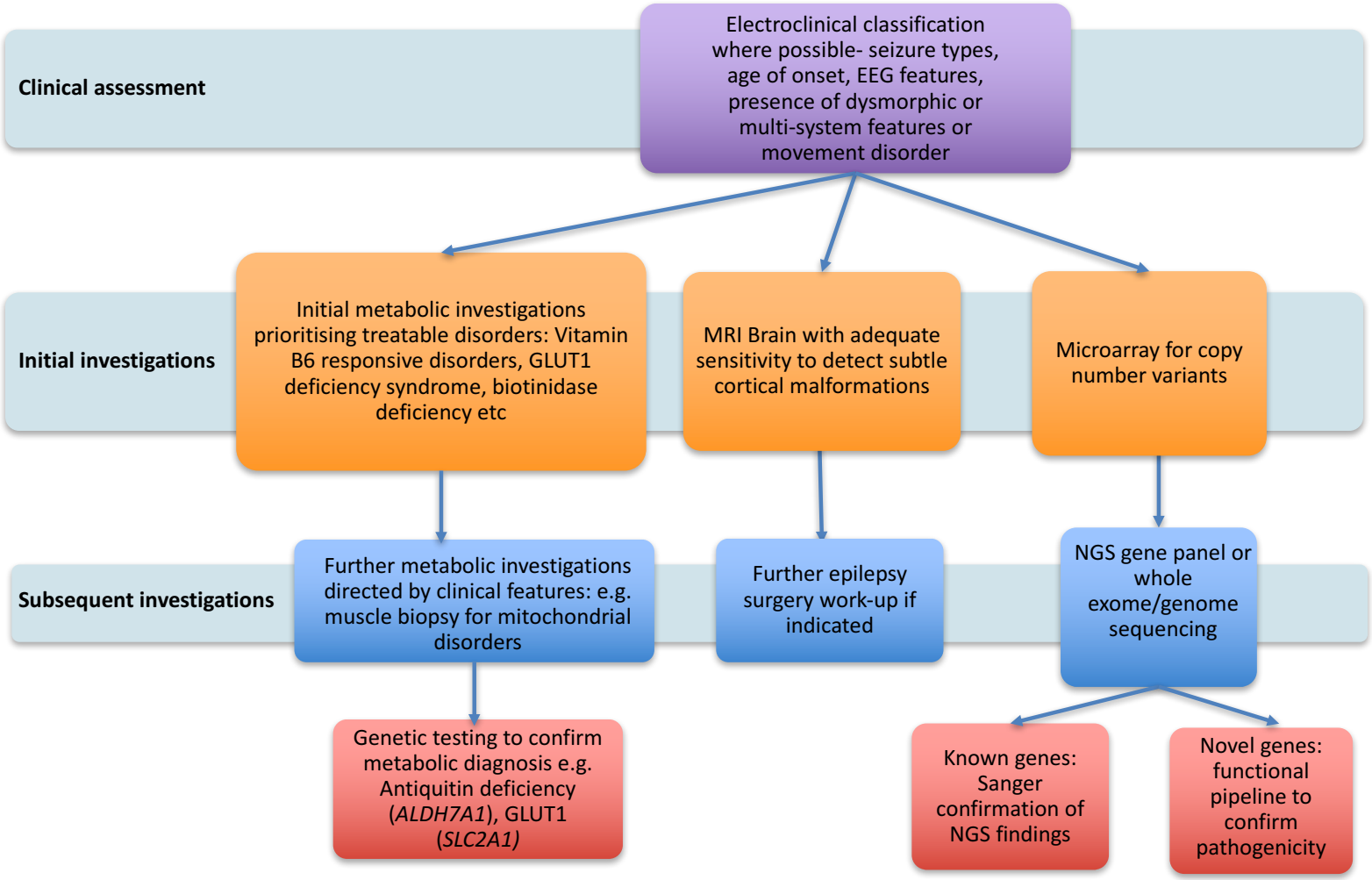

Figure 1-1 A diagnostic approach to early onset epilepsy. GLUT1 Glucose Transporter 1, NGS next generation sequencing

1.2 Epileptic Encephalopathy

The term “encephalopathy” broadly describes an alteration of consciousness that can result from many different aetiologies including infectious, toxic and metabolic causes. Although the concept of an epileptic encephalopathy, that is an alteration of cognition or consciousness associated with epilepsy, appears to be a modern phenomenon, the co-occurrence of frequent seizures with cognitive impairment was first described by Dr West in his own child who presented with infantile spasms and cognitive decline in 1841 (Eling et al. 2002; Duncan 2001). Subsequently, further clinical descriptions of “eclampsia nutans” and tic de Salaams” were published, but the associated chaotic inter-ictal EEG abnormality was not described until 1951 and was then subsequently characterized as “hysparhythmia” by Gibbs and Gibbs (Eling et al. 2002; Capovilla et al. 2013). This, therefore, was the first potential evidence of disturbance of cognitive function by inter-ictal discharges associated with severe epilepsy. From the 1950s, the clinical and electrographic delineation of other severe epilepsy syndromes such as Lennox Gastaut and Landau Kleffner syndromes have further contributed to the concept of inter-ictal EEG abnormalities resulting in a neuropsychological deficit, as discussed below (Capovilla et al. 2013).

The concept of an epileptic encephalopathy was formally defined in the 2001 ILAE Classification Commission Report (Engel 2001) as a state in which the epileptiform abnormalities themselves contribute to the progressive decline in cognitive function seen in some severe epilepsies. This was further discussed in the 2006 ILAE Classification report (Engel 2006) where epileptic encephalopathy was defined as a condition associated with progressive neurodevelopmental impairment which is epilepsy-dependent, rather than solely resulting from an underlying cause such as an encephalitis or a metabolic disorder. In the subsequent 2009 ILAE report on classification and terminology (Berg et al. 2010) the concept was further developed to describe epilepsies where the epileptic activity itself contributes to progressive neurodevelopmental impairment, which is worse that would be expected due to the underlying pathology alone. In support of this concept, there is evidence from animal models that both early-life seizures and the occurrence of inter-ictal spikes, even without overt seizures, predispose to cognitive impairment compared to controls (Chapman et al. 2015) In several studies, longer periods of abnormal electrical activity have been associated with a poorer cognitive outcome in West syndrome of

undetermined aetiology (Matsumoto et al. 1981; Kivity et al. 2004; O'Callaghan et al. 2011). Arguably, this may reflect the underlying cause, rather than the effect of EEG discharges on long-term developmental outcome. However, in studies investigating the impact of infantile spasms in either Down syndrome or tuberous sclerosis, it is evident that earlier, and even pre-symptomatic, treatment is associated with improved cognitive outcome (Humphrey et al. 2014; Jóźwiak et al. 2011). Indeed, in other epileptic encephalopathies, such as Landau-Kleffner syndrome, where disease-onset follows a period of normal development, there is a clear relationship between the onset of EEG abnormalities (in this case electrical status epilepticus in slow wave sleep, ESES), and the observed acquired aphasia and cognitive decline. Resolution of ESES usually, though not always, leads to cognitive improvement (Van Bogaert 2013). Furthermore, in Lennox Gastaut syndrome or epilepsy associated with Ring Chromosome 20, non-convulsive status epilepticus can confer an additional cognitive impairment which resolves with treatment (Chapman et al. 2015). Overall, it is likely that multiple complex factors contribute to the encephalopathy and motor/cognitive decline observed in different epilepsies.

Over time, epileptic encephalopathy has become an umbrella term to describe many of the severe epilepsy syndromes of infancy and childhood (**Table 1.1**) where frequent seizures are accompanied by severe neurodevelopmental delay or regression, cognitive impairment and behavioural difficulties (McTague et al. 2015). However, more recently, the use of this term has become more controversial as the relationship with underlying aetiology has emerged (Howell et al. 2016; Korff et al. 2015). Some authors proposed the term "epileptogenic" rather than epileptic encephalopathy, stating that the underlying pathology leads to cognitive impairment which is independent from the epilepsy (Capovilla et al. 2013). Other authors also assert that the epileptic activity reflects the severity of brain dysfunction resulting from the underlying aetiology (Korff et al. 2015) and that, in the majority of circumstances, resolution of seizures and/or EEG abnormalities does not result in cognitive improvement. Indeed, there a number of chromosomal disorders where epilepsy is a major feature, such as Angelman syndrome, but where significant developmental delay is evident prior to seizure onset (Buiting et al. 2016). In the most common genetic epileptic encephalopathy, Dravet syndrome, cognitive slowing and decline tends to occur before the epilepsy becomes florid, suggesting the cognitive decline may follow a different time-course to the epilepsy, although both are likely to be related to the underlying *SCN1A* mutation (Nabbout et al. 2013; Dravet et al. 2011). Indeed, focal

knockdown of Scn1A in the basal forebrain led to cognitive impairment in the absence of seizures in a rodent model (Bender et al. 2013). In contrast to *SCN1A*-epilepsy, in *STXBP1* and *KCNQ2* related encephalopathies, patients present with a severe early neonatal epilepsy which improves with time or burns out, but patients continue to manifest severe neurological impairment, often with the emergence of other neurological symptoms, such as non-epileptic movement disorders (Weckhuysen et al. 2013; Stamberger et al. 2016; McTague et al. 2015; Scheffer et al. 2017). In the recent report of the ILAE Classification Committee, it was recognized that for many of the genetic early onset epilepsies, there is likely to be a developmental encephalopathy, where the impact of the genetic mutation leads to cognitive impairment which is independent of the electrical activity (Scheffer et al. 2017). Increasingly, patients are described as having a developmental and/or an epileptic encephalopathy, based on the judged additional impact of the epileptic activity to the cognitive burden. It is likely that as we continue to move towards aetiology-led descriptions of early onset epilepsy, both of these terms will be replaced by concepts such as *SCN1A* or *CDKL5* encephalopathy (Scheffer et al. 2017).

While these may seem like semantic discussions, there are practical implications for patients. The importance of this concept lies in our approach to treatment. Aggressive treatment of inter-ictal EEG abnormalities could potentially lead to over-treatment with resultant increased drug load and side-effect burden. Conversely, failure to treat a reversible process could further disadvantage a child in terms of cognitive outcome. It is increasingly recognised that, rather than being a concept which can be applied to all severe epilepsies, there are a limited number of clinical scenarios in which resolution of an inter-ictal EEG abnormality may confer a cognitive gain for the patient. One of the hallmarks of these scenarios is where a previously developmentally normally infant or child develops an EEG abnormality such as in some cases of infantile spasms or Landau Kleffner syndrome. In addition, non-convulsive status epilepticus may confer additional cognitive impairment for children with Lennox Gastaut syndrome or other severe epilepsies. It is vital that appropriate neuropsychological and developmental assessment is utilised alongside medical interventions to monitor treatment response. However, for the majority of the genetic early onset epilepsies, it is much more likely that inter-ictal EEG abnormalities reflect the underlying brain dysfunction and abolishment of these discharges, even if it were possible, would be unlikely to be of cognitive benefit. Therefore, when the term epileptic encephalopathy (EE) is used throughout this thesis, it refers to a

severe epilepsy associated with an encephalopathy or disturbance of cognitive processes, without any imputation of the role of inter-ictal EEG activity in this process.

1.3 Electroclinical syndromes in infancy and childhood

An electroclinical syndrome is defined as the co-occurrence of clinical features including seizure types, EEG abnormalities and other features occurring at a specific age (Berg et al. 2010). A number of electroclinical syndromes are recognised in infancy and childhood and, in the absence of a more specific aetiological diagnosis, remain an important part of epilepsy classification and diagnosis which may guide treatment and indicate prognosis (Scheffer et al. 2017). In the first two years of life, the majority of electroclinical syndromes are severe (**Table 1.1**) and many are described as epileptic encephalopathies, often associated with a poor neurodevelopmental outcome. Self-limited epilepsy syndromes such as familial or non-familial self-limited neonatal or infantile epilepsies do however occur (Gaily et al. 2016). Importantly, many patients present with severe epilepsies which do not fulfil the criteria of the electroclinical syndromes, commonly described as non-specific epileptic encephalopathy.

Epilepsy syndrome	Age at onset	Seizures at onset	EEG	Epilepsy evolution and outcome	Development
OS	0-3 m	Tonic seizures. May have focal seizures and infantile spasms; myoclonus rare	Interictal: BS Ictal: diffuse attenuation or low-voltage fast activity. Focal rhythmic spiking with focal seizures. Frequent evolution to hypsarrhythmia.	75% evolve to WS Ongoing seizures in most	Severe to profound delay
EME	0-3m	Fragmentary myoclonus. May have tonic and focal seizures.	Interictal: burst suppression which is worse in sleep and persists beyond infancy. Ictal: myoclonias do not show EEG correlate.	No evolution in most, but persistent myoclonic and focal seizures	Severe to profound delay
EIMFS	0-6m (median 7wks)	Focal seizures that migrate from one hemisphere to the other. Often adversive, eye involvement, autonomic features, apnoeas.	Interictal: may be normal initially, becomes slow with multifocal epileptiform abnormalities Ictal: migrating ictal focus between hemispheres	May be preceded by or evolve into WS Ongoing seizures in some, others have infrequent seizures after first year of life	May be normal before seizure onset Regression/plateau in many after seizure onset Outcome severe to profound delay in most.
WS	2-12m (peak 6m)	Infantile spasms	Interictal: hypsarrhythmia Ictal: electrodecremental response or high-amplitude midline slow wave with admixed fast activity	May evolve to LGS or develop other seizure types,	May be normal or abnormal before onset Plateau or regression with spasm onset Outcome worse in those with known aetiology; 80% have developmental delay
DS	5—16 m (peak 5-8m)	Febrile or afebrile hemiclonic or generalised tonic–clonic, often febrile status epilepticus	Initial EEG normal and up to 1-2 years Generalised and multifocal epileptiform abnormalities later Photosensitivity	Ongoing seizures From 1-5 years: focal, myoclonic, absence seizures, ± NCSE 10 yrs onwards: brief nocturnal convulsive seizures ± focal	Normal in first year of life (may have subtle visual problems) Slows between 1-2 years; mean age of walking 17 months. Language relatively spared. Regression with

				dyscognitive seizures, myoclonus and absences less common	status epilepticus Outcome mild-severe delay (rare cases of normal development reported) Emerging gait ataxia in later life
EMA	7m-6y (peak 3-4y)	Multiple seizure types: myoclonic-atonic ±myoclonic, absence, tonic-clonic, and episodes of non-convulsive status epilepticus.	Interictal: Hypersynchronous theta or delta slowing; generalized spike-wave or generalized polyspike-wave, increasing in sleep Photosensitivity in some	Remission in most within 3.5 years of onset Persistent seizures in more severe cases, usually as nocturnal tonic or tonic vibratory seizures	Early development normal in most. Regression with epilepsy onset seen. Outcomes from normal intellect to severe ID
LGS	1-8y, rare adult onset cases (peak3-5y)	Multiple seizure types: tonic seizures ± atypical absences, atonic, myoclonic, GTCS, spasms, focal, episodes of tonic SE or NCSE	Interictal: slow background, slow (<2.5 Hz) spike-wave, generalized paroxysmal fast activity in sleep Ictal: electrodecrement or low voltage fast activity (tonic seizures), slow spike-wave (atypical absences), generalized spike- or polyspike-wave activity (myoclonic seizures)	Seizures persist into adulthood in most cases	Developmental delay precedes epilepsy onset in 20-60%. Cognitive impairment in 90% by 5 years after seizure onset. Learning difficulties in remainder.
EAS (including LKS, CSWS, ABRE)	3-7y	LKS: rolandic seizures in 70% ECSWS: rolandic seizures ABRE: rolandic seizures, negative myoclonus, atonic	Centrotemporal spikes, often bilateral independent and bilaterally synchronous increasing in sleep LKS and CSWS: electrical status in sleep (>85% non-REM sleep)	Epilepsy age-limited, resolves by teenage years in almost all patients	Most normal pre-seizure onset. Acquired epileptic aphasia at onset in LKS, more global delay or regression on other EAS disorders. Outcome from normal to severe delay

Table 1.1 Severe electroclinical syndromes of infancy and childhood. Abbreviations: ABRE atypical benign rolandic epilepsy, BS burst suppression, CSWS continuous spike-wave in slow wave sleep, DS Dravet syndrome, EAS epilepsy aphasia spectrum, EIEE early infantile epileptic encephalopathy, EME early myoclonic encephalopathy, EMA epilepsy with myoclonic atonic seizures, EOEE early onset epileptic encephalopathy (epileptic encephalopathy starting before 3 months), LGS Lennox-Gastaut syndrome, LKS Landau Kleffner syndrome, m months, MAE epilepsy with myoclonic-atonic seizures, NCSE non-convulsive status epilepticus, OS Ohtahara syndrome, SE status epilepticus, WS West syndrome, y years. Adapted from McTague *et al The Lancet Neurology* 2015;15(3):304-16.

1.4 The genomic revolution and early onset epilepsy

1.2a

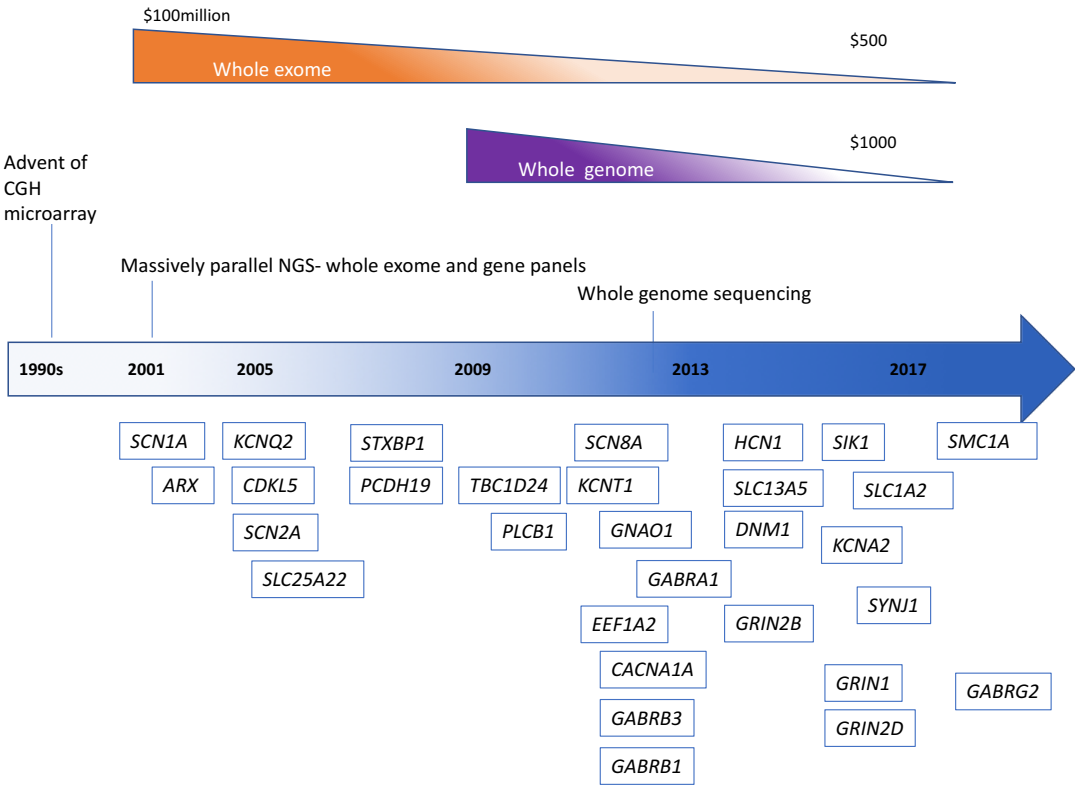

1.2b

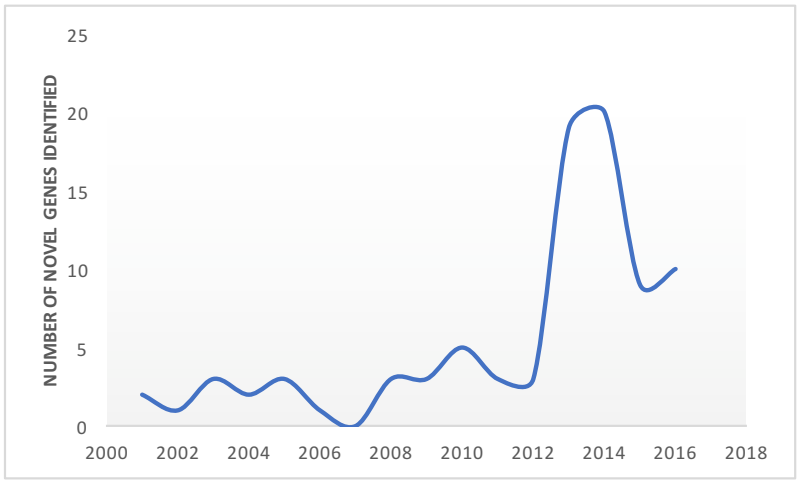

Figure 1-2 A timeline of genetic discovery in the early onset epileptic encephalopathies. **1.2a** Developments in genomic technologies and gene discovery. **a**CGH array comparative genomic hybridization, NGS next generation sequencing. **1.2b** Number of novel genes discovered by year (by Pubmed citation search).

In 2001, *SCN1A* was the first gene identified in an epileptic encephalopathy with the discovery of heterozygous *de novo* mutations in seven unrelated individuals with Dravet syndrome (Claes et al. 2001). *SCN1A* mutations had previously been identified in two families with generalised epilepsy with febrile seizures plus (GEFS+) (Escayg et al. 2000). Early gene discovery relied heavily in mapping and linkage studies in extended kindreds coupled with candidate gene Sanger sequencing. However, the advent of massively parallel, high throughput next generation sequencing (NGS) in the early 2000s led to an explosion in genetic discovery in many conditions, including the early onset epilepsies (Møller et al. 2015).

At this point, it is pertinent to consider what constitutes an "epilepsy gene". There are a large number of multi-system disorders, genetically-defined syndromes and neurodevelopmental disorders where epilepsy is one phenotypic feature. As an illustration, the Online Mendelian Inheritance in Man (OMIM) database contains 1989 entries associated with the search term "seizures" and the ClinVar database has 5424 genetic variants associated with "epilepsy" as a clinical manifestation of disease. Indeed, a recent study interrogated multiple databases and identified 693 genes associated with epilepsy (Wang et al. 2017). Many of these genes were implicated in metabolic disorders, developmental brain malformation disorders, dysmorphic syndromes or other neurological disorders where seizures were one of several phenotypic features. However, 84 genes were classified as "pure" epilepsy genes where mutations caused epilepsy or an epilepsy syndrome with few other additional features. But which genes should be considered to be important in the epileptic encephalopathies? Table 1.2 contains over 80 genes where epilepsy and developmental delay are the core phenotypic features. Although there may be a spectrum of associated features, particularly developmental delay/intellectual disability, movement disorders, and non-specific MRI abnormalities, these alone are not pathognomonic. Malformations of cortical development and inherited metabolic disorders are excluded. It is important to group these epileptic encephalopathy genes together for several reasons. Firstly, it is helpful for clinicians to understand which genes have been implicated in the EEs, and this may aid interpretation of diagnostic tests such as multiple gene panels or clinical exomes. Secondly, as many of these genes may lead to the same phenotype, it is important from a research perspective to consider how their diverse functions may lead to a shared mechanism of neurological dysfunction.

Gene	Age Sz onset	Epilepsy syndromes (% of cases of this syndrome where known)	Sz at onset Sz evolution	EEG at onset EEG evolution	Development at onset Development evolution	Other features – neurologic	Other features – non-neurologic	Magnetic resonance brain imaging	Protein function and mechanistic implications
AARS AR 3 Simons 2015	2-6 m	Non-specific	IS, M, F Refractory Sz	MF UK	UK Profound DD	Microcephaly Spasticity Absent reflexes (likely neuropathy) Movement disorder (mixed)	Congenital vertical tali Short stature	Hypo-myelination Progressive atrophy (cerebral>cerebellar)	Aminoacyl-tRNA-synthetase Mutations impair aminoacylation, affecting protein translation
ALG13 AD *(de novo)* 5 Timal 2012 DeLigt 2012 Epi4K 2013 Michaud 2014 Hino-Fukuyo 2015	4 m (not noted in some)	WS WS → LGS Non-specific	IS Refractory Sz - ES, F, T, aT, M	Hyps SSW, MF	Normal-mild DD Moderate-severe DD	None reported in most Optic atrophy females	Reports of males with abnormal transferrin isoform pattern and multiorgan abnormalities, these not reported in females	UK	N-glycosylation of proteins
AP3B2 AR 12 Theveneon 2017	0-9m	WS Non-specific	IS, M GTC, M	Hyps in 3	Moderate-severe DD (one walked at 12 years)	Stereotypies Dystonia Hyperkinesia choreoathetosis Central hypotonia Peripheral hypertonia Post-natal microcephaly	Optic atrophy	Thin cc, cerebral and cerebellar atrophy in some	neuron-specific subunit of non-clathrin and clathrin-associated adaptor protein complex 3 which plays a key role in signal-mediated trafficking
ARX mutations X-linked (males affected) >30	1d in most	Non-specific	C, M, F Refractory Sz	MF N/A	N/A Profound DD	'XLAG' phenotype Temperature instability Axial hypotonia Spastic quadriplegia	'XLAG' phenotype Ambiguous genitalia	Lissencephaly Agenesis corpus callosum Abnormal basal ganglia	Transcription factor crucial for interneuron migration and function

Berry-Kravis 1994 Dobyns 1999 Kitamura 2002 Kato 2004 Kato 2005						Acquired microcephaly			
ARX expansions X-linked (males affected) >30 Stromme 2002 Guerrini 2007 Kato 2007	0-7 m	EIEE WS Non-specific	IS, T Ongoing Sz in some - T, M or F, some Sz free after infancy	Hyps, B-S N, MF	DD in most Severe-profound DD	'Non-malformative' phenotype Movement disorder (most commonly dystonia +/- episodes status dystonicus)	'Non-malformative' phenotype Micropenis in some	Normal in 50% Non-specific abnormalities in 50% incl. basal ganglia cavitation/ signal change, cerebral atrophy	Transcription factor crucial for interneuron migration and function
BRAT1 AR >15 Puffenberger 2012 Saunders 2012 Saitsu 2014 Straussberg 2015 Hanes 2015 Van de Pol 2015 Mundy 2016 Smith 2016 Horn 2016 Srivastava 2016	0-7 d	EIEE EOEE	T, M, C, F Refractory Sz	B-S, MF N/A	N/A Profound DD	Neonatal rigidity Hypertonia Dysautonomia Microcephaly	Dysmorphism	Normal or mild frontal lobe hypoplasia	DNA repair and apoptosis
CACNA1A AD *(de novo)* 6 EPi4K 2016 Epi4K 2013	1 day-4w	EOEE EIMFS LGS	M, T, F, SE TC, F, SE	MF, GSW, slowing Migrating ictal spikes in 1	Moderate-severe DD	Hypertonia and hyperreflexia Ataxia in 1 Hypotonia in 1 Athetoid movements in 1	Transient VT in 1	Increased T2 temporal lobe signal in 1	Encodes alpha1 subunit of the Cav2.1 P/Q-type calcium channel, first reported in episodic ataxia type 2, spinocerebellar ataxia 6 and familial hemiplegic migraine

						and tremor in 1			type 1.
CDKL5 X-linked (females and males affected) >30 Kalscheuer 2003 Weaving 2004 Bahi-Buisson 2008a and 2008b Klein 2011 Fehr 2013	0-6 m	EOEE (6%) WS	T, TCS IS, then ongoing Sz in 80% (refractory in 50%) - T, M, F, atA and 'hypermotor-tonic-spasms sequence'	Often N Hyps → MF (often 'pseudo-periodic') or N	DD in most Severe DD Autistic features in some	Hypotonia Poor visual interaction Deceleration head growth Rett-like features (hand stereotypies, hand apraxia, bruxism)	-	Cerebral atrophy Posterior white matter T2 hyperintensity	Ubiquitously expressed kinase, involved in multiple cellular functions Mutations impair neuronal morphogenesis and transcriptional regulation
CHD2 AD *(de novo)* >30 Carvill 2013 Suls 2013 Chenier 2014 Thomas 2015	9 m -4 y	Non-specific	M, A, GTCS, A(EM), 'aT-M-A', prominent clinical photosensitivity Refractory Sz - as above plus T, aT, NCSE	GSW, PSW, activates in sleep SSW, MF	DD in most, Mild-severe DD Autistic features in some	Ataxia	-	Normal or vermis hypoplasia	Chromatin remodeler, specific function unknown
DNM1 AD *(de novo)* 33 Epi4K Consortium 2013 EuroEPINOMICS 2014 Nakashima 2016	2-13 m	WS WS→ LGS FIRES	IS Refractory Sz in most - T, aT, F, atA, M	Hyps, MFD SSW, PFA, MFD	DD in some Severe-profound DD	Hypotonia Extrapyramidal movement disorder in 1.	-	Normal or cerebral atrophy	GTPase involved in activity-dependent synaptic vesicle formation at inhibitory synapses. Mutations predicted to impair vesicle recycling and reduce T firing at synapses

Allen 2016 Deng 2016 EuroEPINOMICS 2017									
DOCK7 AR 3 Perrault 2014	2-6 m	EOEE EOEE→ WS Non-specific	T Refractory Sz - IS, M, F, T, T-C	MF Hyps, MF	DD in some Moderate-severe DD	Cortical visual impairment Dysmorphism	-	Occipital atrophy and white matter abnormality Prominent pontobulbar sulcus, mild pontine hypoplasia	Rac-guanine nucleotide exchange factor. Mutations impair neurogenesis and neuronal polarity
EEF1A2 12 de Ligt 2012 Veeramah 2013 Nakajima 2015 Inui 2016 Lam 2016	2m-2y	Non-specific EOEE	My IS, T-C, Abs	MF	Mild to severe delay	Hypotonia	Subtle facial dysmorphism: broad nasal bridge, tented upper lip, everted lower lip and downturned corners of the mouth	Atrophy/thin corpus callosum in some	Elongation factor with key role in protein synthesis, the delivery of amino- acylated tRNAs to the ribosome.
FHF1(FGF12) AD *(de novo)* 5 Siekierska 2016 Al-Mehmadi 2016	Day 2-6w	EOEE with cerebellar atrophy	T, F, Focal SE, TCS T, TCS, F, SE	Low voltage fast followed by long suppression Hyps	Moderate to severe DD	Hypotonia, ataxia, acquired microcephaly, poor visual development	chronic constipation, hypohydrosis, and reduced lacrimation in 1.	Cerebellar atrophy	FHF1 encodes small cytosolic proteins that interact with the cytoplasmic tails of Na_v and elevate the voltage dependence of neuronal sodium channel fast inactivation. Note all cases so far have the same p. R52H mutation.
FOXG1 mutations AD *(de novo)* >30 Ariani 2008[31]	3 m-3 y in most Mid-late child-hood in some	Non-specific Non-specific→ LGS	F, M, T, TCS Ongoing Sz in most, refractory in some	F, MF F, MF, SSW	DD Severe DD with absent language, most non-ambulatory	Rett-like features ('congenital variant') Hypotonia Spastic quadriplegia Movement disorders	Mild postnatal growth impairment Scoliosis	Gyral simplifications frontal lobes Corpus callosum hypoplasia	Transcriptional repressor Mutations impair telencephalon development and postnatal neuronal survival

Kortum 2011 Seltzer 2014 Papandreou 2016 Cellini 2016 Mitter 2017						(stereotypies, dyskinesias, chorea) Acquired microcephaly			
FOXG1 duplications AD *(de novo)* ~15 Yeung 2009 Brunetti-Pierri 2011 Seltzer 2014 Pontrelli 2014 Bertossi 2014	3-7 m	WS	IS None in most, refractory in few - T, M	Hyps N, MF	DD Severe DD with absent language, most ambulatory Autism	Normal head size	-	Normal in most	Transcriptional repressor Mutations impair telencephalon development and postnatal neuronal survival
FRRS1L AR 9 Madeo 2016 Shaheen 2016	4-24 months	NS-EOEE EOEE with CSWS	HC, GTC, my ES, GTC	CSWS in one case, others not stated	Normal until 18-22 months then loss of language and ambulation	Severe choreoathetosis Hypotonia, ballsim, cogwheel rigidity	-	Diffuse cortical and cerebellar volume loss, flattening of the heads of the caudate nuclei, periventricular FLAIR hyperintense signal	Ferric chelate reductase 1-like, important component of the outer core of AMPAR accessory proteins. Loss of FRRS1L would affect AMPAR constituency and thus AMPAR function.
GABRA1 AD *(de novo)* 11 Epi4K 2013 Carvill 2014 Kodera 2016	1-11 m	DS/DS-like Also causes non-EE epilepsy: FS, mild GGE	FS, TCS, HC, SE Refractory Sz - TCS, A, MJ, F, aT	F, GSW, some photo-sensitive As above	UK Mild-moderate DD	-	-	Normal in most	Ligand-gated ion channel responsible for inhibitory neurotransmission Mutations result in loss of function
GABRB1 AD (de novo)	3-12 m	IS NS-EOEE	FS Ep spasms, A, atA, My, aT	Hyps at 35 m in 1. Slow.	Global severe delay	Ataxia	-	Thin corpus callosum	$GABA_A$ receptor ß1 subunit. Funtional validation (Janve 2016) showed altered GABA signalling.

2 Epi4K 2013 Lien 2016									
GABRB3 AD *(de novo)* 34 Epi4K 2013 Papandreou 2016 Le 2017 Moller 2017	5-10 m	WS DS EMA FS Non-specific Also causes non-EE epilepsy: CAE	IS, F Refractory Sz in most - F, TCS, atA, T, aT, M	Hyps, MF MF, hyps, SSW	DD in some Moderate-profound DD ADHD in some	-	-	Normal in most	Ligand-gated ion channel responsible for inhibitory neurotransmission
GABRG2 AD *(de novo)* 16 Harkin 2002 Ishii 2014 Zou 2017 Shen 2017	2-3 m	DS/DS-like Also causes non-EE epilepsy: GEFS+, mild GGE	FS, TCS, HC Refractory Sz - TCS, aT, M, A	UK PSW, photo-sensitive	UK Moderate DD	-	-	Normal	Ligand-gated ion channel responsible for inhibitory neurotransmission
GNAO1 AD *(de novo)* 25 Nakamura 2013 Law 2015 Saitsu 2016 Schorling 2017 Danti 2017 Arya 2017 MArce-Grau 2017	0-2 m in most Mid-child-hood in some	EIEE (5%) WS Non-specific	T Refractory Sz - IS, later to T +/- F	B-S Hyps or MF, later to SSW, F B-S	N/A Severe-profound DD	Movement disorder (most frequently choreoathetosis)	-	Normal early infancy Delayed myelination, thin corpus callosum, progressive cerebral atrophy from later infancy	G protein subunit involved in cell signaling. Mutations impair adrenergic signaling and calcium current, reducing cortical excitability

GRIN1 AD *(de novo)* 21 Epi4K 2013 Ohba 2015 Lemke 2016 Zehavi 2017	2-11m	Non-specific	IS, F, M Ongoing Sz, refractory in 50%, controlled in 50%	F, MF, 'diffuse' As above	DD in some Severe DD	Movement disorder (mixed, hyperkinetic including oculogyric crisis-like eye movements, may precede Sz onset) Spasticity Rett-like features Acquired microcephaly	-	Cerebral atrophy Thin corpus callosum	NMDA receptor subunit Functional effect of reported mutations not studied
GRIN2A AD *(de novo)* >30 Carvill 2013 Lesca 2013 Lemke 2013 Turner 2015 Gao 2017	2-5 y	EAS (9-20%) WS (single report)	None or rolandic, negM, aT, IS Resolution by puberty	CTS (with CSWS in most), hyps N	Language delay in some Language regression at onset, ongoing language impairment post-resolution	Nil	-	Normal	NMDA receptor subunit NR2A Mutations reported to produce variable effects on receptor function NR2A replaces NR2B as dominant NMDA receptor subunit in early development, which may explain age of Sz onset
GRIN2B AD *(de novo)* 34 Epi4K 2013 Lemke 2014 Platzer 2017	1 m – 9 y	WS LGS Non-specific	IS, M Refractory Sz - ES, T C, T, F, A	Hyps SSW, UK	UK Mild-severe DD	Hypotonia 'Episodic hyperextension' Movement disorder (dystonia)	-	Normal in most	NMDA receptor subunit NR2B Mutations reported to result in gain of function
HCN1 AD *(de novo)* 6 Nava 2014	4-13 m	DS-like	FS, TCS, HC, SE Refractory Sz - TCS, A, F, M	N, GSW, PSW, MF GSW, PSW, MF	UK Mild-severe DD Autism Major behavioural disturbance	Ataxia in some	-	Normal	Hyperpolarization-activated, cyclic nucleotide–gated channel Mutations can have either a gain of function or dominant negative effect on channel function

IQSEC2 X-linked (affected males and females reported) 18 Morleo 2008 Shoubridge 2010 Epi4K 2013 Mau-Them 2014 Gandomi 2014 Tzschacht 2015 Zerem 2016	15 m- 4 y	IS LGS Non-specific	M, IS, atA Refractory Sz - M, TCS, aT	Hyps, UK SSW, UK	UK Moderate-severe DD Autistic features	Hypotonia Movement disorder (stereotypies) Strabismus Microcephaly and macrocephaly reported	-	Normal or mild cerebral and cerebellar atrophy	Guanine nucleotide exchange factor for the ARF family of GTP-binding proteins, roles include regulation of organelle formation and vesicular transport
KCNA2 AD *(de novo)* 15 Pena 2015 Syrbe 2015 Hundallah 2016 Corbett 2016	5-17 m	DS-like EMA-like Non-specific	FS, HC, TCS, M, F, SE Refractory Sz (but offset at 4-15 y in some) - FS, F, M, TCS, A, A(EM)	N or F MF with marked sleep activation, GSW, PSW	Normal Mild-severe DD	Ataxia Movement disorder (tremor, myoclonus) Hypotonia 'Hyperkinetic' behaviour	-	Normal	Potassium channel Mutations can result in loss or gain of channel function.
KCNQ2 AD *(de novo for EE, usually inherited in 'benign' epilepsies)* >30 Weckhuysen 2012 and 2013 Kato 2013 Pisano 2015	Most in week 1	EIEE (20%) EOEE Also causes non-EE epilepsy: BFNS	T, F Most settle by 3 y - T, F, TCS, M Evolution to IS rare	B-S, MF, F MF	N/A Moderate-profound DD	Axial hypotonia +/- spastic quadriplegia Movement disorder (dystonia) in some	-	Basal ganglia and thalamic hyperintensity in infancy	Potassium channel 'EE' mutations can result in loss or gain of function, BFNS mutations typically loss of function

Miceli 2015 Hortiguela 2017 BFNS: Singh 1998									
MEF2C AD *(de novo)* >30 Engels 2009 Bienvenu 2013 Novara 2013 Paciokowski 2013	0-18 m in most, child-hood in some	WS Non-specific	IS, M, FS Some Sz-free, some ongoing Sz	Hyps, MF, GSW UK	DD in some Severe DD with absent language, many ambulant Autistic features	Hypotonia Movement disorder (hyperkinesis and stereotypies) Inappropriate laughter High pain tolerance	Abnormal gastrointestinal motility Strabismus Dysmorphism	Corpus callosum dysgenesis Mild asymmetry/ enlargement lateral ventricles Delayed myelination	Transcription factor. Mutations lead to abnormal dendrite and synaptic development and loss of synaptic plasticity. Same cellular pathway as MECP2 and CDKL5, which have overlapping clinical features
PCDH19 X-linked (male sparing unless mosaic) >30 Juberg 1971 Ryan 1997 Scheffer 2008 Dibbens 2008 Depienne 2009 Marini 2010 and 2012 Terracciano 2016 Liu 2017	4 m – 3 y	EFMR DS-like Can manifest in mosaic males	FS, F, SE Sz-free in ~30% Ongoing Sz clusters in ~70%, less frequent over time - F, FS, M, A, SE	N, F, GSW As above	Normal-mild DD Normal-moderate DD Autistic features	Unsteady gait in some	-	Normal in most	Cadherin family of cell-cell adhesion molecules, involved in a variety of functions 'Cellular interference model' proposed, in which mixed population of wild-type and mutant cells required to produce disease (therefore affecting females and mosaic males)
PIGA X-linked 12 Johnston 2012	0-9 m	EME EIEE EOEE WS Non-specific	M, T, F, IS. SE Refractory Sz in most - M, T, F, ES	B-S, hyps, N MF, UK	N/A or DD in most Profound DD	Axial hypotonia Spastic quadriplegia	Polyhydramnios Joint contractures Facial dysmorphism Teeth/gum anomalies	Delayed myelination Thin CC Cerebral and cerebellar atrophy Diffusion restriction in some	Biosynthesis of glycosylphosphotidylinositol anchors, required to attach cell surface proteins to plasma membrane

Van der Crabben 2014 Swoboda 2014 Kato 2014 Kim 2016							Elevated ALP Iron overload Vesicoureteric reflux		
PLCB1 AR 4 Kurian 2010 Poduri 2012 Ngoh 2014 Schhonjans 2016	2-10 m	EIMFS EOEE→WS Non-specific	F, T, IS Refractory Sz - F, T, T-C	B-S, hyps, MF UK	DD Severe-profound DD	Axial hypotonia +/- spastic quadriplegia	-	Normal or Mild cortical atrophy Mildly hypoplastic corpus callosum	Phospholipase enzyme involved in signal transduction across cell membrane
PNKP AR 12 Shen 2010 Poulton 2012 Nakashima 2014	1-6 m	Non-specific LGS Also associated with non-EE epilepsy: spinocerebellar atrophy with neuropathy phenotype	F, FS Refractory Sz in most - F, UK	UK As above	DD in some, UK in some Severe DD Hyperactive behaviour	Congenital microcephaly	-	Mildly simplified gyral pattern Cerebellum proportionate to cerebrum	DNA repair enzyme with both kinase and phosphatase activity Mutations result in increased apoptosis and reduced cell proliferation
PURA AD *(de novo)* 7 Hunt 2014 Lalani 2014	0-14 m in most	LGS Non-specific	ES, M Refractory in some, not reported in others - M, T, TCS, F, aT	UK MF, UK	DD Severe DD in most	Neonatal onset hypotonia, respiratory difficulties, poor feeding 'Myopathic' facies Excess startle Recurrent aspiration Nystagmus	Strabismus Multiple fractures	Normal or delayed myelination	Roles in DNA transcriptional regulation and mRNA trafficking in postnatal brain development
QARS AR	Most in week 1	EIMFS EIEE Non-specific	F, T, SE Refractory Sz	B-S, MF, hyps UK	N/A Profound DD	Microcephaly (congenital in some, progressive in all)	-	Progressive atrophy of cerebrum and cerebellum (vermis >> hemispheres)	Glutaminyl-tRNA synthetase, role in protein translation. Mutations lead to reduced neuronal survival

7 Zhang 2014 Kodera 2015 Salvarinova 2015						Hypotonia +/- spastic quadriplegia Episodes in childhood of agitation, excitement, thrashing, poor sleep, excess sweating during which Sz are absent and may → rhabdomyolysis		Delayed myelination, reduced white matter, thin corpus callosum	
SCN1A AD *(de novo or inherited)* >30 Dravet 1978 Claes 2001 Harkin 2007 Freilich 2011 Catarino 2011 Brunklaus 2012 Kim 2014 GEFS+: Escayg 2000 Wallace 2001	4-15 m	DS (90%) Rare reports in EIFMS, EMA, EAS, other multiocal infantile epilepsy Also causes non-EE epilepsy: GEFS+, others	FS, TCS, HC, SE Refractory Sz - M, A, F, TCS, FS, SE	N, GSW, some photo-sensitive GSW, PSW, MF, some photo-sensitive	Normal in most Normal (rare) to severe DD Neurologic decline in adulthood	Crouch gait in mid-childhood Dysphagia in adulthood	-	Normal in ~90% Cerebral atrophy or temporal/hippocampal changes in 10%	Sodium channel subunit $Na_v1.1$, expressed on GABAergic interneurons. Mutations produce loss of function
SCN2A AD *(de novo for EE, usually inherited in 'benign' epilepsies)* >30	0-3 m in most Early child-hood in some	EIEE (10%) EIMFS (25%) EOEE WS Non-specific Also causes non-EE epilepsy: BFNIS	F, T, IS Refractory Sz - F, IS, T, M	B-S, MF MF, N	N/A or normal in most Severe-profound DD in most, some normal	Movement disorders (mixed) Hypotonia +/- spastic quadriplegia Early handedness Episodic Ataxia	Severe gastrointestinal symptoms	Variety of non-specific findings Signal change in white matter, basal ganglia, thalami, brainstem Atrophy (cortical +/- cerebellar)	Sodium channel subunit $Na_v1.2$, expressed on excitatory neurons Effect of mutations on channel function not well understood Genotype-phenotype difference between 'EE' and BFNIS not understood

Kamiya 2004 Nakamura 2013 Howell 2015 Schwarz 2016 BFNIS: Heron 2002									
SCN8A AD *(de novo)* >30 Veeramah 2012 Carvill 2013 Epi4K consortium 2013 Ohba 2014 Larsen 2015 Kong 2015 Anand 2016	0-22 m	EIMFS WS Non-specific Also causes non-EE epilepsy: BFNS	F, IS, T Refractory Sz in most - F, T, C, M, atA, SE	N, F, MF, hyps MF, SSW	Normal or DD Moderate-profound DD	Movement disorders (mixed, may precede Sz onset) Excess startle Hypotonia Spastic quadriplegia in some Ataxia in some SUDEP	-	Normal or atrophy, thin corpus callosum, delayed myelination	Sodium channel subunit $Na_v1.6$, expressed on excitatory and inhibitory neurons Mutations produce gain of function with increase in persistent sodium current and incomplete channel inactivation $Na_v1.8$ replaces $Na_v1.2$ as dominant sodium channel in excitatory neurons in infancy, which may explain later age of Sz onset with *SCN8A* mutations than *SCN2A*
SIK1 AD *(de novo)* 6 Hansen 2015	0-4 m	EME EIEE WS Non-specific	M, IS, T Refractory Sz - M, ES, T, TCS, aT	B-S, hyps Hyps, UK	N/A in most Severe DD in infant onset cases (no language, some ambulant) Autism	Repetitive and self-injurious behaviours	Scoliosis in some	Normal or mild frontal lobe hypoplasia or mildly simplified gyration	Salt-inducible kinase with roles in circadian rhythm, transcription of corticotrophins in hypothalamus and effects on MEF2C pathway. Truncation mutations result in loss of function. ACTH increases SIK1 activity, may be potential mechanism of treatment response to steroids in infantile spasms.
SLC1A2 AD *(de novo)* 3 Epi4K 2016 Epi4K 2013	2 days-1m	EOEE EME WS	IS, M T, TCS, SE, F	MF, slow, Hyps	Severe DD	Quadriplegia Hypotonia	Kyphoscoliosis Joint contractures	Delayed myelination, cerebral atrophy, thin corpus callosum	Encodes major glutamate transporter, EAAT2. In null mouse model, excess glutamate leads to excitotoxicity, spontaneous seizures and early death.

SLC1A4 AR 15 Conroy 2016 Heimer 2015	2m-1y	IS Non-specific EOEE	IS, F My, F, IS	Hyps MF	Moderate to severe DD	Spasticity Acquired microcephaly		Thin corpus callosum, progressive white matter volume loss, markedly delayed myelination	CNS serine transporter
SLC13A5 AR 8 Thevenon 2014	Week 1	EOEE	F Refractory in most (with periods of relative stability in childhood)	MF UK	N/A Severe-profound DD	Axial hypotonia +/- spastic quadriparesis	Teeth anomalies	UK	Cytoplasmic sodium-dependent citrate carrier Mutations impair citrate transport, impacting multiple cellular functions
SLC25A22 AR 9 Molinari 2005, 2009 Poduri 2013 Cohen 2014	0-6 m	EME EIMFS WS Non-specific	M, F Refractory Sz - IS, M, T	B-S, MF MF, SSW, hyps	N/A or DD Profound DD	Axial hypotonia Spastic quadriparesis Acquired microcephaly Abnormal ERG/VEP in some	Dysmorphism	Normal or a variety of findings including atrophy and delayed myelination	Mitochondrial glutamate transporter
SLC2A1 AD *(de novo or inherited)* >30 De Vivo 1991 Seidner 1998 Brockmann 2001 Suls 2008 Suls 2009 Mullen 2011	0-12 m in most Early child-hood in some	'Glut1 deficiency syndrome' EO-AE (10%) EMA (5%)	TCS, A, F, M, T Ongoing Sz tendency, most on ketogenic diet are Sz free	MF, F, GSW As above	Normal-DD Mild-severe DD	Acquired microcephaly Movement disorders (paroxysmal dystonia, dyskinesia) Ataxia Spasticity	-	Normal in most	Transports glucose across blood-brain barrier Mutations result in inadequate glucose transport

SLC6A1 AD *(de novo)* 10 Rauch 2012 Sanders 2012 Carvill 2015	1-5.5 y	EMA (4%)	M, aT, A Sz free by 3-8 y in ~40% Ongoing Sz in ~60% - M, aT, M-aT, A,	GSW, PSW, some photo-sensitive As above	DD Mild-severe DD Autistic features	Tremor or ataxia in some	-	Normal in most	Voltage-dependent GABA transporter responsible for synaptic GABA reuptake. Mutations reduce GABA transport activity.
SMC1A X-linked dominant *de novo* (truncating) 20 Lebrun 2015 Jansen 2016 Symonds 2017 Gorman 2017 Huisman 2017	1m-28m	IS, focal infantile epilepsy EIMFS	F in clusters, EM IS	Hyps Migrating ictal foci MF, GSW	Severe DD	Stereotypies (Rett-like) Progressive microcephaly	Dysmorphic features in some: mild synophris, small hands and feet, thin nose and upper lip, retrognathia, and triangular shaped face Short stature Structural cardiac anomalies	Small cc	SMC proteins (structural maintenance of chromosome proteins) are important part of functional kinetochores which allow correct segregation of chromosomes during cell division. Missense or in-frame deletions cause Cornelia du Lange syndrome
SPTAN1 AD *(de novo)* 7 Saitsu 2010 Hamdan 2012 Writzl 2012 Nonoda 2013 Tohyama 2015	0-3 m in most Rare child-hood onset cases	WS Non-specific → WS Non-specific	IS, M Refractory Sz in most – T	Hyps, MF MF	DD Profound DD	Axial hypotonia Spastic quadriplegia Acquired microcephaly	-	Severe hypomyelination Progressive cerebral, brainstem and cerebellar atrophy	Membrane scaffolding protein Mutations with dominant negative effect lead to altered clustering of sodium channels at axon initial segment and impaired integrity of myelinated axons. Haploinsufficiency thought not to cause EE
STXBP1 AD *(de novo)*	0-3 m	EIEE (30%) EOEE WS (2%)	T, F, IS, M, FS, TCS	B-S, MF, hyps MF, unusual	N/A or DD Severe-	Movement disorder (tremor - 'figure of 8 head	-	Frontal cortical hypoplasia/atrophy Thin +/- dysmorphic CC	Synaptic protein Mutations disrupt synaptic transmission

>30 Saitsu 2008 Deprez 2010 Otsuka 2010 Mignot 2011 Milh 2011 Carvill 2014 Dl Meglio 2015 Stamberger 2016		DS May have ID without epilepsy	May settle then recur in later infancy Sz free by 2 y in ~50%, refractory Sz in ~50% - F, T, M, A, TCS, aT, FS	back-ground fast without IEDs	profound DD in most	tremor') Hypotonia Spastic quadriplegia Extrapyramidal features in 2 adult patients		Hypo- or delayed myelination	
SYNGAP1 AD *(de novo)* 18 Hamdan 2009, 2011 Vissers 2010 Berryer 2013 Carvill 2013 Dyment 2014	6 m – 4 y	Non-specific	M, A, TCS, F Many refractory	GSW (usually posterior-predominant), SSW, MFD As above	DD in some Moderate-severe DD in most Autism	Acquired microcephaly in some	-	Normal in most	RAS/RAP GTP-activating protein, part of the NMDAR complex Mutations result in impaired interaction between RAS, and NMDA and AMPA receptors
SYNJ1 AR 6 Hardie 2016	Day 1-2.5m	Other focal/multifocal infantile epilepsy	M, IS, F, C M, T, IS	Hyps, MF, F	Severe DD	Spastic quadriplegia Visual impairment Dystonia in 1	All gastrostomy fed Complex III and IV deficiency in liver and fibroblasts in 1.	Thin corpus callosum, limited gliosis and atrophy of the periventricular white matter in 1, rest normal.	Synaptojanin 1 is vital to shedding of the clathrin coat and vesicle exocytosis and recycling. Homozygous missense SYNJ1 associated with early onset parkinsonism.
TBC1D24 AR >30 Corbett 2010 Guven 2012 Milh 2013 Afawi 2013	2-3 m in most	EIFMS Other focal/multifocal infantile epilepsy Also causes non-EE epilepsy: FIME	F, SE, M, TCS, A Refractory Sz - F, M	MF, UK As above	DD in some Mild-profound DD	DOORS syndrome Cerebellar signs Hearing impairment	DOORS syndrome Nail anomalies Bony anomalies	Subtle cortical thickening, progressive signal change and atrophy in cerebellar lobules	GTPase-activating protein involved in cycling of synaptic vesicles, membrane recycling, actin remodelling and neurite development Mutations produce loss of function

Campeau 2014 Balestrini 2016 Ngoh 2016 FIME: Falace 2010									
UBA5 AR 9 Muona 2017	3-12m	IS Other focal/multifocal infantile epilepsy	IS, M	Not stated	Severe DD	Irrritability and jitteriness in neonatal period, early onset dystonia and choreoathetosis Truncal hypotonia		Delayed myelination, cortical atrophy, increased periventricular and frontal WM signal	Ubiquitin fold modifier 1 (UFM1) cascade is a ubiquitin-like modification system
WDR45 X-linked dominant 6 Xixis 2015 Abidi 2016 Nakashima 2016 Redon 2017	3-6m in most	IS Other focal infantile epilepsy	F, ES ES	Hyps MF, slow waves	Severe DD	Dystonia Spastic quadriplegia	-	Brain iron accumulation on MRI in 2 patients	WD40- repeat protein with essential role in the budding of autophagosomes during autophagy WRD45 mutations in females (rarely seen in males) cause BPAN with severe dystonia and childhood onset seizures.
WWOX AR 17 Mallaret 2014 Abdel-Salam 2014 Mignot 2015 Ben-Salam 2015 Tabarki 2015	0-5m in most Up to 2 y in some	WS Non-specific	IS, F, T, TCS, M Refractory Sz - T, F, M	Hyps, MF MF, SSW	DD in some Moderate-profound DD (profound DD in all with 'EE' phenotype)	'EE' phenotype: Axial hypotonia Limb rigidity/ spasticity Hypokinesia Acquired microcephaly Retinal abnormalities or optic atrophy in many Spinocerebellar ataxia (SCAR) phenotype: Ataxia	-	Normal or cerebral atrophy, thin/ hypoplastic corpus callosum, cerebellar sparing	WW-domain containing oxidoreductase, involved in a variety of pre- and postnatal cellular processes (unclear which are relevant to epilepsy pathogenesis) Null mutations produce 'EE' phenotype, hypomorphic mutations 'SCAR' phenotype

Table 1.2 Genes, phenotypic features and pathogenic mechanisms of major single gene causes of epileptic encephalopathies. This table refers predominantly to non-malformation, non-metabolic, non-chromosomal (e.g. CNV, Ring 20) causes of each genetic epilepsy syndrome. Genes associated with (i) mild epilepsies only (ii) those in which only one patient/family is reported (iii) causation is otherwise unclear and (iv) where minimal phenotypic information is available, are not included. AD autosomal dominant, AR autosomal recessive, BFNIS benign familial neonatal-infantile seizures, BFNS benign familial neonatal seizures, CAE childhood absence epilepsy, DS Dravet syndrome, d day, DD developmental delay, DOORS syndrome: deafness, onychodystrophy, osteodystrophy, retardation and seizures syndrome, EAS epilepsy aphasia spectrum, EFMR epilepsy limited to females with mental retardation, EIEE early infantile epileptic encephalopathy (Ohtahara syndrome), EIMFS epilepsy of infancy with migrating focal seizures, EMA epilepsy with myoclonic atonic seizures, EME early myoclonic epileptic encephalopathy, EO-AE early onset absence epilepsy, EOEE early onset epileptic encephalopathy, IGE idiopathic generalised epilepsy, FIME familial infantile myoclonic epilepsy, FIRES febrile infection related epilepsy syndrome, FS febrile seizures, GEFS+ genetic epilepsy with febrile seizures plus, GGE genetic generalized epilepsy, LGS Lennox-Gastaut syndrome, m month, Sz seizures, UK unknown, XLAG X-linked lissencephaly with ambiguous genitalia, WS West syndrome, y years. Seizure types: A absence, A(EM) absence with eyelid myoclonia, aT atonic, atA atypical absence, C clonic, ES epileptic spasms, F focal, FS febrile seizures, IS infantile spasms, M myoclonic, SE status epilepticus, T tonic, TCS tonic clonic seizure. EEG features: B-S burst-suppression, F focal, GSW generalized spike-wave, MF multifocal, PSW polyspike-wave, SSW slow spike-wave. Adapted from McTague *et al The Lancet Neurology* 2015;15(3):304-1

Several sequencing methods/platforms are now available but all share the basic principles of NGS. Essentially, genomic DNA is sheared, then hybridised to a library of probes which either aims to capture all coding regions of the genome (the exome) or a limited panel of genes (multiple gene panel). The high-throughput nature of the technology allows multiplexing of samples. Over time, the cost of sequencing an exome has fallen sharply (**Figure 1-2**, Møller et al. 2015).

Many large cohort studies in epileptic encephalopathy have used a trio design, where the exomes of both the proband and parents are simultaneously sequenced (Veeramah et al. 2013; Allen et al. 2013; Euro-EpinomicsConsortium et al. 2014). Using this approach, an average of 1.58 *de novo* mutations per proband were detected, allowing rapid identification of causative variants in ~30% of patients with an epileptic encephalopathy (Allen et al. 2013). Although it has been clear for some time that familial epilepsies were likely to have a genetic basis, these large scale genetic studies demonstrated that causative *de novo* dominant mutations are a commonly observed in sporadic childhood epileptic encephalopathies. Whole exome approaches are increasingly utilized in clinical practice, yielding genetic diagnoses in a significant proportion of children with neurological diseases (Yang et al. 2013; Mefford 2015; Tarailo-Graovac et al. 2016).

Targeted sequencing using NGS technology in the form of gene panels has been extremely important in providing accurate diagnoses for families, as well as advancing genetic understanding of the severe epilepsies. Genes are selected for panel inclusion based on a number of factors. Firstly, known EE disease genes which affect multiple individuals and which meet American College of Medical Genetics and Genomics (ACMG) guidelines for pathogenicity are prioritised. A gene may also be included based on evidence from animal or other model systems or biological function. Candidate genes may also be selected from previous whole exome or copy number variant data and this approach has been fruitful in large resequencing studies which have confirmed putative disease genes such as *CHD2* and *SYNGAP1* (Carvill et al. 2013). The selected genes are included in panels of 50 to several hundreds of genes, and large cohorts can be rapidly sequenced for pathogenic variants. The diagnostic pick-up rate in studies varies considerably in the literature from 10-50% (Lemke et al. 2012; Carvill et al. 2013; Kwong et al. 2015; Zhang et al. 2017; Gokben et al. 2017; Parrini et al. 2017; Myers et al. 2016). This is likely due to cohort variability (including how much previous genetic testing was done for different patients) affecting the pre-test probability of detecting a genetic disorder in addition to variations in panel design.

However gene panels are an extremely powerful tool in routine clinical practice, as demonstrated by one study which identified pathogenic gene variants in 18% of those tested (Trump et al. 2016), increasing to 39% in the group of patients presenting with seizure onset under 2 months.

Chromosomal micro-arrays are another important diagnostic tool in the epileptic encephalopathies and arguably should be undertaken as a first line investigation. In one study of 349 patients with EE, up to 8% were found to have a causative or potentially contributing copy number variant (CNV) (Mefford et al. 2011). CNVs are present in all human genomes and those frequently reported in the control populations indicate normal genetic variability. When a CNV is identified, careful assessment is required to assess whether it is pathogenic. CNVs which are large, occur *de novo*, are not present in databases of genomic variation such as DECIPHER, and which encompass disease-causing genes are most likely to be pathogenic. CNVs of uncertain significance can play an important role in novel gene discovery, as exemplified by the discovery of *STXBP1* and *CHD2*, where deletions encompassing the candidate gene were initially identified, with subsequent detection of intragenic mutations in patients with similar phenotypes thereafter (Saitsu et al. 2008; Carvill et al. 2013). In contrast, discovery of intragenic missense mutations in a gene in EE can also help confirm the causative gene responsible for patients with small chromosomal deletions associated with complex neurodevelopmental phenotypes, as in the case of *PURA* in patients with 5q31.3 deletions (Hunt et al. 2014; Lalani et al. 2014; Myers & Mefford 2016). Increasingly CNVs can also be identified by NGS sequencing using sequencing read-depths, and an NGS-first approach may be possible in the future as technology improves (Yamamoto et al. 2016).

While *de novo* dominant variants are most commonly reported in the EEs, autosomal recessive and X-linked disorders are also recognised. Autosomal recessive inheritance is particularly suspected when a family is consanguineous (homozygous variants likely) or in an outbred family with more than one affected member (compound heterozygous variants more likely). X-linked inheritance may occur in X-linked dominant disorders such as *ARX*, in X-linked recessive disorders such as *DCX*, or in *PCDH19*-related epilepsy, where females are affected and males are generally unaffected carriers.

1.5 Important genetic concepts in the early onset epilepsies

1.5.1 The importance of a genetic diagnosis

While many new aetiologies for early onset epilepsies have been revealed, some clinicians question the impact of these recent advances for patients. It is clear that for patients with rare diseases and their families, the diagnostic journey is fraught and arduous. Recent reports from Rare Disease UK and Genetic Alliance UK (https://www.raredisease.org.uk, www.geneticalliance.org.uk), highlight the prolonged wait for diagnosis and the emotional, psychosocial and financial burden this places on individuals and their families. The major impact of identifying a genetic aetiology is the ability to offer an accurate diagnosis which may allow prognostication on disease course and associated co-morbidities such as developmental outcome. In addition, a specific diagnosis should prevent the need for further unnecessary, often invasive, investigations. Qualitative research which has been undertaken into the impact of receiving a genetic diagnosis in familial epilepsies, albeit in adult patients, has revealed that patients value this certainty (Vears et al. 2015) and this has been borne out in a study of the impact of a *SCN1A* diagnosis in Dravet syndrome (Brunklaus et al. 2013). There can also be psychological benefits to this certainty; parents may blame themselves or other factors for their child's epilepsy. Furthermore, parents may be able to access patient support groups specific to the genetic condition. An accurate genetic diagnosis also has an impact on the wider family, with parents able to receive genetic counselling including information about recurrence risk, enabling an informed choice regarding future pregnancies, including the use of pre-implantation or prenatal diagnosis. Receiving a specific genetic diagnosis may also have a direct impact upon management of the epilepsy. Although initial hopes of a new era of precision medicine have not, as yet, materialised, there are a number of EEs where the genetic diagnosis alters disease management. Quinidine as a precision therapy in *KCNT1*-related epilepsies is discussed further in Chapter 4. GLUT1 transporter deficiency due to heterozygous mutations in *SLC2A1* can be effectively treated with the ketogenic diet and an early accurate diagnosis may reduce disease burden and possibly improve cognitive outcome (Klepper 2012; Saul A Mullen et al. 2011; Leen et al. 2010; Ramm-Pettersen et al. 2013). Sodium channel blockers (SCBs) such as Lamotrigine are known to worsen myoclonic seizures in Dravet syndrome; the presence of a causative *SCN1A* mutation altered medication choice in 69% of cases in one study (Brunklaus et al. 2013). In the same study, the specific genetic diagnosis also appeared to improve access to other therapies such as

physiotherapy, occupational therapy, and speech and language therapy. Conversely, recent genetic discovery has revealed that SCBs can be very effective in *SCN2A* and *SCN8A* encephalopathies (where a gain of function is implicated*)* and in *KCNQ2* encephalopathy (possibly due to co-localisation and interaction of voltage-gated sodium and potassium channels) (Wolff et al. 2017; Howell et al. 2015; Larsen et al. 2015; Numis et al. 2014).

The ability to make a genetic diagnosis in 20-40% of patients presenting with early onset epilepsy has revolutionised clinical practice for both paediatric and adult neurologists (Scheffer 2014) and appears to have direct clinical benefits for patients. However, there is a pressing need for further translation of genomic advances into clinical practice.

1.5.2 The Online Mendelian Inheritance in Man (OMIM) early infantile epileptic encephalopathy phenotypic series

Within the Online Mendelian Inheritance in Man (OMIM) database, genes causing early onset epileptic encephalopathy are organized in a phenotypic series. To date 54 genes have been included (**Table 1.3)** and the series is included here by way of comparison with Table 1.2. However, there are several limitations to such a classification system. Several genes are included where only a small number of affected individuals with no further cases published in the interim (e.g. *PNKP*) or a single consanguineous family, (e.g. *SZT2)* (Shen et al. 2010; Basel-Vanagaite et al. 2013) have been described, and some without supportive functional validation of mutation pathogenicity. This may lead to the erroneous impression that these genes are as important or as frequently encountered in EE than others which are not included in the OMIM series. Conversely, other well-described epilepsy genes such as *CHD2* are not included (Carvill et al. 2013). There is also inevitably a great deal of phenotypic overlap between the different genes. Therefore, it should not be viewed as either a clinical classification of early onset epileptic encephalopathy or as a comprehensive source of all genes important in the EEs.

OMIM classification	OMIM phenotype number	Gene	Inheritance	Phenotype(s)
Epileptic encephalopathy, early infantile, 1	308350	*ARX*	XLR	OS WS XLAG
Epileptic encephalopathy, early infantile, 2	300203	*CDKL5*	XLD	OS WS
Epileptic encephalopathy, early infantile, 3	609304	*SLC25A22*	AR	EMEE, OS, EIMFS
Epileptic encephalopathy, early infantile, 4	612164	*STXBP1*	AD	OS, WS
Epileptic encephalopathy, early infantile, 5	613477	*SPTAN1*	AD	WS, NS-EOEE
Epileptic encephalopathy, early infantile, 6	607208	*SCN1A*	AD	DS, WS, EIMFS
Epileptic encephalopathy, early infantile, 7	613720	*KCNQ2*	AD	OS, WS, BFNIS
Epileptic encephalopathy, early infantile, 8	300607	*ARHGEF9*	XLR	Hyperekplexia, NS-EOEE
Epileptic encephalopathy, early infantile, 9	300088	*PCDH19*	XL (female sparing)	EFMR
Epileptic encephalopathy, early infantile, 10	613402	*PNKP*	AR	MCSZ
Epileptic encephalopathy, early infantile, 11	613721	*SCN2A*	AD	OS, WS, EIMFS, BFNIS
Epileptic encephalopathy, early infantile, 12	613722	*PLCB1*		WS, EIMFS, NS-EOEE
Epileptic encephalopathy, early infantile, 13	614558	*SCN8A*	AD	WS, NS-EOEE
Epileptic encephalopathy, early infantile, 14	614959	*KCNT1*	AD	EIMFS, ADNFLE, WS, OS
Epileptic encephalopathy,	615006	*ST3GAL3*	AR	WS, NS-EOEE

early infantile, 15				
Epileptic encephalopathy, early infantile, 16	615338	*TBC1D24*	AR	EIMFS, FIME, DOORS
Epileptic encephalopathy, early infantile, 17	615473	*GNAO1*	AD	WS, NS-EOEE
Epileptic encephalopathy, early infantile, 18	615476	*SZT2*	AR	NS-EOEE
Epileptic encephalopathy, early infantile, 19	615744	*GABRA1*	AD	DS
Epileptic encephalopathy, early infantile, 20	300868	*PIGA*	XLR	MCAHS2
Epileptic encephalopathy, early infantile, 21	615833	*NECAP1*	AR	NS-EOEE
Epileptic encephalopathy, early infantile, 22	300896	*SLC35A2*	XLD	NS-EOEE, CDGIIm
Epileptic encephalopathy, early infantile, 23	615859	*DOCK7*	AR	NS-EOEE
Epileptic encephalopathy, early infantile, 24	615871	*HCN1*	AD	FS-EOEE (Dravet-like)
Epileptic encephalopathy, early infantile, 25	615905	*SLC13A5*	AR	NS-EOEE
Epileptic encephalopathy, early infantile, 26	616056	*KCNB1*	AD	NS-EOEE
Epileptic encephalopathy, early infantile, 27	616139	*GRIN2B*	AD	WS
Epileptic encephalopathy, early infantile, 28	616211	*WWOX*	AR	WS, NS-EOEE
Epileptic encephalopathy, early infantile, 29	616339	*AARS*	AR	NS-EOEE
Epileptic encephalopathy, early infantile, 30	616341	*SIK1*	AD	OS, WS, NS-EOEE
Epileptic encephalopathy, early infantile, 31	616346	*DNM1*	AD	WS
Epileptic encephalopathy, early infantile, 32	616366	*KCNA2*	AD	NS-EOEE
Epileptic encephalopathy,	616409	*EEF1A2*	AD	NS-EOEE

early infantile, 33				
Epileptic encephalopathy, early infantile, 34	616645	*SLC12A5*	AR	EIMFS
Epileptic encephalopathy, early infantile, 35	616647	*ITPA*	AR	NS-EOEE
Epileptic encephalopathy, early infantile, 36	300884	*ALG13*	XLD	WS, NS-EOEE, CDGIs
Epileptic encephalopathy, early infantile, 37	616981	*FRRS1L*	AR	NS-EOEE
Epileptic encephalopathy, early infantile, 38	617020	*ARV1*	AR	NS-EOEE
Epileptic encephalopathy, early infantile, 39	612949	*SLC25A12*	AR	NS-EOEE
Epileptic encephalopathy, early infantile, 40	617065	*GUF1*	AR	WS
Epileptic encephalopathy, early infantile, 41	617105	*SLC1A2*	AD	WS, NS-EOEE
Epileptic encephalopathy, early infantile, 42	617106	*CACNA1A*	AD	FHM1, EA2, SCA6, NS-EOEE
Epileptic encephalopathy, early infantile, 43	617113	*GABRB3*	AD	WS, NS-EOEE
Epileptic encephalopathy, early infantile, 44	617132	*UBA5*	AR	WS, NS-EOEE
Epileptic encephalopathy, early infantile, 45	617153	*GABRB1*	AD	NS-EOEE
Epileptic encephalopathy, early infantile, 46	617162	*GRIN2D*	AD	WS, NS-EOEE
Epileptic encephalopathy, early infantile, 47	617166	*FGF12*	AD	NS-EOEE
Epileptic encephalopathy, early infantile, 48	617276	*AP3B2*	AR	WS, NS-EOEE
Epileptic encephalopathy, early infantile, 49	617281	*DENND5A*	AR	NS-EOEE
Epileptic encephalopathy, early infantile, 50	616457	*CAD*	AR	NS-EOEE
Epileptic encephalopathy,	617339	*MDH2*	AR	NS-EOEE

early infantile, 51				
Epileptic encephalopathy, early infantile, 52	617350	*SCN1B*	AR	DS-like FS-EOEE
Epileptic encephalopathy, early infantile, 53	617389	*SYNJ1*	AR	WS, NS-EOEE
Epileptic encephalopathy, early infantile, 54	617391	*HNRNPU*	AR	FS-EOEE, NS-EOEE

Table 1.3 OMIM classification of early infantile epileptic encephalopathy (EIEE). ADNFLE autosomal dominant nocturnal frontal lobe epilepsy, AD autosomal dominant, AR autosomal recessive, CDGIIm congenital disorder of glycosylation type IIm, CDGIs congenital disorder of glycosylation type Is, DOORS deafness, onychodystrophy, osteodystrophy, and mental retardation syndrome**,** DS Dravet syndrome, EA2 episodic ataxia Type 2, EFMR epilepsy in females with mental retardation, EIMFS Epilepsy of infancy with migrating focal seizures, FHM1 familial hemiplegic migraine type 1, FIME familial infantile multifocal epilepsy, FS-EOEE fever-sensitive EOEE, OS Ohtahara syndrome, MCAHS2 multiple congenital anomalies-hypotonia-seizures syndrome-2, MCSZ microcephaly seizures, NS-EOEE non-specific early onset epileptic encephalopathy, SCA6 spinocerebellar ataxia Type 6, WS West syndrome, XLAG X-linked abnormal genitalia, XL X-linked, XLD X-linked dominant, XLR X-linked recessive.

1.5.3 Genetic heterogeneity

Following the explosion in genetic discovery and advent of a multiple gene testing approach, it has become clear that the epilepsy syndromes are genetically heterogeneous (**Table 1.4**). Even the prototypical monogenic epileptic encephalopathy, Dravet syndrome, in which over 80% of patients are found to carry a *SCN1A* mutation, may also be caused by mutations in other genes such as *STXBP1* and *GABRA1*, albeit in a small number of cases (Carvill et al. 2014). As genetic causes are identified, sub-phenotypes with similar but subtly different clinical features can be discerned, as with epilepsy with myoclonic atonic seizures due to *CHD2*, *SLC2A1* and *SLC6A1* where there can be variability in the degree of developmental delay or presence of movement disorders (Mullen et al. 2011; Carvill et al. 2013; Carvill et al. 2015). As further patients are studied, these disorders may become distinct clinical entities rather than part of an electroclinical syndrome. For Ohtahara syndrome, (Kato et al. 2004; Absoud et al. 2010; Fullston & Hons 2011; Saitsu et al. 2012; Nakamura et al. 2013; Nakamura et al. 2013b; Allen et al. 2013; Touma et al. 2013; Lund et al. 2014; Martin et al. 2014; Higurashi et al. 2013), West syndrome (Otsuka et al. 2010; Osborne et al. 2010; Edvardson et al. 2013; Allen et al. 2013; Kato et al. 2013; Kato et al. 2014; Lemke et al. 2014; Michaud et al. 2014; Nakashima et al. 2016; Kodera et al. 2016; Møller et al. 2017) and Lennox Gastaut syndrome (Allen et al. 2013; Lund et al. 2014; Zerem et al. 2016) , many genes have been identified, with a small number of cases per gene (**Table 1.2, 1.4**).This may reflect that the electroclinical syndromes represent an age-related manifestation of a number of genetic defects, which converge on common pathways to result in a similar phenotype, rather than distinct clinical disorders (Paciorkowski et al. 2011).

Epilepsy syndrome	Genes (with approximate proportion of cases with this syndrome and causative gene, where known)
OS	*STXBP1* in ~30% *KCNQ2* in ~20%* *note this is an emerging gene encephalopathy,* *SCN2A* in ~10% *AARS, ARX, BRAT1, CACNA2D2, GABRA1, GNAO1, KCNT1, NECAP1, PIGA, PIGQ, SCN8A, SEPSECS, SIK1, SLC25A22, ZEB2*
EME	*ErbB4, PIGA, SETBP1, SIK1, SLC25A22, WWOX*
EIMFS	*KCNT1* in ~30-50% *SCN2A* in ~25% *ALG1, ALG3, PLCB1, QARS, RFT1, SCN1A, SCN8A, SLC25A22, TBC1D24, SLC12A5*
WS	*CDKL5* in ~10%* *note this is an emerging gene encephalopathy,* *STXBP1* in ~2% *ARX*, *ALG13, CACNA1A, DOCK7, DNM1, FOXG1 (duplications), GABRB1, GABRB3, GNAO1, GRIN1, GRIN2A, GRIN2B, KPNA7, MAGI2, MEF2C, NACC1, NEDDL4, NDP, NRXN1, PIGA, PLCB1, PTEN, SCA2, SCN1A, SETBP1, SIK1, SLC25A22, SLC35A2, SPTAN1, ST3Gal3, TBC1D24, TCF4, UBA5, WDR45, WWOX*
DS	*SCN1A* in 90% cases (mutations in >85%, CNV in <5%; >90% occur de novo; 5-10% inherited (mostly missense mutations) *PCDH19*, GABRA1, GABRG2, HCN1*, STXBP1* * *note most cases have a DS-like syndrome*
EMA	*SLC2A1* in 5%, *SLC6A1 in 4%* *CHD2, GABRA1, GABRG2, GABRB3, SCN1A, SCN1B, KCNA2*
LGS	*ALG13, CACNA1A, CDKL5, CHD2, DNM1, FLNA, GABRB3, GRIN2B, HNPRNU, HNRNPH1, IQSEC1, iQSEC2, KCNQ3, KPNA7, MTOR, SCN1A, SCN2A, SCN8A, STXBP1*
EAS	*GRIN2A* in 10-20% cases

Table 1.4 Electroclinical syndromes and known genetic determinants. ABRE atypical benign rolandic epilepsy, DS Dravet syndrome, EAS epilepsy aphasia spectrum, EIEE early infantile epileptic encephalopathy, EME early myoclonic encephalopathy, EMA epilepsy with myoclonic atonic seizures, EOEE early onset epileptic encephalopathy (epileptic encephalopathy starting before 3 months), LGS Lennox-Gastaut syndrome, MAE epilepsy with myoclonic-atonic seizures, OS Ohtahara syndrome. Adapted from McTague et al *The Lancet Neurology* 2015;15(3):304-1.

1.5.4 Phenotypic pleiotropy and mosaicism

As the genomic revolution has unfolded, it has become clear that mutations in one gene may lead to either varied severity of phenotype or to different phenotypes altogether (**Table 1.2**). It should be noted that the quality and depth of phenotypic data that is reported with novel genes or novel variants in known genes is quite variable, with often extensive data in some small case series and scant information in some large gene panel and exome sequencing studies. This impacts upon the accuracy of the phenotypic spectrum that is reported and should be taken into consideration by clinicians. Databases such as ClinVar attempt to improve the phenotypic annotation of reported variants

(Landrum et al. 2014) but the diagnostic categories are broad and often lack detail. Large databases such as ClinVar require uniformity of vocabulary and therefore phenotypic data is often reduced to simplified MeSH terms (PubMed medical subject heading) or Human Phenotype Ontology (HPO) terms (Robinson et al. 2008). However efforts such as the Monarch Initiative to combine sources of phenotypic data (Mungall et al. 2017), improved curation and advances in search technology may improve the quality and depth of phenotypic data. Phenotypic variability can either occur within families or unrelated individuals. In the 10% of *SCN1A*-positive Dravet syndrome patients with inherited mutations, other family members may be affected by the same mutation but manifest with febrile seizures or other phenotypes which are part of the milder GEFS+ phenotype (Depienne et al. 2010; Singh et al. 2001). This suggests that other modifier genes, epigenetic or environmental factors may be contributing to the expression of the phenotype in these individuals. Mosaicism may be another explanation for the variable phenotypes observed in the genetic EEs. Mosaicism refers to the existence of two populations of cells within a human being, one bearing a mutated allele and one with the wild-type, normal allele (Poduri et al. 2013). Mosaicism may be either somatic or gonadal. Somatic mosaicism occurs during embryonic development and therefore affects cells of certain tissue types or cell lineages. This is an emerging area of interest in childhood neurological disorders such as hemimegalencephaly, where somatic mutations in mTOR pathway genes are found within the abnormal brain tissue but not in the peripheral blood (Poduri et al. 2012). It is conceivable that tissue-level mosaicism is relevant to non-malformation disorders such as the genetic EEs but currently the lack of available brain tissue precludes investigation. Somatic mosaicism may provide an explanation for transmission of dominantly inherited variants by unaffected or mildly affected parents, as has been documented in Dravet syndrome. In 12 cases where parental mosaicism was identified, levels of parental mosaicism varied from 0.04% to 85% of cells, with higher levels correlating with the severity of the phenotype in the parent (Depienne et al. 2010). Gonadal or germline mosaicism is confined to the egg or sperm, conferring risk of mutation inheritance to offspring. Parents are clinically unaffected and such germline mosaic mutations are not detectable on leucocyte DNA testing of the parent. This phenomenon has been reported in Dravet syndrome and must be remembered when counselling families for seemingly *de novo* mutations. Although in this scenario, the likely disease mechanism is *de novo* occurrence of the mutation post-fertilisation during early

embryogenesis, gonadal mosaicism, though rare, remains a small possibility with associated recurrence risk (Depienne et al. 2006; Marini et al. 2006; Morimoto et al. 2006).

Another factor which may account for transmission of a dominant variant by a healthy parent, or the presence of the same variant in a healthy unaffected sibling, is reduced or altered penetrance. This is well-documented particularly in autosomal dominant focal epilepsy genes such as *CHRNA4* and *LGI1* and is discussed further in Chapter 4 relating to *KCNT1* (Leniger et al. 2003; Rosanoff & Ottman 2008; Cooper et al. 2013).

Altered penetrance and mosaicism must also be considered when examining WES data for new dominant EE genes. Indeed, given the observations in *SCN1A*-related epilepsy, as well as other dominant genetic epilepsies, it is increasingly important not to immediately exclude inherited heterozygous variants including those rarely reported in public databases in "control" individuals, without further interrogation as to whether they could be disease-causing (Jenkinson et al. 2016).

In addition to intrafamilial phenotypic variation, wide variation in phenotypes can be seen between unrelated individuals. For example, self-limited familial neonatal and infantile seizures are relatively benign disorders where the majority of infants do not have long-term neurodevlopmental problems after the resolution of their epilepsy, usually by the age of 12 months (Pettit & Fenichel 1980). 80% of individuals have inherited mutations of *KCNQ2*, the voltage-gated potassium channel $K_V7.2$ (Singh et al. 1998), thought to be due to haploinsufficiency (Biervert & Steinlein 1999) with loss of a single allele due to nonsense, splice or frameshift variants. However, it became clear that there were individuals both within families and with sporadic *de novo* missense *KCNQ2* mutations with a severe Ohtahara-like encephalopathy (Dedek et al. 2003; Weckhuysen et al. 2012; Weckhuysen et al. 2013). These mutations are thought to have a greater detrimental functional impact, with some authors finding more markedly abnormal channel function than in benign variants, possibly due to a dominant negative effect of encephalopathy-associated mutations (Orhan et al. 2014; Miceli et al. 2013). A single gene can also lead to quite different epilepsy phenotypes, as is evident for de novo *KCNT1* mutations leading to both epilepsy of infancy with migrating focal seizures and the later onset autosomal dominant nocturnal frontal lobe epilepsy syndrome, discussed further in Chapter 4 (Barcia et al. 2012; Heron et al. 2012). Therefore, many factors may contribute to phenotypic pleiotropy including the nature and timing of mutations during development, the

functional domains affected by the mutation, epigenetic factors and genetic background including possible modifier gene effects (**Table 1.5**).

Gene	Phenotypic variability	Postulated molecular mechanism(s) for variability
ARX	Malformation vs non-malformation phenotypes	Location and functional effect of mutation within gene: malformation phenotypes are caused by truncating mutations (resulting in complete loss of function) and most missense mutations within homeobox (DNA binding) domain. Non-malformation phenotypes result from missense mutations outside the homeobox domain or expansions of the polyalanine tracts. Increased size of polyalanine expansion correlates with increased phenotypic severity in most cases.
KCNQ2	EE vs BFNS	Functional impact of mutation: Most BFNS mutations result in haploinsufficiency. Multiple (conflicting) mechanisms have been reported in EE-causing mutations, including haploinsufficiency, dominant negative effect and gain of channel function.
CDKL5	Variable severity of epilepsy and developmental impairment	Location of mutation within gene: Patients with missense mutations in the ATP binding site typically have a less severe phenotype than those with mutations in the kinase domain or frameshift mutations in the C-terminal region.
SCN1A	1. DS vs milder phenotypes (GEFS+ etc.) in members of families with the same mutation 2. Phenotypic variability within DS	1. Differences can be due to mosaicism or (presumed) modifier genes. Mosaicism: There are multiple reports of children with DS who have inherited an SCN1A mutation from a mildly affected or unaffected mosaic parent. Mosaicism levels of 0.04% to 85% are reported, with more severe parental phenotypes at levels of > 45%. Modifier genes: specific modifier genes are not well established, although models of *SCN1A* mutant mice suggest that concurrent *SCN9A* or *SCN8A* mutations can lower or raise the seizure threshold respectively compared with *SCN1A*-only mutants. 2. Functional impact of mutation: Truncating mutations are associated with slightly earlier age of myoclonic and absence seizure onset compared with missense mutations.
SCN8A	EE vs ID without epilepsy	Functional impact of mutation: gain of function mutations are associated with EE, heterozygous loss of function mutations result in ID without epilepsy in both humans and mouse models.
GRIN2A	EOEE vs EAS	Functional impact of mutation: mutations in EAS result in haploinsufficiency, two mutations associated with the more severe EOEE associated with gain of NMDA receptor complex function (each producing increased current flow via different mechanisms).

Table 1.5 Examples of the proposed molecular bases of phenotype-genotype variability. Abbreviations: ADNFLE autosomal dominant nocturnal frontal lobe epilepsy, BFNS benign familial neonatal seizures, DS Dravet syndrome, EAS epilepsy aphasia spectrum, EIEE early infantile epileptic encephalopathy, EIMFS Epilepsy of infancy with migrating focal seizures, EOEE early onset epileptic encephalopathy, GEFS+ Genetic epilepsy with febrile seizures plus, ID intellectual disability, OS Ohtahara syndrome. Adapted from McTague et al *The Lancet Neurology* 2015;15(3):304-1.

1.6 Genes and mechanisms in the early onset epilepsies

Advances in genetic discovery for the severe epilepsies has revealed a large number of different possible disease mechanisms (**Figure 1-3** and **Table 1.2**). While channelopathies remain perhaps the most common group, genes with key roles in transcriptional regulation, chromatin remodelling, DNA repair, transporter function and cellular metabolism have been implicated. Synaptic dysfunction (associated with mutations in genes encoding proteins involved in synaptic vesicle formation and recycling and synaptic signaling) is an emerging unifying mechanism for some genetic forms of EE (**Figure 1-3**).

Data from animal and recent human-derived induced pluripotent stem cell (iPSC) studies has revealed that certain neuronal sub-types seem to play a significant role in epileptic encephalopathies. In *ARX* and *SCN1A* related encephalopathies, abnormalities of interneuron development, migration or function are implicated (Galanopoulou 2013; Olivetti & Noebels 2012; Sun et al. 2016).

Bioinformatic methods to use statistical gene network analyses using gene expression and protein interaction databases have highlighted forebrain-expressed genes and GABAergic genes in West syndrome (Paciorkowski et al. 2011). It is also clear from bioinformatics studies that certain protein networks such as the FRAX protein network may link neuronal firing to neuronal protein synthesis and regulation (Allen et al. 2013; Barcia et al. 2012).

In conclusion, a large number of genes are now associated with the early onset epileptic encephalopathies which have provided insight into the diverse molecular mechanisms at play. In the following chapters I will investigate the molecular genetic basis of EIMFS and examine the insights into disease pathogenesis that the genomic era has brought for this particularly severe early onset epilepsy.

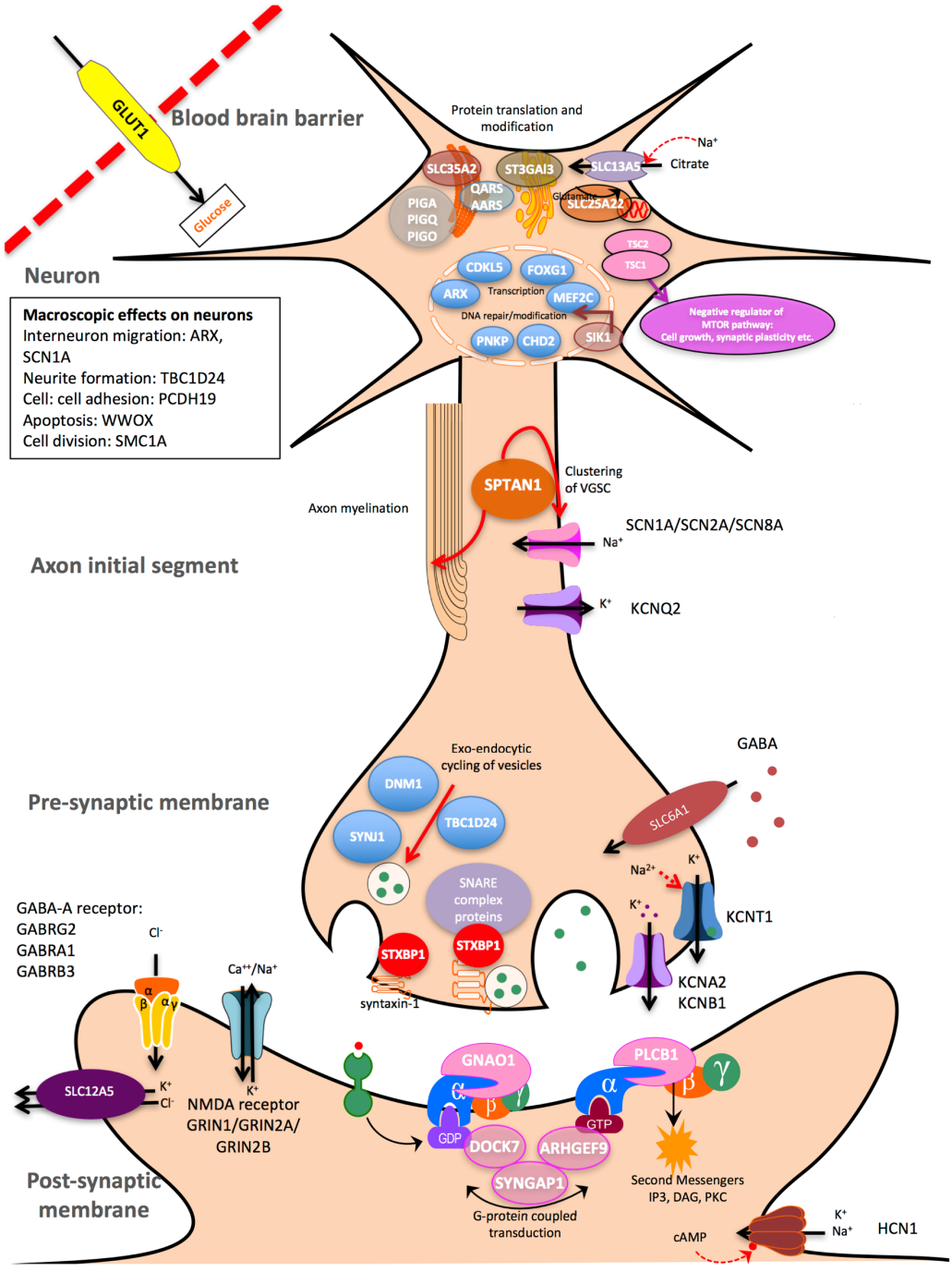

Figure 1-3 Disease mechanisms in childhood epileptic encephalopathies. Schematic drawing of neuron, axon, pre and post synaptic compartments. Many areas of abnormal neuronal function including DNA repair, transcriptional regulation, axon myelination, metabolite transport and peroxisomal function in addition to channelopathies and synaptic dysfunction are implicated in severe childhood epilepsies. Adapted from McTague et al *The Lancet Neurology* 2015;15(3):304-1.

Chapter 2 General Methods

2.1 Clinical data collection

2.1.1 British Paediatric National Surveillance Unit (BPNSU) Study

A national surveillance study of EIMFS was proposed to the BPSNU scientific committee by Dr Rachel Kneen (Paediatric Neurologist, Alder Hey Children's Hospital), and was approved. The project was discussed with the local research ethics committee (LREC) for Alder Hey Children's Hospital but as this was an anonymised surveillance study, it was deemed that ethical approval was not required. A research proforma was designed to collate anonymised clinical information regarding the patient's clinical phenotype including seizure onset, semiology, associated clinical features, EEG and other investigation results, response to treatment and developmental outcome (see Appendix). Members of the British Paediatric Neurology Association (including UK neurologists and paediatricians with an interest in neurology) were emailed once per month over a 2-year period from 2008 to 2010 and asked if they had a current or previous patient fulfilling the diagnostic criteria for EIMFS. If the answer was affirmative, a proforma was emailed to the clinician and followed up by reminder emails until completion of the questionnaire. The proformas along with anonymised clinical data and reports were collated and the data was tabulated in Excel.

2.1.2 Patient recruitment to genetics of early onset epilepsy study

Following the completion of the BPNSU study it was clear that further genetic investigations were required in these patients as none had an established aetiology for their clinical symptoms. As part of a larger Early Onset Epileptic Encephalopathy (EOEE) cohort, I recruited EIMFS patients from Great Ormond Street Hospital (GOSH) that I either saw in Dr Kurian's specialist Neurogenetic clinic or referred by colleagues, UK patients referred by GOSH colleagues, as well as UK patients referred by other paediatric neurologists and geneticists and international patients referred by clinical colleagues and collaborators. The patients were recruited as part of a collaborative study under the project title: "Genetic and biochemical investigations of children with symptoms suspicious for an inherited metabolic disease", of which Dr Kurian is a co-investigator. This encompassed all neurological diseases that are suspected to be (i) genetic in origin and (ii)

due to a gene defect encoding a protein which disrupts any process involved in cell metabolism (including channels, transporters, enzymes and other cell proteins). The study was approved by the National Research Ethics Service (NRES) (London – Bloomsbury, REC reference: 13/LO/0168, IRAS project ID: 95005). Patients were consented using age-appropriate consent forms and parents were supplied with information sheets. Patient data was entered and stored on a secure database for analysis. EIMFS recruited to this study underwent research testing, including targeted single gene analysis (*KCNT1,* KCC2) and/or whole exome sequencing.

2.1.3 Ethical approval for patients tested on the diagnostic panel

Some patients had diagnostic multiple gene panel testing as part of routine clinical care and were found to have a *KCNT1* mutation. For these patients, I undertook an approved case note review project (Great Ormond Street Hospital Research and Development Department, 16NM11). I reviewed anonymised clinical information in conjunction with anonymised EIEE diagnostic panel data.

2.1.4 Clinical endophenotyping

I collated and reviewed all clinical data. EEG data were reviewed as raw EEG data where possible and EEG reports where this was not available. Professor J Helen Cross and Dr Krishna Das from Great Ormond Street assisted in reviewing EEG data. MRI and MRS data were reviewed with Dr Shivram Avula, Alder Hey Children's Hospital, Liverpool (Chapter 3), and Dr Kling Chong, Great Ormond Street Children's Hospital (Chapters 4 and 5). Neuropathology specimens and data were reviewed by two consultant neuropathologists, Dr Michael A Farrell, Beaumont Hospital, Dublin and Dr Thomas Jacques, Great Ormond Street Hospital for Children

2.2 Materials

2.2.1 Chemical reagents

BioMix Red	Bioline
Agarose	Bioline

SYBR Safe DNA gel stain	Invitrogen
Tris-Borate-EDTA (TBE) buffer	Sigma
Hyperladder 100bp	Bioline
GC rich solution of FastStart Taq DNA Polymerase	Roche Diagnostic
Distilled Water (dH_2O)	Gibco
MicroCLEAN	Web Scientific
Sodium Acetate 3M	Ambion
Ethanol 100%/70%	Haymankimia
TE 1x buffer pH 8.0	Applichem
Accuprime Pfx Supermix	Invitrogen
NEbuffer 3.1	New England Biolabs
*EcoR*I	New England Biolabs
*Sal*I	New England Biolabs
T4 DNA ligase	New England Biolabs
T4 DNA ligase 10x Buffer	New England Biolabs
Agar powder	Sigma Aldrich
LB powder	Sigma Aldrich
10 cm petri dishes	Falcon

One Shot™ TOP10 Chemically Competent *E. coli*	Invitrogen
Ampicillin sodium salt	Sigma Aldrich
DMEM	Gibco
HBSS	Gibco
MEM	Sigma Aldrich
OptiMEM	Life Technologies
HEK293 (ATCC® CRL-1573)	ATCC
Fugene6	Promega
Pencillin-Streptomycin (10,000units/ml)	Life Technologies

2.2.2 Kits

BigDye Terminator Cycle Sequencing Kit version 3.1 (Applied Biosystems Inc., Life Technologies Corporation)

Qubit dsDNA BR Assay Kit (Invitrogen)

Stratagene QuikChangeTM Site-Directed Mutagenesis Kit (Agilent)

QIAquick Gel Extraction Kit (Qiagen)

QuikChange Lightning Site-Directed Mutagenesis Kit (Agilent)

QIAprep Spin Miniprep Kit (Qiagen)

HiSpeed Plasmid Maxi Kit(Qiagen).

2.3 DNA sequencing

2.3.1 DNA extraction and measurement

DNA was extracted either by local referring laboratories or by the Great Ormond Street Hospital North East Thames Regional Genetics Service Laboratory using standard methods. I measured aliquots of DNA either using a Nanodrop (ThermoScientific) spectrophotometer or Qubit. The Qubit assay system is a fluorometric system and the Qubit dsDNA BR Assay Kit (Invitrogen) was used according to the manufacturers protocol. In general DNA stock concentrations were in the region of 150-250ng/µl which were diluted to provide working concentrations of 20-40ng/µl for PCR and sequencing purposes.

2.3.2 Polymerase chain reaction (PCR)

The polymerase chain reaction, a method of rapidly producing numerous copies of DNA sequence from a single-stranded template, was one of the most important scientific advances of the 20th century (Saiki et al. 1985). DNA is heated or denatured, leading to separation of the double-stranded structure. Following denaturation, the temperature is lowered to allow binding or annealing of a primer to each strand of DNA. The primers direct the polymerase to a specific section of the template DNA, allowing amplification of a specific DNA fragment. A heat-stable polymerase, *Taq* polymerase which was isolated from *thermus aquaticus*, a bacterium found in hot springs, then synthesizes two new strands using the original strands as templates. Each of these strands can then be denatured and further strands synthesised, with an exponential increase in DNA copies with each cycle in the chain reaction leading to billions of copies or amplicons by the end of the reaction.

I performed PCR reactions in 20 µl aliquots as below:

	Final Concentration	Volume
• DNA (40-80ng)	(2ng/µl)	2µl
• dH_20		7.2µl
• BioMix Red 2X	(1x)	10µl
• Forward primer 10µM	(0.2µM)	0.4µl
• Reverse primer 10µM	(0.2µM)	0.4µl

BioMix Red is a pre-mixed 2X reaction solution containing an ultra-stable Taq DNA polymerase. It also contains an inert red dye to allow easy visualisation during agarose gel electrophoresis. PCR reactions were performed in thin-walled 50µl tubes or 96-well plates. For each set of reactions, a control DNA sample (from a normal subject) and a negative sample containing dH_20 instead of DNA was included.

PCR was performed using an Applied Biosystems Thermocycler. The standard PCR settings were an initial denaturation of 95^0C for 5 minutes; followed by 40 cycles of 95^0C for 45 seconds, annealing at 60^0C for 45 seconds, extension at 72^0C for 1 minute; followed by 72^0C for 5 minutes.

For GC-rich templates, the PCR reaction was adapted as below:

	Final Concentration	Volume
• DNA (40-80ng)	(2ng/µl)	2µl
• dH_20		3.2µl
• BioMix Red 2X	(1x)	10µl
• Forward primer 10µM	(0.2µM)	0.4µl
• Reverse primer 10µM	(0.2µM)	0.4µl
• GC rich solution		4 µl

2.3.3 Primer design and optimization for sequencing

I mainly used Primer3 (http://fokker.wi.mit.edu/primer3/input.html) (Untergasser et al. 2012) to design primers. The parameters in Primer3 were set as: length 18-20 nucleotides, 50% maximum GC content, exclusion of sequences with hairpin loops or self-complementarity, product size of 300-500 base pairs. I also specified that the T_M or melting temperature of the oligonucleotides should not differ by more than 5^0C. For smaller exons or where intronic length allowed, I designed primers to cover two exons at once. Following successful primer generation, I blasted the sequences against the human genome using BLASTN to ensure they were specific to the targeted region of interest.

Where Primer3 was not able to generate primers, I used manual primer design with the Ensembl transcript as a template. The following criteria were used: (i) oligonucleotide length 18-20 base pairs (ii) no more than 50% GC content (iii) 3" sequence ending in a G or a C and (iv) a product size of 250-500 base pairs. Again, these were blasted to ensure

specificity. In addition, I checked them in Primer3 to ensure there was no self-complementarity or potential to form secondary structures.

In general, I tested primers with control DNA at 60^0C and a standard thermocycling regime of 95^0C for 5 minutes; 40 cycles of 95^0C for 45 seconds, 60^0C for 45 seconds 72^0C for 1 minute; followed by 72^0C for 5 minutes.

Where there was no band, or a weak PCR product of the correct size, the T_M or melting temperature of the primer pairs was taken into consideration and I adjusted the annealing temperature either using a gradient PCR, where a range of annealing temperatures is tested simultaneously, or with sequential trials of different temperatures. Annealing temperature was thus manipulated until a strong clean band was obtained. Furthermore, I often modified PCR conditions (such as adjusting the temperature, annealing time or cycle numbers) for PCR optimisation. If these strategies were unsuccessful, design of new primers was necessary.

Where there were multiple non-specific PCR products present, specificity was mainly achieved by increase of the annealing temperature but I also tested decrease of annealing time and cycle numbers. When these strategies were not effective, I designed new primers were designed. For some fragments (e.g. *KCNT1* exon 29, Chapter 4) where primer re-design and adjustments of the PCR parameters was initially not successful, I used touchdown (TD) PCR. In TD PCR, the initial annealing temperature is set above the T_M and decreases over subsequent cycles, conferring an advantage to the specific annealing of primers to template over the non-specific priming that may occur at lower temperatures (Don et al. 1991). This can be useful where mispriming may be a factor as in GC-rich sequences (Lorenz 2012) (see below). Where primer dimers were present the primers were diluted further in case of excess primer concentrations.

Although the average guanine-cytosine (GC) content of the human genome varies widely from 35-60% (Romiguier et al. 2010; Lander et al. 2001), some genes are particularly GC-rich. A good example of this is *KCNT1* (Chapter 4) which has 61.7% GC content (http://grch37.ensembl.org/biomart). PCR and sequencing of GC-rich genes can be difficult as the G-C bonds are particularly stable due to base stacking leading to stable secondary structure formation and mispriming during PCR (Jensen et al. 2010). Various strategies are available including use of DMSO, which reduces secondary structure formation, or betaine

and increasing annealing temperature (Strien et al. 2013). Several commercial GC-enhancer solutions are also available. I used GC-RICH Reaction Buffer, 5X concentrated, which contains 7.5 mM MgCl2 and DMSO.

Lastly, where the negative sample contained a DNA band suggesting a DNA contamination, I repeated the reaction with fresh primer dilutions. If the negative contamination persisted, new primer stocks and reagents or a change of set-up location were used which was effective.

2.3.4 Agarose gel electrophoresis

I verified PCR products by running samples on horizontal agarose gels to ensure the PCR product was the correct size and that there was no contamination. Gels were 1.5% agarose made by adding 1.5 grams of agarose powder to 100mls of 1X TBE Buffer. This was dissolved in a 250ml conical flask using a standard domestic 800W microwave, cooled to hand-hot temperatures and 5µl of SybrSafe (10,000X concentration) was added. SybrSafe enables DNA denaturation and visualisation. The agarose was poured onto a gel casting tray and left for 15-25 minutes to solidify under an extraction hood. I then loaded samples and 5µl of ladder into the wells created by inserting plastic combs during the solidification process. After electrophoresis at 120V for 30-40 minutes, the gel was visualised using a Gel Doc™ XR+ Gel Documentation System and ImageLab software.

2.3.5 Sanger sequencing of PCR products

The chain termination or dideoxy technique, which was developed by Sanger in 1977, exploits the fact that dideoxynucleotides (ddNTPs) cannot be incorporated into DNA during an extension reaction due to the lack of a 3' hydroxyl group (Heather & Chain 2016). As chemical ddNTP analogues are incorporated into the DNA strand, they result in chain termination. The technique was further refined as dye-terminator sequencing, where fluorescently labelled ddNTPs emit signal at differing wavelengths as they are incorporated during DNA extension. This innovation led to the development of automatic sequencers such as the ABI PRISM sequencer used in this study.

I purified PCR products using MicroCLEAN (Web Scientific) to remove reaction buffers, enzymes, primers, primer dimers or dNTPs which could interfere with downstream processing. 2.5-3.5 µl of microclean was added to the equivalent volume of PCR product in

a 96 well plate. This was centrifuged at 4000rpm at 4^0C for 40 minutes, followed by another short centrifugation step in which the unwanted chemicals were removed by inverting the plate. The cleaned-up PCR product was resuspended in distilled water.

2.3.5.1 Sequencing reaction set-up

I set up each 10µl reaction as follows:

- PCR product re-suspended in dH_20 4.5µl
- dH_20 2µl
- BigDye Sequencing buffer 5X 2µl
- BigDye 1.1 Reaction Mix 0.5µl

1µl of either forward or reverse primer was then added to each well.

I ran the sequencing reaction on an Applied Biosystems Thermocycler using the following parameters: 96^0C for 3 minutes; followed by 35 cycles of 96^0C for 30 seconds, 50^0C for 15 seconds and 60^0C for 4 minutes.

2.3.5.2 Precipitation of sequenced DNA

Following the sequencing reaction, I added 2µl of Sodium Acetate (3M) and 50µl of 100% ethanol to each well. The reaction was mixed by briefly vortexing and left at room temperature for 20 minutes. The plate was then centrifuged at 3000rpm for 40 minutes at 4^0C and subsequently inverted and centrifuged at 300rpm for 1 minutes to remove excess ethanol. A further precipitation sand centrifugation step with 70% ethanol at 3000rpm for 10 minutes was followed by centrifugation of the inverted plate at 300 rpm for 1 minute. The plate was air dried to eliminate excess ethanol and 10 µl of TE was added to each reaction.

2.3.5.3 Sequencing reaction and analysis

The samples that I prepared for sequencing were run by laboratory technicians within the Great Ormond Street Hospital NE Thames Regional Genetics Service Laboratory on an ABI PRISM 3730 DNA Analyzer (Applied Biosystems Inc). This is part of a mutual agreement and is the standard service for sequencing within the UCL Institute of Child Health. I analysed sequencing data either with Chromas (Technelysium Pty Ltd, Australia) or Sequencher (GeneCodes Corporation, USA) software. I checked samples for read quality before aligning

to a control sequence to analyse sequence for coverage of exon and exon-intron boundaries and the presence of abnormal variants.

2.4 Mapping and single nucleotide polymorphism(SNP) arrays

Illumina CytoSNP12 arrays were performed by the local UCL Genomics Service in both parents, affected and unaffected children from Family 1 (Chapter 5), see Appendix for methods. Analysis of SNP data is considered in 5.2.1.

2.5 WES and analysis

For Family 1, described in Chapter 5, whole exome sequencing was performed by the Institute of Neurology(IoN) Next Generation Sequencing service (Molecular Neurosciences, Institute of Neurology, London). The methods used in the IoN laboratory are detailed in the Appendix. WES described elsewhere in this thesis was performed externally and methods are also described in the Appendix. I received the data from IoN as a .csv file which I then analysed in Excel, using series of filtering steps based on the hypothesis that the underlying condition was a rare, likely recessive disorder. Firstly, I excluded all synonymous variants and retained non-synonymous single nucleotide variants (SNVs), frameshift and non-frameshift deletions or insertions and stop-loss or stop-gain SNVs. Secondly, I excluded all variants with a mean allele frequency of >0.01 in genome databases (1000 Genomes, Exome Variant Server) to retain only rare variants. Subsequently I selected homozygous and compound heterozygous variants. Within this data I then focused my analysis on variants lying within the homozygous regions identified by autozygosity mapping.

Further WES described in Chapters 3, 4 and 6 was performed externally to UCL and methods are described in the Appendix. Analysis is described in the relevant chapters.

2.6 *In situ* mutagenesis of pCMV6-XL5-KCC2 plasmid

2.6.1 Preparation of materials for bacterial culture

2.6.1.1 Lucia Bertani (LB) medium

I mixed 10g of LB broth base (Sigma) with 500ml of water and the solution was autoclaved to sterilize the solution.

2.6.1.2 Ampicillin solution

I added 1 gram of ampicillin sodium salt (Sigma Aldrich) to 10mls of distilled water under a fume hood. For sterilisation, the solution was passed through a washed 0.22 µm filter, aliquoted and stored at -20^{0}C.

2.6.1.3 Ampicillin agar plates

I mixed 8g of LB broth base and 6g of agar powder with 400ml of distilled water and autoclaved the solution. Once cooled to a hand-hot temperature (approximately 50^{0}C), 400µl of 100mg/ml ampicillin was added. Before pouring into 10cm petri dishes, the opening of the bottle was flamed with a Bunsen burner to ensure sterile conditions and left to set under a fume hood.

2.6.2 Amplification of commercial *SLC12A5* clone in *E coli*

I obtained a pCMV6-XL5 plasmid with a full length *SLC12A5* wild-type human insert from Origene (catalogue number SC304801) (**Figure 2-1**).

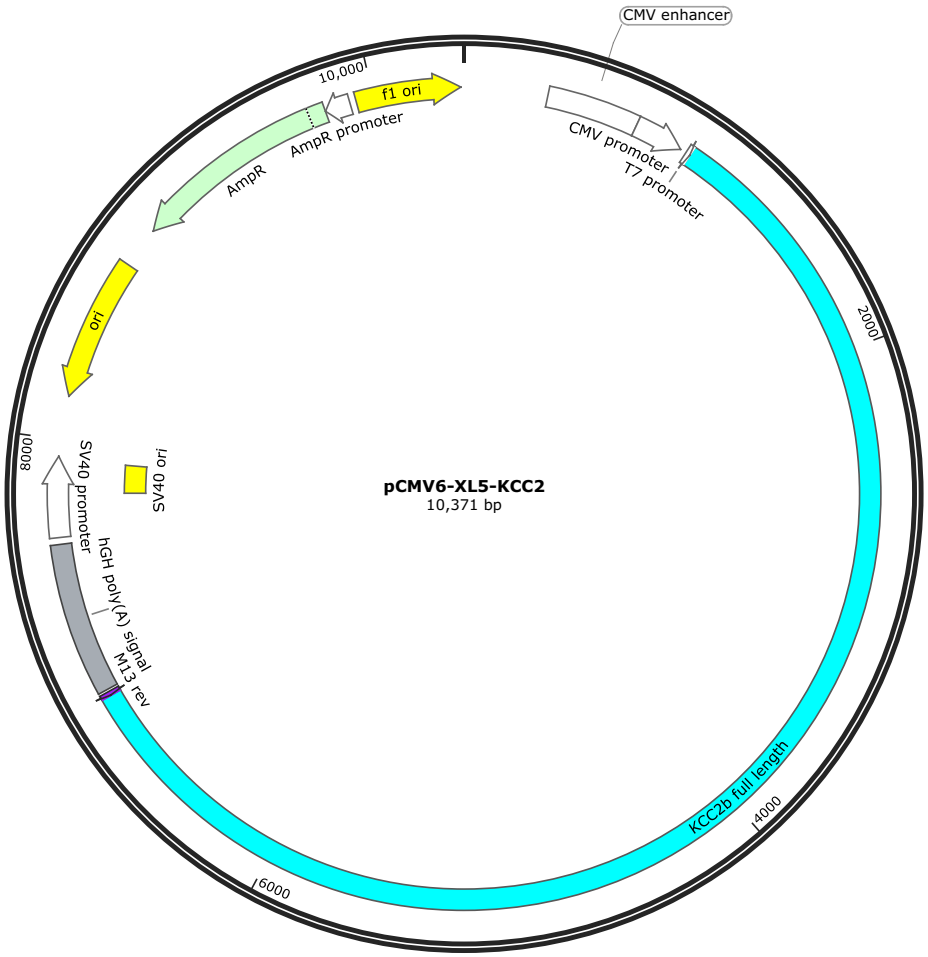

Figure 2-1 pCMV6-XL5-KCC2 plasmid map

For amplification of the plasmid, I transformed One Shot™ TOP10 Chemically Competent *E. coli*. with 1µl of the resuspended clone. After incubation on ice for 30 minutes, the cells were heat shocked at 42^0C for 30 seconds in a water bath and then put back on ice. I added 250µl of SOC medium and the cells were incubated at 37^0C for 1 hour with shaking. To ensure only amplification of cells containing the plasmid, I plated them onto warmed LB-Agar Ampicillin plates using two different volumes, 10µl and 100µl, and incubated overnight at 37^0C. The following day, I picked discrete colonies which were then inserted into 5mls of LB medium with 5µl of ampicillin (100mg/ml) followed by incubation at 37^0C overnight with shaking. From the overnight cultures, I purified DNA using a Qiaprep Mini Prep kit (Qiagen) in accordance with the manufacturers protocol. I measured DNA using a Nanodrop and then sequenced this directly with cDNA primers (see Chapter 5 Methods) to verify the presence of the full-length wild type *SLC12A5* cDNA insert without mutations. Following confirmation of the correct sequence, I inoculated 250mls of LB broth containing

250µl of ampicillin (100mg/ml) with 2.5mls of the overnight culture which was incubated with shaking overnight at 37^0C. I extracted the plasmid DNA using a Qiaprep Maxi Prep kit. I then measured the DNA and sequenced it directly with cDNA primers.

2.6.3 *In situ* mutagenesis

In situ, or site-directed, mutagenesis is the introduction of a mutation into a gene of interest at a specific location. Several methods are available, but one of the most efficient uses complementary mutagenesis primers and a high-fidelity non-strand displacing polymerase such as *pfu* polymerase to amplify plasmid DNA in a thermocycler. This creates a nicked circular DNA containing the desired mutation. As the template DNA has been created within *E coli* it will be methylated and can be digested with the methylation sensitive restriction enzyme *Dpn*I. However, the mutated plasmids have been generated *in vitro* and are therefore unmethylated and will escape digestion. Hence, I chose to use a Stratagene Quikchange Site-Directed Mutagenesis kit which is based on this principle. I designed mutagenesis primers for each of the *SLC12A5* mutations in keeping with guidance in the Stratagene QuikChangeTM manual using Primer3 (detailed in Chapter 5). In brief, the primers should be 25-45 nucleotides in length, with the desired mutation in the middle of the primers and a $T_M \geq 78^0$C with minimum T_M mismatch between primers. In accordance with the kit instructions, I set up the mutagenesis reaction in 50µl aliquots, keeping primers in excess of the DNA template. Cycling parameters were: 95^0C for 1 minute; followed by 18 cycles of 95^0C for 50 seconds, 60^0C for 50 seconds and extension at 68^0C for 10 minutes (1 minute per Kb of plasmid); followed by 68^0C for 7 minutes. Subsequently, the reaction was placed on ice, *Dpn*I was added and samples incubated at 37^0C for 1 hour. *E. coli* were then transformed and plated onto ampicillin LB Agar plates as detailed above. The following day I selected colonies which were added to 5mls of LB medium containing ampicillin and incubated overnight. I extracted DNA the following day using a Qiaprep kit as above. Plasmid DNA was sequenced using cDNA primers to verify the introduction of the mutation and to ensure no additional mutations had been generated during mutagenesis. Using this method, I successfully introduced all three *SLC12A5* mutations into the pCMV6-XL5-KCC2 plasmid.

2.7 Cloning of pRK5 plasmid

To investigate the impact of *SLC12A5* mutations on transporter function, I planned to express the mutants in a cell system. For this purpose, the insertion of the wildtype and mutated *SLC12A5* sequence into a robust expression plasmid was required. The pRK5 plasmid was kindly provided by Professor Robert Harvey (**Figure 2-2**). This is an expression plasmid previously successfully used by the Harvey lab in studies of glycine receptor function (Rees et al. 2006).

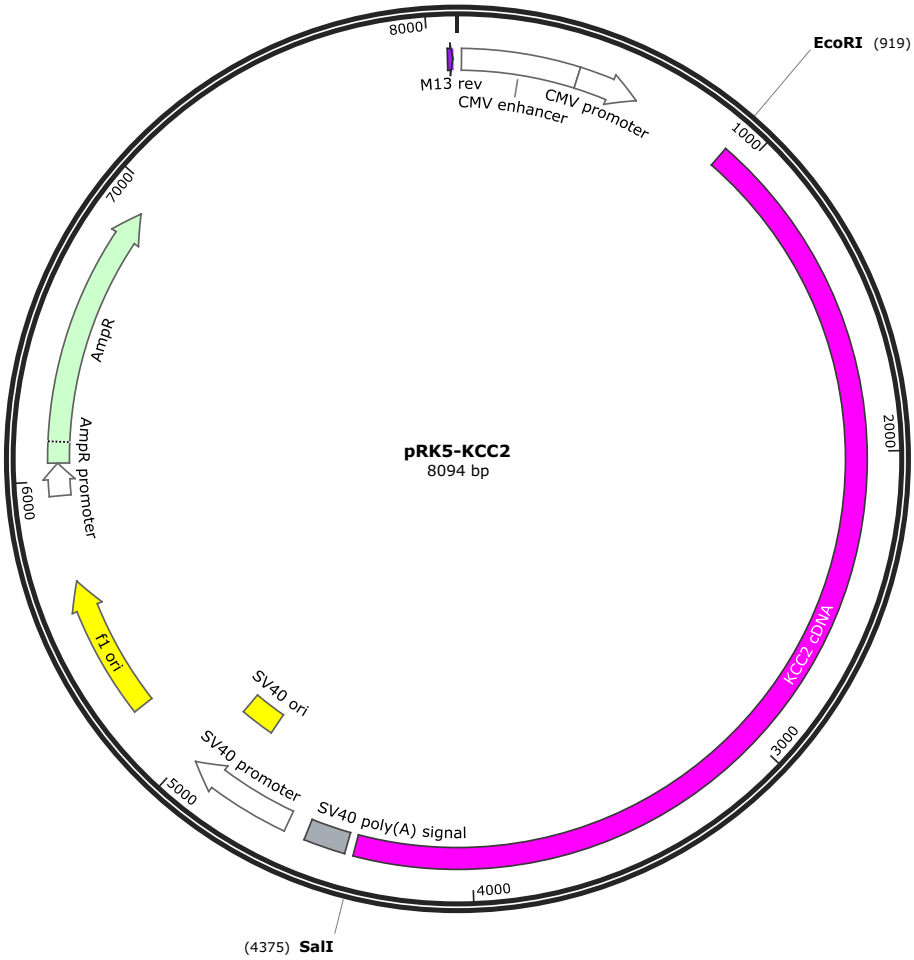

Figure 2-2 pRK5-KCC2 plasmid map. pRK5 sequence based on publicly available Addgene data https://www.addgene.org/browse/sequence_vdb/3944/

2.7.1 Amplification of insert

PCR-based cloning involves PCR-based amplification of the gene of interest from a donor plasmid with incorporation of restriction enzyme recognition sites. This enables the insert to be cut out and incorporated into a recipient plasmid or vector. Using NEBcutter, I interrogated the donor plasmid (pCMV6-XL5-KCC2) and recipient plasmid (pRK5) sequence for common bacterial enzyme recognition sites located within the multiple cloning site (MCS) and which were unique in the recipient plasmid and the *SLC12A5* cDNA sequence to prevent cutting elsewhere in the vector or the insert. As a result, I chose *EcoR*I and *Sal*I as enzymes which would cut out the *SLC12A5* insert from the donor plasmid and also cut the recipient pRK5 plasmid, resulting in complementary ends between the donor and recipient plasmids. I also chose a different restriction enzyme site for each end to avoid re-ligation of the donor plasmid. I manually designed primers with a three-base overhang or initial sequence followed by the recognition for the upstream restriction enzyme in the forward primer and the downstream restriction site in the reverse primer. I then incorporated a Kozak sequence, the eukaryotic translation initiation consensus sequence which helps to align the ribosome with the start codon. Inclusion of a Kozak sequence in primers can improve expression (Kozak 1986). This was followed by the ATG start codon for the forward primer and the first 18 nucleotides of the gene, and the stop codon and last 18 nucleotides for the reverse primer. Both primers were finally checked in Primer3 for self-complementarity and secondary structure formation. Primer details are found in Chapter 5.

I performed the PCR in the Harvey laboratory using an in-house protocol. 25µl reactions were set up as follows:

	Final concentration	Volume
• Forward primer (10µM)	0.4 µM	1µl
• Reverse primer (10µM)	0.4 µM	1µl
• Accuprime Pfx Supermix		22µl
• pCMV6-XL5-KCC2 DNA (50ng/µl)		1µl

I set up reactions were set up for pCMV6-XL5-KCC2 wild type and all three mutations. Thermocycler conditions were as follows: 95^0C for 3 minutes; followed by 25 cycles of 95^0C for 1 minute; 50^0C for 1 minute and 68^0C for 16 minutes (2 minutes per Kb).

After the PCR, I added 1 µl of *Dpn*I restriction enzyme, followed by incubation at 37^0C for 90 minutes. The PCR product was run on an agarose gel to ensure successful amplification. A QIAquick Gel Extraction Kit was then used for extraction of the DNA from the agarose gel according to the manufacturers protocol.

2.7.2 Restriction digest

I performed a double digest on both the gel-extracted PCR product (amplified from the donor plasmid) and the recipient plasmid as follows:

Donor plasmid (25µl):

- NEbuffer 3.1 3µl
- *EcoR*I 1µl
- *Sa*lI 1µl

pRK5 plasmid (2µl):

- NEbuffer 3.1 2µl
- dH_20 14µl
- *EcoR*I 1µl
- *Sa*lI 1µl

The digests were pulsed for 30 seconds in a bench-top centrifuge and incubated at 37^0C for 2 hours.

2.7.3 Phenol-chloroform extraction

I added distilled water to the vector and insert to result in a final volume of 100µl. 100µl of phenol-chloroform isoamyl alcohol was added to each sample under the fume hood and tubes were centrifuged at 13000rpm for 10 minutes. The aqueous phase of each sample was each added to a tube containing 250µl 96% ethanol, 10µl 3M sodium acetate and 1.5µl Glycogen.

The mixture was chilled on dry ice for 30 minutes and then centrifuged for 18 minutes. I discarded the supernatant and the pellet washed with 250µl 80% ethanol, centrifuged and air dried. The pellet was then eluted in 14µl EB buffer for the insert and 50µl for the pRK5 vector.

2.7.4 Ligation

The next step of the cloning process it to ligate the insert, which has been cut from the surrounding donor plasmid DNA, into the recipient plasmid which has been cut at the same restriction sites. The T4 DNA ligase enzyme forms phosphodiester bonds between the 3'-hydroxyl of one DNA terminus with the 5'-phosphoryl of another using ATP as a co-factor.

Varying ratios of vector to insert were trialled but 1:3 was the most successful. I set up the ligation reaction as follows:

- Insert 3µl
- Vector 1µl
- 10X ligation buffer 1µl
- T4 DNA ligase 1µl

Tubes were spun for 1 minute and then incubated at 4^0C overnight.

2.7.5 Transformation of *E coli*

I transformed TOP10 cells as detailed above and plated them onto ampicillin LB Agar plates. As described previously, colonies were selected into mini cultures and I extracted DNA using the Qiaprep Mini Prep kit.

I performed a diagnostic double digest to ascertain whether the gene had been successfully inserted using *EcoRI* and *SalI* as described above. The digest was separated and visualised by gel electrophoresis at 120mV for 2 hours on a 0.8% agarose gel. Only the DNA of plasmids that possibly contained the insert was sent for sequencing using cDNA primers to ensure the presence of the gene of interest. Once the success of the cloning was confirmed, I performed a maxi prep to generate DNA stocks for each mutation.

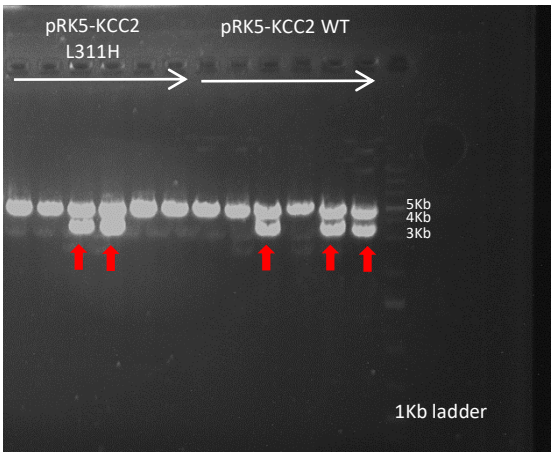

Figure 2-3 Agarose gel electrophoresis of diagnostic digest of pRK5 cloning product for wild-type KCC2 and L311H. 0.8% gel run at 120mV for 2 hours. For 5 samples (red arrows), 2 bands at~ 5Kb and ~3Kb are seen, indicating successful insertion of the 3.3 Kb KCC2 insert into the pRK5 plasmid

2.8 *In situ* mutagenesis of pRK5 plasmid

As PCR-based cloning was not successful for all of the mutations, I undertook in situ mutagenesis of the generated pRK5-KCC2 wild-type plasmid to generate the L426P and G551D mutant plasmids. Essentially the principles and the primers used are as described above, but a QuikChange Lightning Site-Directed Mutagenesis Kit was used. I set up 50µl reactions as follows:

	Final Concentration	Volume
• Lightning Reaction Buffer		5µl
• Template DNA		1µl
• Forward primer(10µM)	0.4 µM	1µl
• Reverse primer(10µM)	0.4 µM	1µl
• dNTP mix		1µl
• QuikSolution		1.5µl
• dH_20		39.5µl
• LightninqQuik enzyme		1µl

Thermocycling parameters were as follows: 95^0C for 2 minutes; followed by 18 cycles of 95^0C for 20 seconds, 60^0C for 10 seconds and extension at 68^0C for 4 minutes (30 seconds per Kb of plasmid); followed by 68^0C for 5 minutes. 2µl of *Dpn* was then added to digest the parental DNA template. To amplify the mutant plasmids, *E. coli* were transformed and cultured under selective conditions as above. To ensure the presence of the mutant KCC2

insert, I extracted and sequenced DNA as above. Using these methods, I successfully generated the remaining two mutant plasmids.

2.9 Cell culture and transfection

2.9.1 Maintenance of HEK293 cells in culture

I grew HEK293 cells in 25cm^2 flasks in Dulbecco's Modified Eagle Medium (DMEM) supplemented with 10% FBS and 1% pencillin-streptomycin (5 ml of 10,000units/ml) and incubated in a CO_2 incubator at 37^{0}C.

2.9.2 Transfection of HEK293 cells for electrophysiology experiments

Once cells were confluent, I split for transfection into 100mm round Petri dishes. Cells were washed with HBSS and 1ml of Trypsin-EDTA was added. I agitated the culturing flask until cells detached and then reconstituted the cells in 9mls of DMEM. Cells were added 1:10 to the 100mm dishes and a further aliquot added to a new 25cm^2 flask of DMEM to be kept in culture. After 24 hours in culture, the cells in the 100mm dishes were washed with HBSS twice to remove any DMEM to avoid interference with downstream processing. I prepared a transfection mixture was prepared for each construct:

- Optimem 230µl
- Fugene 30µl
- Plasmid DNA 4 µg per construct varying by concentration

I co-transfected cells with three constructs:

1. pRK5-eGFP
2. pRK5-GlyR α2 subunit
3. pRK5-KCC2, either wild type or mutant, or pRK5 alone (empty vector)

The Optimem and Fugene were combined and incubated for 5 minutes, followed by addition of the DNA with incubation at room temperature for 15 minutes. 9ml of MEM was added to the cells. As DMEM contains glycine and the cells were transfected with a glycine receptor (Chapter 5), it was essential that only MEM was used post-transfection. I dropped the transfection mixture onto the cells and they were incubated for 24 hours.

2.9.3 Preparation of transfected cells for electrophysiology

I aspirated the medium from the transfected cells and HBSS was used to wash the cells. Cells were detached with 1ml of Trypsin-EDTA and 9ml of MEM added. The contents of the dish were transferred to a 15cm Falcon tube and centrifuged at 1000rpm for 2 minutes. The supernatant was discarded, and the pellet was resuspended in 1ml of perfusion solution (see below).

2.10 Electrophysiology

I undertook electrophysiology experiments under close supervision from Dr Arnaud Ruiz. I prepared the cells for patching and set up the electrophysiology rig including pipette and solution preparation. I worked alongside Dr Ruiz who patched the majority of the cells from which the experimental data is derived but as I acquired better technical skills, I was able to successfully patch several cells, generating data that was included in the analysis. Patch pipettes (3-5 MΩ) were pulled from borosilicate glass (1.5 mm outer diameter, 0.5 mm wall thickness) and recordings were obtained from eGFP-positive HEK293 cells under infra-red differential interference contrast imaging. I prepared the perfusion solution containing NaCl (140mM), KCl (4mM), $MgCl_2$ (1mM), $CaCl_2$ (2mM), D-glucose (5mM), HEPES (10mM) (pH 7.2, osmolarity 298mOsm.l^{-1}). Currents were recorded with a Multiclamp 700-B amplifier (Molecular devices), filtered at 2 kHz (internal 4-pole low-pass Bessel filter) and sampled at 10 kHz. The access resistance, monitored throughout the experiments was <15 MΩ and results were discarded if it changed by more than 20 %. The pipette solution contained CsCl (50mM), NaCl (10mM), CsF (60mM), EGTA (20mM), HEPES (10 mM) (pH 7.2, osmolarity 310mOsm.l^{-1}). Local pressure application of glycine (1mM in control HEPES solution) was delivered via a patch pipette connected to a Picospritzer (General Valve Corporation). The puff pipette was positioned roughly 10-20µm away from the recorded cell and the bath perfusion arranged to keep it downstream of this position. Cells were first held at –80mV while several glycine applications were made at 30 seconds intervals to ensure that no desensitisation occurred. Glycine puffs (3-5 ms, 5-10 PSI) were then delivered every minute at different holding potentials (–80 mV to +20 mV, 20 mV increment). A linear regression of I_{Gly} amplitude plotted against the holding potential was used to analyse the voltage dependence. The intercept of the I-V relation with the abscissa was then extrapolated as E_{Cl}. (As experiments were performed in bicarbonate-free solution buffered with HEPES I_{Gly} was solely mediated by Cl^- and thus we report E_{Cl}). E_{Cl} predicted

from the Nernst equation was -21.3 mV. Data are expressed as mean ± S.E.M and were considered significant if $P < 0.05$.

Chapter 3 Epilepsy of Infancy with Migrating Focal Seizures

3.1 Historical background and first description

Epilepsy of infancy with migrating focal seizures was originally described in 1995 (Coppola et al. 1995) in a series of 14 children with severe epilepsy. Since this original report, over 170 patients have been described (Coppola et al. 1995; Coppola et al. 2006; Coppola et al. 2007; Okuda et al. 2000; Wilmshurst et al. 2000; Gross-Tsur et al. 2004; Marsh et al. 2005; Hmaimess et al. 2006; Hahn et al. 2007; Jocic-Jakubi & Lagae 2008; Caraballo et al. 2008; Caraballo et al. 2014; Caraballo et al. 2016; Cilio et al. 2009; Nabatame et al. 2010; Bedoyan et al. 2010; Djuric et al. 2011; Freilich et al. 2011; Gilhuis et al. 2011; Irahara et al. 2011; Sharma et al. 2011; Vendrame et al. 2011; Carranza Rojo et al. 2011; Chien et al. 2012; Fasulo et al. 2012; Barcia et al. 2012; Lee et al. 2012; Need et al. 2012; Poduri, Chopra, et al. 2012; Annapurna Poduri et al. 2013; Dhamija et al. 2013; Ishii et al. 2013; Merdariu et al. 2013; Milh et al. 2013; Ünver et al. 2013; De Filippo et al. 2014; Iyer et al. 2014; Bearden et al. 2014; Ohba et al. 2015; Segal et al. 2014; Shimada et al. 2014; Howell et al. 2015; Mikati et al. 2015; Møller, Heron, et al. 2015; Saade & Joshi 2015; Selioutski et al. 2015; Stödberg et al. 2015; Appavu et al. 2016; Barba et al. 2016; Mori et al. 2016; Rizzo et al. 2016a; Saitsu et al. 2016). Coppola reported children presenting with frequent focal seizures with onset before six months of age in most patients, associated with a unique, multifocal, shifting pattern of EEG activity, amounting to an unusual focal status epilepticus. In this seminal paper, several key features were delineated, including:

- Disease onset before six months of age
- Frequent focal seizures that are intractable to treatment
- Ictal EEG showing rhythmic alpha or theta activity independently involving multiple areas of the cortex and moving from one area to another in consecutive seizures
- Normal development prior to onset of seizures followed by developmental regression

Although a poor developmental outcome was seen in ten of 14 patients, two patients had seizure control after one year and made subsequent developmental progress, attaining

independent walking by three years of age. Other clinical features were noted, including a choreoatheoid movement disorder in two patients, acquired microcephaly and severe hypotonia.

EIMFS has been previously termed migrating partial seizures of infancy, migrating focal seizures of infancy and malignant migrating partial seizures of infancy. With the reorganisation of epilepsies proposed by the International League against Epilepsy (ILAE, http://www.ilae.org) in 2010 (Berg et al. 2010), the term malignant was removed as this was felt to be an emotive and upsetting term. In line with other focal epilepsies, the term partial was changed to focal. While there is no formal ILAE classification of electroclinical syndromes, EIMFS currently remains the preferred descriptor (Scheffer et al. 2016; Scheffer et al. 2017).

3.2 The British Paediatric Neurology Surveillance Unit study of EIMFS

At the beginning of my research project, I noted that EIMFS was purported to be a rare condition. However, an increasing number of cases were being reported in the literature and I had met a number of affected families in my clinical practice. I therefore aimed to determine the incidence and prevalence of EIMFS in the UK. A national surveillance study was undertaken in conjunction with the British Paediatric Neurology Surveillance Unit (BPNSU, www.bpnsu.co.uk) to investigate the incidence of EIMFS and to further delineate the clinical features of this disorder.

3.2.1 Methods

A national surveillance study was performed in conjunction with the BPNSU over a 27-month period (February 2008 to May 2010). Study inclusion criteria (Coppola et al. 1995) were as follows:

- Seizure onset before age of nine months
- Focal motor seizures at onset
- Multifocal seizures proving intractable to conventional anti-epileptic drugs
- EEG criteria: initial EEG can be normal but characteristic changes emerge over time, including interictal multifocal spikes and ictal independent, unilateral and migrating involvement of varying cortical areas with electroclinical correlation.

- Developmental delay or developmental regression with seizure onset.
- Presentation not consistent with another recognised electro-clinical syndrome (although evolution from/to other syndromes e.g Ohtahara and West syndrome may occur)

These features were derived from the first description of EIMFS by Coppola *et al* in 1995 as discussed above. British Paediatric Neurology Association (BPNA) members (285 paediatric neurologists, paediatricians with an interest in neurology and clinical trainees) were sent a monthly email during a two year period and asked to notify new or previous cases of EIMFS. Those who responded positively were sent a proforma (see Appendix) to collect anonymised clinical data regarding disease evolution, EEG features, neuroimaging, neurometabolic and genetic investigations.

3.2.2 Results

3.2.2.1 Epidemiology

Over the course of this study overall response rate was 68.4%. Of 17 patients notified to the BPNSU study, 14 met the inclusion criteria. Based on these figures, I estimated the UK prevalence of EIMFS to be 0.11 per 100,000 over the two years of the study. The incidence of new cases of EIMFS was 0.26 cases and 0.55 cases per 100,000 live births in the first and second years of the study respectively.

3.2.2.2 Clinical features

All identified patients were singleton cases with no affected siblings. There was no parental consanguinity. In three cases, there was a family history of adult-onset generalised or focal seizures but not in a first degree relative. One patient was born at 35 weeks, whilst the rest were born at full term. Mean birth weight was 3.0kg (10^{th}-16^{th} centile, range: 2.18-3.69 kg). Three of the children manifested early feeding difficulties; one of these had concurrent neonatal seizures.

The median age at seizure onset was seven weeks (range: four days to five months). Most had focal motor seizures at onset. Adversive seizures with head turning and eye deviation or eye flickering were frequent. Autonomic features such as facial flushing, drooling, apnoea, epiphora and changes in pupil size were seen in 12 (88%) of the patients. Patients without autonomic features at disease onset did not develop such symptoms later in the

disease course. Notably, five patients did not manifest motor seizures at onset but all patients had frequent focal motor seizures by six months of age.

Over time, all patients developed multiple seizure types. Multifocal or clinically migrating seizures were seen in six patients. Infantile spasms with hypsarrhythmia were evident in two of the patients at two and eight months of age respectively. As the disease progressed, seizures became very frequent in all patients, ranging from three to over 100 episodes each day. Clustering of seizures was common, most frequently on waking and falling asleep. Within the cohort, age at peak seizure frequency was variable from three weeks to three years. However, in the seven patients where the clinician reported a reduction over time in seizure frequency, the median age of peak seizure frequency was four months (range three weeks to one year).

None of the patients had specific dysmorphic features as reported by their paediatric neurologist but five were reported to have coarse facial features. All patients had a normal occipito-frontal head circumference (OFC) at birth which then declined with age, resulting in microcephaly in seven patients. Most patients had a normal neurological examination at presentation. However three patients displayed abnormalities of tone with central hypotonia and/or peripheral limb spasticity. After 12 months from onset of the disorder, one patient had developed spasticity with increased peripheral reflexes and seven had become hypotonic.

I also identified several less commonly reported clinical features. Firstly, a variety of non-epileptic movement disorders were seen in four patients. One patient manifested a severe cervical dystonia, one a limb dystonia with subsequent four limb dyskinesia, and two patients displayed generalised choreoathetosis. Secondly, a very severe gastrointestinal dysmotility disorder was reported in three patients.

All patients received multiple antiepileptic medications in varying combinations and none resulted in seizure freedom for a significant period of time. Some reduction in seizures or a brief period of seizure freedom was seen with oxcarbazepine, phenytoin, topiramate, levetiracetam, vigabatrin, stiripentol and lacosamide. Bromide salts were used in three patients with no evidence of efficacy and excessive sleepiness in one leading to cessation. Corticosteroids were used in nine patients and effective in two; ACTH in one case and oral

prednisolone combined with the ketogenic diet in another. Nine patients were treated with the ketogenic diet of which one became seizure free for approximately two years.

The outcome for patients in this UK cohort was uniformly poor. Over half of the cohort died at between two months and eight years of age. In seven patients, there was a gradual reduction of seizures over time; however although they seemed to have "burnt out" in terms of seizure frequency, the patients were not completely seizure free and had significant neurodisability. The developmental outcome in general was poor with two-thirds of children showing developmental regression at seizure onset and the remainder having never made any significant developmental progress. The best developmental stage attained beyond one year of age was at three to four month level with some degree of head control, rolling and visual fixing and following.

3.2.2.3 EEG Features

While in the majority the inter-ictal EEG showed multifocal spikes and background slowing, the initial inter-ictal EEG was normal in three patients. Novel inter-ictal abnormalities included periods of relative suppression in two patients and frank burst suppression in one patient. In addition, hypsarrhythmia (**Figure 3-1**) was noted in three patients, with infantile spasms evident in 2/3 of these infants.

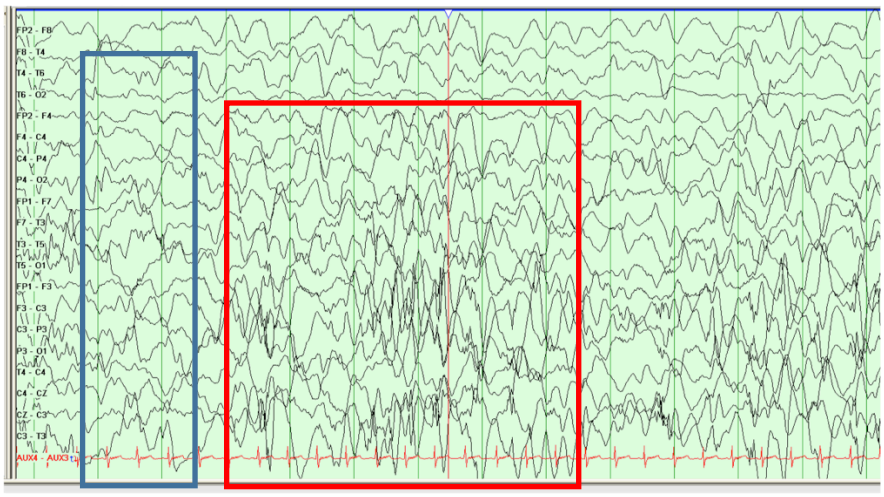

Figure 3-1 EEG recording reveals modified hypsarrhythmia at 2 months of age in Patient 9. The EEG reveals arrhythmic, high-amplitude, asynchronous delta activity with independent, multifocal spike discharges which is more prominent in the left sided electrodes than the right (red box). It is also interspersed by periods of lower-amplitude semirhythmic delta and theta activities (blue box). Adapted from McTague et al, Brain 2013;136:1578-91.

Ictal EEG was performed in all patients and captured either migrating ictal foci within the same seizure or closely overlapping seizures with differing sites of onset (**Figure 3-2).** The majority of seizures showed a characteristic pattern with one seizure dying out and another seemingly independent seizure starting in a different cortical location.

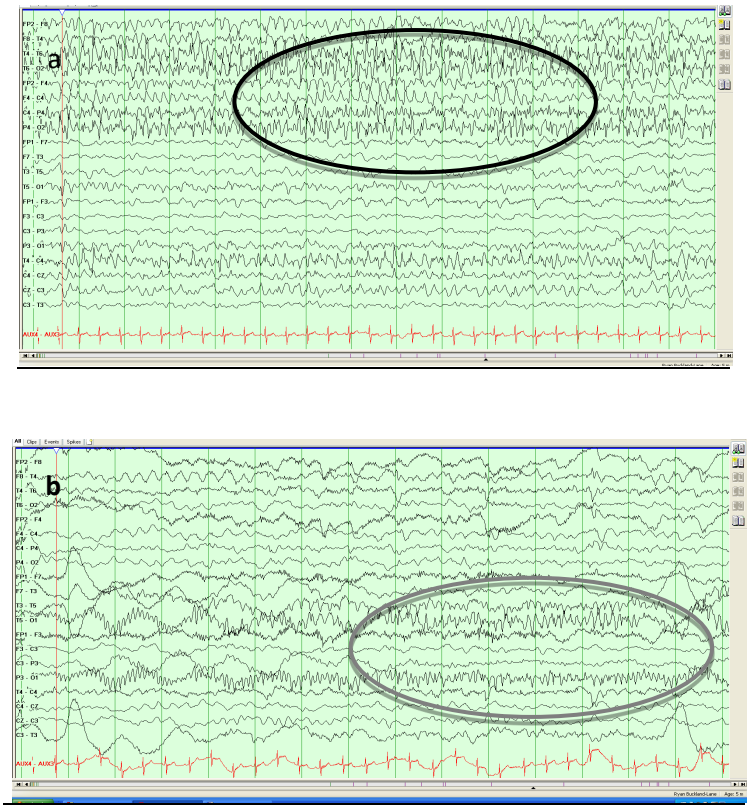

Figure 3-2 Migrating ictal foci at 5 months of age. 3.2a Rhythmic theta activity detected in the right temporo-parietal electrodes (black oval). **3.2b** The right temporo-parietal activity wanes, as similar theta activity begins independently in the left temporo-parietal electrodes (grey circle). (Adapted from McTague et al, Brain 2013;136:1578-91.).

3.2.2.4 Radiological features

MRI and MRS data were reviewed by me with expert input from Dr Shivaram Avula, Consultant Radiologist, Alder Hey Children's Hospital. Six of the fourteen patients had normal brain magnetic resonance imaging (MRI); however, five of these only had a single scan with the latest performed at five months of age. One patient did have two normal scans but again the last scan was undertaken at only five months of age. Of the eight patients who had abnormal cranial imaging, the initial scan was normal in four. The most frequently identified abnormality was cerebral atrophy, detected in seven patients. The

earliest age at which this abnormality was identified was four months (range four to 42 months). Delayed myelination with increased T2 signal in the white matter was seen in four patients (**Figure 3-3**).

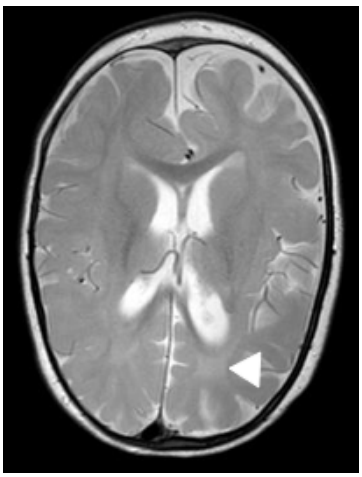

Figure 3-3 Axial T2 weighted MRI at 16 months of age. Relative hyperintensity of the deep white matter (white arrowhead) is suggestive of delayed myelination. Adapted from McTague et al, *Brain* 2013;136:1578-91.

Lastly in Patient 7, abnormal bilateral increased signal in the putamen and caudate nuclei was seen accompanied by cerebral atrophy (**Figure 3-4**). Comprehensive metabolic investigations and an autopsy were unrevealing in this patient (see below). Magnetic resonance spectroscopy (MRS) was performed in four patients. In three patients, a reduced N-acetyl aspartate (NAA) peak relative to the choline and creatine peaks was seen, in keeping with delayed neuronal maturation (**Figure 3-5**).

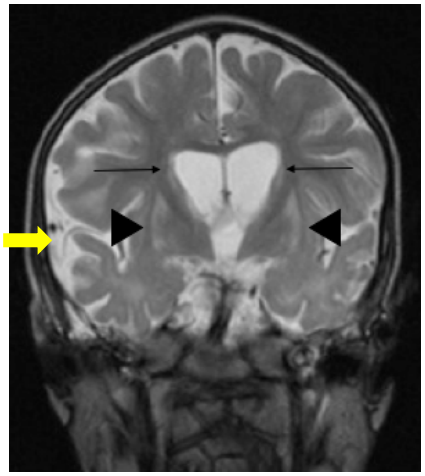

Figure 3-4 T2 weighted MRI at 39 months of age. Bilateral symmetrical signal abnormality of putamen (black arrowheads) and caudate (black arrows) is seen in addition to cerebral atrophy, indicated by increased extra-axial spaces (yellow arrow). Adapted from McTague et al, *Brain* 2013;136:1578-91.

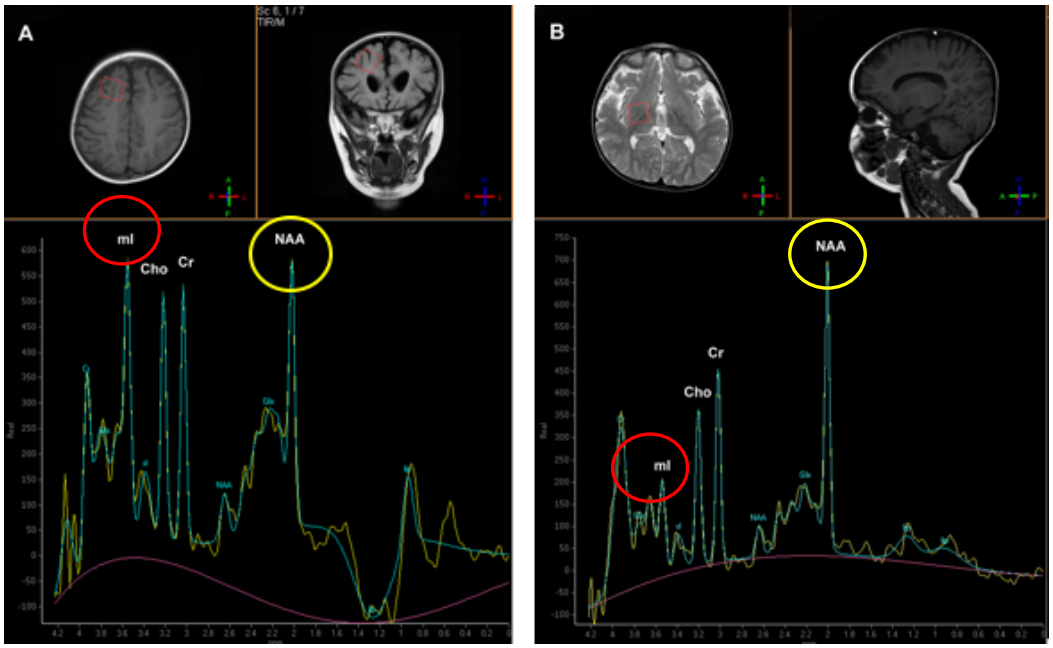

Figure 3-5 Single voxel MRS: (A) MRS at 24 months of age demonstrating a relatively high myoinositol (mI) peak (red circle) and a relatively low NAA peak (circled in yellow) in relation to the creatine (Cr) and choline (Cho) peaks signifying immaturity. (B) For comparison, MRS obtained with similar acquisition parameters of a normal 24 month old child is shown with mI peak (red circle) much lower than the NAA peak (yellow circle). Adapted from McTague et al, *Brain* 2013;136:1578-91.

3.2.2.5 Pathological features

Two patients from the cohort underwent post mortem (PM). Post-mortem data were reviewed by two consultant neuropathologists, Dr Michael A Farrell, Beaumont Hospital, Dublin and Dr Thomas Jacques, Great Ormond Street Hospital for Children. Patient 12 died of respiratory failure at nine months of age. On PM there was bilateral hippocampal gliosis with neuronal loss in the CA4 regions bilaterally and areas of granule cell dispersion in the dentate gyri. There was some minor extension into CA3 but CA2 and CA1 were well-preserved (**Figure 3-6**). Patient 7 died at 54 months due to respiratory complications. As seen in Patient 12, there was again bilateral hippocampal sclerosis in CA4 and CA3 and also in CA1 (**Figure 3-7)**. In addition, there was striking bilateral putaminal atrophy with marked neuronal loss and gliotic changes, also seen to a lesser degree in the caudate nucleus (**Figure 3-8**).

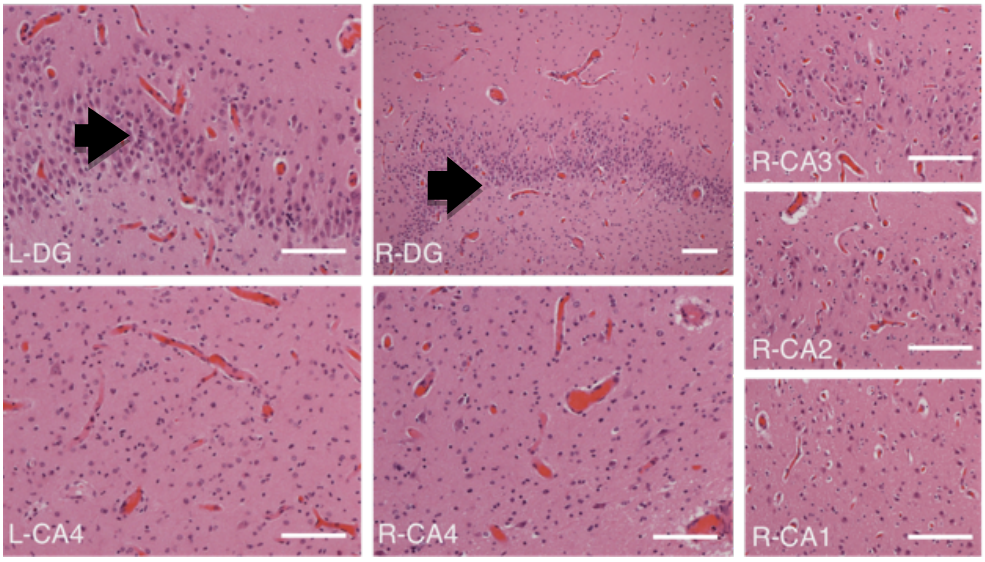

Figure 3-6 Hippocampal sections from Patient 12 revealing a pattern of hippocampal sclerosis. Right and left CA4 layers show depletion of neurones and end folial sclerosis. R-DG (right dentate gyrus) and L-DG (left dentate gyrus) have an extra band of cells (black arrows) due to granule cell dispersion by proliferation of glial cells. Right CA2/CA1 normal (see R-CA3. R-CA2 and R-CA1). Adapted from McTague et al, *Brain* 2013;136:1578-91.

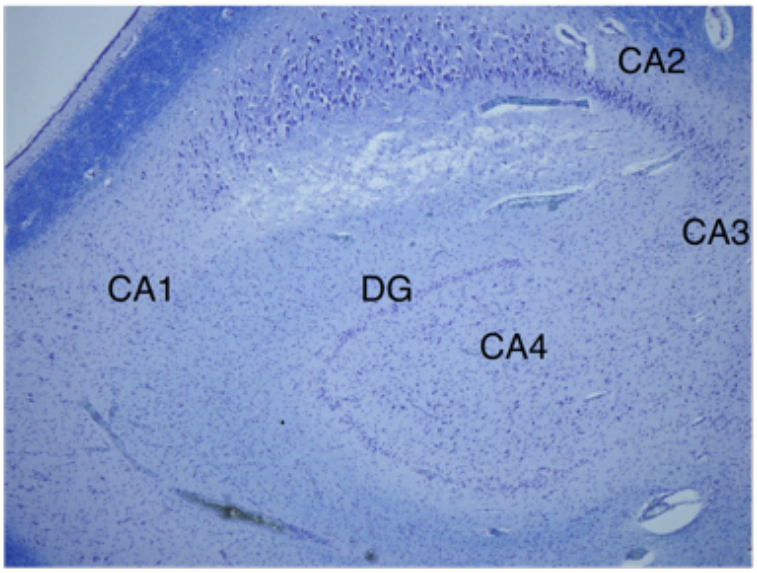

Figure 3-7 CA3, CA4 layers and dentate gyrus of hippocampus from Patient 7. Evidence of cell depletion consistent with a form of hippocampal sclerosis. Adapted from McTague et al, *Brain* 2013;136:1578-91.

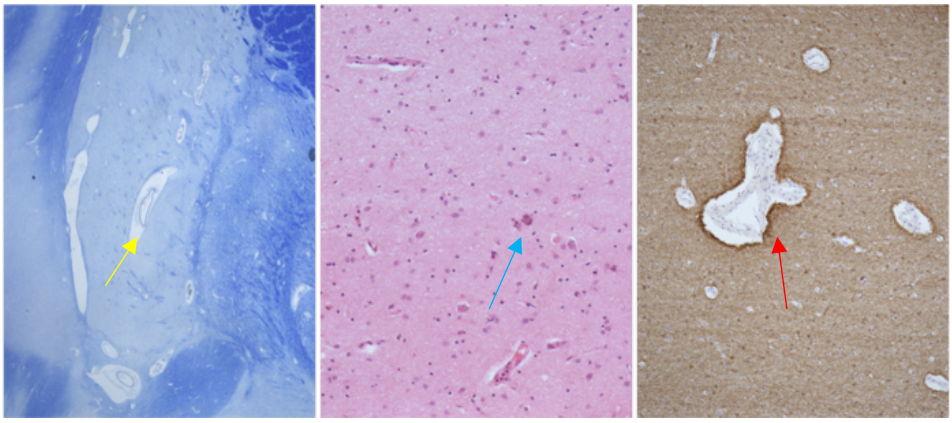

Figure 3-8 Abnormal putaminal findings in Patient 7. 7a: Large perivascular spaces (yellow arrow) (Luxol Fast Blue/Nissl). **7b:** Neuronal depletion and gliosis with focal calcification as indicated by deep purple staining (blue arrow) (Hematoxylin and eosin). **7c:** Glial fibrillary acidic protein stain reveals astrocytosis (red arrow). Adapted from McTague et al, *Brain* 2013;136:1578-91.

3.2.2.6 Other investigations

As part of their diagnostic work-up, all patients had comprehensive metabolic testing including muscle biopsies in seven patients. Three of these were abnormal with slightly low

Complex I levels (Patients 6, 7 and 9). A number of patients had targeted single gene testing and comparative genomic hybridization (CGH) micro-array performed (**Table 3.1**). In addition, six patients underwent testing with a multiple gene next generation sequencing (NGS) panel. None of these investigations revealed a genetic diagnosis.

		1	2	3	4	5	6	7	8	9	10	11	12	13	14
Single gene testing	***ARX***	-	N	-	-	-	-	N	N	-	-	-	-	-	-
	CDKL5	-	N	N	-	-	N	N	-	-	-	-	-	-	-
	SCN1A	N	N	N	N	-	-	N	N	N	N	N	N	-	-
	MECP2	N	N	N	N	-	-	N	-	-	-	-	-	-	-
	SLC25A22	-	-	-	-	-	-	N	-	-	-	-	-	-	-
	PLCB1	-	-	-	-	-	-	N	-	-	-	-	-	-	-
	SLC2A1	N	-	-	-	-	-	N	-	-	-	-	-	-	-
	STXBP1	-	-	-	-	-	N	-	-	-	-	-	-	-	-
CGH micro-array		-	-	-	-	-	N	N	N	N	-	N	-	N	-
Multiple NGS gene panel including exon-level CGH*		-	-	-	-	-	N	N	N	N	-	-	N	N	-

Table 3.1 Molecular genetic investigation of BPNSU cohort

- Investigation not undertaken,

N Negative (no abnormality identified),

* *CDKL5*, *MECP2*, *ARX*, *ATRX*, *SLC9A6*, *SLC16A2*, *ADSL*, *CNTNAP2*, *NRXN1*, *PNKP*, *KIAA1279*, *UBE3A*, *EHMT1*, *FOXG1*, *MEF2C*, *SIP1*, *ZEB2*, *TCF4*, *STXBP1*, *SLC25A22*, *PCDH19*, *SCN1A*, *PLCB1*, *SPTAN1*, *KCNQ2*, *ARHGEF9*, *SCN2A*, *MAGI2*.

CGH Comparative genomic hybridization

Adapted from McTague et al*, Brain* 2013;136:1578-91.

.

3.3 Further expansion of the clinical cohort

Following the completion of the BPNSU study in 2010, clinicians from both the UK and overseas continued to refer patients with EIMFS. From 2010-2016, a further twenty patients were ascertained, yielding a total cohort of 34 patients recruited for research molecular genetic investigations. Written informed consent was obtained, and clinical information was gathered. Original EEG data and MRI brain imaging were reviewed where possible. My strategy for molecular genetic investigation is described in Chapters 4 and 5. Overall a monogenic aetiology was identified in 16/29 (55%) patients (**Table 6.1**, Chapters 4, 5, 6).

3.4 Discussion

At the time of the BPNSU study there had been 100 published cases describing patients with EIMFS. My study was the first attempt to establish the prevalence and incidence of EIMFS. A rare disease is defined by the European Union as affecting less than 5 per 10,000 of the general population (http://www.raredisease.org.uk). Therefore, the estimated prevalence and incidence would be in keeping with EIMFS being a rare disorder.

This study has a number of limitations in epidemiological terms. Firstly, this may not be a true population-based estimate as only one method of data capture was employed. Secondly, only 68.4% of BPNA members responded, so it is possible that not all EIMFS cases were reported during the time period of the BPNSU study. Thirdly, there may have been patients presenting to clinicians who were not members of the BPNA and hence not reported through this surveillance study. This is unlikely, given the complexity and severity of this condition. Since the findings of this study were published (McTague et al. 2013), a further twenty-six papers have been published, with a total of 173 EIMFS patients with a clinical diagnosis of EIMFS now described (Coppola et al. 1995; Okuda et al. 2000; Wilmshurst et al. 2000; Gross-Tsur et al. 2004; Marsh et al. 2005; Coppola et al. 2007; Coppola et al. 2006; Hmaimess et al. 2006; Hahn et al. 2007; Jocic-Jakubi & Lagae 2008; Caraballo et al. 2008; Cilio et al. 2009; Nabatame et al. 2010; Djuric et al. 2011; Vendrame et al. 2011; Freilich et al. 2011; Gilhuis et al. 2011; Irahara et al. 2011; Carranza Rojo et al. 2011; Sharma et al. 2011; Lee et al. 2012; Fasulo et al. 2012; Chien et al. 2012; Poduri,

Chopra, et al. 2012; Barcia et al. 2012; Merdariu et al. 2013; Milh et al. 2013; Ünver et al. 2013; Dhamija et al. 2013; Ishii et al. 2013; De Filippo et al. 2014; Shimada et al. 2014; Poduri et al. 2013; Ohba et al. 2014; Bearden et al. 2014; Caraballo et al. 2014; Iyer et al. 2014; Selioutski et al. 2015; Saade & Joshi 2015; Caraballo et al. 2015; Ohba et al. 2015; Møller et al. 2015; Howell et al. 2015; Stödberg et al. 2015; Mikati et al. 2015; Rizzo et al. 2016b; Mori et al. 2016; Barba et al. 2016; Saitsu et al. 2016; Need et al. 2012; Appavu et al. 2016; Caraballo et al. 2016; Segal et al. 2014; Bedoyan et al. 2010; Veneselli et al. 2001). I will now discuss the clinical features of EIMFS as revealed in the BPNSU study in relation to the current literature (**Table 3.2**).

The most frequently reported initial seizure types in the BPNSU series were focal motor seizures, accompanied by head and eye deviation. This was also borne out in the published cases where 78% presented with focal motor seizures at onset (**Table 3.2)**. In the remaining patients, subtle seizures with behavioural arrest, apnoea and cyanosis or generalised tonic or tonic-clonic seizures are seen. Over time, all patients in the BPNSU study developed focal motor seizures, as reported in the literature (**Table 3.2**). However, many infants with EIMFS may also manifest subtle seizures which are barely noticeable clinically, as is the case in other neonatal epilepsies (Plouin & Kaminska 2013).

Clinically migratory seizures, defined as focal motor seizures affecting alternating sides of the body were not seen at onset but later developed in approximately half of our study patients. In the cases reported to date, alternating focal motor seizures were reported in 44.5% of patients. Although this is not a pathognomonic feature, it would be strongly suggestive of EIMFS, although differential diagnoses include alternating clonic seizures in self-limited familial and non-familial neonatal epilepsies (previously known as benign familial/non-familial neonatal seizures) (Panayiotopoulos 2005).

Autonomic features such as facial flushing, salivation, apneas and cyanosis were seen in the majority of the patients on our study. However, only 50.3% of reported cases describe autonomic features (**Table 3.2**). I actively sought the presence of autonomic features in my BPNSU cohort, through direct questions in my proforma (see Appendix). I found the most commonly reported autonomic features to be facial flushing followed by hypersalivation, whereas apnoea and cyanosis are most frequently described in the literature (**Table 3.2**). Autonomic seizures are a well-described feature of neonatal epilepsies due to diverse

aetiologies, including self-limited familial and non-familial neonatal and infantile epilepsies (Panayiotopoulos 2005) and temporal lobe seizures in older patients (Jan 2007).

I also identified two EIMFS patients with infantile spasms associated with hypsarrhythmia. There are now 14 reported cases of infantile spasms in patients with EIMFS, of which four manifest the EEG correlate of hypsarrhythmia (Coppola et al. 1995; Jocic-Jakubi & Lagae 2008; Carranza Rojo et al. 2011; Lee et al. 2012; Chien et al. 2012; Caraballo et al. 2015). As in our study, infantile spasms have emerged either prior to or after the onset of EIMFS. Indeed, one patient presented with early myoclonic encephalopathy associated with typical burst suppression on EEG, followed by an EIMFS phenotype which then developed into infantile spasms with hypsarrhythmia (Chien et al. 2012). This observation may reflect the age-dependent manifestation of the underlying epilepsy aetiology, as is well-documented in the evolution from Ohtahara syndrome to West syndrome (Ohtahara & Yamatogi 2006a).

The natural history of EIMFS appears to fall into a continuum of three phases. As illustrated by the BPNSU study, the early stage is characterised by the onset of seizures at a median of seven weeks (range: 4 days to 5 months), similar to that observed in published cases (median age of onset 8.5 weeks, mean 6.6 weeks, range one day to nine months of age) (**Table 3.2**). Of note there are four cases reported with disease onset at greater than six months but these were accepted as EIMFS as they met the remainder of the diagnostic criteria (Coppola et al. 1995; Barcia et al. 2012; De Filippo et al. 2014). Phase two of disease is typically characterised by a stormy period with increasing seizure frequency to a peak seizure frequency at a median of 16 weeks of age (range: 1 to 40 weeks) with up to 200 seizures per day. Infants develop either a form of focal status epilepticus or frequent clusters of focal seizures. In the third phase, for many patients there is a reduction of seizures with time, leading to either survival with continuing but less frequent seizures or death. Of the reported cases, 25 have died at between five months and six years of age. This is likely to be an underestimate as the majority of published papers are single case reports or case series rather than longitudinal or cohort studies. SUDEP is uncommon in the literature with four cases reported (Hmaimess et al. 2006; Fasulo et al. 2012; Milh et al. 2013). The remainder of patients die of respiratory failure, infection, status epilepticus or unstated causes.

As we reported, the developmental outcome is extremely poor for EIMFS, with all but ten of the 186 cases published to date displaying severe developmental delay. However, six of the reported patients have achieved independent ambulation (Coppola et al. 1995; Marsh et al. 2005; Carranza Rojo et al. 2011; Howell et al. 2015) with normal development before and after seizures in one patient (Howell et al. 2015). Unfortunately, in general the best developmental stage achieved for most patients is rolling and visual fixation, although some patients regain developmental milestones following periods of good seizure control (Merdariu et al. 2013; Bearden et al. 2014; Caraballo et al. 2015; Mikati et al. 2015; Mori et al. 2016).

The BPNSU study also highlighted the presence of non-epileptic abnormal movements in EIMFS. A spectrum of movement disorders has now been reported in 19 EIMFS patients (**Table 3.2**) with dystonia in seven patients and choreoathetosis in five (Coppola et al. 1995; Hahn et al. 2007; Cilio et al. 2009; Caraballo et al. 2008; Møller, Heron, et al. 2015; Ohba et al. 2014; Ohba et al. 2015; Howell et al. 2015; Barba et al. 2016). Non-epileptic movement disorders are increasingly recognized in a number of early onset epileptic encephalopathies due to genetic abnormalities, as will be discussed further in Chapter 4.

The BPNSU study revealed both typical and unusual EEG findings in the EIMFS cohort. Inter-ictal EEG can be normal initially but slowing of the background with multi-focal abnormalities emerge over time. Ictal discharges are often of theta or alpha frequency and are located in the centro-temporal or temporo-occipital regions initially. In general there is good electro-clinical correlation with head and eye deviation and eye jerking associated with occipital discharges, focal tonic seizures associated with contralateral frontal EEG discharges, rolandic changes with contralateral limb clonic seizures and behavioural arrest and oral automatisms associated with temporal involvement (Coppola et al. 1995; Caraballo et al. 2008). The characteristic migrating ictal focus, where seizure onset will appear in one area of the cortex and then wane as independent discharges commence in another region (commonly the contralateral hemisphere), may take some time to emerge. Although this characteristic EEG appearance is required for the diagnosis of EIMFS, migration of ictal foci is described in other neonatal epilepsies, particularly self-limited familial neonatal seizures (Wilmshurst et al. 2000). This may be an aetiology-related phenomenon, as interestingly, mutations of *SCN2A* have been identified in both of these epilepsies. Fast intra-ictal activation may also be seen in infants with neonatal seizures due to a wide range of causes including hypoxic ischaemic encephalopathy (Alix et al. 2016).

The pathophysiology of these migrating ictal discharges is unclear. Some have postulated that they reflect an abnormally excitable cortex resulting in multifocal discharges. Another explanation could be a deficit of interhemispheric inhibition normally mediated by transcallosal pathways (Freilich et al. 2011). The occurrence of EIMFS in a patient with Aicardi syndrome and an absent corpus callosum might lend weight to this theory (Jocic-Jakubi & Lagae 2008) but further study is needed.

Our study also identified hypsarrhythmia, electrodecrement and periods of EEG suppression. These are classically features of West syndrome and Ohtahara syndrome respectively and again are likely to reflect the continuum of age-related electroclinical manifestations of cerebral dysfunction.

The most commonly reported abnormality on MR imaging of the brain is cerebral atrophy, seen in 41.6% of reported cases. The BPNSU study also identified delayed myelination and white matter hyperintensity, which has since been noted in further published cases. It has been postulated that the cerebral atrophy may result from excitotoxic damage to the developing brain due to excessive glutamatergic neurotransmitter activity (Gross-Tsur, Varda, Ben-Zeev, Bruria, Shalev, Ruth S 2004). However, another possibility is a failure of normal brain development and growth. This would be supported by the abnormally delayed myelination seen in our patients and other reported cases, as well as the acquired microcephaly that is frequently seen in EIMFS. We found MRS changes in our patients, also in keeping with delayed myelin development and brain maturation as similarly reported in three other cases (Gross-Tsur, Varda, Ben-Zeev, Bruria, Shalev, Ruth S 2004; Cilio et al. 2009; Freilich et al. 2011) although MRS was normal in three other studies (Poduri, Chopra, et al. 2012; Chien et al. 2012; Dhamija et al. 2013). The basal ganglia changes identified in one of our patients are unusual. Recently, eight of 12 EIMFS patients with de novo *SCN2A* mutations were reported to have a variety of basal ganglia abnormalities on MR imaging, including basal ganglia swelling and T1 and T2 hyperintensities of basal ganglia and thalami (Howell et al. 2015). These resolved in one patient with time, but were persistent in the remainder. Of note Patient 7 was not found to have pathogenic variants of *SCN2A* on whole exome sequencing.

The treatment of EIMFS is extremely difficult. In our study one of the more effective treatments was the ketogenic diet. This has been used in 32 of the reported patients, was partially effective in 13 and led to seizure freedom in one patient (Caraballo et al. 2015).

Potassium bromide or triple bromides were found to be effective in 16 patients, with three patients becoming seizure free (Fasulo et al. 2012; Ünver et al. 2013; Caraballo et al. 2014). However significant side effects including bromoderma and excessive sedation were seen in two patients (Nabatame et al. 2010; Mori et al. 2016). A wide range of standard antiepileptic medications in various combinations have been reported to be useful in EIMFS including levetiracetam, rufinamide, stiripentol and clonazepam. Most recently cannabinoids have been used with some effect in one patient (Saade & Joshi 2015). However, although new treatments may result in early reductions in seizure burden, a lack of longitudinal data means that it is difficult to judge the efficacy of these interventions on long-term seizure control and outcome.

Post-mortem data on EIMFS is reported for five patients reported in the literature. In the original case series, Coppola described neuronal loss and gliosis in the hippocampal CA1 region in two patients (Coppola et al. 1995). Microcephaly and low brain weight was noted in another patient (Hahn et al. 2007) with a normal post-mortem examination in the fourth patient (Wilmshurst et al. 2000). Fasulo *et al* described several different types of cortical malformation in one patient, with polymicrogyria, microscopic cortical features consistent with focal cortical dysplasia and neuronal loss in CA1, CA3 and CA4 in keeping with hippocampal sclerosis (Fasulo et al. 2012). Bilateral hippocampal damage was seen in both patients from the BPNSU study who underwent autopsy. It is unclear whether these changes are secondary to the extremely frequent focal seizures or whether there may be a pre-existing developmental brain malformation. Indeed, one patient displayed left temporal lobe atrophy, hippocampal sclerosis and cortical-subcortical blurring on MRI imaging (Coppola et al. 2007). However, this is an unusual case and the majority of patients do not have focal MRI abnormalities. One patient in the BPNSU study had evidence of marked putaminal injury. This patient underwent extensive metabolic testing including muscle and skin biopsies which were unrevealing.

	BPNSU cohort	**Published cases 1995-2017**
Mean/median age and age range at disease onset (weeks)	10/7, range 4-20	7/9, range 0.1-36
Mean/median age and age range at peak seizure frequency (weeks)	38/20, range 3-150*	17/16, range 1-40
Number of seizures at peak	9-150	1-200
Focal motor seizures at onset (%)	15 (100)	135 (78)
Generalized tonic-clonic seizures (%)	9 (65)	20 (12)
Head and eye deviation (%)	6 (43)	105 (61)
Clinically migrating seizures (%)	8 (57)	77 (50)
Epileptic spasms	2	7
Autonomic features (%)	12 (86)	87 (50)
Apnoea/cyanosis	2	73
Facial flushing	9	57
Lacrimation	1	4
Tachycardia	0	2
Salivation	3	9
Chewing	0	2
Hyperthermia	0	2
Hyperventilation	0	1
Movement disorder (%)	4 (28)	19 (7)
Choreoathetosis	1	5
Dystonia	2	7
Ataxia	0	2
Myoclonus	0	1
Tremor	0	2
Dyskinesia	1	0
Hypotonia (%)	8 (57)	117 (42)
Increased tone/spasticity	3	31
Developed cerebral atrophy on MRI	7	72
Deaths	8	25
SUDEP	0	4

Table 3.2 Clinical Features of the BPNSU cohort in comparison to 173 reported patients with EIMFS. *in those whose seizures reduced with time, median age of peak seizure frequency was 16 weeks (range 3 weeks to 1 year).

When EIMFS was first described, the aetiology was largely unknown and possible metabolic, structural and genetic aetiologies were considered. In general, extensive metabolic investigations of patients described to date have been unrevealing. However, recently four patients with congenital disorder of glycosylation Type 1 (CDG-I) were described (Barba et al. 2016). They presented with the electroclinical features of EIMFS in addition to a spectrum of multi-systemic involvement including gastro-intestinal problems, coagulopathy, dysmorphic facial features and a spastic quadriparesis. MRI brain revealed cerebellar atrophy in all four patients, with brainstem atrophy in three. Transferrin isoelectric focussing (TIEF) testing was consistent with CDG-I. Although the remaining 12 patients of this CDG-I cohort did not manifest the clinical features of EIMFS, it would be prudent to consider testing TIEF in patients presenting with EIMFS, particularly in those with multisystemic features and cerebellar atrophy on MRI. The specific association of CDG-I with EIMFS is interesting and further research may provide insights into EIMFS pathogenesis. In general, MRI imaging has not revealed structural abnormalities other than in one case as described above (Coppola et al. 2007). Whilst structural abnormalities are often reported in other electroclinical syndromes such as Ohtahara's syndrome (Ohtahara & Yamatogi 2006b), there is no convincing evidence for an underlying structural aetiology in EIMFS patients.

The first evidence for a possible genetic basis for EIMFS came from the finding of a patient with a 16p11.2 duplication, previously associated with autism and epilepsy (Bedoyan et al. 2010). This finding has not been replicated in other EIMFS patients. Furthermore, mutations in genes within this duplicated region have not been reported in EIMFS. Although *PRRT2* was within the duplicated region, the associated infantile convulsions with choreoathetosis (ICCA) phenotype differs from the reported clinical features and is also due to haploinsufficiency (Ebrahimi-Fakhari et al. 2015). Therefore, the relevance of this duplication is unclear. With the recent explosion in genetic discovery for the early onset epilepsies, the genetic basis of EIMFS has now begun to emerge and will be further explored in Chapters 4 and 5.

In conclusion, EIMFS is a rare electroclinical syndrome characterised by onset of frequent focal seizures in the first six months of life associated with migrating ictal EEG foci, evolving into a severe epileptic and developmental encephalopathy. As demonstrated by both the BPNSU study and the reported cases, typical and atypical features are seen, possibly representing overlap with other severe electroclinical syndromes such as Ohtahara and

West syndromes. Other than the ketogenic diet, response to treatment is poor. It should be noted that the accumulated knowledge on EIMFS is based on single case reports or small series. The BPNSU study represents a national cohort of patients, but to fully understand the natural history, evolution of seizure disorder and developmental trajectory, longitudinal data is required. This would necessitate an international patient registry collecting prospective patient data following a diagnosis of EIMFS, which could be achieved by collaboration between national and international epilepsy or rare disease networks. In addition, a longitudinal study with serial EEGs could further delineate the evolution of the ictal and inter-ictal abnormalities. This data would be essential to future assessment of the effevts of novel therapies on both sezure frequency and developmental outcomes. As with other electroclinical syndromes, EIMFS likely represents the age-related manifestation of a range of aetiologies, although these are most likely to be mainly genetic in origin, rather than underlying metabolic or structural causes. Further investigation of the aetiology of EIMFS is essential to understand to attempt to understand disease mechanisms amd how these disparate aetiologies may result in a similar phenotype, and this will now be explored in the remainder of this thesis.

Chapter 4 Heterozygous mutations of *KCNT1* in Epilepsy of Infancy with Migrating Focal Seizures

4.1 Introduction

In 2012, autosomal dominant gain of function mutations of *KCNT1* were identified in patients with EIMFS (Barcia et al. 2012). *KCNT1*, also known as KCa4.1, SLACK (sequence like a calcium-dependent potassium channel) and Slo2.2, encodes the sodium-activated potassium channel responsible for slow hyper-polarisation following action potential generation (Kaczmarek 2013). Mutations of *KCNT1* have since been identified in a wide spectrum of epileptic disorders.

In order to investigate *KCNT1*-related epilepsy in my expanded EIMFS cohort, I sought to undertake (i) deep endophenotyping to delineate the salient clinical features and (ii) molecular genetic investigations by Sanger sequencing of *KCNT1* in the research laboratory.

4.2 Methodology

4.2.1 Patient recruitment:

Following the BPNSU study during which 14 patients were ascertained, I recruited a further 20 patients to a research study, resulting in an EIMFS cohort of 34 patients (Chapter 3). 28 of the total EIMFS cohort (n=34), including 9 from the BPNSU study, were tested for mutations in *KCNT1* using a variety of different genetic approaches. I undertook direct Sanger sequencing in the research laboratory. NGS multiple gene panel and diagnostic microarray and karyotype were taken in local diagnostic molecular genetic laboratories. Whole exome sequencing was undertaken at Duke University and I analysed the data as described below (**Table 4.1**, Patients 1,3, 6-9, 11-13, 15-32, 34). Of the remaining unscreened six cases, one (Patient 33) was the similarly affected sibling of Patient 32; this sibship is further discussed in Chapter 5. For the other 5 patients, either DNA was not available for the proband, or parents did not consent to further genetic investigations

(**Table 4.1**). Written informed consent was obtained from families in whom research genetic investigations were undertaken. The study was approved by the National Research Ethics Service (NRES) (London – Bloomsbury, REC reference: 13/LO/0168, IRAS project ID: 95005). In order to better understand genotype-phenotype correlations in *KCNT1*-related epilepsy, two additional patients with non-EIMFS presentations (EOEE1 and 2, Table 4.1) in whom a *KCNT1* mutation was identified on routine local diagnostic multiple gene panel testing (n=2) were also included in this study. Anonymised data from patients tested on the diagnostic NGS panel (n=2) was collected as part of an approved case note review project (Great Ormond Street Hospital Research and Development Department, 16NM11).

EIMFS Cohort Patient No	Phenotype	Screening Method			Diagnostic chromosomal microarray	Diagnostic karyotype
		Research-based Sanger sequencing	NGS Diagnostic Panel*	WES		
1	EIMFS	+	-	+	-	N
2	EIMFS	No DNA				
3	EIMFS	+	-	+	-	N
4	EIMFS	No DNA				
5	EIMFS	No DNA				
6	EIMFS	+	-	-	N	-
7	EIMFS	+	-	+	N	-
8	EIMFS	+	-	-	N	-
9	EIMFS	+	-	+	N	-
10	EIMFS	No DNA				
11	EIMFS	+	-	-	N	-
12	EIMFS	+	-	-	-	N
13	EIMFS	+	-	+	N	-
14	EIMFS	Parents did not consent to further testing				
15	EIMFS	+	+	-	-	-
16	EIMFS	+	-	-	-	N
17	EIMFS	+	-	-	N	-
18	EIMFS	-	+	-	N	-
19	EIMFS	+	-	-	N	-
20	EIMFS	-	+	-	N	-
21	EIMFS	-	+	-	N	-
22	EIMFS	+	-	-	N	-
23	EIMFS	+	-	-	N	-
24	EIMFS	+	-	-	N	-
25	EIMFS	+	-	-	N	-
26	EIMFS	+	-	-	N	-
27	EIMFS	+	-	-	N	-

28	EIMFS	+	+	-	11.8 Mb heterozygous deletion Chr 20q11 copy number variant of uncertain significance	-
29	EIMFS	-	+	-	N	-
30	EIMFS	-	+	-	N	-
31	EIMFS	-	+	-	N	
32	EIMFS	-	-	+	N	
33#	EIMFS	-	-	-	N	-
34	EIMFS	-	-	+	N	-
EOEE1	NFLE-like	-	+	-	2.4Mb heterozygous duplication Chr 15q14 Inherited from mother	-
EOEE2	NFLE-like	-	+	-	N	-

Table 4.1 Summary of genetic investigation for *KCNT1* mutations in the EIMFS cohort and in two patients with early onset epilepsy. EIMFS epilepsy of infancy with migrating focal seizures, N normal, NFLE nocturnal frontal lobe epilepsy, NGS next generation sequencing, WES whole exome sequencing. * Patients 6-9, 12 and 13 had NGS panel testing which did not include *KCNT1* (Table 3.1). # Patient 33 had direct sequencing of *SLC12A5* only as he is the affected sibling of Patient 32 (Chapter 5).

4.2.2 PCR sequencing

All annotations are as described in the NCBI GRCh37.p13 build. The DNA template for the longest protein-coding transcript of *KCNT1* (ENST00000298480.5) located at Chromosome 9: 138,594,031–138,684,992 was obtained from the Ensembl genome browser. Primer3 (http://fokker.wi.mit.edu/primer3/input.html) was used to design primers (as described in **Methods 2.3.3**) to cover all exons and exon-intron boundaries of *KCNT1*, ensuring coverage across all nine protein-coding transcripts (**Table 4.2**). Where Primer3 could not successfully generate an appropriate oligonucleotide, primers were designed manually.

Transcript number									Primer	Primer Sequence	Annealing temperature ^{0}C	GC rich solution	Product size
202	002	001	201	004	005	007	006	010					
1F	1F	1F							1F	aacgcgagggaagaaggt	60	-	243
1R	1R	1R							1R	ggaacttgggggtcttaggt			
			1bF	1bF	1bF		1bF		1bF	cgggtgcttgaaccttctc	58	-	499
			1bR	1bR	1bR		1bR		1bR	gtgggcttaggaggggagac			
2F	2F					1F		1F	2dF	atgacagctcccgtccc	62	yes	585
2R	2R					1R		1R	2dR	gaagccgggaaaagttgaag			
			2bF		2bF	2bF	2bF		2bF	ccatctgtctgtctactgcc	58	-	215
			2bR		2bR	2bR	2bR		2bR	gctctcacacctctaagagc			
3F	3F	2F	3F	2F	3F	3F	3F	2F	3F	cagttggaaagttggaagaagtc	60	-	358
3R	3R	2R	3R	2R	3R	3R	3R	2R	3R	gtctcagacagtgtgaagctaag			
4F	4F	3F	4F	3F	4F	4F	4F	3F	4F	cagagagcccagccagac	60	-	346
4R	4R	3R	4R	3R	4R	4R	4R	3R	4R	ctttttccatcctgggacag			
5F	5F	4F	5F	4F	5F	5F	5F	4F	5F	cttgtctcccaggtgttagagct	60	-	552
5R	5R	4R	5R	4R	5R	5R	5R	4R	5R	aactggctgggaactcacaat			
6F	6F	5F	6F	5F	6F	6F	6F	5F	6F	agtggaggccaatggttatg	60	yes	396
6R	6R	5R	6R	5R	6R	6R	6R	5R	6R	gctcactgagttggagtcacc			
7F	7F	6F	7F	6F	7F	7F	7F	6F	7F	ctggctttgtgtggtacctg	60	yes	242
7R	7R	6R	7R	6R	7R	7R	7R	6R	7R	gagagggtgggggaggtg			
8F	8F	7F	8F	7F	8F	8F	8F	7F	8/9F	acttcccagcctcatccac	60	-	475
8R	8R	7R	8R	7R	8R	8R	8R	7R	8/9R	cggtcctctacaggtcatgc			
9F	9F	8F	9F	8F	9F	9F	9F	8F	8/9F	acttcccagcctcatccac	60	-	475

9R	9R	8R	9R	8R	9R	9R	9R	8R	8/9R	cggtcctctacaggtcatgc			
10F	10F	9F	10F	9F	10F	10F	10F	9F	10F	cgtctgctttccactgtcct	60	-	291
10R	10R	9R	10R	9R	10R	10R	10R	9R	10R	ccgatagcttggacataggc			
11F	11F	10F	11F	10F	11F	11F	11F	10F	11F	ctggtgatgcacagctcagt	62	-	378
11R	11R	10R	11R	10R	11R	11R	11R	10R	11R	agtggcaccctccctctact			
12F	12F	11F	12F	11F	12F	12F	12F		12F	ggcccctaacagacagtcg	60	-	400
12R	12R	11R	12R	11R	12R	12R	12R		12R	gaggcatctgccctcact			
13F	13F	12F	13F	12F	13F	13F	13F		13F	gtgggcacaaacacagtcc	60	-	287
13R	13R	12R	13R	12R	13R	13R	13R		13R	tgagcagccgacctgact			
14F	14F	13F	14F	13F	14F	14F	14F		14bF	ctccacccacgctcag	60	yes	179
14R	14R	13R	14R	13R	14R	14R	14R		14R	ggcaggtctcttccctcag			
15F	15F	14F	15F	14F	15F	15F	15F		15cF	agcccgtctgcact	58	yes	251
15R	15R	14R	15R	14R	15R	15R	15R		15bR	caccatcacccaacagcat			
16F	16F	15F	16F	15F	16F	16F	16F		16F	gcaccttcaggaagtgagca	60	-	294
16R	16R	15R	16R	15R	16R	16R	16R		16R	ctcctctgggaagcccatc			
17F	17F	16F	17F	16F	17F	17F	17F		17F	ggcaaaagtcctgcataggg	60	-	338
17R	17R	16R	17R	16R	17R	17R	17R		17R	gagggcacagagcagagc			
18F	18F	17F	18F	17F	18F	18F	18F		18bF	gactctggtgatttgcaggaa	60	-	384
18R	18R	17R	18R	17R	18R	18R	18R		18bR	ctggtctcccgccaaag			
19F	19F	18F	19F	18F	19F	19F	19F		19F	tcacctgagctctgggaact	60	-	394
19R	19R	18R	19R	18R	19R	19R	19R		19R	accaaggatgctccgacac			
20F	20F	19F	20F	19F	20F	20F	20F		20bF	tgtgcagctgtgctgag	59	-	220
20R	20R	19R	20R	19R	20R	20R	20R		20R	gagaaaccagggcaggtatg			
21F	21F	20F	21F	20F	21F	21F	21F		21F	gtggccagcaggaaccac	62	yes	288

21R	21R	20R	21R	20R	21R	21R	21R		21R	ctggctgcaggtctgagg			
22F	22F	21F	22F	21F	22F	22F	22F		22F	ctctgtgcatggagggtagg	60	-	234
22R	22R	21R	22R	21R	22R	22R	22R		22R	caccccagactttggaagag			
23F	23F	22F	23F	22F	23F	23F	23F		23F	gtcctgtgggtggggagt	60	-	238
23R	23R	22R	23R	22R	23R	23R	23R		23bR	gggcttgtggtcatagctg			
24F	24F	23F	24F	23F	24F	24F	24F		24cF	accctgagagtcccacagccatga	60	yes	234
24R	24R	23R	24R	23R	24R	24R	24R		24cR	tttccctgaccgcgtgtgaggcact			
25F	25F	24F	25F	24F	25F	25F	25F		25F	tgtacggtgcacacacagt	60	-	215
25R	25R	24R	25R	24R	25R	25R	25R		25R	ggagtcctatcattcagaac			
26F	26F	25F	26F	25F	26F	26F	26F		26fB	agaaaaggcctcccagaactctgcc	55	yes	332
26R	26R	25R	26R	25R	26R	26R	26R		26R	agagcctcctggccaccgtgaatca			
27F	27F	26F	27F	26F	27F	27F	27F		27bF	agccaactcagggttcc	60	-	381
27R	27R	26R	27R	26R	27R	27R	27R		27R	atctagcccaggtccctgac			
28F	28F	27F	28F	27F	28F	28F	28F		28F	ctaagcatgttccgtgcaga	60	-	189
28R	28R	27R	28R	27R	28R	28R	28R		28R	ctggcaggcttctccatgt			
29F	29F	28F	29F	28F	29F	29F	29F		29F	gagcccacacctcttcctaa	TD	-	566
29R	29R	28R	29R	28R	29R	29R	29R		29.2Rb	ccgactgttcttggctgtg			
30F	30F	29F	30F	29F	30F	30F	30F		30F	gcacctcgcttgctgatatt	60	-	241
30R	30R	29R	30R	29R	30R	30R	30R		30R	ctcacagctcctgtccacct			
31F	31F	30F	31F	30F	31F	31F	31F		31F	atgaggtgctggagcagaat	60	yes	299
31R	31R	30R	31R	30R	31R	31R	31R		31R	gtgcctgtggcctcatct			
32F		31F		31F	32F	32F	32F		32F	gggcactggggagatgag	60	-	293
32R		31R		31R	32R	32R	32R		32R	ctcctccacgtccttcctg			

Table 4.2 Primer coverage and PCR conditions for Sanger sequencing of *KCNT1*. TD touchdown PCR: 95^{0}C 5 minutes; 8 cycles of (95^{0}C 30 seconds, 60^{0}C 30 seconds, 72^{0}C 1 minute); 20 cycles of (95^{0}C 30 seconds, 60^{0}C 30 seconds [decreasing by 0.5^{0}C each cycle], 72^{0}C 1 minute); 15 cycles of (95^{0}C 30 seconds, 50^{0}C 30 seconds, 72^{0}C 1 minute); 72^{0}C 5 minutes

To optimize primer PCR conditions (see Chapter 2), I initially trialled primers with control DNA at 60^0C and a standard thermocycling regime of 95^0C for 5 minutes; 40 cycles of 95^0C for 45 seconds, 60^0C for 45 seconds 72^0C for 1 minute; followed by 72^0C for 5 minutes. These conditions were effective for the majority of the primer pairs but some required alterations in annealing temperature and/or use of a GC-rich reaction buffer (**Table 4.2**). Touchdown PCR (see **Methods 2.3.3**) was required for exon 29.

Following successful PCR amplification, I sequenced PCR products using the primers detailed in **Table 4.2** and the methods described in **Chapter 2.3.5**. I analysed sequencing data was analysed using Chromas (Technelysium Pty Ltd, Australia) or Sequencher (GeneCodes Corporation, USA) software.

4.2.3 Next generation sequencing panel

Eight patients from the EIMFS cohort and two patients with EOEE (**Table 4.1**) were tested for *KCNT1* mutations by the Great Ormond Street Hospital Regional Genetics laboratory using their in-house diagnostic next generation sequencing panel (see Appendix).

4.2.4 Whole exome sequencing

Whole exome sequencing was performed in collaboration with Professor Ann Poduri, Harvard Medical School, Boston, USA and Dr Erin Heinzen, Duke University, North Carolina, USA (see Appendix). I then took a candidate gene approach to interrogate the filtered data for mutations in previously reported EIMFS genes (**Table 1.2**).

4.2.5 Protein homology modelling

In order to better understand the effects of mutant KCNT1 on protein structure-function properties, protein homology modelling was undertaken by Dr Maya Topf and Dr Sony Malhotra from the Institute of Structural and Molecular Biology, Birkbeck College, University of London, UK (see Appendix).

4.2.6 Electrophysiology in a xenopus oocyte model

In order to investigate the effects of mutant KCNT1 on potassium channel function, electrophysiology experiments were undertaken by Dr Umesh Nair and Dr Steve Petrou, Florey Institute of Neuroscience and Mental Health, Melbourne, Australia. Methods are described in detail in the Appendix. In brief, variants were introduced into a wild-type human KCNT1 expression construct using in situ mutagenesis. *Xenopus laevis* oocytes were transfected with either wild type or mutant cRNA and whole cell patch clamping performed, both before and after the application of Quinidine. Of note, KCNT1 subunits form either homotetramers, or heterotetramers with KCNT2 in vivo. As xenopus oocytes do not have endogenous KCNT1 or KCNT2 expression, it expected that channels formed in this over-expression system would be KCNT1 homotetramers.

4.3 Results

Of the 30 patients tested, heterozygous *KCNT1* mutations were identified in 12. Five were detected through direct Sanger sequencing alone, two on whole exome sequencing and five from the Great Ormond Street Hospital diagnostic multiple gene panel. Of note in the two patients diagnosed by WES and in one of the panel diagnosed patients, Sanger sequencing of the entire *KCNT1* gene was also performed (**Table 4.1**).

4.3.1 Clinical features of *KCNT1*-EIMFS

Clinical features for Patients 1,3 and 6 were briefly described in Chapter 3. Considering the *KCNT1*-positive patients as a group, the median age of seizure onset was 3.5 weeks, with a range of one day to six months. The majority of patients, as expected, had seizure semiology consistent with EIMFS as discussed in Chapter 3. Two of the 12 patients (EOEE1 and EOEE2, **Table 4.3**) presented with severe, early onset nocturnal frontal lobe epilepsy, characterized by asymmetric tonic posturing and later fencing posture. These two patients had presented with early onset epilepsy and were referred for testing on the GOSH EIEE panel. Similar frontal seizure semiology was also noted in some EIMFS patients (Patients 1,6,16,17, 21). All patients developed marked axial hypotonia and three patients displayed pyramidal motor features. A choreiform movement disorder (onset 14-24 months) was seen in four patients (also discussed for Patient 6 in Chapter 3); one developed generalised dystonia at 18 months. The onset of the hyperkinetic movement disorder did not appear to

be related to medication (including Vigabatrin) or intercurrent illness. All patients had normal 12-lead electrocardiograms, but no patients underwent more extensive cardiac testing. All patients were extensively investigated for an underlying metabolic or structural aetiology for their epilepsy and these tests were unrevealing in most patients. However, abnormal muscle respiratory chain enzyme activity for complex I and/or II was detected in Patients 6 and 16 of uncertain significance (**Table 4.4**). In Patient 6 a routine muscle biopsy revealed borderline abnormalities in Complex I and II ratios (as discussed in Chapter 3). The muscle biopsy in Patient 16, was taken during an intercurrent illness, revealing Complex I deficiency. This was repeated following clinical recovery, with a more borderline result. Notably, neither patient had any other systemic, biochemical or radiological indicators of mitochondrial disease nor concurrent Sodium Valproate treatment. In general, the majority of EIMFS patients had a poor neurodevelopmental outcome. All patients had a trial of at least five different medications (**Table 4.3**), though seizures remained intractable to most medical interventions. Eight patients with *KCNT1* mutations received the ketogenic diet in combination with other anti-epileptic drugs. Three responded with approximately 75% seizure reduction. Three patients were treated with quinidine based on early reports of therapeutic benefit (Bearden et al. 2014). Patient 15 tolerated 40mg/kg/day without adverse events (prior to the *in vitro* data being available), but no effect on seizure burden was noted. Patient 17 was treated with Quinidine at 30mg/kg/day and had a marked reduction in seizure frequency. Patient 18 showed some initial reduction in seizure frequency at 30mg/kg/day, but this effect was transient. For this patient, the unexpected development of a severe proliferative pulmonary and mediastinal vasculopathy resulted in life-threatening pulmonary haemorrhage. Investigations failed to identify an underlying vasculitis and quinidine was subsequently withdrawn. The patient later died despite initial successful pulmonary embolization.

EIMFS Patient Cohort No	Electroclinical syndrome	Age of onset	Initial seizure type	Subsequent seizure types	Autonomic features	Movement disorder (age at onset)	Additional features	Best developmental stage attained	Effective anti-epileptic treatments
1	EIMFS	2 weeks	HV, eye jerking, oral automatisms, FM upper limbs	Asymmetric tonic posturing, My, GTCS	Facial flushing	-	-	No developmental milestones achieved	None
3	EIMFS	2 weeks	HV, ED, vocalisation	TS with adversive component	Facial flushing, pupillary dilation	-	Gastrointestinal dysmotility	Partial head control, smiling	Nitrazepam at 5 months
6	EIMFS	4 weeks	HV, ED, fisting of hands	Asymmetric tonic posturing, ED, oral 9automatisms	Facial flushing	Limb dystonia and severe scoliosis (18 months)	Peripheral hypertonia	Babbling, some degree of head control	Steroids and KD in combination at 7-12 months
15	EIMFS	Day 1	HV, ED and jerking, TS upper limbs	FM seizures of face and arm	-	-	-	No developmental milestones achieved	None (including quinidine)
16	EIMFS	7 weeks	Exaggerated startle, reflex warm water clonic/My, evolved to HV and ED, tonic posturing upper limbs, FM all limbs	Rapid alternating ED, facial grimacing leading to airway obstruction	Drooling, salivation, apneas	Hyperkinetic movement disorder affecting upper limbs (18 months)	Coarse facial features, gum hypertrophy	Normal development until 10 weeks, then regression with loss of social smile and head control	None
17	EIMFS	3 months	Behavioural arrest, staring, upward eye rolling, HV and ED to either side, asymmetric tonic posturing and elevation of limbs	Flexor spasms involving the trunk, clonic seizures of limbs, eyelid twitching, gelastic seizures		Hyperkinetic movement disorder involving head and all limbs (18 months)	Cleft of hard palate	Early social smile and visual interaction, lost after onset of epilepsy	Ketogenic diet with Vigabatrin, effect later lost Quinidine-effective
18	EIMFS	2 weeks	Brief FM all limbs (twitching)	HV, dystonic posturing upper limbs, ED and jerking	Facial flushing, noisy breathing	Hyperkinetic movements perioral muscles,	Systemic proliferative vasculopathy of	No developmental milestones achieved	None (some initial response to

						tongue, hand and wrists (2 years)	pulmonary and mediastinal vessels		quinidine)
19	EIMFS	5 months	HV, TS	TS, gelastic seizures	-	Hyperkinetic movement disorder (14 months)	-	Normal until seizure onset, (smile and head control), regression at 5 months with no further development	None
20	EIMFS	3 weeks	HV, ED with pupil jerking, FM arm and face, oral automatisms	HV, ED12, drooling, TS upper limbs, FM upper limbs	Facial flushing	-	-	Smiling, visual awareness, some head control, rolling	Stiripentol, levetiracetam and clonazepam in combination
21	EIMFS	3 weeks	ED with eye flickering, HV, TS upper limbs	FM upper and lower limbs with lip smacking, hand fisting, HV and ED, fencing posture of arm	Facial flushing	-	-	Social smile and reaching for objects until regression and loss of these skills at 5 months	KD and lacosamide in combination
EOEE1	NFLE	6 months	Predominantly nocturnal, asymmetric tonic posturing	ED, choking noises, fencing posture, brief generalised TS and GTCS	Facial flushing	-	Right sided neglect, increased tone on right side, peripheral hyperreflexia in lower limbs	Grasps objects and standing briefly at 2.5 years, vocalising and babbling	None resulted in seizure freedom
EOEE2	NFLE	8 weeks	Focal motor seizures hands, ED and jerking, TS upper limb and FM contralateral lower limb Seizures only in sleep Stopped at 4-5 months	From 11 months: GT with fist clenching, ED, asymmetric tonic posturing, mainly from sleep	-	-	Right sided weakness with peripheral hyperreflexia	Walking prior to regression at 11 months, best subsequent stage sitting independently	No sustained response

Table 4.3 Clinical features of patients with KCNT1 mutations ED eye deviation, EIMFS epilepsy of infancy with migrating focal seizures, FM focal motor, GTCS generalised tonic-clonic seizures, HV head version, KD ketogenic diet, My myoclonic seizures, NFLE nocturnal frontal lobe epilepsy, TS tonic seizures. Adapted from McTague et al Neurology 2018 Jan 2;90(1):e55-e66**.**

	Patient 6	Patient 16
Muscle Biopsy	Normal	2014: slight prominence of intermyofibrillar mitochondria 2016: Coarse clumps of mitochondria suggesting mitochondrial abnormality
Respiratory chain enzymes	Complex I ratio: 0.077 (normal range 0.104-0.268) Complex II ratio: 0.029 (normal range 0.040-0.204)	2014: Complex I 68.6nmol/min/UCS 2016: Complex I 84.5 nmol/min/UCS (normal range>94.17)
***POLG* sequencing**	Normal	Normal
Mitochondrial common deletions	Normal	Not done
Whole Mitochondrial Genome sequencing	Normal	Not done

Table 4.4 Mitochondrial investigations in Patients 4 and 8. UCS units of citrate synthase. Adapted from McTague et al Neurology 2018 Jan 2;90(1):e55-e66**.**

4.3.2 EEG findings

All patients with an EIMFS phenotype had a "migrating" ictal focus with discrete ictal involvement of differing cortical areas within the same EEG (**Table 4.5**) as discussed in Chapter 3. Although this was not always evident at initial presentation, it emerged by 7 months of age in most patients. Periods of EEG suppression or burst suppression were noted in 8/10 EIMFS patients with *KCNT1* mutations. Of note, six of these had seizure onset in the first four weeks of life. Further atypical EEG features included a generalised electrodecremental response in five patients and hypsarrhythmia in one case (**Figure 4-1**).

Patient Cohort No	Age at 1st EEG	Features on initial EEG		Suppression (age)	Further EEG evolution	Atypical EEG features (age)
		Ictal	Interictal			
1	4 w	MIF	Slow background, MF Sh/SW	Inter-ictal suppression (6 weeks)	-	Brief ED (4 weeks) Atypical hyps (6 months)
3	3 w	L temporal ictal focus	MF Sh/SW and slowing	-	MIF (4 months)	-
6	2 m	L or R temporal ictal foci with theta/alpha discharges	Independent MF Sh over the post-central regions	Asynchronous BS (7 months)	MIF (7 months)	ED (7.5 months)
15	1 m	MIF	MF Sh/SW	Brief periods of suppression (1 month)	-	-
16	5 m	Onset left OL but also independently within the right OL, spreading anteriorly/to the CL hemisphere	Frequent bilateral independent spike wave discharges in posterior temporal regions	Post-ictal suppression (6 months)	MIF at 6 months	-
17	4 m	Continuous focal epileptiform activity (rhythmic theta) arising from either hemisphere	Diffuse background slowing	-	MIF at 4.5 months	ED at 7 months Bilateral asymmetric tonic posturing with frontal ictal theta activity at 15 months
18	2 m	Rhythmic delta left parietal	Slow background, MF Sh/SW	Asynchronous BS (2 months)	MIF at 3 months	ED at 2 months
19	5 m	Right mid-temporal region Sp-SW complexes, subsequent seizure arising from left temporal region	Runs of discrete Sp-SW R temporo- parietal regions, and independently L parieto-occipital region	Brief ictal suppression (15 months)	MIF noted at 14 months	-
20	1 m	Initial suppression followed by focal seizure	MF Sp/Sh and SW	Ictal suppression (1 month and 7 months	MIF (7 months)	-

				with tonic seizure)		
21	1 m	No ictal features	MF Sp/Sh and SW	Inter-ictal suppression (from 1 month, still seen at 7 months)	MIF 5 months)	ED (2 months)
EOEE1	6 m	Onset right anterior quadrant	Asymmetric right sided slowing	-	MF Sh/SW. Left frontal or posterior ictal onset (12 months)	-
EOEE2	2 m	Information unavailable	-	-	MF anterior independent asymmetric Sh Ictal focus R mid-temporal at 3 years and L mid-temporal at 11 years	-

Table 4.5 EEG features in 12 patients with *KCNT1* mutations BS burst suppression, ED electrodecrement, hyps hypsarrhythmia, L left, m months, MIF migrating ictal focus, MF multifocal w weeks, OL occipital lobe, R right, Sh sharp waves, Sp spikes, SW slow waves. Adapted from McTague et al Neurology 2018 Jan 2;90(1):e55-e66**.**

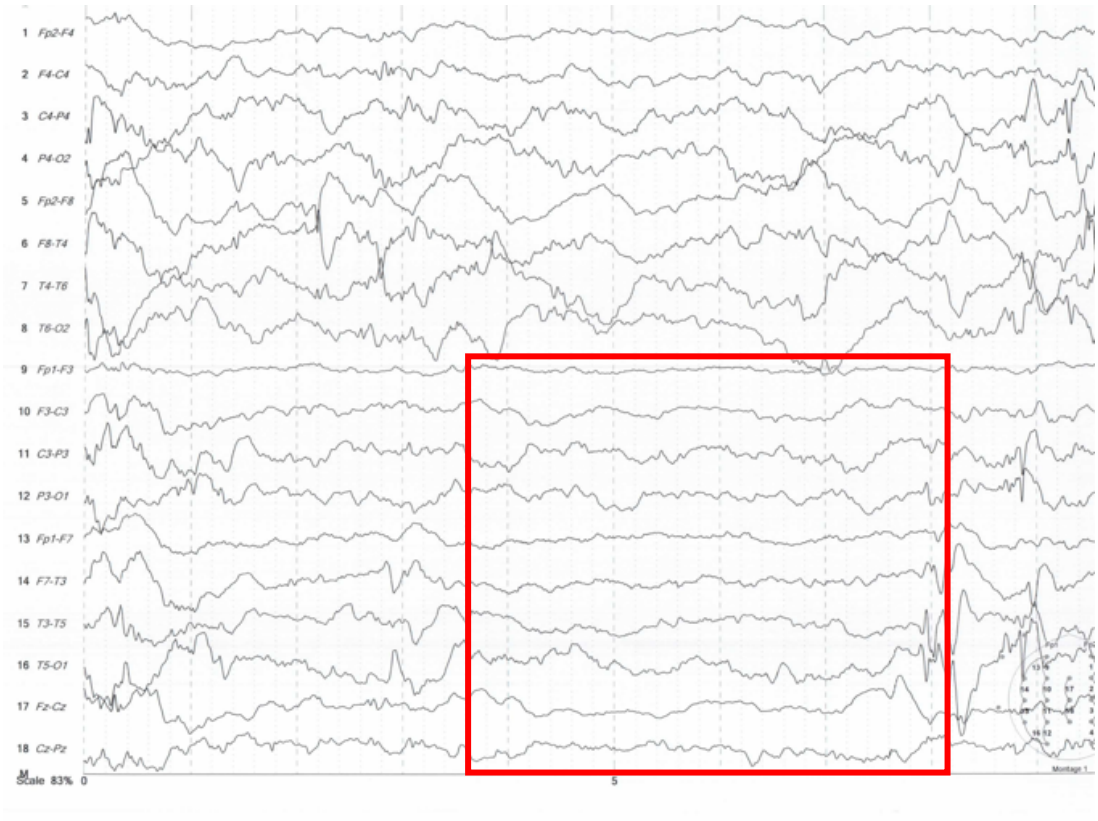

Figure 4-1 Left sided post-ictal suppression at 6 months of age in Patient 16. Suppression indicated by red box.

4.3.3 MRI findings

Neuroimaging was available in 11/12 patients and was reviewed with Dr Kling Chong, consultant neuroradiologist, Great Ormond Street Children's Hospital. Note Patients 1, 3 and 6 were also discussed in Chapter 3. The majority developed cerebral atrophy by three years of age, with predominantly frontal involvement (**Figure 4-2, Table 4.6**). Cerebellar atrophy was also evident in four patients (**Figure 4-2c**). An open operculum was evident in the first six months of life in Patient 16 (**Figure 4-2b**). Delayed myelination was evident in 9/11 patients (including Patients 3 and 6) who had imaging after three months of age. In some patients, early brain imaging undertaken under five months of age was normal. Magnetic resonance spectroscopy was abnormal with a relatively reduced N-acetylcholine peak in 3/4 patients (including Patients 1 and 3 as described in Chapter 3) in whom this investigation was undertaken.

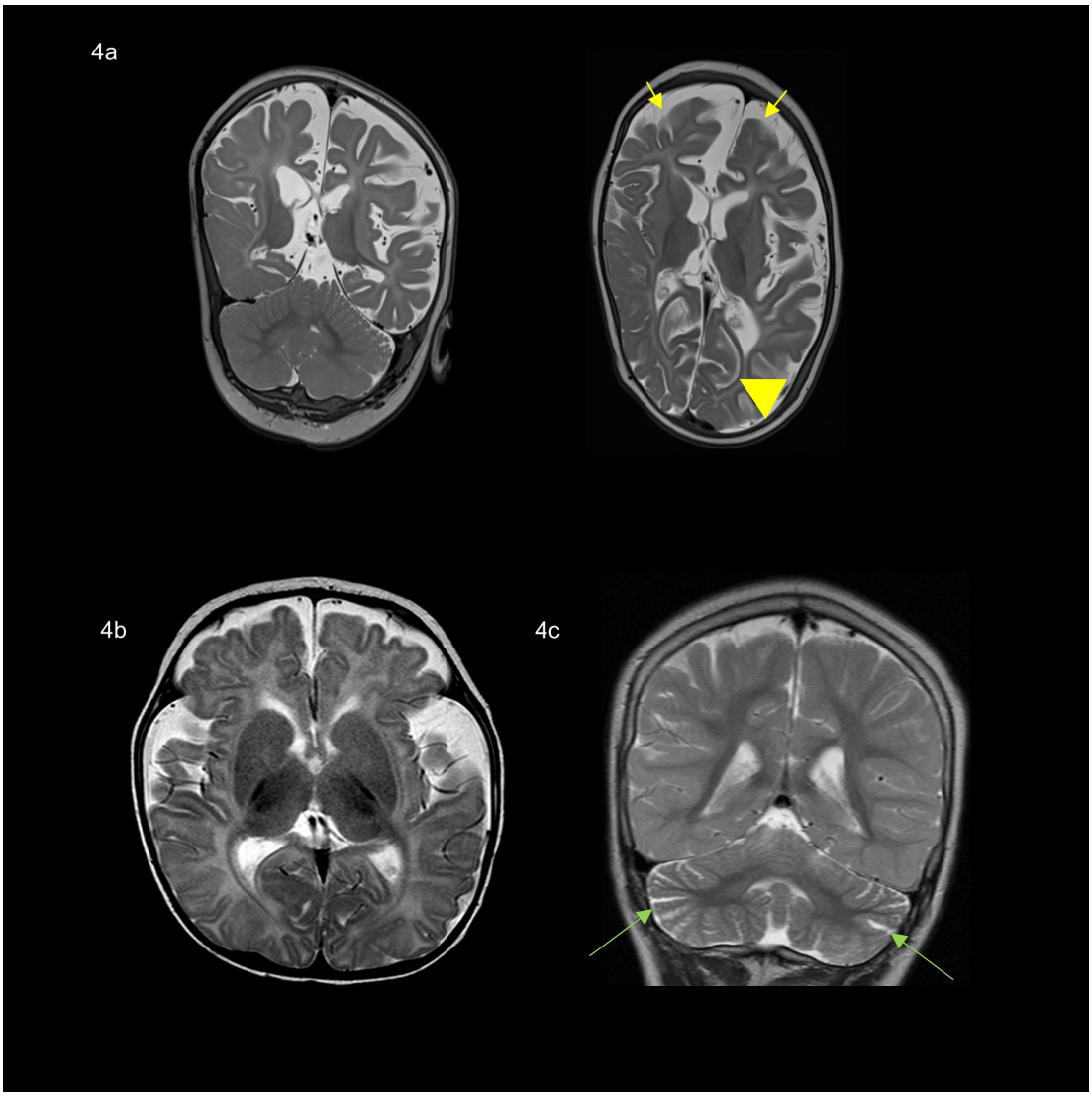

Figure 4-2 MRI features in KCNT1-related epilepsy

4-2a: Coronal(left) and axial (right) T2 weighted images in Patient 15 at 10 months of age reveal severely delayed myelination (yellow arrowhead), volume loss and frontal predominant atrophy(yellow arrows) with plagio/dolichocephaly. 4-2b: Axial T2 weighted images in Patient 16 at 5 months of age show abnormally open operculum (black arrows) with lack of brain development. 4-2c: Coronal T2 weighted images with cerebellar atrophy indicated by prominent cerebellar foliae (green arrows) in Patient EOEE2 at 8 years of age. Adapted from McTague et al Neurology 2018 Jan 2;90(1):e55-e66.

Patient Cohort No	Age at imaging	MRI	MRS
1	31 days	WNL	-
	4 months	Dolicocephaly; DM	Relative choline elevation and NAA reduction
3	11 weeks	DM	Low NAA
	3 years	DM and global CA	
6	9 weeks	DM	-
	4 months	DM	-
	2 years	Very little myelination maturation after 6-8 months with decreased white matter volume, volume loss/CA	-
15	10 weeks	DM already apparent, underdeveloped FL, slim CC	-
	10 months	Plagio and dolicocephaly, severe volume loss/CA, fronto-temporal worse than parieto-occipital, thin corpus callosum	
16	4 months	Underdevelopment of frontal and temporal lobes and cerebellum	Normal
	5 months	Abnormally open operculum, CA/lack of brain development	-
17	3 months	WNL	-
18	10 weeks	WNL	-
	10 months	DM, CA and cerebellar atrophy	
19	5 months	DM	-
20	23 days	WNL	-
21	7 weeks	WNL	Relative NAA reduction
	5 months	WNL	-
	6 months	Marked CA /volume loss, cerebellar atrophy	-
	8 months	Worsened CA & DM	-
	1 year	Further atrophy with left subdural effusion, cerebellar atrophy & DM	-
EOEE1	5 months	WNL	-
	18 months	DM	-
	3 years	DM (18/12 stage), CA, cerebellar atrophy	-
EOEE2	2 years	WNL	-
	5 years	Global CA and cerebellar atrophy	-
	8 years	Progression of CA, cerebellar atrophy, DM	-

Table 4.6 Radiological features of patients with *KCNT1* mutations. CA cerebral atrophy, CC corpus callosum, DM delayed myelination, FL frontal lobe, WNL within normal limits. Adapted from McTague et al Neurology 2018 Jan 2;90(1):e55-e66**.**

4.3.4 Molecular genetic findings

12 patients with missense mutations in *KCNT1* were identified; eight of these have been previously reported and four are novel unreported mutations (McTague et al. 2013; Ishii et al. 2013; Ohba et al. 2015; Møller, Heron, et al. 2015; Hildebrand et al. 2016) (**Table 4.7**). 8/12 patients had variants located in the carboxy terminus, of which five had the A934T variant, reported in multiple cases. Of these five cases, four had an EIMFS presentation and one (Patient EOEE2) had a NFLE-like phenotype. In addition, I identified a total of four (including two previously unreported) variants around transmembrane (TM) domains 5 and 6 (V271F, L274I, G288S and F346L).

In order to determine the potential effect of identified missense variants, I undertook pathogenicity predictions using a variety of *in silico* tools. Polyphen2 scores variants based on both phylogenetic, sequence-based and structural features integrating predictions on the impact of the variant on protein structure and function (Adzhubei et al. 2010). The Sorting Tolerant from Intolerant (SIFT) score uses sequence-based homology data to assess pathogenicity based on conservation and the tolerance of that residue to substitution, with changes at highly-conserved residues scored as deleterious(Ng & Henikoff 2001). The Protein Variant Effect Analyzer (Provean) tool uses multiple protein sequence alignments to assess the impact of a change in sequence homology amino acid variation to the query sequence(Choi et al. 2012). While each of these tools has advantages, they tend to use a single measure such as sequence alteration based on conservation or protein structure and are not directly comparable. As a result, tools which integrate multiple annotations of variant effects such as the Combined Annotation Dependent Depletion (CADD) tool have been developed. CADD enables calculation of a single score for deleteriousness (Kircher et al. 2014) by comparing the combined predictions for simulated variants with those of fixed or nearly-fixed alleles in humans i.e. those which have survived natural selection. Using a combination of these methods, the majority of the *KCNT1* variants are predicted to be pathogenic (**Table 4.7**). F346L has a CADD score of 14 and is only predicted to be pathogenic on one tool, Provean. All variants including F346L affect highly conserved amino acid residues (**Figure 4-3**). They are not reported in databases of normal genetic variation including 1000 Genomes, the ExAC database, the Exome Variant Server or the gnomAD database (see Appendix for websites).

For 9/12 cases variants occurred *de novo* (Patients 3,6,15,16,18,20,21, EOEE1 and EOEE2). Parental DNA was not available in Patient 1. For Patient 17, the same *KCNT1* variant was found in an asymptomatic mother. A lower heterozygous peak was noted on Sanger sequencing of both salivary and blood-derived maternal genomic DNA (**Figure 4-4)**. In Patient 19, the variant was inherited from an unaffected father with no difference in peak size on Sanger sequencing (**Figure 4-5**). The recurrent A934T variant was identified in five patients, four with a EIMFS presentation and one (EOEE2) with a NFLE phenotype.

Patient Cohort No	CDS	Protein change	PP2	SIFT (<0.05)	Provean (<-2.5)	CADD (scaled)	In ExAC, 1000G, EVS, gnomAD	Inheritance	Previous functional validation?
1	c.811G>T	V271F	0.773 PD	0.092 T	-3.29 Del	23.0	No	Unknown (parental DNA not available)	Gain of function (McTague et al. 2013; Q.-Y. Tang et al. 2016)
15	c.820C>A	L274I	0.947 PD	0.002 D	-1.76 N	28.7	No	*De novo*	No
EOEE1	c.862G>A	G288S	0.978 PrD	0.086 T	-5.27 Del	24.8	No	*De novo*	Gain of function (Kim et al. 2014; Ohba et al. 2015; Møller, Heron, et al. 2015; Rizzo et al. 2016b; Q.-Y. Tang et al. 2016; Arai-Ichinoi et al. 2015)
16	c.1038C>G	F346L	0.043 B	0.341 T	-3.62 Del	14.44	No	*De novo*	No
17	c.1504T>G	F502V	0.051 B	0.004 D	-6.29 Del	23.6	No	Maternal inheritance, likely somatic mosaicism	No
18	c.2687T>A	M896K	0.978 PrD	0.001 D	-4.82 Del	29.2	No	*De novo*	No
7	c.2800G>A	A934T	0.602 PD	0.064 T	-2.51 Del	23.6	No	*De novo*	Gain of function (Barcia et al. 2012; McTague et al. 2013; Kim et al. 2014; Ohba et al. 2015; Milligan et al. 2014)
3	c.2800G>A	A934T	0.602 PD	0.064 T	-2.51 Del	23.6	No	*De novo*	
20	c.2800G>A	A934T	0.602 PD	0.064 T	-2.51 Del	23.6	No	*De novo*	
EOEE2	c.2800G>A	A934T	0.602 PD	0.064 T	-2.51 Del	23.6	No	*De novo*	
21	c.2800G>A	A934T	0.602 PD	0.064 T	-2.51 Del	23.6	No	*De novo*	
19	c.2849G>A	R950Q	0.941 PD	0.012 D	-2.95 Del	23.6	No	Paternally inherited	No

Table 4.7 *KCNT1* mutations identified in 12 patients. 1000G 1000 genomes database, B benign, CADD Combined Annotation Dependent Depletion**,** CDS coding sequence, D damaging, Del deleterious, EVS exome variant server, ExAC Exome Aggregation consortium, gnomAD Genome Aggregation database, N neutral,

NGSP next generation sequencing panel, PD possibly damaging, PP2 Polyphen2, PrD probably damaging, SS sanger sequencing, T tolerated, WES whole exome sequencing. Adapted from McTague et al Neurology 2018 Jan 2;90(1):e55-e66.

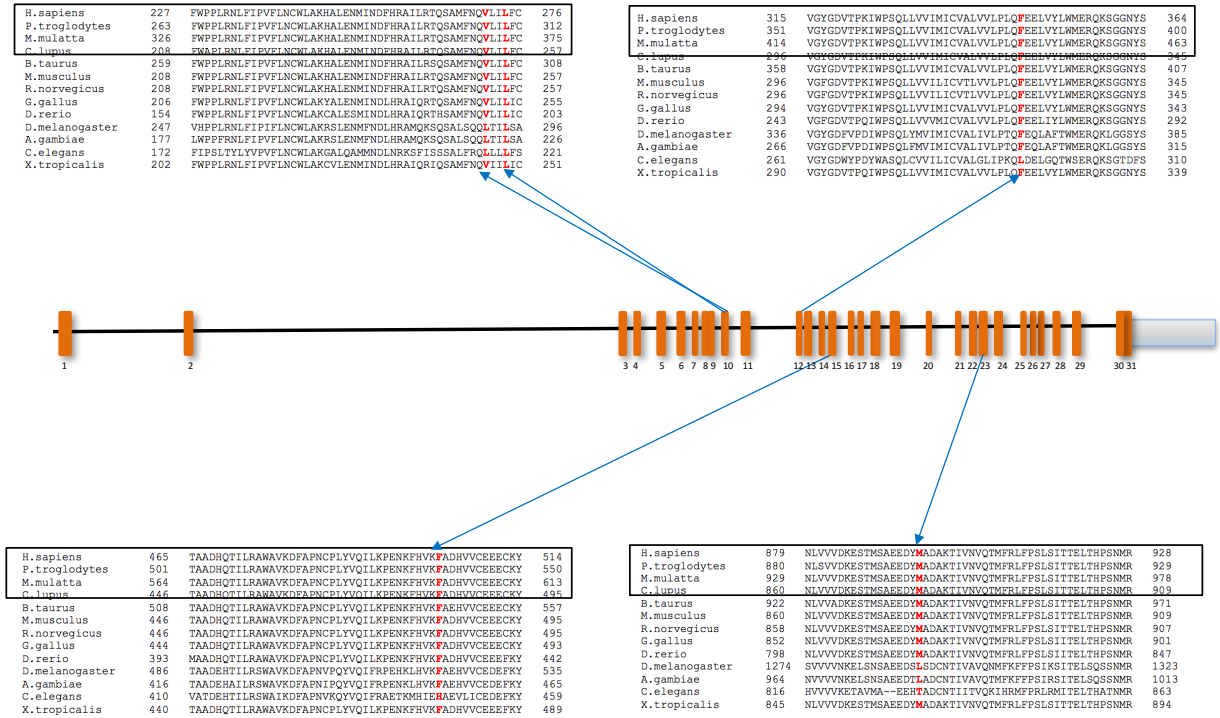

Figure 4-3 Conservation of amino acid residues affected by novel variants. Schematic drawing of the 31 exons of *KCNT1* with multiple protein alignments from different species (*H. sapiens*, *P. troglydytes*, *M. mulatta, C. lupus*, *B. taurus*, *M. musculus*, *R. norvegicus*, *G. gallus*, *D. rerio, D. melanogaster, A. gambiae, C. elegans, X. tropicalis*). The residues involved in the five novel mutations (F271 and L274, F346, F502 and M896) are highly conserved throughout species. Adapted from McTague et al Neurology 2018 Jan 2;90(1):e55-e66.

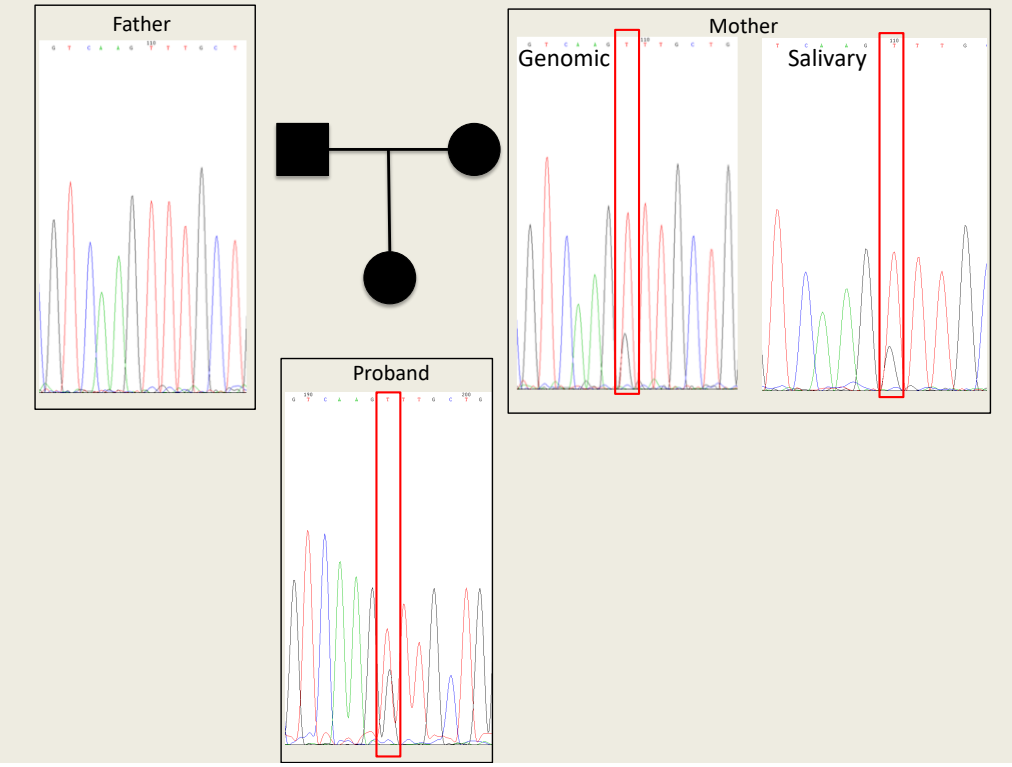

Figure 4-4 Evidence of possible maternal mosaicism for Patient 17. A lower heterozygous peak for variant 1504T>G, F502V is evident in both maternal lymphocytic and salivary DNA. Adapted from McTague et al Neurology 2018 Jan 2;90(1):e55-e66**.**

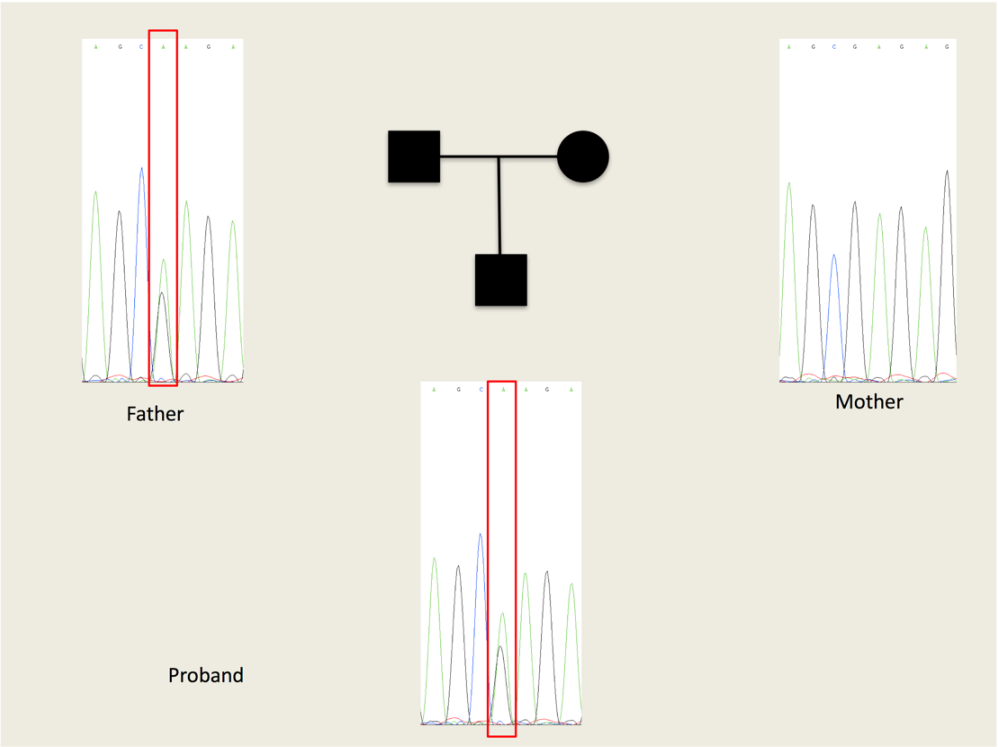

Figure 4-5 Evidence of parental inheritance for Patient 19. The mutation c.2849G>A, R950Q in Patient 19 is paternally inherited. Adapted from McTague et al Neurology 2018 Jan 2;90(1):e55-e66**.**

4.3.5 Protein homology modelling

To further understand how the identified previously unreported missense variants could impact on protein structure, homology modelling was performed by Dr Sony Malhotra and Dr Maya Topf. Due to availability of homologous sequences, only two of the novel variants were amenable to modelling, F346L, located in the ion-channel domain (residues 270-353) and F502V, located in the gating region (residues 373-1174. F346 is located on the inner helix (**Figure 4-6a, b**) within the ion channel transmembrane domain (residues 270-353 that form the transmembrane pore region) and is part of the hydrophobic cavity, which mediates interactions between the inner-membrane helices of two adjacent subunits (**Figure 4-6c).** As in the modeled open conformation, F346 is surrounded by many hydrophobic residues of the inner helix of other protomer and hence responsible for maintaining the stability of the open conformation. It is observed in the modeled closed state conformation that the helix containing F346 and the inner helix from the other protomer undergo conformational changes (**Figure 4-7**). Therefore, mutation to leucine (F346L) is likely to destabilize the open state by perturbing the hydrophobic interactions as the side chain of leucine is smaller (**Figure 4-6c**). If the open state is less stable, then the

overall dynamics of the channel (i.e. equilibrium between the open and closed) is likely to be affected. Also, the packing arrangement in the K^+ channels involving the pore and the inner helix is known to be critical for the stability of the tetrameric assembly, the ion conduction function and also for its selectivity for the cation (Doyle et al. 1998). F346 lies on the inner helix and F346L might be detrimental for these functions.

F502 is in the KCNT1 gating region (373-1174). Within each protomer of the gating region, there are two tandem RCK domains (RCK1 and RCK2), which serve as regulators of potassium conductance (**Figure 4-6e**). The two RCK domains form flexible intra- and inter-subunit (**Figure 4-6e**)**.** interfaces which facilitate channel assembly into a functional tetramer (Yuan et al. 2010). F502 is in RCK1 and predicted to form a pi-pi interaction (a non-covalent attractive force) with W476 from αD (**Figure 4-6f**)**.** F502 is also surrounded by several hydrophobic residues (I472, L473, A475, V500 and A503) which may play a role in stabilising the overall assembly structure of the gating ring (**Figure 4-6f**). The amino acid substitution F502V is predicted to result in (i) destabilisation of these hydrophobic interactions, given the smaller valine side chain (**Figure 4-6g**) and (ii) abolition of potential pi-stacking with resultant disruption of the stable assembly interface.

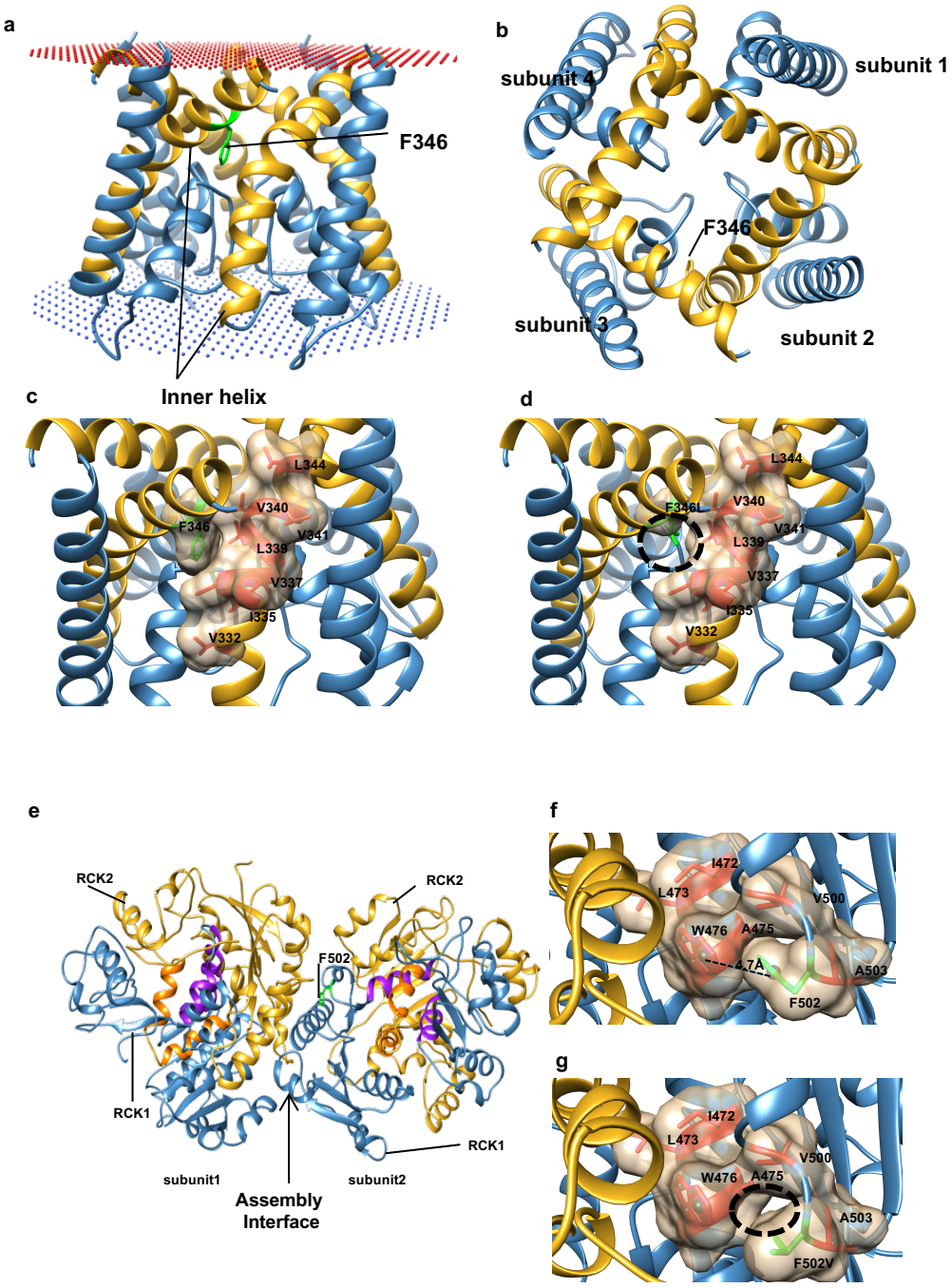

Figure 4-6 Modeling the ion channel and gating apparatus of KCNT1. (a) Side view of the homology model of the KCNT1-ion channel (residues 278-346) as a tetramer. F346 is present on the edge of the inner helix (gold) and interacts with the inner helix of the adjacent subunit. Membrane position is shown in spheres. **(b)** Top-view of the tetramer and location of F346 on the inner helix. **(c)** F346 is part of the hydrophobic cavity (shown as surface), which mediates interactions between the inner-membrane helices of the two subunits. F346 (green) and the surrounding hydrophobic residues (red) **(d)** Upon mutation to leucine (F346L, green), hydrophobic interactions between the two subunits are likely to be reduced (black circle), as the side chain of leucine is much shorter than phenylalanine.

(e) A model of a dimer of the gating ring (residues 372-1044), which is a tetramer, based on recent cryo-EM structure at 4.5 Å (PDB ID: 5A6F). Each subunit has two RCK domains; RCK1 (blue) and RCK2 (gold). F502 (green) is in the RCK1 domain, near the inter-subunit interface (assembly interface). The RCK1-RCK2 intra-subunit interface is purple (residues from RCK1) and orange (residues from RCK2). The dimer interfaces formed by both RCK-1 and RCK-2 is pointed with an arrow. **(f)**: F502 (green) and its neighbouring hydrophobic residues (red), including W476, with which it could potentially form a pi-pi interaction. The distance between the centroid (indicated as spheres) of the two rings (F502 and W476) is 4.7 Å and the angle between the ring planes is 27.3 degrees. **(g)**: F502V could abolish the formation of the potential pi-pi interaction with W476 and is likely to reduce the hydrophobic interactions (pointed using a black circle), as the side chain of valine is smaller than that of phenylalanine. Adapted from McTague et al Neurology 2018 Jan 2;90(1):e55-e66**.**

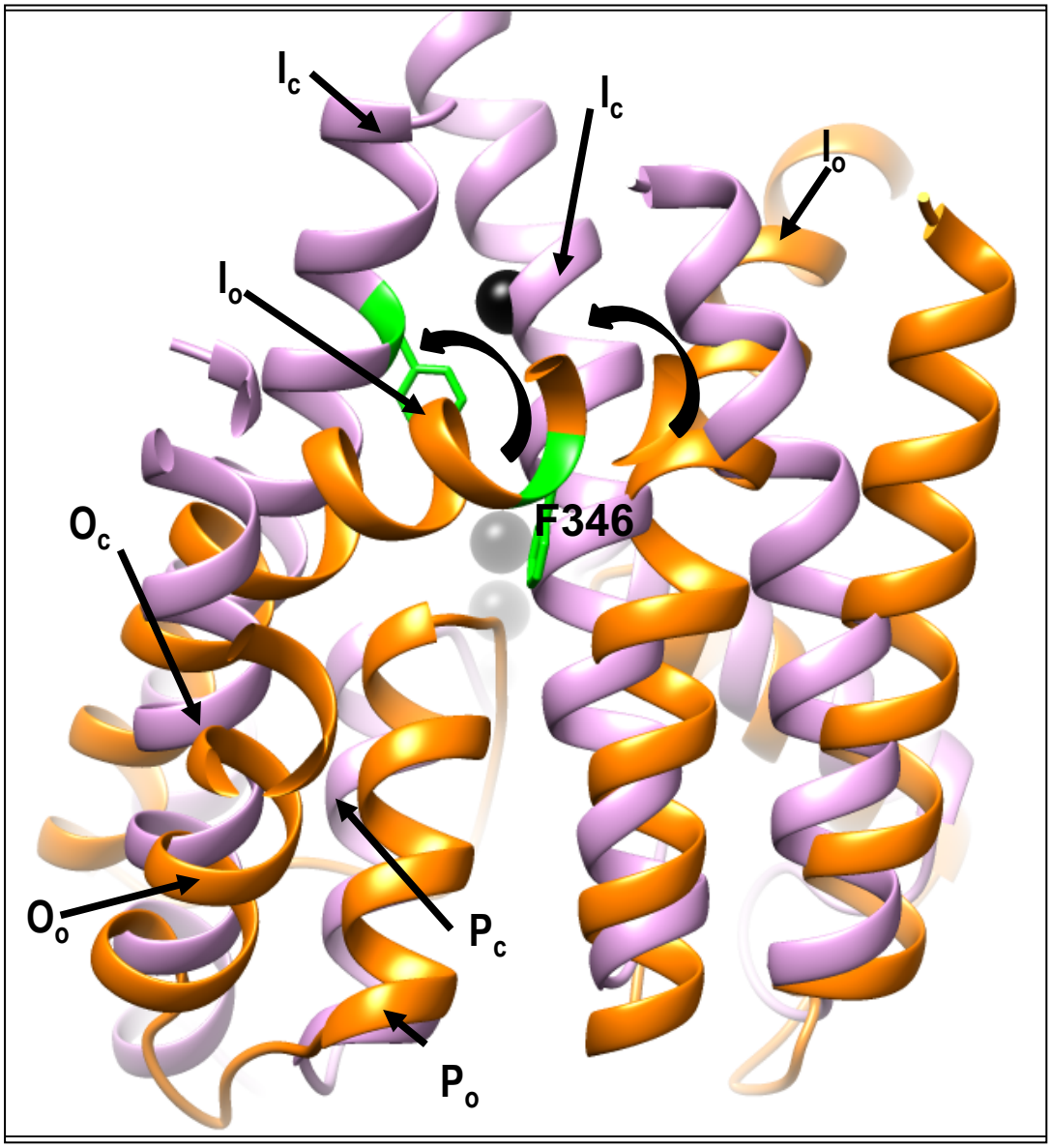

Figure 4-7 Open-state (in orange) vs. closed state (in pink) model of the ion channel domain. F346, which is shown in green, is present at the dimeric interface between two inner helices (I_o and I_c for open and closed state respectively) (see Figure 4-6) in the open state, but the two helices undergo conformational change in the closed state, as pointed out using black arrows. Potassium ions (black spheres) are modelled into the tetrameric model using structure superposition with the K^+-bound open form (PDBID: 3LDC). The dimer of the open state is modeled based on the biological assembly of the open state of MthK from *Methanothermobacter thermautotrophicus* (PDBID: 3LDC). The dimer of the closed form of the ion channel domain is modeled using the closed form of potassium channel from *Streptomyces lividans* (PDBID: 2A9H). O_c and O_o correspond to outer helices in closed and open states and P_o and P_c represent the pore helices in closed and open state respectively. Adapted from McTague et al Neurology 2018 Jan 2;90(1):e55-e66**.**

4.3.6 Electrophysiology

Electrophysiology experiments were performed by Dr Umesh Nair and Dr Steve Petrou. The four previously unreported variants and V271F, which I described previously (McTague et al. 2013) and which was recently studied in a xenopus oocyte system (Q.-Y. Tang et al. 2016), were chosen for evaluation. All variants led to an increase in current magnitude compared to wild type (WT) (**Figure 4-8a**). Notably, for the mutants V271F and F346L, the rate of activation was slowed at higher voltages compared to WT, whereas in others (M896K, F502V and L274I) activation rates were faster than WT (**Figure 4-8a**). Assessment of the current-voltage relationship showed that mutant channels were either very weakly voltage-dependent or, in some cases, there was absence of voltage dependence of steady state activation (**Figure 4-8b** and **c**). In addition, only residual Goldman–Hodgkin–Katz rectification was seen. This refers to the phenomenon where currents flowing across permeable membranes are larger when flowing in one direction e.g inward versus outward, due to ion flow across membranes as determined by ion concentrations and gradients (Goldman 1943). Evaluation of average peak currents at +10mV revealed a highly statistically significant difference between both individual mutant channels and summated data when compared to WT (**Figure 4-8d** and **e**). Therefore, not only did mutant channels exhibit increased channel amplitude, but several aspects of channel kinetics were observed to be altered in mutant KCNT1 channels.

Quinidine responsiveness was assessed in the xenopus oocyte system (**Figure 4-9**). Four of the five novel mutations showed some degree of reduction in channel current amplitude with quinidine application. This was variable and only reached statistical significance for M896K and F502V (**Figure 4-9c**). There was no effect of quinidine on channel amplitude in F346L. Correlation with clinical response to quinidine will be discussed in section 4.4.

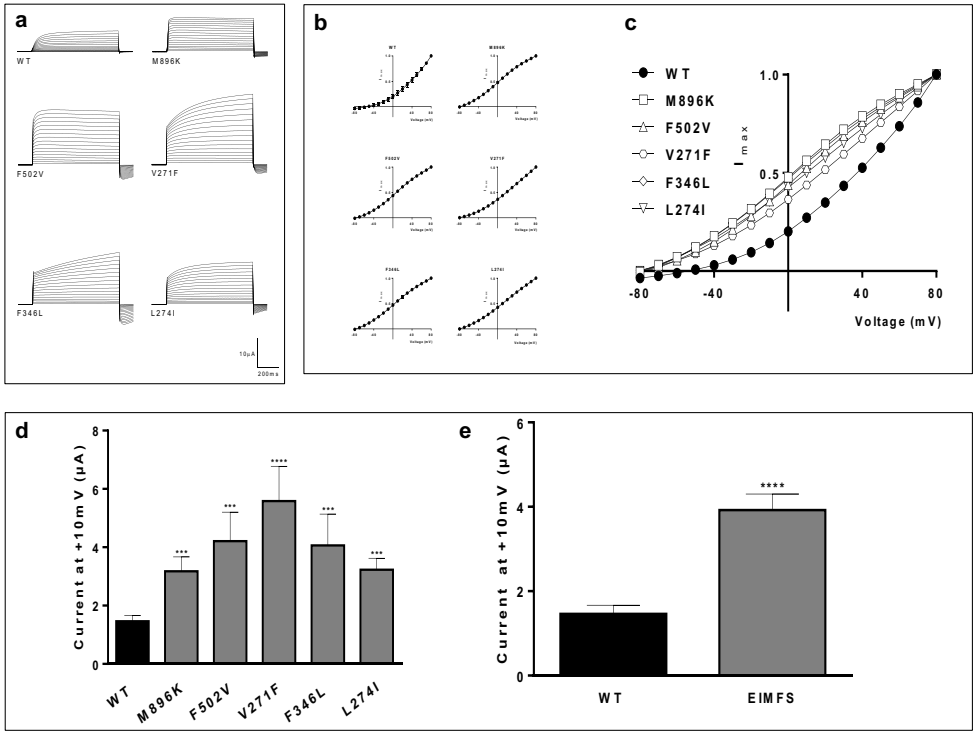

Figure 4-8 Functional investigation of *KCNT1* mutations in a xenopus oocyte model. a: Representative current traces from oocytes expressing WT or EIMFS mutants (M896K, F502V, V271F, F346L and L274I). Oocytes held at -90mV and stepped from -80mV to 80mV for 600 ms every 5 s. Scale bars apply to all traces. b Current–voltage (IV) relationships WT (n = 32), M896K (n = 15), F502V (n = 13), V271F (n = 9), F346L (n = 11) and L274I (n = 12). Currents averaged, then normalized to the value at test potential of +80mV (Imax). c Comparison of IV relationships between WT (solid circles, n = 32) and EIMFS mutations [M896K (squares, n = 15), F502V (triangles, n = 13), V271F (hexagons, n = 9), F346L (diamonds, n = 11) and L274I (inverted triangles, n = 12)]. d Average peak currents at +10mV for WT (n = 44), M896K (n = 19), F502V (n = 16), V271F (n = 10), F346L (n = 11), L274I (n = 12), channels. Peak currents for mutant channel at +10mV compared to the peak currents for the WT channel at +10mV. ***p < 0.001, ****p < 0.0001. e Comparison of pooled WT (n = 44) and EIMFS (n = 68) currents at +10mV. ****p < 0.0001. Adapted from McTague et al Neurology 2018 Jan 2;90(1):e55-e66**.**

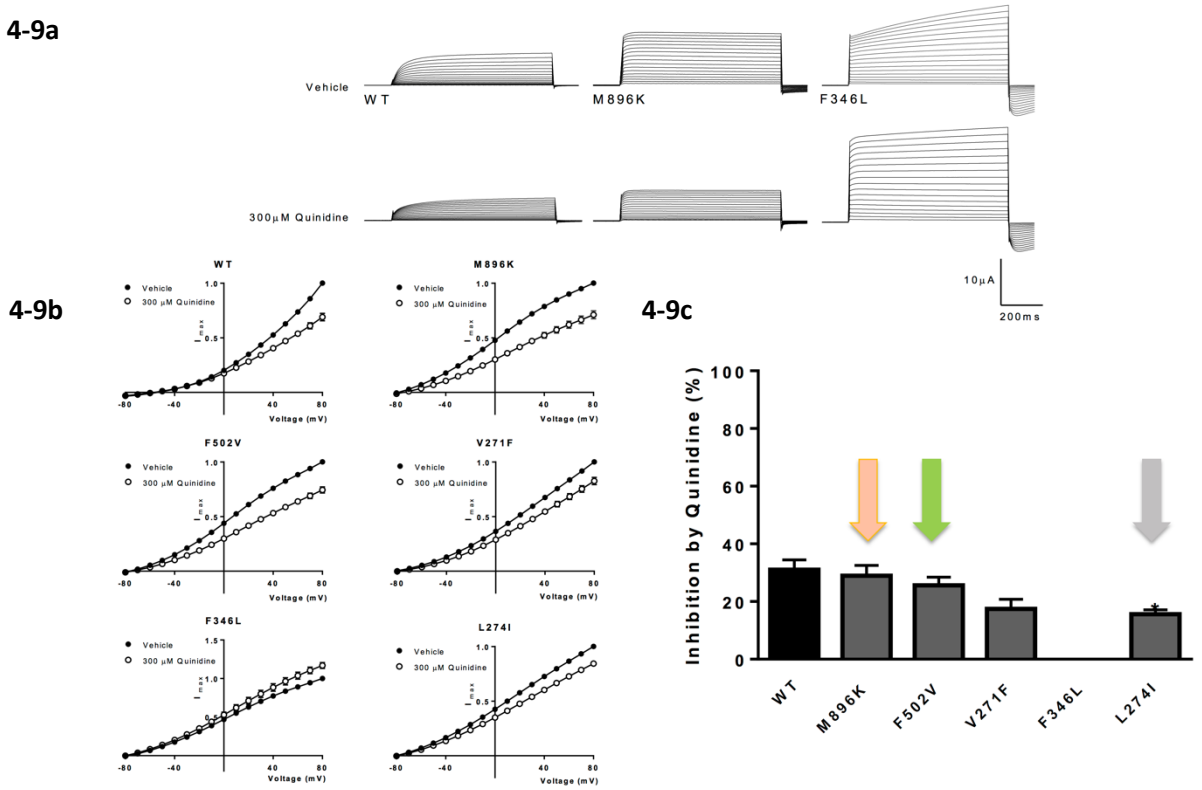

Figure 4-9 Effect of quinidine on *Xenopus* oocytes expressing h*KCNT1* channels. 4.9a Representative current traces obtained from oocytes expressing WT and EIMFS mutants (M896K and F346L) with application of vehicle (ND96) and 300 µM quinidine. Oocytes were held at -90mV and stepped from -80mV to +80mV for 600 milliseconds every 5 seconds. Scale bars apply to all traces. 4.9b Current–voltage relationships for WT (n = 32), M896K (n = 15), F502V (n = 13), V271F (n = 9), F346L (n = 11) and L274I (n = 12) h*KCNT1* channels in the presence of vehicle (ND96) and 300 µM quinidine. Currents were averaged, then normalized to the value at a test potential of +80mV (Imax). 4.9c Average percent inhibition at +80mV of WT (n = 31) and EIMFS (M896K, n = 15; F502V, n = 13; V271F, n = 9; F346L, n = 11;L274I, n = 12) h*KCNT1* channels by quinidine (300 µM) depicting the variable degree of block by 300 µM quinidine (One-way ANOVA followed by Bonferroni *post hoc* analysis). *p < 0. Arrows indicate

patients treated with quinidine and clinical response: orange arrow indicated minimal response, green arrow indicates good response, grey arrow indicates no response – see section 4.4. Adapted from McTague et al Neurology 2018 Jan 2;90(1):e55-e66**.**

4.4 Discussion

KCNT1 encodes the sodium-activated potassium channel KCa4.1 (SLACK: sequence like a calcium-dependent potassium channel, Slo2.2). KCNT1 is broadly expressed throughout the brain, as well as in the dorsal root ganglia and kidney. Activation of KCNT1 channels following bursts of action potentials results in slow hyperpolarization (Kaczmarek 2013; Brown et al. 2008). KCNT1 also has direct interactions with Fragile X related protein (FMRP) (Kim & Kaczmarek 2014). In contrast to other potassium channels, KCNT1 is involved in a wide protein network, which may indicate an important role, not only in neuronal excitability but also in cognitive developmental processes (Kim et al. 2014; Barcia et al. 2012; Kim & Kaczmarek 2014; Kaczmarek 2013).

KCNT1-related disease includes a range of heterogeneous and typically severe epilepsies associated with severe neurodevelopmental delay and cognitive difficulties. *KCNT1* mutations have been reported in Ohtahara syndrome, West syndrome/infantile spasms, ADNFLE, non-specific early onset epileptic encephalopathy (EOEE) and hypomyelinating leucoencephalopathies (**Table 4.8**) (Barcia *et al.*, 2012b; Heron *et al.*, 2012; Allen *et al.*, 2013, 2015; McTague *et al.*, 2013b; Ishii *et al.*, 2013b; Kim *et al.*, 2014; Martin *et al.*, 2014; Vanderver *et al.*, 2014; Bearden *et al.*, 2014a; Mikati *et al.*, 2015; Møller *et al.*, 2015; Ohba *et al.*, 2015; Arai-Ichinoi *et al.*, 2015; Rizzo *et al.*, 2016; Chong *et al.*, 2016; Hildebrand *et al.*, 2016; Fukuoka *et al.*, 2017). Recently, two siblings with childhood onset learning difficulties with ensuing adult onset epilepsy with hippocampal sclerosis and cerebellar ataxia were reported (Hansen et al. 2017). In addition, a patient with Brugada syndrome and seizures has been described (Juang et al. 2014). Notably, an ADNFLE patient was found to have a concurrent cardiac arrhythmia , similar to Brugada syndrome, and a member of the same family who harboured an identical mutation died from SUDEP (Møller et al. 2015).

Given case acertainment bias, the majority of patients with *KCNT1* mutations in my cohort had electroclinical EIFMS. A broader phenotypic range may be seen in a larger multi-centre study. Indeed, two of the five *KCNT1* positive patients identified by the NGS panel from a larger pool of 800 patients with EOEE/developmental delay referred for panel testing had a NFLE-like presentation. Several atypical EEG features are evident in these patients. Generalised electrodecrement and hypsarrhythmia, more classically associated with

infantile spasms, have been previously described in EIMFS (Fukuoka et al. 2017; McTague et al. 2013; Ohba et al. 2015; Møller, Heron, et al. 2015; Allen et al. 2015). While EEG suppression, classically seen in Ohtahara syndrome (Ohtahara 1977), has been described in EIMFS before (McTague et al. 2013; Ohba et al. 2015), it was found in most the *KCNT1*-EIMFS patients and it seemed to be associated with earlier seizure onset. These findings may reflect the age-dependent expression of KCNT1 dysfunction.

Extensive diagnostic investigations performed in *KCNT1* patients prior to diagnosis were mainly uninformative, other than abnormal muscle respiratory chain enzyme analysis of muscle tissue in two patients. As in other severe epilepsies, this may be evidence of secondary mitochondrial dysfunction in *KCNT1*-epilepsy (Folbergrová & Kunz 2012). Other genetic and environmental influences on mitochondrial function may also play a role.

Genomic mutation	Effect on protein	Age of seizure onset	Phenotype	Additional features							Inheritance	Functional validation (references
				Seizure types	EEG	MRI	Pyramidal features	Movement disorder	Psychiatric	Other		
c.769C>G	H257D	2 weeks	EIMFS	-	-		-	-	-	-	*De novo*	No (Møller et al. 2015)
c.785G>A	R262Q	8 weeks	EIMFS	-	-		-	-	-	-	*De novo*	No (Møller et al. 2015)
c.808C>G	Q270E	2 days	EIMFS	-	Brief EEG suppression		Spasticity	-	-	-	*De novo*	No (Ohba et al. 2015)
c.811G>T	V271F	2 weeks	EIMFS	-	Subtle BS (6 weeks) Hyps (6 months)		-	-	-	-	Unknown (donor egg IVF)	Gain of function (McTague et al. 2013; Tang et al. 2016)
c.862G>A	G288S	2 months	EIMFS	-	-		-	-	-	-	*De novo*	Gain of function (Møller et al. 2015; Ohba et al. 2015; Tang et al. 2016; Ishii et al. 2013; Kim et al. 2014; Arai-Ichinoi et al. 2015; Rizzo et al.
c.862G>A	G288S	2 months	EIMFS	-	-		-	-	-	-	*De novo*	
c.862G>A	G288S	3 years	ADNFLE	-	-		-	-	-	-	Unknown	
c.862G>A	G288S	4 months	EIMFS	-	-		Spasticity	Chorea (left finger)	-	-	*De novo*	
c.862G>A	G288S	2 months	EIMFS						-	-	*De novo*	
c.862G>A	G288S	3 months	EIMFS	Spasms	-		-	Choreiform movements	-	-	Unknown	
c.862G>A	G288S	5 weeks	EIMFS	-	-		-	-	-	-	Unknown	

c.862G>A	G288S	3 months	EOEE	-	-	Severe DM (HL)	-	-	-	-	Unknown	2016a)
c.862G>A	G288S	2 months	EIMFS	-	-	-	-	-	-	-	*De novo*	
c.1018G>A	V340M	3 years	Multifocal epilepsy	-	-	-	-	Limbic encephalitis	-	-	*De novo*	No (Møller et al. 2015)
c.1193G>A	R398Q	Median 5.5 years (range 5–18)	ADNFLE	-	-	-	-	Psychiatric/ behavioural problems in 2/4 No ID		-	Familial (AD)	Gain of function (Mølleet al. 2015; Kim et al. 2014; Allen et al. 2015; Milligan et al. 2014; Heron et al. 2012)
c.1193G>A	R398Q		ADNFLE	-	-	-	-		-	-		
c.1193G>A	R398Q		ADNFLE	-	-	-	-		-	-		
c.1193G>A	R398Q		ADNFLE	-	-	-	-		-	-		
c.1193G>A	R398Q	10 days	EIMFS	-	-	-	-	-	-	-	Unknown	
	R398Q	Unknown	Likely ADNFLE	-	-	-	-	-	-	-	Familial (AD)	
	R398Q	8-14 months	ADNFLE	-	-	-	-	-	-	-		

c.1193G>A	R398Q	3 months	EIMFS	-	-	-	-	-	-	-		
c.1193G>A	R398Q	6 months	Focal epilepsy	-	-	-	-	-	-	-		
c.1193G>A	R398Q	5 months	EIMFS	-	-	-	-	-	-	-		
c.1193G>A	R398Q	10 weeks	EIFMS	-	-	-	-	-	-	-	*De novo*	
c.1225C>T	P409S	2 months	EIMFS	-	-	-	-	-	-	-	*De novo*	No (Ohba et al. 2015)
c.1283G>A	R428Q	2 months	EIMFS	-	-	-	-	-	-	-	*De novo*	Gain of function (Møller et al. 2015; Ohba et al. 2015; Barcia et al. 2012; Bearden et al. 2014)
c.1283G>A	R428Q	17 hours	EIMFS	-	-	-	-	-	-	-	*De novo*	
c.1283G>A	R428Q	2 hours	EIMFS	-	-	-	-	-	-		*De novo*	
c.1283G>A	R428Q	10 weeks	EIMFS	Apnoea with seizure (2 years)	-	-	-	-	-	-	Unknown	
c.1283G>A	R428Q	1 month	EOEE	-	Brief period of EEG suppression	-	-	-	-	-	*De novo*	
c.1283G>A	R428Q	3 weeks	EIMFS	Spasms	-	-	-	-	-	-	Unknown	
c.1420C>T	R474C	Day 1	EIMFS		Hyps-like when awake BS in sleep		Spasticity	Tremor	-	-	*De novo*	No (Ohba et al. 2015)
c.1421G>A	R474H	2 weeks	EIMFS	-		-	-	-	-	-	*De novo*	Gain of function (Ohba et al. 2015; Tang et al. 2016; Barcia et al. 2012)
c.1421G>A	R474H	4 days	EIMFS	-	-	-	-	-	-	-	*De novo*	
c.1421G>A	R474H	15 days	EIMFS	-	-	-	-	-	-	-	*De novo*	
c.1421G>A	R474H	2 months	WS	Spasms	-	-	-	-	-	-	*De novo*	

c.1429G>A	A477T	1-2 weeks	EIMFS	-	-	-	-	-	-	-	*De novo*	No (Ohba et al. 2015)
c.1546A>G	M516V	Day 2	EIFMS	-	-	-	-	-	-	-	*De novo*	Gain of function (Rizzo et al. 2016a)
c.1694G>A	R565H	18 years	MTLE	-	-	Enlarged amygdala and HS	-	Cerebellar ataxia Nystagmus	Learning difficulties from childhood	-	Maternally inherited	No (Hansen et al. 2017)
c.1694G>A	R565H	25 years	MTLE	-	-		-			-		
c.1887G>C	K629N	4 months	EIMFS	-	-	-	-	-	-	-	*De novo*	Gain of function (Mikati et al. 2015)
c.1955G>T	G652V	5 months	West syndrome	Spasms	-	-	-	-	-	-	Unknown	No (Fukuoka et al. 2017)
c.2280C>G	I760M	3 days	EIMFS	-	-	-	-	-	-	-	*De novo*	Gain of function (Barcia et al. 2012)
c.2386T>C	Y796H	Median 5.5 years (range 3–8)	ADNFLE	-	-	-	-	-	Psychiatric and behav problems in 2/4	-	Familial AD	Gain of function (Tang et al. 2016; Milligan et al. 2014; Heron et al. 2012; Mikati
c.2386T>C	Y796H		ADNFLE	-	-	-	-			-		
c.2386T>C	Y796H		ADNFLE	-	-	-	-			-		
c.2386T>C	Y796H		ADNFLE	-	-	-	-			-		

												et al. 2015)
c.2386T>C	Y796H	18 months	Sporadic NFLE	-	-	-	-	-	-	--	*De novo*	Gain of function (Mikati et al. 2015)
c.2688G>A	M896I	9 years	Sporadic FLE	-	-	-	-	-	No ID	--	*De novo*	Gain of function (Kim et al. 2014; Milligan et al. 2014; Heron et al. 2012)
c.2718G>T	Q906H	3 months	EOEE	-	-	Severe DM (HL)	-	-	-	-	*De novo*	No (Arai-Ichinoi et al. 2015)
c.2771C>T	P924L	1 month	EIMFS	Spasms	-	-	-	-	-	-	*De novo*	Gain of function (Ohba et al. 2015; Allen et al. 2015; Milligan et al. 2014)
c.2771C>T	P924L	1.5 months	EIMFS	-	-	-	-	-	-	-	Inherited (maternal somatic mosaicism)	
c.2782C>T	R928C	Median 2 years (range 1-15)	ADNFLE	-	-	-	-	-	Psychiatric and behav problems in 5/6		Familial AD	Gain of function (Møller et al. 2015; Tang et al. 2016; Kim et al. 2014; Milligan et
c.2782C>T	R928C		ADNFLE	-	-	-	-	-		-		
c.2782C>T	R928C		ADNFLE	-	-	-	-	-		-		
c.2782C>T	R928C		ADNFLE	-	-	-	-	-		-		
c.2782C>T	R928C		ADNFLE	-	-	-	-	-		-		
c.2782C>T	R928C		ADNFLE	-	-	-	-	-		-		
c.2782C>T	R928C	-	Unaffected	-	-	-	-	-		-	Familial (AD)-	

											reduced penetrance	al. 2014; Heron et al. 2012)
c.2782C>T	R928C	1 year	ADNFLE	-	-	-	-	-	-	-	Familial (AD)	
c.2782C>T	R928C	12 years	ADNFLE	-	-	-	-	-	-	-	Familial (AD)	
c.2782C>T	R928C	15 years	ADNFLE	-	-	-	-	-	-		Familial (AD)	
c.2782C>T	R928C	7 years	ADNFLE	-	-	-	-	-	-		Familial (AD)	
c.2782C>T	R928C	6 years	ADNFLE	-	-	-	-	-	-		Familial (AD)	
c.2782C>T	R928C	5 years	NFLE	-	-	-	-	-	-	-	Unknown	
c.2794T>A	F923I	1 month	EOEE with myoclonic seizures	-	-	Severe DM and HL	-	Choreo-athetosis (2 years).	-	-	*De novo*	Gain of function (Tang et al. 2016; Vanderver et al. 2014)
c.2800G>A	A934T	2 weeks	EIMFS	-	-	-	-	-	-	-	*De novo*	Gain of function (Ohba et al. 2015; McTague et al. 2013; Tang et al. 2016; Ishii et al. 2013; Kim et al. 2014; Barcia et al.
c.2800G>A	A934T	1 month	EIMFS	-	-	-	-	-	-	-	*De novo*	
c.2800G>A	A934T	2.5 months	EIMFS	-	-	-	-	-	-	-	Unknown	
c.2800G>A	A934T	1 month	EIMFS	-	-	-	Spasticity	-	-	-	*De novo*	
c.2800G>A	A934T	8 weeks	EIMFS	-	-	-	Spasticity, hyper-reflexia	-	-	-	Inherited (maternal somatic mosaicism)	
c.2800G>A	A934T	2 months	EIMFS	-	-	-	-	-	-	-	*De novo*	

												2012)
c.2849G>A	R950Q	5 months	EIMFS	-	-	-	Hyper-reflexia	-	Autistic traits		*De novo*	No (Ohba et al. 2015)
c.2849G>A	R950Q	3 years	NFLE	-	-	-	-	-	Psychosis, depression	-	*De novo*	Gain of function (Hildebrand et al. 2016)
c.G2896G>A	A966T	Day 1	Ohtahara syndrome	-	BS	-	-	-	-	-	Paternal isodisomy (autosomal recessive mutation)	Marked gain of function (Martin et al. 2014)

Table 4.8 Published mutations in *KCNT1* leading to epilepsy and other neurodevelopmental disorders. Recurrent mutations are shaded in blue or grey. AD autosomal dominant, ADNFLE autosomal dominant frontal lobe epilepsy, behave behavioural, BS burst suppression, DM delayed myelination, EIMFS epilepsy of infancy with migrating focal seizures, EOEE early onset epileptic encephalopathy, FLE frontal lobe epilepsy, GI gastrointestinal, HL hypomyelinating leucoencephalopathy, hyps hypsarrythmia, ID intellectual disability, MTLE mesial temporal lobe epilepsy, NFLE nocturnal frontal lobe epilepsy, SUDEP sudden unexplained death in epilepsy, WS West syndrome. Adapted from McTague et al Neurology 2018 Jan 2;90(1):e55-e66**.**

In this study I identified patients with identical mutations associated with different electroclinical phenotypes (**Table 4.4** and **Table 4.8**). Such phenotypic pleiotropy (see Chapter 1) is a recurrent theme in the early onset genetic epilepsies, and it is postulated that other genetic/epigenetic for environmental factors may play a role (Zuberi et al. 2011; Lim et al. 2016). Variation of the phenotype caused by *KCNT1* mutations has been reported even within single families, where different individuals may present with either ADNFLE or EIMFS (Møller, Heron, et al. 2015) resulting from the same mutation. This intrafamilial phenotypic variability is also described in *SCN1A*-kindreds, where Dravet syndrome, febrile seizures and a variety of other generalized epilepsies may be reported within the same family (Scheffer et al. 2009). While most of the mutations in this cohort occurred *de novo*, two patients inherited mutations from an unaffected parent. Parental inheritance of disease-associated variants has significant implications for future genetic counselling.

How can an unaffected parent transmit a dominant disease-causing mutation to their offspring? Two possibilities are reduced penetrance and somatic mosaicism. Penetrance refers to the proportion of individuals in a population harbouring a mutation who manifest the disease associated with that mutation (Cooper et al. 2013). If the mutation is present in unaffected individuals within this population, the mutation shows reduced penetrance. This differs from variable expressivity which describes differing phenotypes in affected individuals with the same mutation. Apparent reduced penetrance in *KCNT1*-related epilepsy has been reported previously in a single individual from a family with multiple members affected with ADNFLE due to the R298C mutation (**Table 4.9**) (Møller, Heron, et al. 2015). In addition, the healthy father of a patient with Ohtahara syndrome, thought to be due to a homozygous *KCNT1* mutation (but due to paternal isodisomy for chromosome 9) was found to be heterozygous for the A966T mutation (Martin et al. 2014). Most recently, two siblings with adult-onset mesial temporal lobe epilepsy were found to have a novel mutation that was maternally inherited, although this variant has not yet been functionally validated (Hansen et al. 2017). Reduced penetrance is also well documented in other autosomal dominant focal epilepsies, for example those caused by mutations of *CHRNA4* or *DEPDC5* (Lal et al. 2014; Leniger et al. 2003) . Possible mechanisms for reduced penetrance identified in other disorders such as cystic fibrosis include a mutation-specific effect, where certain mutations are highly penetrant but others less so (Cooper et al. 2013). This seems not to be the case for *KCNT1*, as penetrance appears to vary for the same mutation between different individuals. Other possible mechanisms include altered

effects on protein function in low penetrance mutations. Again, this does not seem pertinent to *KCNT1*, as the mutations identified with lower penetrance have similar gain of function identified in functional studies, albeit in over-expression systems. However, factors which have not yet been explored for *KCNT1* penetrance include modifying effects of polymorphisms within the same gene, or within different genes, which may rescue the phenotype in unaffected individuals. In addition, alterations in gene expression and epigenetic differences between individuals or environmental factors may play a role.

As discussed in Chapter 1, somatic mosaicism has been reported in other genetic early onset epilepsies such as Dravet syndrome, resulting in transmission by an apparently unaffected parent (Depienne et al. 2010). Parental mosaicism has also been previously reported in two cases of *KCNT1*-related epilepsy (Møller, Heron, et al. 2015; Ohba et al. 2015). It is possible that mosaicism may also contribute more widely to variable expression of phenotypes and the difficulties in correlating phenotype with genotype.

Differential expression of alternative *KCNT1* transcripts may also play a role in phenotypic variability. In rodents it has been shown that there are several differing amino-terminus SLACK isoforms under the control of differing promoters (Brown et al. 2008). The original SLACK sequence is denoted as SLACK-B and other transcripts with an alternate exon 1 are termed SLACK-A. In addition, a further transcript was denoted as SLACK-M. All transcripts are highly expressed throughout the brainstem and olfactory bulb and more variably in the cerebral cortex and hippocampus. Interestingly, cortical expression of SLACK-B is restricted to the frontal cortex (Bhattacharjee et al. 2002). Channels derived from SLACK-B versus SLACK-A transcripts have different electrical properties when studied *in vitro* with slow activation in B and rapid activation in SLACK-A (Brown et al. 2008). Therefore conceivably the functional impact of a mutation may be mediated by which isoform is predominantly affected. Lim et al discuss that seizures in ADNFLE may be a result of mutations more affecting SLACK-B isoforms with predominant expression in frontal cortex, whereas disruption of SLACK-A function could result in EIMFS or ADNFLE (Lim et al. 2016). However, although sequences orthologous to the SLACK-A and B isoforms are present within the human *KCNT1* gene, the relative expression and significance of these transcripts has not been shown in humans. To date, all *KCNT1* disease-causing mutations described appear to affect the latter transmembrane domains and carboxy terminus of KCNT1 (**Figure 4-10**), which theoretically should equally impact on all isoforms.

A further layer of functional complexity is the influence of different isoforms on heteromer formation with SLICK (KCNT2) channels. Only the SLACK-B isoform is able to form heterotetramers with SLICK and these channels have markedly different electrical properties and response to protein kinase C (PKC) regulation compared to homomeric SLICK or SLACK channels (Chen et al. 2009; Kaczmarek 2013). The effect of a mutation on channel function may therefore also be mediated by the impact on heteromeric or homomeric channel formation. Again, this is speculative, as although co-expression of SLICK/SLACK channels has been shown with co-immunoprecipitation and co-staining on immunocytochemistry (Chen et al. 2009), this has not been demonstrated in humans. Functional studies of KCNT1 function have largely taken place in oocyte systems where *KCNT2* is not expressed and therefore have studied KCNT1 homomers. In addition, the extent to which mutant and wild-type subunits form tetramers may also influence the functional impact of mutations. In one study, co-transfection of mutant KCNT1 constructs revealed a more marked gain of function than mutant-WT co-transfection, albeit in a heterologous, over-expression cell model system (Rizzo et al. 2016a). Further study in a patient-derived or animal neuronal model could evaluate the effect on tetramer function which might contribute to genotype: phenotype correlation.

KCNT1 tetramers form a transmembrane (TM) sodium-activated potassium channel. Each subunit consists of six TM domains with an extended cytoplasmic carboxy (C-) terminus (Figure 4-10)**.** Most reported mutations (**Table 4.8**), as seen in this study, are in the C-terminus with clustering around the RCK (regulators of potassium conductance) and nicotinamide adenine dinucleotide (NAD) binding domains (**Figure 4-10**). More recently, several mutations have been identified within TM domain 5 and in the pore forming regions between TM domains 4 and 5 (**Table 4.8**), (McTague et al. 2013; Ishii et al. 2013; Kim et al. 2014; Møller, Heron, et al. 2015). This study further demonstrates epilepsy-associated mutations in transmembrane domains.

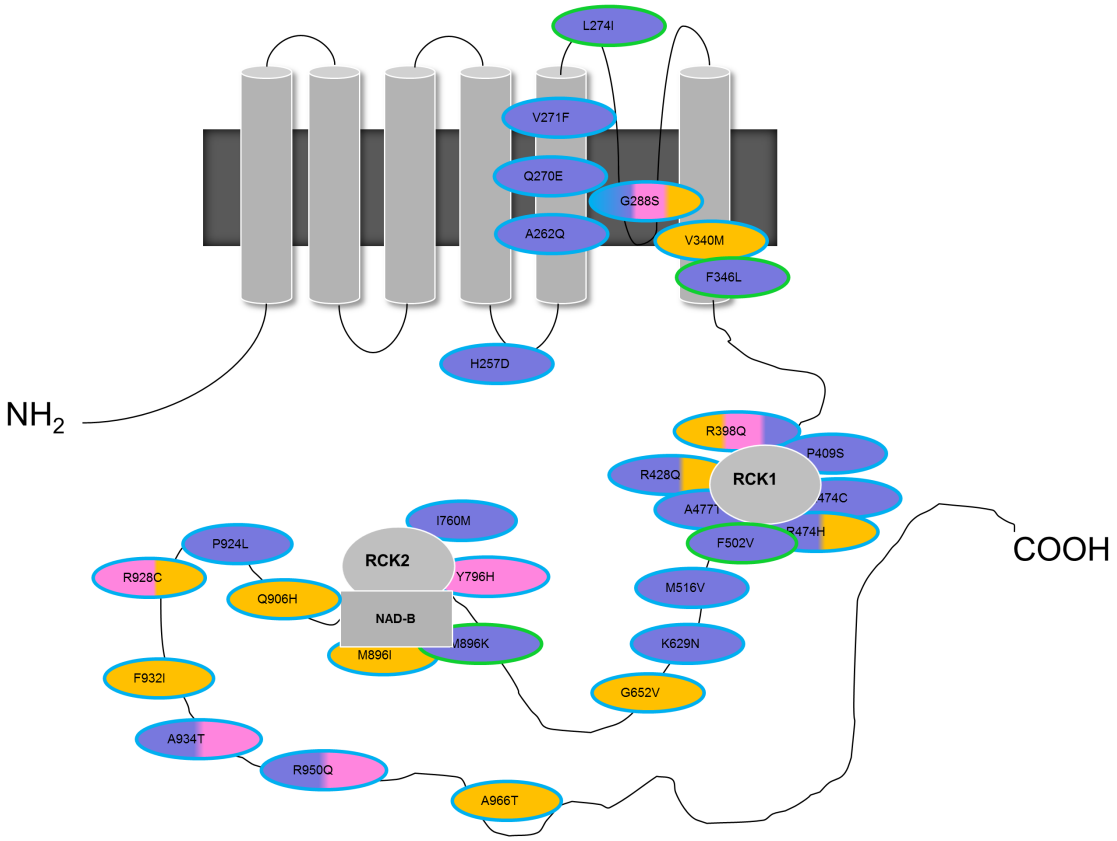

Figure 4-10 Schematic diagram of mutations in *KCNT1* in this and previously published studies. 6 transmembrane domains with a pore-forming region, RCK (regulator of potassium conductance) and NAD-binding domains are shown. EIMFS phenotypes (purple), ADNFLE/NFLE (pink), others [Ohtahara syndrome, leucoencephalopathy, focal epilepsy, EOEE, West syndrome, unaffected] (orange). Mutations giving rise to more than one phenotype are shaded with a combination of the corresponding colours. Novel mutations identified in this study are outlined in green, those identified in previous studies in turquoise. Adapted from McTague et al Neurology 2018 Jan 2;90(1):e55-e66**.**

Although there does not appear to be a clear genotype: phenotype correlation in terms of mutation location, there is clustering of 90% of reported mutations around functional domains (**Figure 4-10, Table 4.8**), namely the pore-forming transmembrane domains (20%), the RCK1 domain (30%), the RCK2 and nicotinamide acid (NAD^+) sensing domains (10%) and the distal carboxy terminus (30%). For example, as discussed in Milligan et al, NAD^+ regulates KCNT1 channels and shows circadian oscillation, which may be associated with the nocturnal occurrence of seizures in some ADNFLE-associated *KCNT1* mutations (Milligan et al. 2014).

Therefore, due to the inter-individual and intra-familial phenotypic variability seen in *KCNT1* disease, genotype: phenotype correlation or prediction of the resultant phenotype based on the mutation is complex. For clinicians making this diagnosis in a patient with EIMFS, it is worth observing that the initial age of presentation, disease course, response to medication, MR brain imaging and EEG findings were similar for both *KCNT1* mutation-positive and negative patients from the EIMFS cohort. However, 5/10 mutation-positive patients with EIFMS presented with a severe movement disorder, as opposed to 2/18 *KCNT1* negative cases. Although movement disorders are increasingly reported in other severe early onset genetic epilepsies (Chapter 1), they have only previously been described in three patients with *KCNT1*-epilepsy (Ohba et al. 2015; Møller, Heron, et al. 2015; Vanderver et al. 2014). As in our study, the movement disorder was described as "choreiform". Further details are limited but both generalised and finger chorea are described. While mechanisms are unclear, it is notable that particularly strong immunoreactvity for SLACK was seen in the substantia nigra, globus pallidus and cerbellar cortex of mouse brain, possibly indicating a role for *KCNT1* in motor control (Rizzi et al. 2016).

Do functional studies of *KCNT1* mutations enable us to better correlate genotype with phenotype? A variety of different model systems have been utilised to determine the functional impact of *KCNT1* mutations (Martin et al. 2014; Ishii et al. 2013; Bearden et al. 2014; Møller, Heron, et al. 2015; Rizzo et al. 2016b; Milligan et al. 2014; Q.-Y. Tang et al. 2016; Evely et al. 2017). Most functional assessments have been performed in the xenopus oocyte system, although several authors have used mammalian cell systems, namely CHO cells (Evely et al. 2017; Rizzo et al. 2016b) as discussed below. The *Kcnt1* null mouse displays altered cognitive function but no epileptic seizures; a knock-in model is not

currently available (Bausch et al. 2015). Most recently, a drosophila model of two recurrent KCNT1 variants has been generated (Ehaideb et al. 2017).

In this study I used data from both protein homology modelling and electrophysiology to evaluate the functional impact of novel *KCNT1* variants. This approach is useful in the assessment of novel variants such as F346L where the CADD score was not significant and further evidence of pathogenicity is crucial. The American College of Medical Genetics and Genomics guidelines for variant classification also use this integrative approach combining evidence from variant segregation, effect on protein, functional studies and presence in control databases to come to a final classification of pathogenic, likely pathogenic, benign or uncertain significance (Richards et al. 2015). For example, F346L is a *de novo* variant which is PS2 or strong evidence of pathogenicity. There is also moderate evidence of pathogenicity (PM2) as F346L does not feature in Exome Sequencing Project (EVS), the 1000 Genomes Project, or ExAc (**Table 4.7**). However, without the electrophysiology studies, this variant would not qualify for final classification as pathogenic by ACMG standards.

The structural modelling performed by Dr Topf and Dr Malhotra suggests anomalous gating or protein instability within the pore-forming region as possible disease mechanisms for the novel mutations F346L and F502V. This information has been particularly useful in understanding the differential response of the F346L variant to quinidine (see below). *In silico* modelling of G288S, suggests a similar functional effect to F502V (Ishii et al. 2013) whilst Y775H is projected to influence sodium sensitivity of the channel (Q.-Y. Tang et al. 2016). *KCNT1* mutations may therefore change protein structure, possibly leading to altered channel function. As reported previously (Martin et al. 2014; Rizzo et al. 2016b; Barcia et al. 2012; Milligan et al. 2014; Q.-Y. Tang et al. 2016)(Table 4.8), the *Xenopus* oocyte model showed that all novel *KCNT1* mutations identified in this study display a gain-of-function effect, with increased current amplitude (**Figure 4-8**). Initially several studies correlated disease severity with the fold-change increase in channel amplitude of gain-of-function (Martin et al. 2014; Milligan et al. 2014). However, in keeping with more recent studies (Kim et al. 2014), such genotype-phenotype correlation was not evident in our study, albeit with smaller numbers of mutations studied. A finding that is common to several studies is that *KCNT1* mutations result in an increased P_o (probability of the channel being open), which may be due to increased mutant channel cooperativity or altered sodium sensitivity (Kim et al. 2014; Q.-Y. Tang et al. 2016). Indeed, in this study, altered

voltage sensitivity of mutant channels was seen, with the rate of activation slowed at higher voltages compared to WT in F346L and V271F. V271F could not be modelled, but the abnormal gating revealed by modelling of F346L may indicate that altered channel dynamics influence the ability of the mutant channel to respond to voltage changes in the same way. Assessment of the effect of sodium removal from the pipette solution revealed a less negative impact on G288S channel amplitude than WT, suggesting altered sodium sensitivity in the mutant (Rizzo et al. 2016b). Recently functional assessment of F932I, a mutation identified in a patient with an epileptic encephalopathy, generalised seizures and severely delayed myelination (**Table 4.8**) was undertaken (Vanderver et al. 2014). Surprisingly, using a CHO model system, a loss of function was noted with reduced channel amplitude and reduced cell surface expression of the mutant construct (Evely et al. 2017). Co-expression of wild-type and mutant constructs indicate a possible dominant negative effect of the mutation. The reasons for this difference from a previous study of this mutation in a xenopus oocyte model (which found a gain of function, altered sodium sensitivity and similar surface expression to WT, although measured by a different method) are unclear (Tang et al. 2016). The authors postulate that these differences may be attributed to their use of a mammalian heterologous expression system, rather than the xenopus oocytes used in ours and many previous studies. Study of a different mutation (G288S) found a similar gain-of-function between CHO cells and xenopus oocytes (Rizzo et al. 2016b; Tang et al. 2016; Kim et al. 2014). The carboxy terminus of KCNT1 has recently been identified as a site of p38 Mitogen-Activated Protein Kinase (MAPK) phosphorylation which regulates trafficking of KCNT1 to the cell surface (Gururaj et al. 2016) . However, previous studies in a CHO cell system, (albeit of non-C terminus variants G288S and M516V), and in a xenopus system (studying several carboxy terminus variants) did not reveal any differences in mutant KCNT1 cell surface expression (Rizzo et al. 2016b; Kim et al. 2014). Further evidence for a gain of function mechanism in *KCNT1*-epilepsy can be derived from a study of human induced pluripotent stem cell (iPSC) derived neurons where the P924L mutation was engineered using nuclease technologies in a control line (Mangan et al. 2015). Details are limited but a gain of function with increased channel bursting was reported. Most recently, a drosophila model which over-expressed two recurrent KCNT1 variants (G288S and R928C) also showed a gain of function with an increase in potassium conductance (Ehaideb et al. 2017). Finally, the phenotype related to the F932I mutation is somewhat “atypical” with generalised myoclonic rather than focal seizures and severely abnormal myelination (**Table 4.8**). This could indicate that LOF variants may be associated

with a slightly different phenotype to EIFMS but that both LOF and gain-of-function results in overall brain neuronal hyperexcitability. To date, no patients with deletions or stop-gain mutations have been identified and many healthy individuals with LOF variants of *KCNT1* are represented in the ExAC and gnomAD databases, but it remains to be seen whether further patients with atypical phenotypes and loss of function mutations are identified. In addition, the complete knock-out mouse does not have an epilepsy phenotype(Bausch et al. 2015).

Overall, this work shows that in patients with severe early onset epilepsy, mutations in *KCNT1* lead to both an increase in *in vivo* channel amplitude and alterations in channel dynamics as revealed by electrophysiology and modelling studies. This study is in keeping with the overwhelming evidence of *KCNT1* mutations leading to a gain of channel function, albeit in non-neuronal, artificial in vitro over-expression models.

A significant remaining question is how *KCNT1* gain-of-function mutations (which would be presumed to lead to neuronal hyperpolarisation) result in epilepsy (Kaczmarek 2013). The altered voltage sensitivity as demonstrated in this study may result in KCNT1 channels opening at more depolarised potentials allowing for a persistent hyperpolarising current. If this predominantly affected inhibitory interneurons, which are richly expressed in the frontal lobes, this could result in interneuronal disinhibition, analogous to the proposed disease mechanism in *SCN1A*-related epilepsy (Bhattacharjee et al. 2002; Yu et al. 2006; Tang et al. 2016). Conversely, more rapid repolarisation in excitatory neurons permitting more frequent and fast action potentials may be a factor in disease pathogenesis (Tang et al. 2016; Lim et al. 2016). These hypotheses were recently further explored in a drosophila model where the R298C variant, previously characterised in xenopus oocytes as gain of function, was over-expressed using a conditional knock-in system in GABAergic inhibitory neurons, leading to increased seizure susceptibility compared to control flies and flies over-expressing wild type *KCNT1*. Therefore, silencing of inhibitory interneurons due to gain of function *KCNT1* mutations could lead to neuronal excitability and epilepsy. In the same study, high levels of mutant *KCNT1* expression in motor neurons was lethal. However low levels (or adult expression) of mutant *KCNT1* in motor neurons did not lead to silencing, but spontaneous synaptic potentials which could be blocked by the calcium channel blocker cadmium. In addition, there was a compensatory increase in the expression of Shaker (a homologue of human *KCNA3*). Therefore, this study shows that there are differential effects of *KCNT1* variants on differing neuronal subtypes and that these compensatory

mechanisms may negatively or positively contribute to the phenotype. A further interesting finding of this study was that over-expression of mutant *KCNT1* variants in motor neurons led to uncoordinated ventral ganglion firing resulting in abnormal larval movement. This may bear some relevance to the movement disorder seen in the patients in this study. Overall, a number of mutation-dependent complex disease mechanisms might be implicated in *KCNT1*-epilepsy.

Recently, quinidine has been identified as a novel therapeutic option for patients with *KCNT1*-related epilepsy. *In vitro* models have shown that quinidine reduced the abnormal increase in mutant KCNT1 channel amplitude (Milligan et al. 2014). In a EIMFS patient harbouring the *KCNT1* mutation R428Q, *in vitro* testing showed a significant threefold gain of function and quinidine sensitivity. Quinidine therapy led to a marked improvement in seizure control with neurodevelopmental gains (Barcia et al. 2012; Bearden et al. 2014). However, in more recent studies patient response has varied and is not always as anticipated by the *in vitro* data (Mikati et al. 2015). Another patient with the R428Q mutation, but with unclassified EOEE rather than EIMFS, did not respond to quinidine therapy. This patient started treatment at a later stage in the disease course (Chong et al. 2016) which may have impacted upon the therapeutic response. Most recently, a patient with West syndrome had a positive response with reduced seizure frequency and improvement in developmental progress but only at a higher dose of 60mg/kg/day (Fukuoka et al. 2017). Although the therapeutic effect may possibly be determined by the specific *KCNT1* mutation, other genetic factors, epilepsy phenotype and drug timing within a "therapeutic window" may also play a role. Indeed, a further study of three more patients recently confirmed that of the eight published patients, the four patients treated at less than 4 years of age responded and those treated after four years of age did not (Abdelnour et al. 2018). Further, in a blinded randomised controlled study of adult patients with ADNFLE, quinidine was not effective and dosages were limited by cardiac toxicity (Mullen et al. 2017). A further explanation for the variability in response is that the xenopus oocyte model where a single channel is studied in isolation, does not adequately recapitulate the situation *in vivo* and therefore may falsely represent the effects of quinidine. In this study, Patient 15 (L274I), Patient 17(F502V) and Patient 18 (M896K) were treated with quinidine (up to 40mg/kg/day) at ages of 2 years, 5 years and 2 years respectively. Only Patient 17 showed a significant response, which correlated with the *in vitro* studies (**Figure 4-9**). The L274I mutation did not show a statistically significant

response to quinidine *in vitro*, which also appears to reflect the clinical response (the patient in this case was treated prior to availability of in vitro data). In contrast, the M896K mutation showed the most marked *in vitro* response to Quinidine and there was indeed felt to be some initial clinical benefit in the patient harbouring this mutation. However, a severe pulmonary vasculopathy resulting in pulmonary haemorrhage emerged. Systemic vasculitis has been previously reported with quinidine treatment (Lipsker, D, Walther, S, Schulz, R, Nave, S, Cribier 1998). Initially there was concern that this might represent an adverse response to quinidine, but recently three further patients with different *KCNT1* mutations, who have not been treated with quinidine, presented with severe pulmonary haemorrhage secondary to massive systemic to pulmonary collateral arteries(Kawasaki et al. 2017). Although *KCNT1* mutations have been associated with Brugada, the expression of *KCNT1* in cardiac and vascular tissue is not understood and the mechanisms remains unclear. The patient harbouring the other mutation which showed blockade by quinidine, V271F, was not treated with Quinidine. Interestingly, the F346L mutation showed no quinidine response at all and this patient was also not treated with quinidine. Although quinidine is a direct KCNT1 blocker, the precise mechanism of blockade is unclear (Yang et al. 2006). It is possible that the disease mechanism for the F346L mutation, perhaps involving abnormal channel opening dynamics as suggested by the homology modelling data, is not modifiable by quinidine.

Overall, the data from this study supports the consideration of a trial of quinidine therapy for patients with *KCNT1* mutations and early onset epilepsy where *in vitro* data have shown a gain of function and blockade by quinidine. However, it should be used with care and in consultation with cardiology colleagues, including a baseline cardiac evaluation, consideration of concurrent medications which affect QT interval and meticulous monitoring during treatment. Larger multi-centre evaluation of clinical utility, patient selection, optimum age of administration and dosing may be helpful in guiding patient management and an international effort would be required to gather sufficient patient numbers in this rare disorder. There are other KCNT1 blockers such as bepridil (Kaczmarek 2013), which reversibly blocks mutant KCNT1 channels *in vitro* at a lower concentration than wild type channels (Rizzo et al. 2016b). However, similar to quinidine, potential cardiac effects and lack of specificity may limit usage in patients and it is not currently available. For true “precision medicine” to be achieved, what is really needed is identification of specific *KCNT1* blockers which lack the non-specific actions of quinidine on

other potassium channels, particularly on channels expressed in the myocardium. This could be investigated in a high-throughput assay using available drug libraries in a xenopus oocyte system. Alternatively, a drosophila model as described above could be used in a high throughput assay, with conditional expression systems allowing the study of effects of drugs in both excitatory and inhibitory neurons. Another model to consider would be a human-derived neuronal model using induced pluripotent stem cells derived from fibroblasts to generate cortical neurons. In addition to shedding light on disease mechanisms (see below), this would also be suited to a high throughput approach, for example using multi-electrode arrays to assess the impact of compounds on channel bursting. Identification of test compounds from a high-throughput system could then be further studied in a knock-in mouse model.

In conclusion, I have shown that heterozygous mutations in *KCNT1* cause a severe early onset epilepsy typically associated with severe neurodevelopmental impact and significant disease burden. Ten of 34 EIMFS patients in this cohort were identified to have *KCNT1* mutations, confirming that it is a major disease gene in this syndrome. Movement disorders appear to be more frequent in *KCNT1*-EIMFS than in EIMFS in general. Otherwise *KCNT1*-EIMFS does not seem to have specific features which distinguish it from the EIMFS electroclinical syndrome in general. However, the reports of massive systemic to pulmonary collateral artery formation in three published cases and one case from this cohort are concerning and should be borne in mind in any *KCNT1* patient with respiratory deterioration or haemoptysis. While the majority of mutations occur *de novo*, inheritance from an unaffected parent is possible due to somatic mosaicism as demonstrated in this study, or reduced penetrance which requires further investigation. This has significant implications for genetic counselling. Importantly, clinicians should not exclude either novel or previously reported variants which are also found in healthy parents. These issues highlight the importance of functional validation of novel variants. As demonstrated, both protein homology modelling and *in vitro* model systems may be used in a complementary approach to investigate variant pathogenicity. Many *KCNT1* mutations including the recurrent mutations have now been validated in over-expression model systems and have indicated, in general, a gain of channel function with increased channel amplitude. One of the challenges following initial gene discovery in rare disorders is whether and how further novel variants in a rare gene continue to be functionally validated without research-based testing pipelines. It could be argued that for a patient with a typical EIMFS phenotype who

is identified to have a heterozygous *KCNT1* mutation located in the pore-forming region or carboxy terminus and predicted to be pathogenic using *in silico* tools, this is very likely to be the disease-causing variant. Functional validation using a xenopus oocyte system would afford the opportunity to assess blockade by quinidine. As in the example of the L274I variant, lack of in vitro response may predict lack of clinical response and allow the patient to avoid a trial of a drug with potentially serious side effects. Unfortunately, the converse is not true, as *in vitro* blockade may not predict clinical response. This likely reflects the limitations of the model, and the research community should now focus its efforts on creating useful models to investigate *KCNT1* variants, as this carries the highest likelihood of identifying better treatments. Several complementary approaches are possible. Firstly, generation of knock-in mouse models of the recurrent *KCNT1* variants would enable a systems-level assessment of mutant *KCNT1* expression with the opportunity to investigate cardiac and vascular tissue in addition to phenotypic evaluation and the opportunity of testing novel compounds. However, an approach which allows the possibility of a human-derived neuronal model would be achieved with iPSC-derived cortical neurons. This would allow investigation of the impact of *KCNT1* mutations in both inhibitory interneurons and excitatory neurons, which would help delineate disease mechanisms, as has already been achieved in Dravet syndrome using an iPSC model (Sun et al. 2016), and provide a platform for high throughput testing of novel compounds as discussed above. Further research is now essential to allow the pursuit of new therapies for this devastating pharmacoresistant group of epilepsies.

Chapter 5 Identification of a novel gene for Epilepsy of Infancy with Migrating Focal Seizures

5.1 Introduction

Over the course of my PhD, I recruited a consanguineous family of Pakistani origin with two affected children to my cohort of EIMFS patients. Although heterozygous *de novo* gene mutations are more commonly reported in the early onset epileptic encephalopathies (see Chapter 1), recessive disease inheritance has been described, often in consanguineous families with multiple affected children (McTague et al. 2015). Indeed, EIMFS due to biallelic mutations in *SLC25A22, PLCB1, ALG1, ALG3, RFT1, QARS,* and *TBC1D24* have been reported (see Conclusion, Chapter 6) (Barba et al. 2016; Poduri, Chopra, et al. 2012; Annapurna Poduri et al. 2013; Milh et al. 2013; Zhang et al. 2014). I therefore hypothesised that these children I had recruited could be affected by a disease gene with an autosomal recessive inheritance pattern and prioritised them for further genetic investigation, using an autozygosity mapping strategy.

Consanguinity is defined as a union between two individuals who are second cousins or more closely related, indicated by a co-efficient of inbreeding of ≥0.0156 (Hamamy 2012). The number of genes shared by two individuals, or the coefficient of relationship, R, for those two individuals, can be established by detailed pedigree evaluation. The co-efficient of inbreeding (*F*) for offspring resulting from that relationship can then be calculated (**Table 5.1**) This represents the probability that two copies of an allele at a locus are homozygous by descent (Spence & Hodge 2000). Consanguineous relationships occur worldwide, with one billion of the global population estimated to live in communities where this is a widespread practice (Hamamy 2012). In the United Kingdom, certain communities have increased rates of consanguineous relationships, such as the UK Pakistani community where 37.5% of Pakistani mothers are married to first cousins in one survey (Sheridan et al. 2013). In addition, complex relationships with multiple loops of consanguinity may exist and marriages restricted to culturally specified groups may contribute (Corry 2014). It is

well established that consanguinity within UK ethnic populations significantly increases the risk of a congenital disorder (Sheridan et al. 2013).

Relationship	Proportion of genes shared	Coefficient of inbreeding (F)	Risk to offspring of autosomal recessive disease*
Siblings or parent-child	1/2	1/4	1/8
Aunt-nephew/Uncle-niece	1/4	1/8	1/16
Double first cousins	1/4	1/8	1/16
First cousins	1/8	1/16	1/32
First cousins once removed	1/16	1/32	1/64
Second cousins	1/32	1/64	1/128

Table 5.1 Coefficient of inbreeding in consanguineous relationships. Adapted from (Bennett et al. 2002) and (Spence & Hodge 2000). *this is a general risk, recurrence risk for specific genes may vary depending on a number of factors including parental carrier status.

Individuals within consanguineous kindreds share many genomic regions of homozygosity due to their descent from a common ancestor. A recessive condition will therefore often be the result of inheriting two disease alleles (one from each parent) which are derived from a mutually common ancestor. Both alleles will be surrounded by regions of homozygosity (Lander & Botstein 1987) (**Figure 5-1**). Lander and Botstein were the first to describe the mathematical model showing that the probability of "homozygosity by descent" at a given locus in a child of a consanguineous relationship is high for rare alleles (Lander & Botstein 1987). This paved the way for autozygosity mapping strategies in consanguineous families as a powerful way to identify disease-causing recessive genes in many conditions, including the early onset epileptic encephalopathies (e.g. *CACNA2D2* and *NECPA1*) (Alazami et al. 2014; Pippucci et al. 2013). Originally, genome-wide microsatellite markers or restriction fragment length polymorphisms (RFLPs) were used to define regions of genomic homozygosity and potential disease loci. However, the advent of microarray technology has allowed a much denser interrogation of the genome, allowing genotyping of hundreds of thousands of single nucleotide polymorphisms (SNPs) per individual (Lander & Botstein 1987; Woods et al. 2004). SNP data can then be used to define homozygous regions which, if shared by affected family members (and different to unaffected family members), can be prioritised. Such potential disease loci can then be further interrogated for disease-causing variants either by direct sequencing of genes contained within the homozygous region or using whole exome sequencing data.

I thus utilised an autozygosity mapping approach to identify potential disease loci in the consanguineous family I had recruited for research. During this process, my supervisor was contacted by Dr Anna Wedell from the Karolinska Institute, Sweden. They had investigated a family with two children affected by EIMFS and had found mutations in a novel gene located within one of the homozygous regions that I had identified in our UK family. A research collaboration was formed and I will present data from all four affected children in the following chapters.

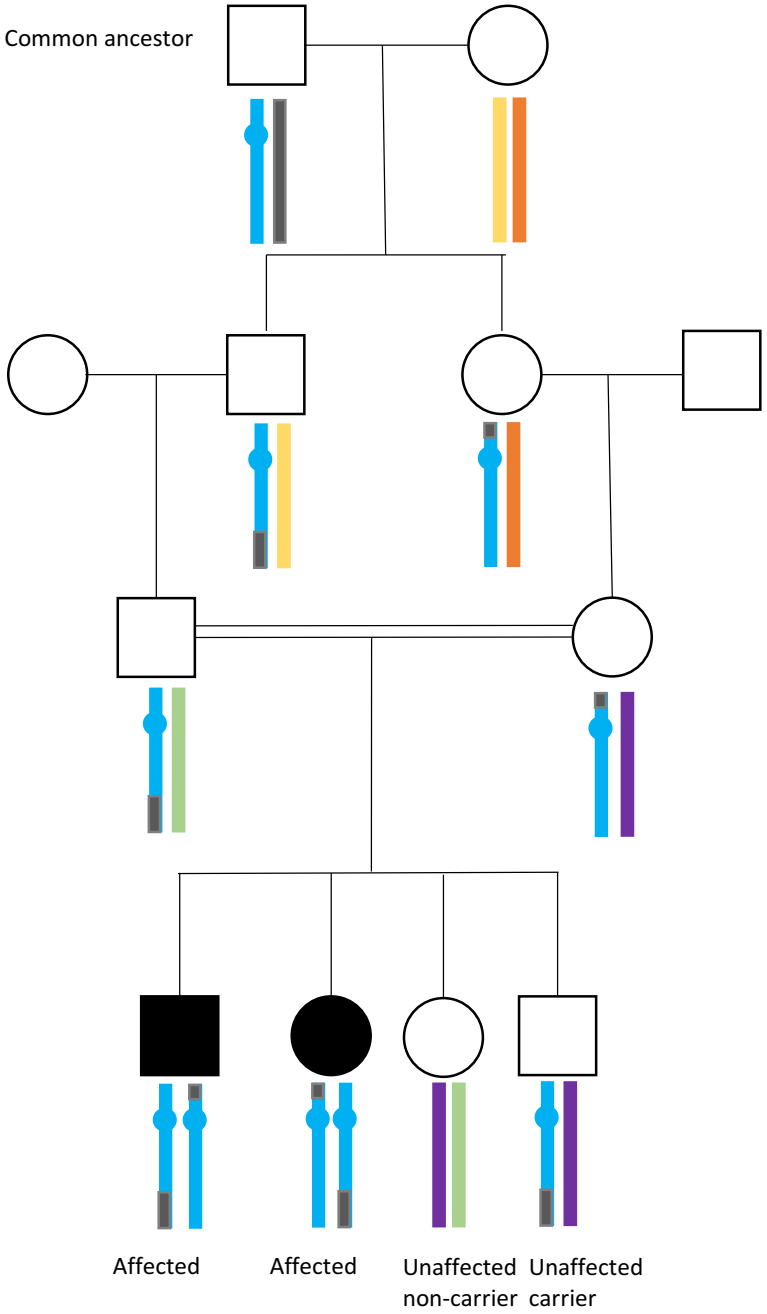

Figure 5-1 The principle of autozygosity mapping. A homozygous region (turquoise) containing a gene of interest (turquoise circle) is inherited from a common ancestor and becomes smaller through successive generations as a result of crossing over (recombination) during meiosis. As a result of a consanguineous marriage (indicated by double horizontal lines), several affected children may inherit two disease alleles by descent.

5.2 Methods

5.2.1 Autozygosity mapping.

In order to identify disease loci, autozygosity mapping, using the Illumina CytoSNP12 array was undertaken (see **Methods 2.4**). Overall, the array genotyped 294,975 single nucleotide polymorphisms across the genome. I manually analysed the data in an excel table and identified regions of homozygosity using colour coding for the genotypes AA, AB and BB. I sorted regions by chromosome and physical position to allow assessment of the size of the homozygous regions. In addition, the UCL Genomics Service used BedTools to analyse the data, confirming the same homozygous regions as the manual method described above.

5.2.2 Whole exome sequencing

Whole exome sequencing was performed for Family 1 by UCL Institute of Neurology Next Generation Sequencing Service using an Illumina platform (see **Methods 2.5**). Data were provided as csv files which I converted to Excel and analysed as described below. The whole exome sequencing methods for Family 2 are described in the Appendix.

5.2.3 Genetic screening of UK EIMFS cohort and other EIMFS/EOEE cases

Throughout this chapter, *SLC12A5* will be used to refer to the gene and KCC2 will be used to refer to the protein, as this is the convention in the literature. I undertook Sanger sequencing in UK patients from the UK EIMFS cohort. Annotations are as described in the NCBI GRCh37.p13 build. The DNA template for the longest protein-coding transcript of *SLC12A5* (ENST00000454036.2) located at Chromosome 20: 44,650,356-44,686,341 was obtained from the Ensembl genome browser. I used Primer3 (http://fokker.wi.mit.edu/primer3/input.html) to design primers (as described in Chapter 2.3.3) to cover all 26 exons and exon-intron boundaries of *SLC12A5*, with coverage across all four protein-coding transcripts **(Table 5.2)**. The standard thermocycling regime of 95^0C for 5 minutes; 40 cycles of 95^0C for 45 seconds, 60^0C for 45 seconds 72^0C for 1 minute; followed by 72^0C for 5 minutes was successful for the majority of exons. Exon 1 required a

longer annealing time of 1 minute and exons 6, 18 and 21 required different annealing temperatures **(Table 5.2**). The same primers were used for sequencing the PCR products (**Methods 2.3.5**).

A further 17 patients who were *KCNT1*-negative from the EIMFS cohort (n=34) were prioritised for *SLC12A5* screening (**Table 5.3**). As described in Chapter 4, for five patients either DNA was not available or parents did not wish further investigation. A variety of approaches were used (**Table 5.3**) including Sanger sequencing and whole exome sequencing (see **Methods 4.2.3**). In addition, several patients were investigated using the GOSH EIEE next generation sequencing panel which includes *SLC12A5* (see **Methods 4.2.2**) and some patients had diagnostic microarray studies as detailed in **Table 5.3**.

In addition, through the collaborations formed for this project, 12 unrelated Swedish patients with EOEE (including 1 patient with EIMFS) were sequenced by whole exome sequencing at the Karolinska Institute. Exome sequencing data (undertaken at Duke University, USA) for a further 19 patients from separate Australian and American EIMFS cohorts were evaluated by collaborators for putative pathogenic variants in *SLC12A5.*

SLC12A5 Transcript number				Primer	Primer Sequence	Annealing temperature ^{0}C	GC rich solution
003	002	001	004				
1F				1F	aagtggccagattcaggaac	60	yes
1R				1R	ctgccccctcaacagac		
	1bF	1bF	1bF	1bF	atacgggatgaggtgagcag	60	
	1bR	1bR	1bR	1bR	cccagcctcctctctgaag		
2F	2F	2F	2F	2F	acaccactgtatgcccaggt	60	
2R	2R	2R	2R	2R	agggagagagcagctgatga		
3F	3F	3F	3F	3F	tgtccccatctcttcctctg	60	
3R	3R	3R	3R	3R	attttcctcccccatcctc		
4F	4F	4F	4F	4F	acctggggtgttcgtaatga	60	
4R	4R	4R	4R	4R	ggtctcatgcttccatcctc		
5F	5F	5F	5F	5F	ggtttggctggtgtttatgg	60	
5R	5R	5R	5R	5R	tctctcttgggccttgatgt		
6F	6F	6F	6F	6F	cttacggcagcccagtgc	62	
6R	6R	6R	6R	6R	cagggagcactgattaactga		
7F	7F	7F		7F	tttttcctaaagcgctgcat	60	
7R	7R	7R		7R	ggggagtttggcagagact		
8F	8F			8F	gcgtccgtgtgtttaaaagg	60	
8R	8R			8R	cccttaatcctgaccgctta		
9F	9F			9F	agagctctggtccccttatg	60	
9R	9R			9R	ctctcttccccatccactca		
10F	10F			10/11F	catctgtctggtctcctgtgg	60	
10R	10R			10/11R	cacctcctgatgggtctgtt		
11F	11F			10/11F	catctgtctggtctcctgtgg	60	
11R	11R			10/11R	cacctcctgatgggtctgtt		
12F	12F			12F	tggaaatccaggcagcact	60	
12R	12R			12R	tcactgtgtggtctctctgg		
13F	13F		7F	13F	ggagagggctgagaaatcct	60	
13R	13R		7R	13R	acggctgcaggattcagata		
14F	14F			14F	tctgtttctgcctccctttg	60	
14R	14R			14R	gaggggatggactggagtaag		
15F	15F			15F	agtcccagcttcagcaacag	60	
15R	15R			15R	ctccttcccaccacccttc		
16F	16F			16F	agctggtgcagtgtagatgg	60	

16R	16R			16R	gtctcctgagccttgcactc		
17F	17F			17F	tatggtgtgtggatggttgg	60	
17R	17R			17R	gagactgtcttcctaagtgtcctg		
18F	18F			18F	agggaaggaggctacaatgg	58	yes
18R	18R			18R	aaaggagcggaaatccagtt		
19F	19F			19F	ggtgttgggagaaccagagt	60	
19R	19R			19R	agagcccctgagtctgacct		
20F	20F			20F	ccctggatctcctcatcaca	60	
20R	20R			20R	ggggccaagaggaaagag		
21F	21F			21F	ctcatgctttcctccgtgtt	58	yes
21R	21R			21R	cctgaggcatcctaaacctg		
22F	22F			22F	agggcatgggtggtgact	60	
22R	22R			22R	ggcagttgagtcctttggag		
23F	23F			23F	gtgcagcttgggtggttt	60	
23R	23R			23R	ggatgccttctgctctcttg		
24F	24F			24F	ctggcagagcaggactcag	60	
24R	24R			24R	tcagagatcccagaggtcgt		
25F	25F			25F	cgactggctccaatcttctc	60	
25R	25R			25R	acagctcagctcttccatcc		
26F	26F			26F	aggtggacgtcagggaatct	60	
26R	26R			26R	ACGGGCACAGGGTCTGTA		

Table 5.2 *SLC12A5* primer sequences and PCR conditions

Patient Cohort Number	Screening Method			Diagnostic chromosomal microarray*	Karyotype*
	Sanger sequencing in research laboratory	NGS Diagnostic Panel*	WES#		
7	-	-	+	N	-
8	+	-	-	N	-
9	-	-	+	N	-
11	+	-	-	N	-
12	+	-	-	-	N
13	-	-	+	N	-
22	+	-	-	N	-
23	+	-	-	N	-
24	+	-	-	N	-
25	+	-	-	N	-
26	+	-	-	N	-
27	+	-	-	N	-
28	+	+	-	11.8 Mb heterozygous deletion Chr 20q11 copy number variant of uncertain significance	-
29	-	+	-	N	-
30	-	+	-	N	-
31	-	+	-	N	
34	+	-	+	N	-

Table 5.3 *SLC12A5* screening of KCNT1-negative EIMFS cohort patients. + test performed, - test not done, N normal. *by GOSH regional or local genetic laboratory # sequenced at Duke University, USA, analysis by Dr McTague

5.2.4 Protein homology modelling- see Appendix

In order to determine structure-function properties of SLC12A5 mutants, protein homology modelling was undertaken by Dr Maya Topf (Birkbeck) (see Appendix for methods).

5.2.4.1 *In situ* mutagenesis to investigate mutant SLC12A5 in an over-expression model

I obtained an expression vector (pCMV6-XL5) containing the full-length human *SLC12A5* cDNA from Origene, USA and validated the sequence by Sanger DNA sequencing. I performed *in situ* mutagenesis was performed using the QuikChange site-directed mutagenesis kit (Agilent, Santa Clara, USA) to generate the three mutations (L311H, L426P, G551D) identified in EIMFS patients (see **Methods 2.6**) using custom-designed mutagenesis primers (**Table 5.4**). I performed PCR-based cloning into a pRK5 expression vector (courtesy of Professor R. Harvey) using custom-designed cloning primers (**Table 5.5**). This was successful for the wild type (WT) DNA and for L311H (see **Methods 2.7**).

For the remaining two mutations, I used custom-designed mutagenesis primers (**Table 5.4**) and a QuikChange II site-directed mutagenesis kit (Agilent Technologies, USA) to mutagenise the wild-type KCC2 in the pRK5 expression vector. In this way I successfully generated plasmids containing each of the three mutations. I performed Sanger sequencing to ensure only the desired mutations had been introduced using cDNA primers (Table 5.6). I transiently co-transfected HEK293 cells (Fugene) with plasmids encoding pRK5-GFP, the human GlyR α2 subunit in a pRK5 expression vector and equal amounts of WT, L311H, L426P or G551D pRK5-KCC2 (**Methods 2.9.2, Figure 5-2**).

Mutation	Forward primer	Reverse primer
SLC12A5-L311H	ttcccgatctgccacctgggtaaccgc	gcggttacccaggtggcagatcgggaa
SLC12A5-L426P	tcctacttcaccctgccggttggcatctacttc	gaagtagatgccaaccggcagggtgaagtagga
SLC12A5-G551D	caggtctttggccatgacaaggccaatggagag	ctctccattggccttgtcatggccaaagacctg

Table 5.4 Mutagenesis primers for the three *SLC12A5* mutations detected in EIMFS patients.

Cloning primer	Primer Sequence
*SLC12A5-Eco*RI	5'-ggcgaattcgccaccatgctaaacaacctgacggac-3’
SLC12A5-SalI	5'-tccgtcgactcaggagtagatggtgatgac-3'

Table 5.5 Cloning primers for PCR-based cloning of *SLC12A5* from pCMV6 topRK5 vector. The recognition sequence for the respective restriction endonuclease is underlined.

cDNA primer	Primer sequence
SLC12A5-c1F	ACCATGCTAAACAACCTGAC
SLC12A5-c1R	CTCCTACTACATGATTTCCAG
SLC12A5-c2F	CATCTCCATGAGTGCAATTGCAA
SLC12A5-c2R	AAACAATGTCACAGAGATCCAGG
SLC12A5-c3F	AAATGAGACGGTGACCACACGGCTA
SLC12A5-c3R	TGGCCTGGCCATCTCATGGGTAATT
SLC12A5-c4F	GTCTACATCAGCTCCGTTGTTCTG
SLC12A5-c4R	TCTCACTGACCTCCCAGCTGAA
SLC12A5-c5F	ACACACCAAGAACTGGAGGCCACAG
SLC12A5-c5R	CCAGATGGATGACAATAGCATCCAG
SLC12A5-c6F	CATGCTCATGCTGCTGCCCTT
SLC12A5-c6R	TCACCTGGACCAAGGACAAGT
SLC12A5-c7F	AGCTGATCCACGATCAGAGTGCT
SLC12A5-c7R	CTGTCACCGTTTACATACAGACCC
SLC12A5-c8F	ACCATCTACTCCTGAGAACCAGGA
SLC12A5-c8R	ACATAGTGTACAGGAGACATCGCGT

Table 5.6 cDNA primers for sequencing of the *SLC12A5* insert. Eight pairs of over-lapping primers were designed to provide full coverage of the cDNA sequence of the gene.

5.2.5 Immunoblotting, surface biotinylation and immunocytochemistry studies in an overexpression model

For detailed methods, see Appendix. In brief, a myc-tagged construct was created from a pCMV6-KCC2 clone (Origene, Rockville, USA). Full-length human KCC2 was cloned into the myc-tagged construct using similar methods to those described in Methods 2.7. This was undertaken by Dr Esther Meyer from the Kurian laboratory. An anti-myc antibody was then used for immunoblotting, undertaken by Dr Juan Zhen from the Reith laboratory, New York.

Biotinylation exploits the strong interaction between avidin and biotin, allowing extraction of biotin-labelled proteins (Elia 2008). Surface biotinylation uses a hydrophilic reagent which cannot cross the hydrophobic plasma membrane, ensuring only cell surface proteins are biotinylated. Streptavidin coated beads can then be used to capture the biotinylated proteins, which are eluted and separated by gel electrophoresis, before immunoblotting to identify the protein of interest, in this case myc-tagged KCC2. Total cell lysate was also analysed by immunoblotting to establish total KCC2 expression.

For confocal microscopy, a pCAGG-KCC2 construct with a FLAG-tagged extracellular epitope was kindly donated by the Levi laboratory, Institut National de la Santé et de la Recherche Médicale, Paris. My collaborator Dr Philip Long (Harvey laboratory, UCL School of Pharmacy) performed *in situ* mutagenesis (see Methods and Appendix) to create the three mutant constructs of interest. Non-permeabilised HEK293 cells were transfected with either WT or mutant constructs, then subsequent immunoblotting (anti-FLAG antibody) allowed assessment of KCC2 cell surface expression. This experiment was repeated with permeabilised HEK293 cells for quantification of total KCC2 expression.

5.2.6 Electrophysiology

For detailed methods, see **Methods 2.10**. In brief, a cell-based system was designed in collaboration with Dr Arnaud Ruiz and Professor Robert Harvey, UCL School of Pharmacy. HEK293 cells were transfected with green fluorescent protein (GFP), the α_2 subunit of the glycine receptor and either pRK5 alone, pRK5-WT KCC2 or pRK5-mutant KCC2. The glycine receptor is essentially a ligand-gated chloride channel and therefore assessment of glycine-induced chloride currents can be used to calculate the reversal potential of chloride (E_{Cl^-}), a

read-out of KCC2 transporter function. The α_2 subunit of the glycine receptor was chosen as it forms homopentameric glycine-gated chloride channels (Hoch et al. 1989) unlike the $GABA_A$ receptor which requires co-transfection of several different subunits to form a functional receptor.

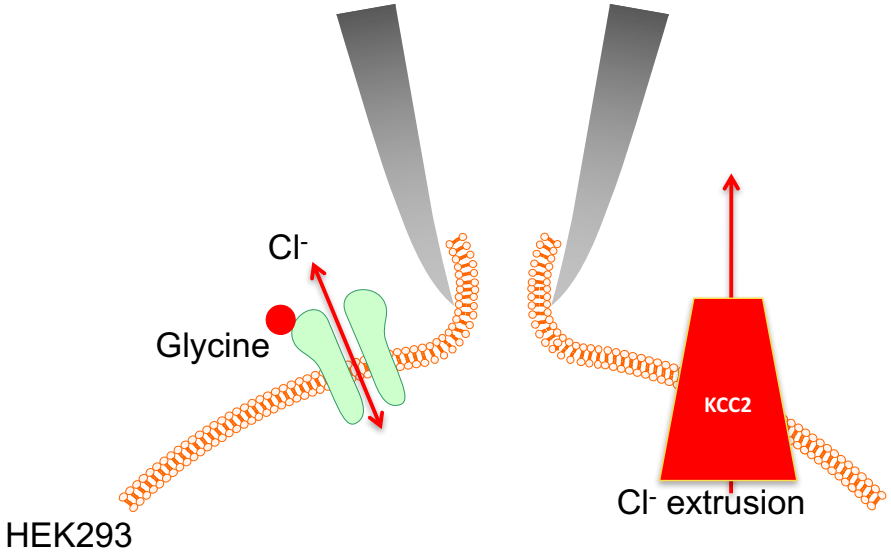

Figure 5-2 Cell system set up for electrophysiology experiments

5.2.7 Zebrafish knockout model

To assess the effects of mutant KCC2 at a whole organism level, a collaboration was formed with Professor Hiromi Hirata (Aoyama Gakuin University, Japan) and Dr Atsuo Kawahara (University of Yamanashi, Japan). Zebrafish experiments were undertaken by Professor Hirata and Dr Kawahara (see Appendix for detailed methods).

5.3 Results

5.3.1 Clinical features of patients with *SLC12A5* mutations

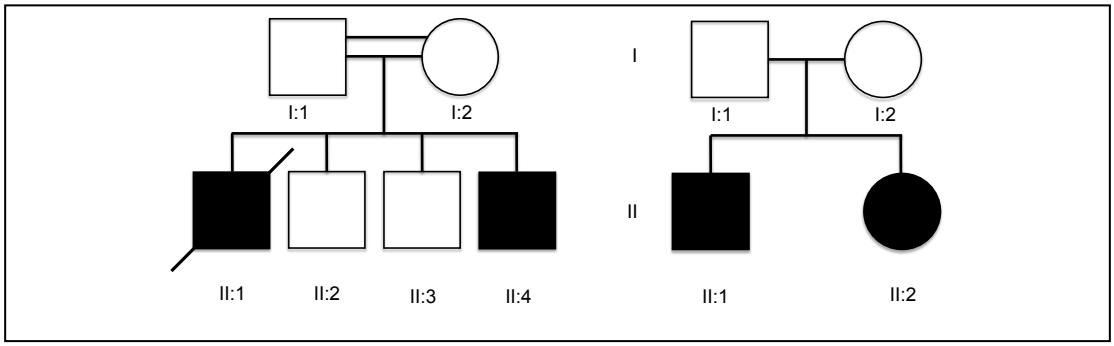

Figure 5-3 Family tree of both families with multiple affected children with EIMFS. Family 1 (Pakistani, left) and Family 2 (Swedish European, right). Squares represent males. Circles represent females. Affected individuals are represented by black shading. Double parallel horizontal bars indicate consanguinity.

In Family 1, the proband (1-II:4) was born following a normal pregnancy and delivery. He is the second child of first cousin Pakistani parents and had an affected older brother (whose history and clinical presentation was re-examined in light of his younger brother's similar presentation) and two unaffected brothers (**Figure 5-3**). He presented at 10 weeks with migrating focal seizures consisting of facial and limb twitching with excessive salivation. Seizures were short-lasting, approximately 20 seconds, and frequent, up to 70 times per day. Prior to seizure onset, developmental attainment was satisfactory, but there was neurological regression after seizure onset. Neurological examination revealed a head circumference of 38 cm (0.4th percentile) with weight on the 10th percentile, global hypotonia, and normal antigravity movements. Phenobarbitone was commenced initially with some reduction in seizure frequency but this was not sustained. Trials of pyridoxine and folinic acid were ineffective, as were levetiracetam and sodium valproate. The addition of topiramate to phenobarbitone led to a period of relative stability, but clusters of focal seizures continued particularly during febrile illnesses. He continues to have short-lived focal seizures characterised by eyelid, facial or arm twitching, which becomes more prolonged and evolves to generalised seizures during intercurrent illnesses. At the last assessment at 17 months, he is significantly developmentally delayed but can fixate visually. There is evidence of ongoing regression with the gradual loss of swallowing skills over recent months. Examination reveals pyramidal signs on the left with microcephaly (head circumference 42 cm at 14 months, below 0.4th percentile).

The proband's oldest brother (1-II:1) had a similar clinical presentation at 6 weeks of age. After a period of early normal development, frequent, migratory focal seizures of the face and limbs occurring in clusters with intermittent evolution to bilateral convulsions were noted. Twitching of the tongue, apnea and drooling were prominent ictal features. Seizures were refractory to multiple antiepileptic drugs and there was no response to pyridoxine. Head circumference at birth was 36 cm (50th percentile) but by 6 months was 40.5cm (below the 0.4th percentile). He died at 2.5 years following a chest infection, increased seizures and cardiac arrest.

In Family 2, two children with EIMFS were born to non-consanguineous Caucasian parents. The following data was derived from clinical information provided by local clinicians. The older male child (2-II:1) was born without complications following an uneventful pregnancy and neonatal period. His early developmental progress was within normal limits. Seizure onset was at 12 weeks of age during an intercurrent illness with fever. The seizure semiology consisted of brief behavioural arrest and eye deviation, followed by afebrile hemiclonic seizures. By 15 weeks of age, numerous and repeated focal seizures emerged, characterised by behavioural arrest, hemiclonic twitching, tonic and atonic features, and eye deviation with clinically migratory seizures. He was admitted to hospital from five to ten months of age due to refractory status epilepticus. During this period there was loss of developmental skills and cognitive decline.

Seizures were resistant to all anticonvulsants. Treatment with intravenous methylprednisolone followed by oral prednisolone at 8 months of age resulted in a noticeable reduction in seizure frequency, with electroencephalographic improvement. He remained on alternate day therapy with oral prednisolone for the next few years, although he continued to have 1-79 seizures per month occurring approximately once per week in clusters. Introduction of the ketogenic diet, at 5 years led to a reduction in seizures to one nocturnal seizure. Here was also an increase in alertness on the diet. Current treatment includes sodium valproate and clobazam. Weaning of the ketogenic diet led to an increase in seizure frequency. Patient 2-II:1 made slow developmental gains. He crawled at 1.8 years of age,and walked independently from the age of 2.8 years. He was able to grasp for objects. He had no dysmorphic features apart from acquired microcephaly (birth head circumference 2.5th percentile, current head circumference 0.1st percentile). He had normal

tendon reflexes but general hypotonia hyperkinetic and dystonic movements. He smiled responsively and made eye contact but was non-verbal.

The younger sister, Patient 2-II:2, currently aged 7.9 years, had onset of focal seizures at 4 months. Hospital admission for 3 months was required due to migrating focal seizures refractory to medication. Treatment with a variety of corticosteroids (IV methylprednisolone, oral prednisolone and ACTH) was not beneficial. At 7 months she commenced the ketogenic diet, with some response. She is globally developmentally delayed with more motor delay than her brother; she is not able to walk or reach for objects and the best motor milestone achieved is sitting with support.

5.3.2 EEG features

Inter-ictal EEG at 4 weeks in patient 1-II:4 revealed slowing with multifocal spikes. Ictal EEG recorded consecutive seizures with central/vertex onset followed by left hemisphere onset associated with facial twitching (**Figure 5-4a**). An EEG at 10 weeks in patient 1-II:1 captured two seizures with eye deviation to the right, chewing automatisms, and right eyelid twitching followed by unresponsiveness with loss of tone. Epileptiform activity over the left temporal region was captured, and other EEGs captured similar seizures with ictal activity in other foci. In Patient 2-II:1, two consecutive EEGs at presentation were normal. Subsequent EEGs revealed status epilepticus with migrating foci, some without clinical correlate. Ictal migration within seizures and between hemispheres was evident (**Figure 5-4b**). Interictal background showed diffuse slowing and multifocal spikes. The EEG in Patient 2-II:2 also showed multifocal spikes with background slowing and ictal migration.

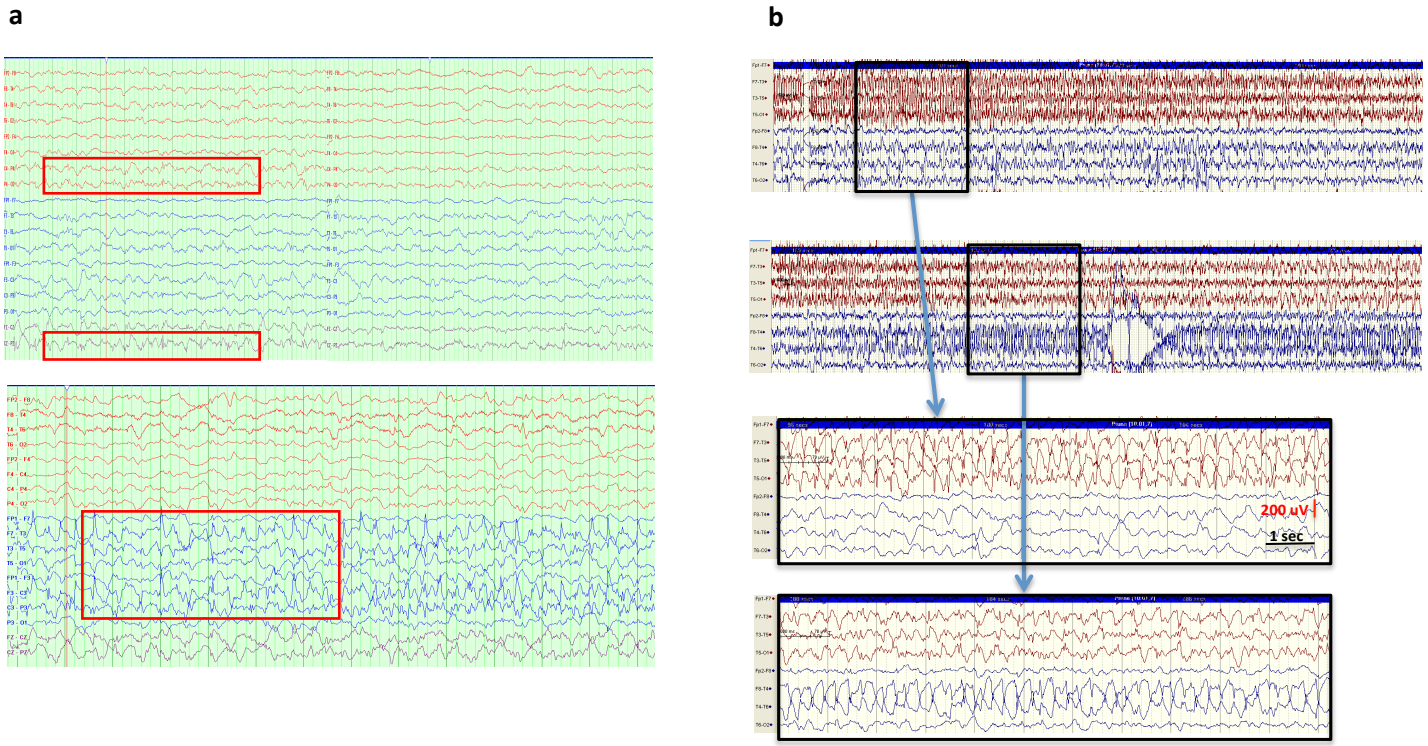

Figure 5-4 Ictal EEG in Patient 1-II:4 (a) and Patient 2-II:1(b). Figure 5-4a: In Patient 1-II:4 the upper (compressed) and lower EEG recording reveal central/vertex and right parietal epileptiform activity (purple/red and boxed in red, upper right figure) that wanes with a return to the interictal state before onset of left centro-temporal ictal activity associated with facial twitching (blue and boxed in red, lower figure). **Figure 5-4b:** The upper two boxes are consecutive EEG segments each 1 minute long. Seizure activity is boxed in black with rhythmic spike-waves evident initially on the left hemisphere (red), then fading and seizure activity starting up in the right (blue) temporal area. Expanded segments below (10 sec) show the spike-wave activity in more detail. Montage: Longitudinal bipolar according to the 10-20 system. Only lateral channels shown. Adapted from McTague *et al* Nat Commun. 2015 Sep 3;6:803.

5.3.3 MRI features

I analysed MRI imaging in the context of clinical data, together with Dr Kling Chong, Consultant Neuroradiologist, Great Ormond Street Hospital. MRI of the brain at eight months in Patient 1-II:4 showed marked delay of myelination and an increase in white matter signal (**Figure 5-5a**). Magnetic resonance spectroscopy (MRS) revealed a relatively reduced N-acetyl aspartate (NAA) peak (**Figure 5-5a**). In Patient 1-II:1 CT brain at 10 weeks showed progressive generalized atrophy compared to CT at 6 weeks. MRI brain at 10 weeks revealed prominent extra-axial CSF spaces with evidence of thin subdural collections (hygromas) bilaterally, the right slightly larger than the left. There were no structural abnormalities. In Patient 2-II:1 MRI brain at 4 months showed delayed myelination and at 29 months, global cerebral atrophy (**Figure 5-5b**).

5.3.4 Autozygosity mapping (Family 1)

Manual SNP array analysis revealed 7 common regions of homozygosity (6-43 Mb in size) in the affected children (**Figure 5-6** and **Table 5.7**). Filtering for rare homozygous, potentially pathogenic variants within these homozygous regions identified 4 genes, which are detailed in **Table 5.7.**

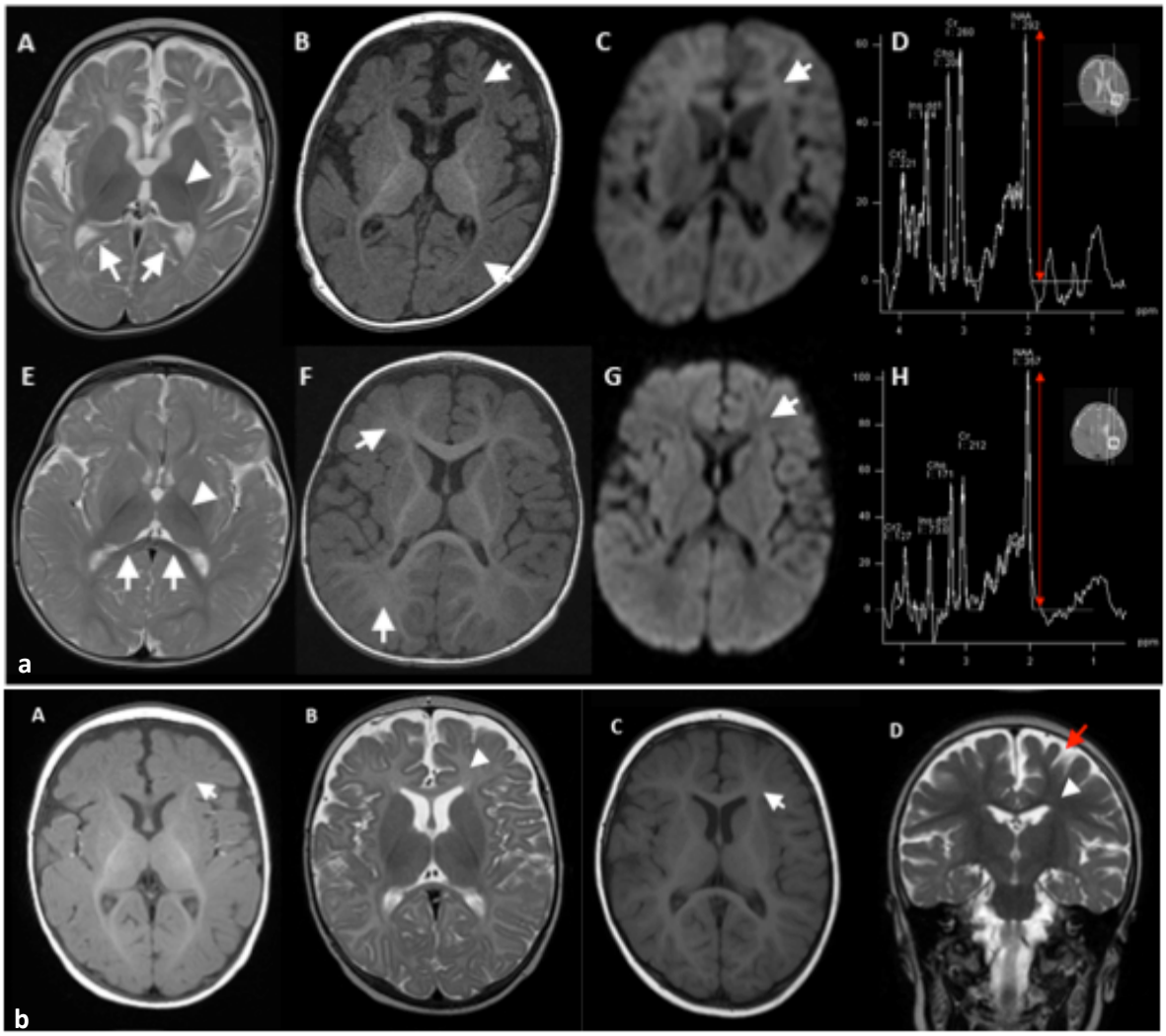

Figure 5-5 Global cerebral atrophy and delayed myelination on MR imaging and spectroscopy in *KCC2*-EIMFS. Figure 5-5a: selected images from Patient 1-II:4 at 8 months (A-D) with normal age-matched control (E-H). Axial T2 sequences (A&E) reveal reduced myelination in the posterior limb of the internal capsule (arrowhead) compared to the normal with lack of myelination in the posterior fornices heading towards the splenium of the corpus callosum (arrows). Axial T1 (B&F) also demonstrates delayed myelination in the frontal and occipital white matter (arrows) compared to normal. Diffusion imaging (C&G) demonstrates increased signal in white matter compared to cortex (arrows). MRS in the occipital white matter (D&H) demonstrates a relatively normal choline (Cho) /creatine (Cr) ratio, but marked reduction in the relative N-acetyl aspartate peak (NAA-red arrow), consistent with delayed myelin maturation**. Figure 5-5b:** Selected images from Patient 2-II:1 at 4 months (A&B) and 29 months (C&D). The axial T1 and T2 images show delayed myelin maturation in the white matter (A arrow & B arrowhead). By 29 months (C arrow and D arrowhead), myelination has progressed. However coronal T2 (D) shows significant prominence of the extra-axial CSF space due to a reduction in overall brain volume (red

arrow) in keeping with global cerebral atrophy. Adapted from McTague *et al* Nat Commun. 2015 Sep 3;6:803.

Name	Chr	Position	Father	Mother	Patient1:II-1	Patient1:II-4	Unaffected sib	Unaffected sib
rs6065453	20	40900992	AB	AB	AB	AB	AB	AA
rs6072674	20	40907054	AA	AA	AA	AA	AA	AA
rs6030107	20	40912801	AA	AA	AA	AA	AA	AA
rs13040321	20	40922844	AB	AB	AA	AA	BB	AB
rs6130099	20	40928973	BB	BB	BB	BB	BB	BB
rs6016741	20	40935515	BB	AB	BB	BB	AB	AB
rs8122334	20	40941198	AA	AA	AA	AA	AA	AA
rs6030128	20	40943696	BB	BB	BB	BB	BB	BB
rs6030129	20	40946744	BB	BB	BB	BB	BB	BB
rs6102774	20	40952914	BB	BB	BB	BB	BB	BB
rs6093621	20	40953408	AB	AA	AA	AA	AB	AA
rs6072686	20	40953812	AB	AB	AA	AA	BB	AB
rs8119920	20	40960421	BB	BB	BB	BB	BB	BB
rs6093624	20	40966154	BB	BB	BB	BB	BB	BB
rs929071	20	40979430	BB	BB	BB	BB	BB	BB
rs6072697	20	40987533	BB	BB	BB	BB	BB	BB
rs4812591	20	40994026	AA	AB	AA	AA	AB	AB
rs6072705	20	40999761	AB	BB	BB	BB	AB	BB
rs10485692	20	41010564	BB	BB	BB	BB	BB	BB
homozygous region continues in two affected children								
rs6019167	20	47057046	BB	BB	BB	BB	BB	BB
rs6122682	20	47063883	AB	BB	BB	BB	AB	BB
rs16993809	20	47070022	AA	AA	AA	AA	AA	AA
rs16993816	20	47076182	AA	AA	AA	AA	AA	AA
rs12480256	20	47082177	BB	BB	BB	BB	BB	BB
rs4810796	20	47088200	BB	BB	BB	BB	BB	BB
rs6125340	20	47092846	AB	BB	BB	BB	AB	BB
rs17347022	20	47097755	AA	AA	AA	AA	AA	AA
rs6019224	20	47103614	BB	BB	BB	BB	BB	BB
rs2869385	20	47111947	AA	AA	AA	AA	AA	AA
rs6125345	20	47119981	AB	AB	BB	BB	AB	AB
rs6019243	20	47126541	AB	BB	BB	BB	AB	BB
rs6095168	20	47141521	AB	AB	BB	BB	AB	AB
rs17347590	20	47141752	BB	BB	BB	BB	BB	BB
rs6122695	20	47142287	AB	AB	BB	BB	AB	AB
rs6019266	20	47147210	BB	BB	BB	BB	BB	BB
cnvi0117575	20	47150301	NC	NC	NC	NC	NC	NC
rs6019272	20	47153207	BB	BB	BB	BB	BB	BB
rs6095179	20	47158886	BB	BB	BB	BB	BB	BB
rs6019278	20	47164777	AB	AB	BB	BB	AB	AB
rs1883888	20	47171338	AB	BB	AB	AB	BB	AB

Figure 5-6 Homozygous region on chromosome 20. The 7 MB region begins at 40,900,992 (top row) and ends at 47,171,338 (bottom row).

Chromosome	Start of homozygous region	End of homozygous region	Size of region (Mb)	Candidate genes from whole exome (homozygous model) before filtering using dbSNP135	Candidate genes from whole exome (homozygous model) after filtering with dbSNP135	Filtering by ExAC/gnomAD	Nature of candidate gene	Nature of mutation in candidate gene	Polyphen2, SIFT Provean2, Mutation Taster, CADD scaled scores (if applicable)
3	156,581,034	172,339,752	16	None	None	-	-	-	-
4	48,283	10,728,759	10	*CPZ, LOC650293*	*CPZ*	Not in ExAC/ gnomAD	Carboxypeptidase Widely expressed in tissues Role in proteolysis and Wnt signalling pathway	Missense	PolyPhen2 = 0 (benign) SIFT= 0.09 (tolerated) Mutation Taster = 1.05 (N-denotes polymorphism) CADD 5.548
					LOC0650293	Not in ExAC/ gnomAD	Pseudogene with one exon only.	Missense	-
6	13,361,927	56,208,751	43	*ZNF187, HLA-H, AK309533, HLA-A, HLA-L, PSORS1C1, HLA-B, MICA, HLA-DRB1, HLA-DQA1, SLC26A8, KIAA0240*	*SLC26A8*	gnomAD: MAF 0.00003 no homozygotes	Testis anion transporter-implicated in spermatogenic failure	Missense	PolyPhen2 = 0.071 (benign) SIFT= 0.81 (tolerated) Mutation Taster =3.06 (N-denotes polymorphism) CADD 9.3601
					PSORS1C1	rs375095896 MAF 0.00002558 in gnomAD, no homozygotes	Psoriasis susceptibility variant, widely expressed, weakly in brain	Frameshift insertion	- CADD 19.09

					MICA *HLA-DQ1*	rs41293539 MAF 0.2145 in gnomAD, frequently homozygous Not in ExAC/ gnomAD	Major histocompatibility complex type 1 related gene, role in immunity Major histocompatibility complex gene, role in immunity	Frameshift insertion Stop loss SNV	- CADD 23.0 -
7	146,711,789	152,600,817	6	*KRBA1, SSPO, ABP1, ATG9B,*	ABP1	rs529653297 (dbSNP142) MAF 0.0002 in ExAc, one homozygote (South Asian)	Metal-binding membrane glycoprotein, mostly expressed in kidney, not expressed in brain.	Missense	PolyPhen2= 0.959 (probably damaging) Provean -1.43 (neutral) SIFT=0.174 (Tolerated) Mutation Taster=0.985901 (D- denotes disease causing)
16	49,866,005	65,809,044	15	None	None	-	-	-	-
20	40,900,992	47,171,338	7	*SLC12A5*	*SLC12A5*	Not in ExAC/ gnomAD	Neuronal-specific potassium-chloride co-transporter	Missense	PolyPhen2 = 0.994 (probably damaging) SIFT = 0.0 (deleterious) Provean = -4.420 (damaging) CADD 27.3

									(deleterious)
21	10,734,842	26,514,597	15	*POTED*	*POTED*	Not in ExAC/ gnomAD	Ankyrin repeat domain-containing protein 21, prostate-, ovary-, testis-, and placenta-expressed gene	4 Missense changes in exon 1	PolyPhen2 = 0.04, 0.001, 0, 0.022 (all benign) SIFT = 0, 0, 0.66 (all tolerated), 0.98 (deleterious) Mutation Taster = 0.001146, 1, 2.2, 3.8 (N-denotes polymorphism) CADD 8.954

Table 5.7 Homozygous regions and filtering of whole exome data for candidate genes in Family 1. Whole exome data were filtered for exonic, damaging (non-synonymous missense, frameshift deletion or insertion, stop-gain or stop-loss), rare (MAF<0.01 in 1000 Genomes and EVS) variants. Variants were then also assessed by presence of other databases, including dbSNP135, ExAC and gnomAD, biological function and predicted pathogenicity using in silico tools Polyphen2, SIFT, Provean and Mutation Taster. MAF mean allele frequency SNV single nucleotide variant.

5.3.5 Whole exome sequencing

Exome sequencing was performed in Patient 1-II:4 from Family 1. An average 32.7-fold coverage of the exome (2x coverage in 93.5% of bases and 10x coverage in 84.0% of bases, **Methods 2.5**). Overall, 21,381 exonic or splice site variants were identified, of which 1173 were non-synonymous or stop-gain. Of these, 262 variants fitted a recessive model (homozygous or compound heterozygous inheritance). My analysis for changes within the 7 identified homozygous regions revealed 20 potential candidate genes. After filtering against dbSNP135 excluding all variants with a mean allele frequency of greater than or equal to 0.01, I found that 9 rare variants in candidate genes remained (*SLC12A5*, *CPZ, SLC26A8, POTED, LOC0650293D, PSORS1C1, MICA, HLA-DQ1* and *ABP*). When the data was first filtered, the next step of variant assessment involved assessing the gene function and pathogenicity as predicted by *in silico* tools Polyphen2, SIFT and Provean. It was possible using this approach to exclude several of the variants on the basis of biological function and known disease associations; for example, *SLC26A8* and *POTED* have roles in testicular and ovarian tissue and are not known to be expressed in brain. The disadvantage of this approach would be falsely excluding a gene whose function or role is unknown. The ExAC and gnomAD databases of normal genetic variation, which have become available since this data was first filtered, were subsequently interrogated for the presence of these variants. They were particularly helpful in excluding the *MICA* variant which was not present in dbSNP135 but present in ExAc and gnomAD, with a MAF of 0.2145 and frequently found in the homozygous state in the normal population.

Based on biological function, absence in databases of normal genetic variation, *in silico* predictions of pathogenicity and data from animal models (see discussion), *SLC12A5* was determined to be by far the most likely and biologically plausible candidate gene for our clinical phenotype of infantile onset epilepsy (**Table 5.7).** The single homozygous variant identified in *SLC12A5,* c.932T>A, results in the missense change L311H (**Figure 5-7**) occurring within the 7Mb homozygous region on chromosome 20. Appropriate familial segregation was verified by Sanger sequencing (**Figure 5-7**)**.** This variant is not reported in established variant databases (including dbSNP137, 1000 Genomes SNP calls, the NHLBI Exome Sequencing Project, ExAC and gnomAD) and is highly conserved (**Figure 5-8**). Further analysis indicated that L311H is predicted to be damaging with a PolyPhen2 score of 0.994

(sensitivity: 0.69; specificity: 0.97), SIFT score of 0.00 (≤0.05 predicted to be deleterious) and Provean score of -4.420 (≤-2.5 is considered "deleterious").

Whole exome filtering performed by our Swedish collaborators is described in detail in Appendix. In brief, the Mutation Identification Pipeline (MIP) weighted sum model (which uses multiple parameters, but emphasizes Mendelian inheritance patterns, conserved, rare and protein damaging variants) was utilised. Filtering resulted in only one gene, *SLC12A5,* with adequate coverage in all sequenced individuals that conformed to autosomal recessive inheritance. *SLC12A5* was also marked out as a likely candidate gene, due to its predicted critical function in neuronal chloride homeostasis and role in GABAergic and glycinergic transmission. The two affected children from Family 2 were found to harbor compound heterozygous mutations of *SLC12A5*, with variants c.1277T>C (L426P) and c.1652G>A (G551D). Sanger sequencing confirmed these changes in both affected siblings from Family 2 (**Figure 5-7)**. L426P was inherited maternally and G551D paternally. Neither variant is reported in established variant databases (including dbSNP137, 1000 Genomes SNP calls, the NHLBI Exome Sequencing Project, ExAC and gnomAD) and both are highly conserved (**Figure 5-8**). L426P is predicted to be damaging using PolyPhen2 (score 1.000, sensitivity: 0.00; specificity: 1.00), PROVEAN score was -6.554 and SIFT score was 0. G551D was also predicted to be damaging, with a PolyPhen2 score of 0.931 (sensitivity: 0.81; specificity: 0.94) and PROVEAN score -4.020.

In addition, no pathogenic variants in genes associated with EIMFS and other early infantile epileptic encephalopathies (see Chapter 1 and Chapter 6) were identified on exome sequencing analysis in any of the affected children from Families 1 and 2.

No mutations were identified in the additional patients who were screened from the UK, Swedish, Australian and American EIMFS/EOEE cohorts, and variants R952H and R1049C (see Discussion) were also not identified in the screened cohorts.

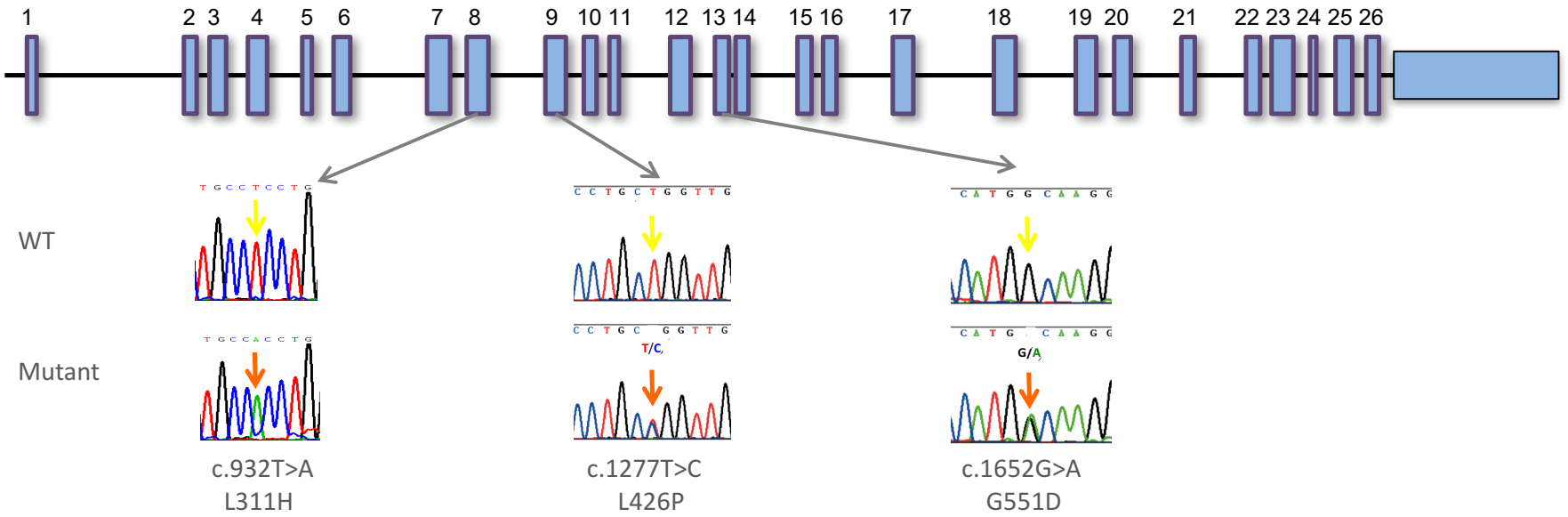

Figure 5-7 Schematic of SLC12A5 gene with mutations identified in four patients. *SLC12A5* consists of 26 exons (blue rectangles). Both wild type (WT) and mutant DNA sequence is displayed. Three point mutations were identified in four patients with EIMFS (wild-type sequence indicated by black arrow, mutated base by orange arrow). The children from Family 1 were homozygous for missense variant c.932T>A (L311H) in exon 8, whilst the two affected Family 2 patients harboured missense mutations in exon 9 (c.1277T>C, L426P) and 13 (c.1652G>A, G551D). Adapted from McTague *et al* Nat Commun. 2015 Sep 3;6:803.

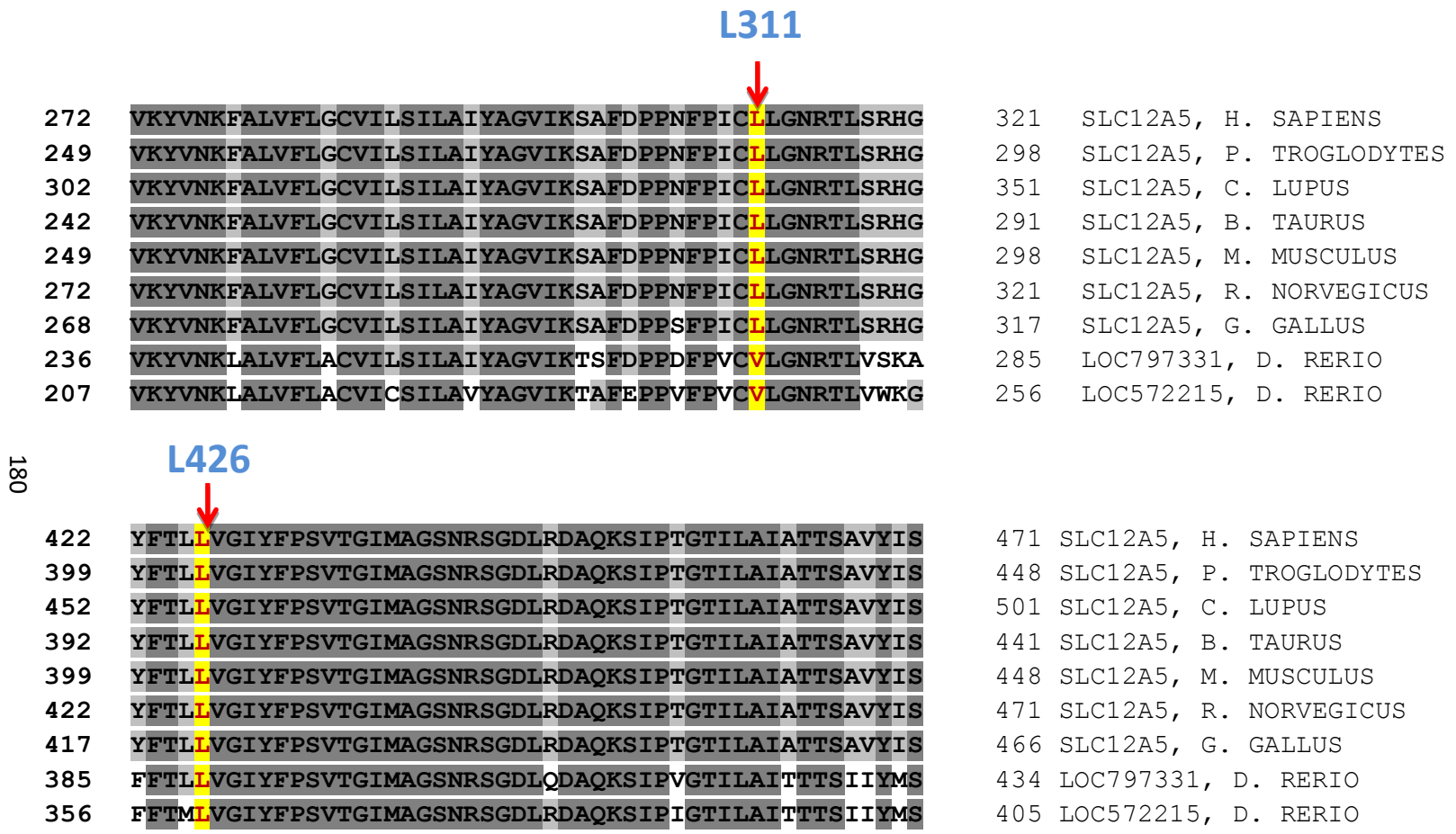
L311
272 VKYVNKFALVFLGCVILSILAIYAGVIKSAFDPPNFPICLLGNRTLSRHG 321 SLC12A5, H. SAPIENS
249 VKYVNKFALVFLGCVILSILAIYAGVIKSAFDPPNFPICLLGNRTLSRHG 298 SLC12A5, P. TROGLODYTES
302 VKYVNKFALVFLGCVILSILAIYAGVIKSAFDPPNFPICLLGNRTLSRHG 351 SLC12A5, C. LUPUS
242 VKYVNKFALVFLGCVILSILAIYAGVIKSAFDPPNFPICLLGNRTLSRHG 291 SLC12A5, B. TAURUS
249 VKYVNKFALVFLGCVILSILAIYAGVIKSAFDPPNFPICLLGNRTLSRHG 298 SLC12A5, M. MUSCULUS
272 VKYVNKFALVFLGCVILSILAIYAGVIKSAFDPPNFPICLLGNRTLSRHG 321 SLC12A5, R. NORVEGICUS
268 VKYVNKFALVFLGCVILSILAIYAGVIKSAFDPPSFPICLLGNRTLSRHG 317 SLC12A5, G. GALLUS
236 VKYVNKLALVFLACVILSILAIYAGVIKTSFDPPDFPVCVLGNRTLVSKA 285 LOC797331, D. RERIO
207 VKYVNKLALVFLACVICSILAVYAGVIKTAFEPPVFPVCVLGNRTLVWKG 256 LOC572215, D. RERIO
L426
422 YFTLLVGIYFPSVTGIMAGSNRSGDLRDAQKSIPTGTILAIATTSAVYIS 471 SLC12A5, H. SAPIENS
399 YFTLLVGIYFPSVTGIMAGSNRSGDLRDAQKSIPTGTILAIATTSAVYIS 448 SLC12A5, P. TROGLODYTES
452 YFTLLVGIYFPSVTGIMAGSNRSGDLRDAQKSIPTGTILAIATTSAVYIS 501 SLC12A5, C. LUPUS
392 YFTLLVGIYFPSVTGIMAGSNRSGDLRDAQKSIPTGTILAIATTSAVYIS 441 SLC12A5, B. TAURUS
399 YFTLLVGIYFPSVTGIMAGSNRSGDLRDAQKSIPTGTILAIATTSAVYIS 448 SLC12A5, M. MUSCULUS
422 YFTLLVGIYFPSVTGIMAGSNRSGDLRDAQKSIPTGTILAIATTSAVYIS 471 SLC12A5, R. NORVEGICUS
417 YFTLLVGIYFPSVTGIMAGSNRSGDLRDAQKSIPTGTILAIATTSAVYIS 466 SLC12A5, G. GALLUS
385 FFTLLVGIYFPSVTGIMAGSNRSGDLQDAQKSIPVGTILAITTTSIIYMS 434 LOC797331, D. RERIO
356 FFTMLVGIYFPSVTGIMAGSNRSGDLRDAQKSIPIGTILAITTTSIIYMS 405 LOC572215, D. RERIO

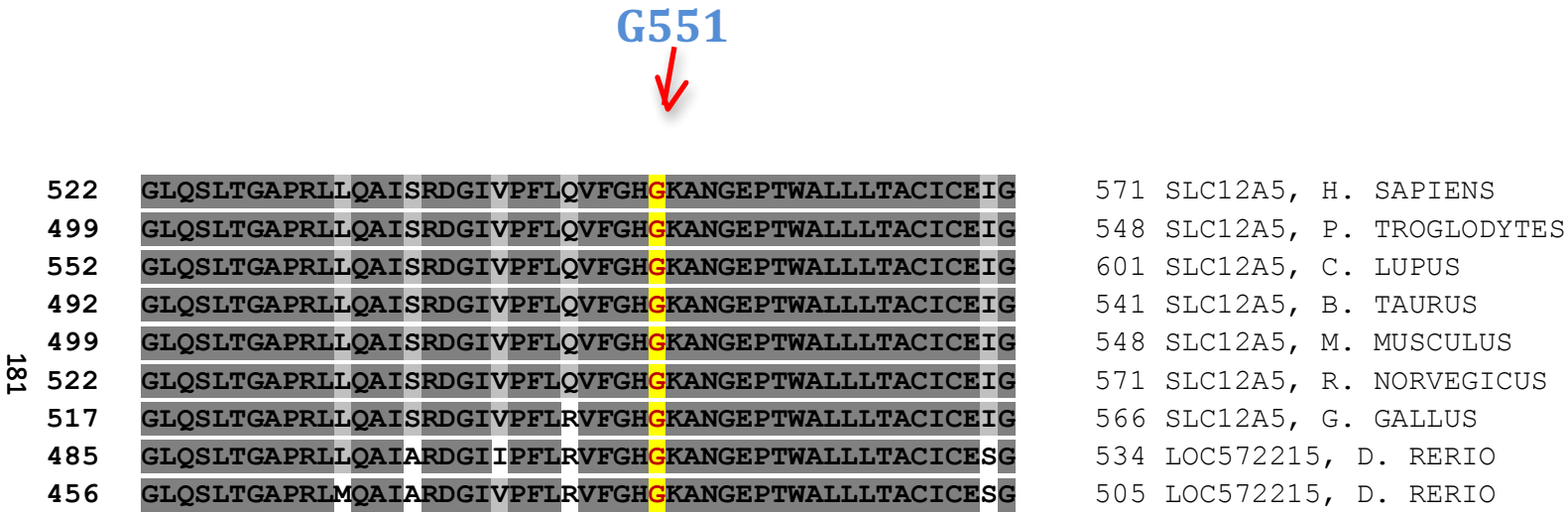

Figure 5-8 Conservation in species for identified *SLC12A5* mutations. The mutated amino acid residues L311, L426 and G551 are highly conserved throughout species. ENSEMBL-id for the different species are: *H. sapiens*, ENSP00000387694; *P. troglydytes*, ENSPTRP00000023337; *C. lupus*, ENSCAFP00000014673; *B. taurus*, ENSBTAP00000018852; *M. musculus*, ENSMUSP00000096690; *R. norvegicus*, ENSRNOP00000062103; *G. gallus*, ENSGALP00000011213; *D. rerio* (loc797331), ENSDARP00000119636; *D. rerio* (loc572215), ENSDARP00000057257. Adapted from McTague *et al* Nat Commun. 2015 Sep 3;6:803.

5.3.6 Protein homology modelling

KCC2 consists of 12 transmembrane (TM) helices interconnected by a series of extracellular and intracellular loops (**Figure 5-9**). Two isoforms KCC2a and KCC2b, differing by an extra 40 amino acids in the N-terminus of KCC2b arise due to differential splicing (Uvarov et al. 2007). The protein can exist as either a monomer or oligomer (Blaesse et al. 2006).

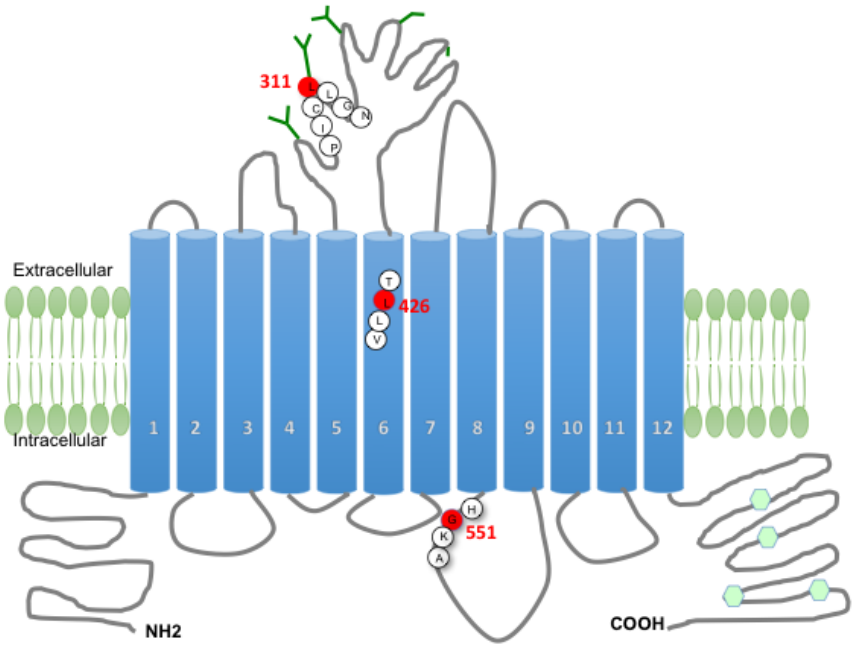

Figure 5-9 Schematic representation of KCC2. The structure consists of 12 transmembrane (TM) helices (numbered blue cylinders) interconnected by a series of extracellular and intracellular loops. Sites of phosphorylation at the C-terminus are depicted as light green hexagons. N-linked glycosylated sites are indicated as dark green Y-shaped structures present at the extracellular loop between TM5 and TM6. The EIMFS mutations are indicated in red circles, located in the extracellular loop between TM5 and TM6 (L311H), within TM6 (L426P) and in the intracellular loop between TM8 and TM9 (G551D). Adapted from from McTague *et al* Nat Commun. 2015 Sep 3;6:803.

KCC2b expression is strongly up-regulated during post-natal development in rodent models and is the most abundant transcript in the adult brain (Uvarov et al. 2007). The variants identified in our patients are present in both isoforms. Computational protein

homology modelling studies were undertaken by our collaborators Maya Topf and Sony Malhotra to study the impact of the pathogenic variants on the structure-function properties of KCC2. L426 is situated in TM6 and is almost universally conserved in the one hundred most similar proteins. Mutation to a proline residue is predicted to disrupt this TM helix (**Figure 5-10**). G551 is located in the intracellular loop between TM8-TM9 (**Figure 5-10**) is also well conserved, and mutation to a much larger negatively-charged aspartate residue may alter the interactions with other residues in the loop region or limit other molecular interactions. It was not possible to accurately model L311H due to a lack of sequence identity for the extended loop region between residues 303 and 407. However, the majority of the homologous proteins possess a hydrophobic residue at the 311 position. Thus, substitution with histidine would be predicted to potentially disrupt hydrophobic interactions, and potentially structural integrity, of the TM5-TM6 loop. Four evolutionarily conserved cysteines (C310, C325, C345 and C354) in the TM5-TM6 region are vital for KCC2 transport activity and are located close to L311 (Hartmann et al. 2010). L311 may form a hydrophobic pocket with a cysteine disulphide bond, in which case L311H would interfere with this process.

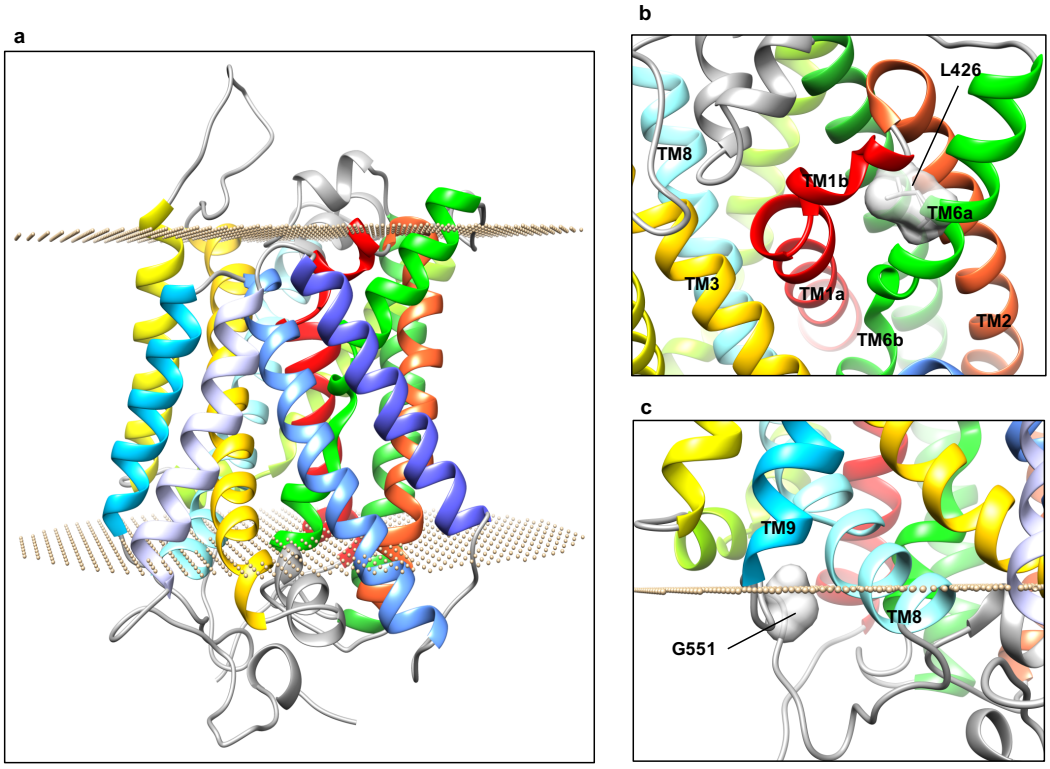

Figure 5-10 Homology modelling of mutations in *SLC12A5*. 5.10a: A homology model of KCC2 showing a transmembrane protein consisting of 12 transmembrane (TM) helices interconnected by intracellular and extracellular loops. **5.10b:** L426 (shown in a surface representation) is located in the unwound TM6 (TM6a). This helix, together with TM1, is pivotal for transporter function. In the L426P mutant, the substitution of a leucine with a proline (not shown) is likely to introduce a kink in TM6, which will result in alteration of the interaction with TM1b. A comparative analysis of different structures of transporters (LeuT, vSGLT and ApcT structures) shows that the conformation of TM1b plays a key role in allowing access to the substrate binding pocket (maintaining a conformation that completely occludes access to the post-synaptic space but only partially occludes access to the cytosolic side). Thus, the presence of a proline in KCC2 TM6 could lead to an alteration of the extracellular occlusion formed by TM1b and TM6. **5.10c**: Our KCC2 model predicts that G551 (shown in a surface representation) is located in the intracellular loop between TM8 and TM9 (residues 539-557). In the G551D mutant, the substitution of the glycine with an aspartic acid – a larger and negatively-charged amino acid – is likely to introduce a distortion in the orientation of TM8. The latter helix contains the putative substrate binding residues A521 and S525, based on homology to the amino acid, polyamine, and organocation ApcT receptor (A287 and T291, respectively (Protein Data Bank Reference 3GIA) (Shaffer et al. 2009). Therefore, introducing an aspartic acid in position 551 could lead to disruption of the binding site thereby affecting substrate binding. Modelling interpreted by Dr Malhotra and Dr Topf. Adapted from McTague *et al* Nat Commun. 2015 Sep 3;6:803.

5.3.7 Evaluation of KCC2 expression by immunoblotting and immunocytochemistry

Using a heterologous expression system, a myc-tagged construct was created by Dr Meyer to assess total and surface expression of KCC2 by Western blotting and biotinylation in the Reith laboratory by Dr Zhen (see Appendix, (**Figure 5-11**). All three mutants displayed significantly reduced cell surface protein expression compared to wild type (WT). Two bands are visible on immunoblotting, with the upper band likely to represent mature glycosylated KCC2 (~130 kDa). There was also a significant difference between the proportion of glycosylated (i.e. mature) versus unglycosylated protein in all three mutants both in in the cell surface protein fraction and in total cell lysate, compared to WT (**Table 5.8**). All variants therefore appear to affect both cell surface expression and post-translational modification of KCC2.

To further evaluate KCC2 cell surface expression, LLC-PK1 cells were transfected with KCC2, using a construct FLAG-tagged at the second extracellular loop by Dr Long in the Harvey laboratory (see Appendix). When permeabilised cells were stained with an anti-FLAG antibody, KCC2 expression in the three mutants was similar to wild type KCC2 (**Figure 5-12**). However, in non-permeabilised cells, reduced immunostaining was seen in cells transfected with KCC2-L311H, -L426P or -G551D versus WT KCC2 transfected cells, again reflecting decreased cell surface expression (**Figure 5-12**).

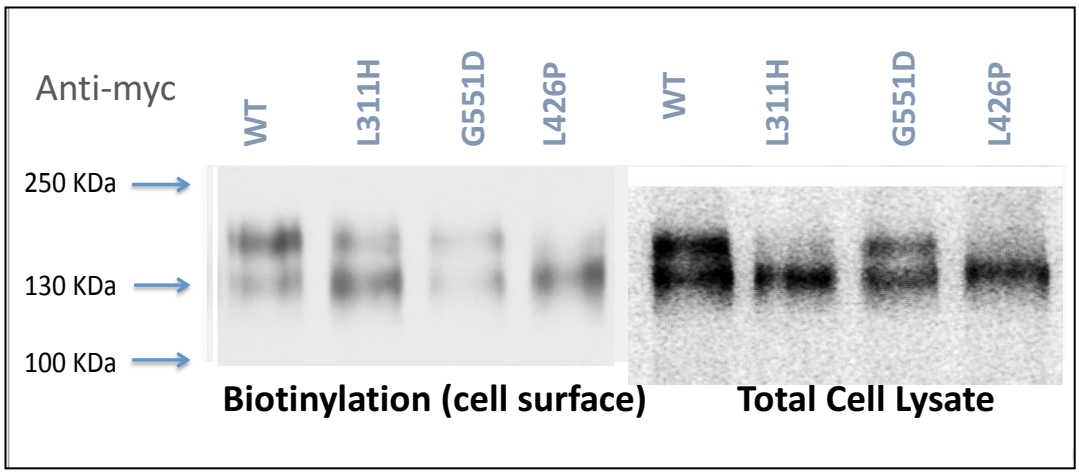

Figure 5-11 Immunoblotting studies including cell surface biotinylation and total cell lysate studies. Two bands are observed for WT and the three mutant KCC2 proteins closely located to each other at ~130kDa and corresponding to glycosylated (upper band) and unglycosylated (lower band) states. Adapted from McTague *et al* Nat Commun. 2015 Sep 3;6:803.

	Glycosylated plus unglycosylated KCC2 at the surface *(fraction of total, % of wild-type)*	*Glycosylated KCC2* *(% of glycoslyated plus unglycosylated)*	
		Surface fraction	*Total fraction*
WT	100[±]±0%	50±13%	43±1%
L311H	34±7%**	22±5%*	17±1%**
G551D	41±10%*	32±7%	38±1%*
L426P	55±13%*	10±3%**	16±4%*

Table 5.8 Quantification of total and glycosylated sub-fraction of KCC2 at the cell surface and in whole cell lysate. All three mutants showed significantly reduced levels of cell-surface over total expression of KCC2 when compared to WT with reduced levels of glycosylated KCC2 protein evident at the cell surface and also in total cell lysates. n=4 * $P < 0.05$, ** $P < 0.005$ (compared with WT, one-sample Student's t-test).

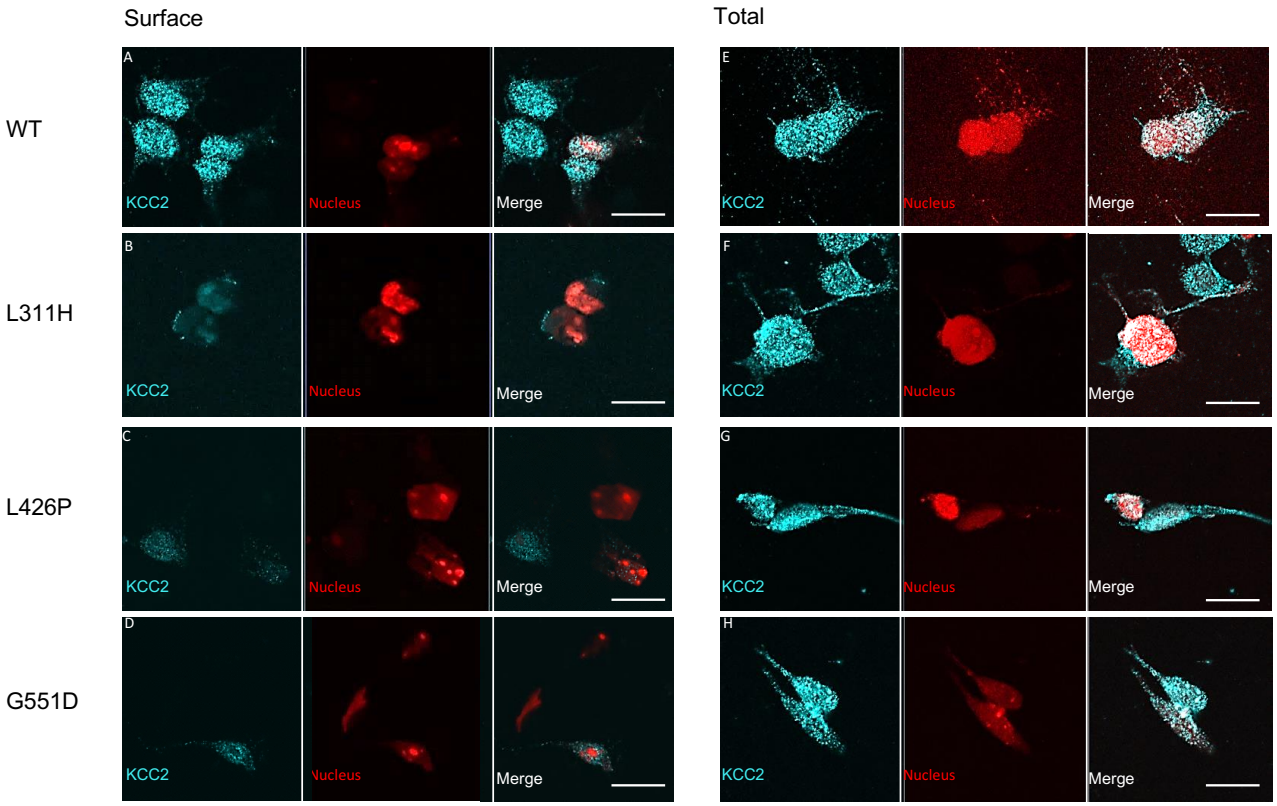

Figure 5-12 L311H, L426P and G551D substitutions impair cell-surface expression of KCC2. HEK293 cells were co-transfected with KCC2-FLAG and HsRed-NLS and immunostained using anti-FLAG and AlexaFluor 488 antibodies. KCC2 WT is detected at the cell surface of intact cells (A), whereas KCC2-L311H, -L426P and -G551D display very little cell surface expression (B, C, D). Expression of KCC2-WT,-L311H,-L426P and -G551D is detected in permeabilised cells (E, F, G, H). Scale bar = 20 µm. Adapted from McTague *et al* Nat Commun. 2015 Sep 3;6:803.

.

5.3.8 Electrophysiology

Given the importance of KCC2 in neuronal chloride homeostasis, I wished to investigate the impact of the EIMFS mutations on chloride transport function. As described above, a cell-based system was devised in collaboration with Dr Ruiz. I performed transient transfection of HEK293 cells with GFP, the α_2 subunit of the glycine receptor (GlyR) and either empty vector, WT KCC2 or mutant KCC2. As described in Methods 2.10, I assisted Dr Ruiz in the experiments and analysis including patching several cells which generated data that was included in the overall data analysis. We were able to measure glycine induced large inward currents (I_{Gly}) at -80mV in GFP positive cells but not in GFP negative, presumably untransfected, cells. A linear relationship between the membrane potential at which the cell was clamped (the holding potential) and the amplitude of I_{Gly} was seen, and a reversal in polarity with changes in holding potential occurred. From the current-voltage, or I-V, relationship we were able to calculate the chloride reversal potential (E_{Cl}^-), that is the membrane potential at which there is no net flow of chloride across the cell membrane and therefore at which it is in equilibrium. In cells transfected with both GlyR α_2 and wild-type KCC2 a more negative, hyperpolarising E_{Cl} was seen than in cells solely expressing GlyR α_2 (**Figure 5-13a**). For the KCC2 mutants, a depolarised E_{Cl} relative to wild type KCC2 was seen. The E_{Cl} was similar in all mutants and resembled the E_{Cl}^- seen in cells without KCC2 (**Figure 5-13b** and **c**), consistent with passive equilibration of Cl^- ions as predicted from the pipette and extracellular solutions. In order to measure transporter function under dynamic conditions, we measured the ability of transfected cells to recover from chloride loading, as described previously (Staley & Proctor 1999). Cells were held at -80 then +40mV while glycine puffs were applied at intervals of 30 seconds to load with chloride (**Figure 5-13d**)**.** When the holding potential was returned to -80mV, the glycine-evoked currents were larger due to the increased driving force provided by higher intracellular chloride. In cells transfected with wild-type KCC2, glycine-evoked currents I_{Gly} returned over time to the initial amplitude consistent with transporter-mediated extrusion of chloride. The rate of I_{Gly} amplitude recovery for the three KCC2 mutants was much longer (**Figure 5-13e** and **f**). In cells expressing L426P and G551D mutants, recovery time was not significantly different from cells without KCC2 (that is, transfected with GlyR α_2 and eGFP alone). This appears to be consistent with near complete loss of KCC2 function. However, the recovery rate for L311H was intermediate between WT and the other mutants, suggesting some residual

KCC2 activity. Therefore, the three missense variants appear to alter E_{Cl^-} with variable abnormal recovery from chloride loading. This impairment of KCC2 function may lead to intracellular Cl^- accumulation in neurons with loss of a hyperpolarizing driving force for $GABA_A$ and glycine receptors.

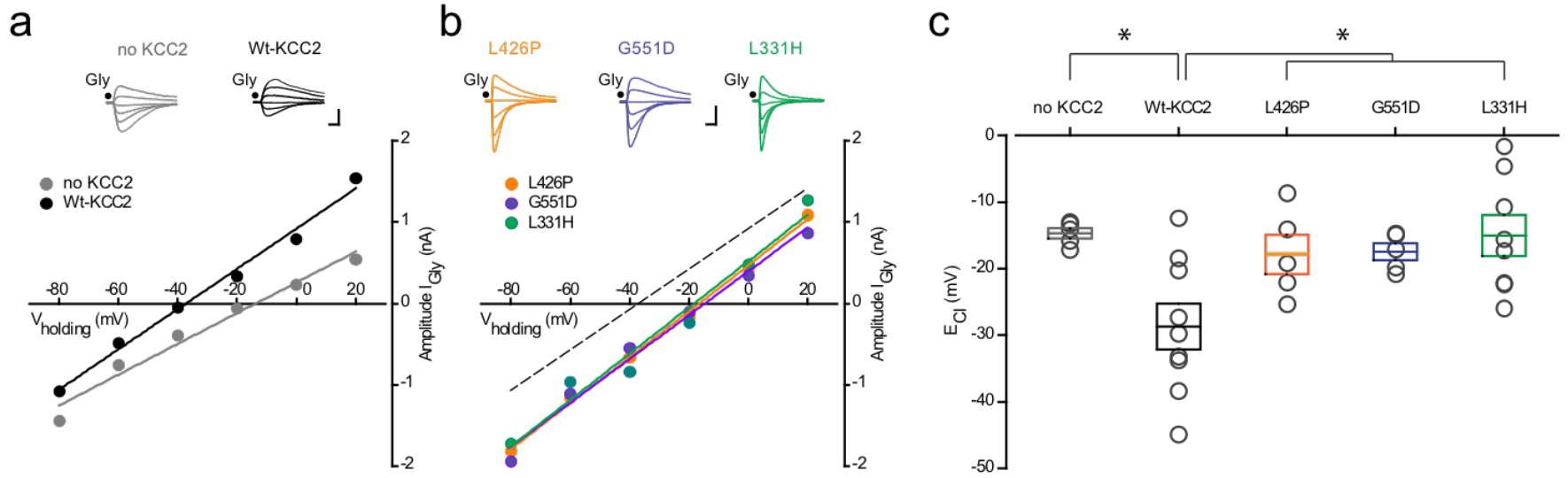

Figure 5-13 Assays of KCC2 function in a HEK293 cell system. 5-13a Examples of I-V relationships in HEK293 cells transfected either with GlyR α_2 alone (no KCC2), or GlyR α_2 with a wild type KCC2 construct. I_{Gly} amplitude was plotted against the holding potential and the intercept of the line of fit of this relation with the abscissa was taken as E_{Cl}. Superimposed traces show examples of glycine-evoked currents recorded from individual cells at different holding potentials (–80 mV to +20 mV). **5-13b:** Examples of I-V relationships in HEK293 cells co-transfected with GlyR α_2 and mutant KCC2, as indicated. E_{Cl} in mutant KCC2 is depolarised in comparison to wild type (fit of I-V relation indicated by dashed-line). Calibration bars for 3a and 3b: 1nA, 1sec. **5-13c:** Summary chart plotting the distribution of E_{Cl} for each cell group: no KCC2: –14.7 $\pm$ 0.8 mV (n = 5), GlyR-KCC2: –29 $\pm$ 3.5 mV (n = 9), G551D: –17.4 $\pm$ 1.2 mV (n = 5), L426P: –17.9 $\pm$ 2.9 mV (n = 5), L311H: –15 $\pm$ 3.1 mV (n = 9); *P = 0.006, one-way ANOVA. Grey symbols represent measurements from individual cells. Boxes represent the mean $\pm$ standard error of the mean. GlyR α_2: glycine receptor α_2, Wt KCC2: wild type K^+-Cl^- co-transporter. Adapted from McTague *et al* Nat Commun. 2015 Sep 3;6:803.

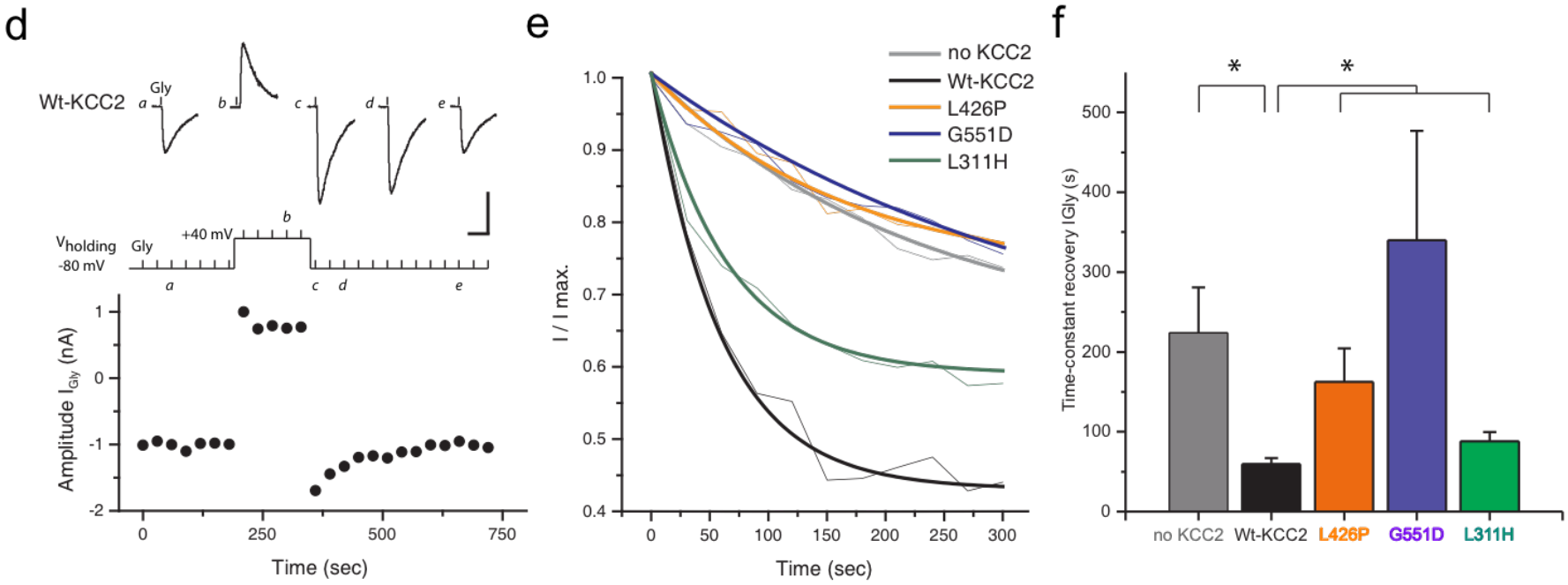

Figure 5-13 continued: 5-13d: I_{Gly} amplitude plotted against time in a HEK293 cell co-transfected with GlyRα_2 and wild type KCC2 and held at different membrane potentials as indicated in the top image. Vertical bars indicate the times of successive glycine applications. Example traces show glycine-evoked currents at times indicated by letters in italic. Calibration bars: 1nA, 300ms. **5-13e:** Rate of recovery of I_{Gly} amplitude after switching back the holding potential from +40mV to -80mV. Fine lines replace symbols and error bars are omitted for legibility. An exponential decay function was used to fit I_{Gly} amplitude ratio in each cell group. **5-13f:** Summary bar graph of the time-constant of I_{Gly} recovery in each group (no KCC2: 224 $\pm$ 56.7 s, n = 6; WT KCC2: 59.5 $\pm$ 7.7 s, n = 13; L426P: 162.5 $\pm$ 42.1 s, n = 4; G551D: 340.1 $\pm$ 137 s, n = 4; L311H: 88.1 $\pm$ 11.5 s, n = 7). *Different from WT KCC2 ($P < 0.01$), ANOVA. Adapted from McTague *et al* Nat Commun. 2015 Sep 3;6:803.

5.3.9 Zebrafish model

In collaboration with Dr Hiromi Hirata (Aoyama Gakuin University, Japan) a zebrafish disease model was generated (see Appendix) to study the impact of KCC2 loss of function. Zebrafish have two KCC2 orthologues, KCC2a and KCC2b (due to ancestral gene duplication). TALEN-mediated genome editing was undertaken to generate knockout zebrafish models. An 8-bp deletion was induced in exon 4 of *KCC2a* to disrupt *KCC2a* and similarly, a 5-bp deletion was induced in exon 4 of *KCC2b* to disrupt *KCC2b*. A phenotype was not seen in neither single KCC2a nor KCC2b knockout zebrafish with normal survival into adulthood. A KCC2a-KCC2b double knockout zebrafish model was then generated, and tactile-induced motor behaviour was assessed. Wild type zebrafish larvae at 2 days post-fertilization (dpf), showed a typical escape swimming response upon touch, with rhythmic side-to-side contraction of the trunk. In contrast to wild type, the KCC2a-KCC2b double knockout zebrafish showed abnormal jerky spasmodic movements during the escape response.

5.4 Discussion

SLC12A5 encodes KCC2, the neuronal-specific potassium chloride co-transporter which is a member of the cation-chloride co-transporter (CCC) family that includes NKCC1 (Payne et al. 1996). KCC2 may exist in monomeric or oligomeric forms (Blaesse et al. 2006). Until pancreatic expression was demonstrated in a recent study (Kursan et al. 2017), KCC2 was thought to show specific neuronal expression. Of note, hypoglycaemia was not reported for any of the patients in this study although two of the patients required nasogastric or gastrostomy feeding and therefore did not have significant periods of fasting. In the central nervous system it is expressed in mature neurons from all layers of the cortex, CA1-4 layers of the hippocampus and the cerebellum (Chamma et al. 2012) (**Figure 5-14**).

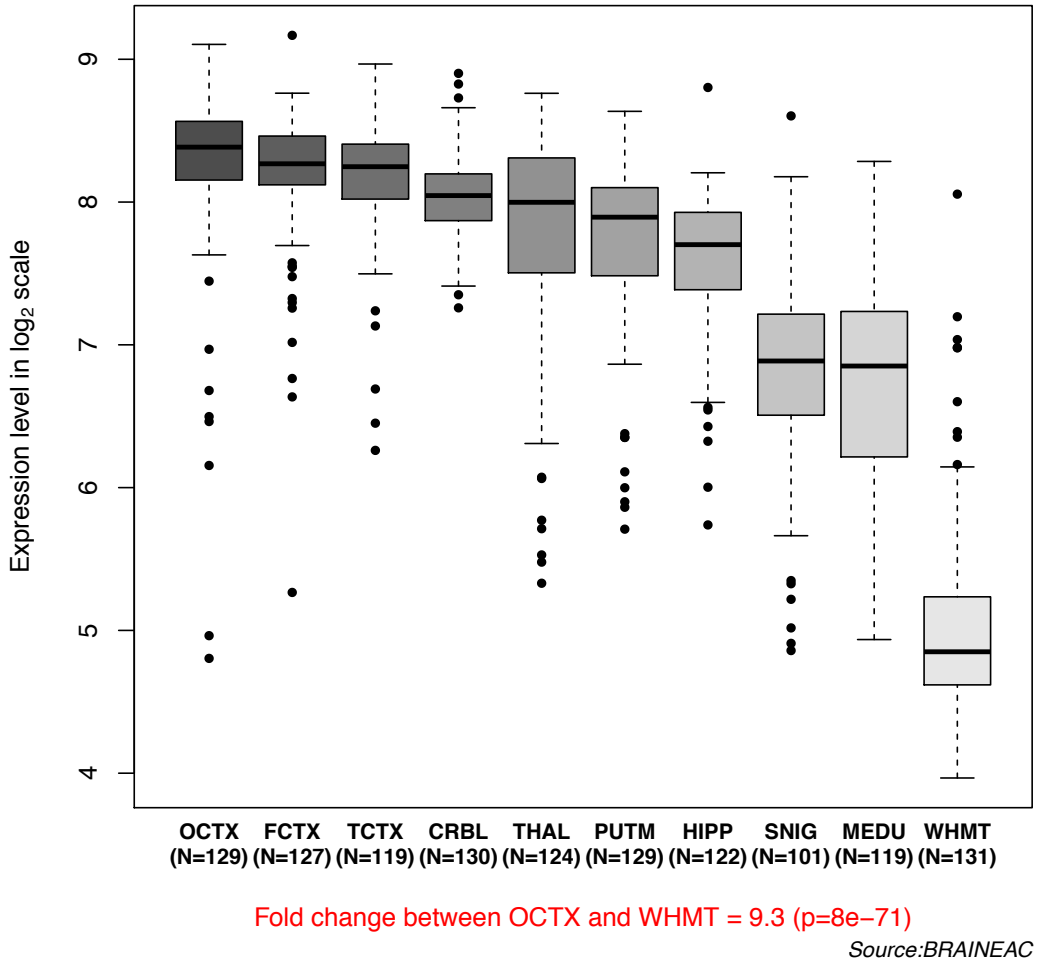

Figure 5-14 *SLC12A5* (transcript variant 2, KCC2b) expression across the human brain. *SLC12A5* is highly expressed in the cerebral cortex, cerebellum, basal ganglia and hippocampus, with levels in the cerebral cortex nine times higher than the intralobular white matter. Data derived from UK Brain Expression Consortium server (http://www.braineac.org), a repository of RNA expression data from 134 normal human brains. OCTX occipital cortex, FCTX frontal cortex, TCTC temporal cortex, CRBL cerebellum, THAL thalamus, PUTM putamen, HIPP hippocampus, SNIG substantia nigra, MEDU medulla, WHMT intralobular white matter.

KCC2 is the major extruder of chloride in neurons and thus mediates the inhibitory effects of GABA/glycine. In the presence of low intraneuronal chloride levels, the binding of GABA/glycine to their receptors results in an influx of chloride and subsequent hyperpolarization, thereby contributing to neuronal inhibition (**Figure 5-15**) (Rivera et al. 1999).

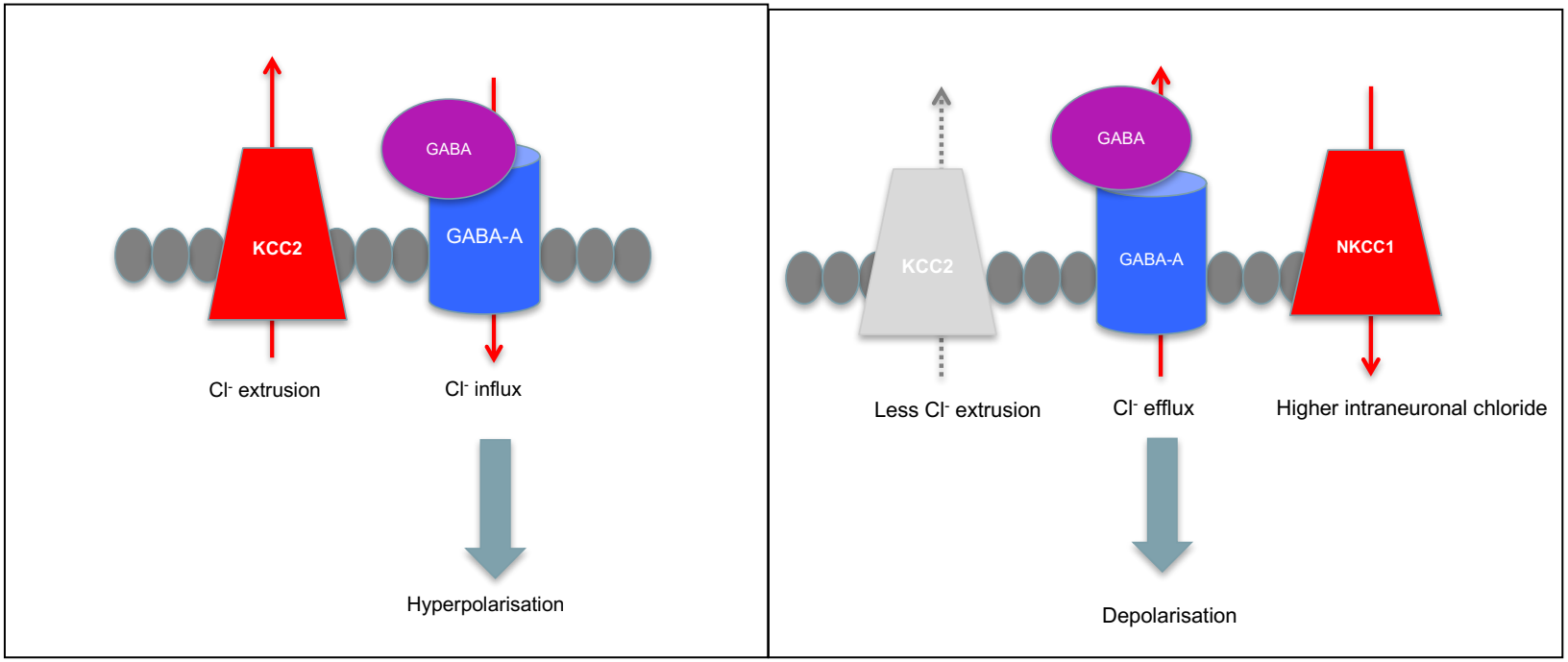

Figure 5-15 Schematic representation of the function of KCC2. In mature neurons (left panel), KCC2 maintains low intraneuronal chloride thus with GABA binding, there is chloride influx leading to hyperpolarization. In immature neurons/pathological states such as post-hypoxia (right panel), low KCC2 and higher NKCC1 expression lead to higher intraneuronal chloride, so GABA binding results in chloride efflux, contributing to depolarization (Vanhatalo et al. 2005; Kahle et al. 2008; Ben-Ari et al. 2012)**.**

KCC2 is thought to be integral to the "developmental switch", a concept whereby GABA and glycine switch from depolarizing to hyperpolarizing neurotransmitters. This conversion is purported to result from a gradual decrease in the chloride electrochemical equilibrium potential (E_{Cl}) of developing neurons, associated with an up-regulation of KCC2 and a downregulation of NKCC1 (Vanhatalo et al. 2005; Ben-Ari et al. 2012). In addition to its critical role governing neuronal inhibition, KCC2 also has a role in early brain neuronal and network development (Blaesse et al. 2009; Hübner et al. 2001).

Although the findings of this study represent the first recessive disease-causing mutations in *SLC12A5*, two independent groups previously identified rare heterozygous variants in the carboxy terminus domain of *SLC12A5* as putative disease-susceptibility alleles for idiopathic generalised epilepsy and febrile seizures. Enrichment of two rare non-synonymous KCC2 variants was identified in a cohort of patients with idiopathic generalized epilepsy (IGE) (Kahle et al. 2014) compared to a cohort of healthy controls. The heterozygous variant R1049C was identified in three individuals with IGE (inherited from an unaffected mother in two cases) and in one control patient with no family history of IGE. The second variant identified, R952H, was identified in five IGE cases but also in five controls. For all three patients where parental DNA was available, the variant was found to be inherited from an unaffected parent. An independent research group (Puskarjovet al. 2014) also identified the variant R952H, but in a family with febrile seizures affecting multiple members of the pedigree. In 3/4 probands where DNA was available, the variant was identified as a heterozygous change. Affected individuals had infrequent febrile seizures (1–3 brief episodes on average) occurring between 12 months and 2.5 years of age. The variant was inherited from an affected mother who had inherited the change from an unaffected grandparent. Functional assessment of the impact of the R952H variant revealed decreased cell surface expression and altered transporter function in both studies, albeit in over-expression systems (Kahle et al. 2014; Puskarjov et al. 2014). In addition, an alteration in the ability of R952H-KCC2 to induce dendritic spine formation in cultured neurons from KCC2 knockout mice was seen (Puskarjov, Seja, et al. 2014). R1049C did not result in altered cell surface expression and had a similar impact on $E_{glycine}$ to R952H when solely expressed, but reduced impact when co-expressed with WT KCC2 in an attempt to mimic the *in vivo* status of the variant (Kahle et al. 2014). Interestingly, both R952H and R1049C were shown to have decreased serine 940 phosphorylation, a major regulatory mechanism for KCC2 expression (see below) (Kahle et al. 2014). Subsequently, a further paper from the

same group examined large cohorts of individuals with autistic spectrum disorder (ASD) and schizophrenia and found an enrichment of the R952H and R1049C variants, and a further C-terminal domain variant, R1048W, in the patient cohorts when compared to controls (Merner et al. 2015). Of note R1048W, while closely located to R1049C and predicted by *in silico* tools to be pathogenic, has not undergone functional validation. Overall studies to date have shown that these rare non-synonymous variants are found in the heterozygous state in both healthy carriers and for some variants in unaffected transmitting parents as well as in individuals with IGE, febrile seizures, ASD and schizophrenia. The clinical significance of these variants remains yet to be fully understood, but it is possible they represent susceptibility alleles within a complex genetic framework that contributes to the multifactorial aetiology underpinning these epilepsies. To investigate these variants further, larger cohorts of patients with IGE from international consortia could be interrogated to see if these findings are replicable in larger populations. However, to fully understand the contribution of these variants to epilepsy, we would need to study them in better model systems. One possible way that this could be achieved is by generating a knock-in mouse harbouring these reported variants. Alternatively it would be interesting to generate cortical neurons from an IGE patient-derived iPSC with the R952H variant in tandem with an age-matched and CRISPR-corrected control as well as an unaffected family member with the same variant , to assess the impact on transporter function and dendritic branching in a human model system

Since our identification of biallelic disease-causing mutations in *SLC12A5* (Stödberg et al. 2015), five similar patients with EIMFS or EIMFS-like phenotypes have been described (Saitsu et al. 2016; Saito et al. 2017). The clinical features are in keeping with our description of a classical EIMFS phenotype (**Table 5.9**). One patient (Patient 4 in **Table 5.9**) had clinical features in keeping with EIMFS but early ictal EEGs were not available to make a formal diagnosis. In keeping with our patients, cerebral atrophy and delayed myelination was seen on MR brain imaging. However, some additional imaging features were also noted in these patients. Unilateral hippocampal sclerosis was noted at the age of four years (Saito et al. 2017). In another patient who was imaged at 10 and 20 years of age, cerebellar atrophy and bilateral hippocampal atrophy with increased signal on FLAIR imaging was seen (Saitsu et al. 2016). It is unclear whether this latter case represents long-term radiological sequelae of *SLC12A5*-EIMFS as, except for this case, the oldest age at reported imaging is 4 years. Focal MRI changes have only rarely been described in EIMFS (Fasulo et

al. 2012; Coppola et al. 2007) as discussed in Chapter 2 and it is not clear whether this may be a secondary phenomenon related to frequent focal seizures or due to underlying aetiology. While most reported patients showed severe neurological impairment, one patient achieved independent ambulation and others regained some neurodevelopmental skills with seizure control (**Table 5.9**). This is also in keeping with our patients, indeed Patient 2-II:1 walked and also made some developmental gains.

The type of the mutations identified in these five further cases is of interest (Saitsu et al. 2016; Saito et al. 2017). Three of the patients harbour loss of function (LOF) variants in *SLC12A5,* namely a splice site mutation leading to an in-frame deletion with loss of exon 3 in two individuals, and a three base-pair deletion leading to an in-frame loss of one amino acid in another. Both these LOF variants occur as compound heterozygous variants in conjunction with a missense variant (**Table 5.9**). This lends further weight to our assertion that the disease mechanism in *SLC12A5*-epilepsy is related to loss of normal transporter function. As in our cases and in contrast to the C-terminus variants discussed above, the presence of a heterozygous variant in both parents and siblings does not seem to confer disease susceptibility in these individuals. While all previous mutations including those detected in our cases have been inherited from unaffected parents, one of the variants in a patient bearing compound heterozygous mutations was *de novo* (Saito et al. 2017).

Electrophysiological assessment of these newly reported *SLC12A5* variants in a heterologous system, where cells were co-transfected with different mutant constructs to recapitulate the compound heterozygous *in vivo* state, demonstrated that the mutants led to a depolarised E_{Cl^-} compared to wild type, albeit not to the same degree as the untransfected cells without KCC2. This partial loss of transporter function with depolarized E_{Cl^-} (Saitsu et al. 2016) is in keeping with our study. However, they did not identify a deficit in surface expression using both confocal microscopy, surface biotinylation studies and immunoblotting. It may be that these variants do not affect transporter trafficking to the same degree as we observed for our mutations. The newly described mutations are located in the N-terminal domain (E50_Q93del), transmembrane domains (A191V and M415V) and the largest extracellular loop (S323P) (**Figure 5-16**). Two of the compound heterozygous variants in this study (W318S/S748del) and the most recently identified compound heterozygous mutations (S399L/R880L) have not yet been functionally validated.

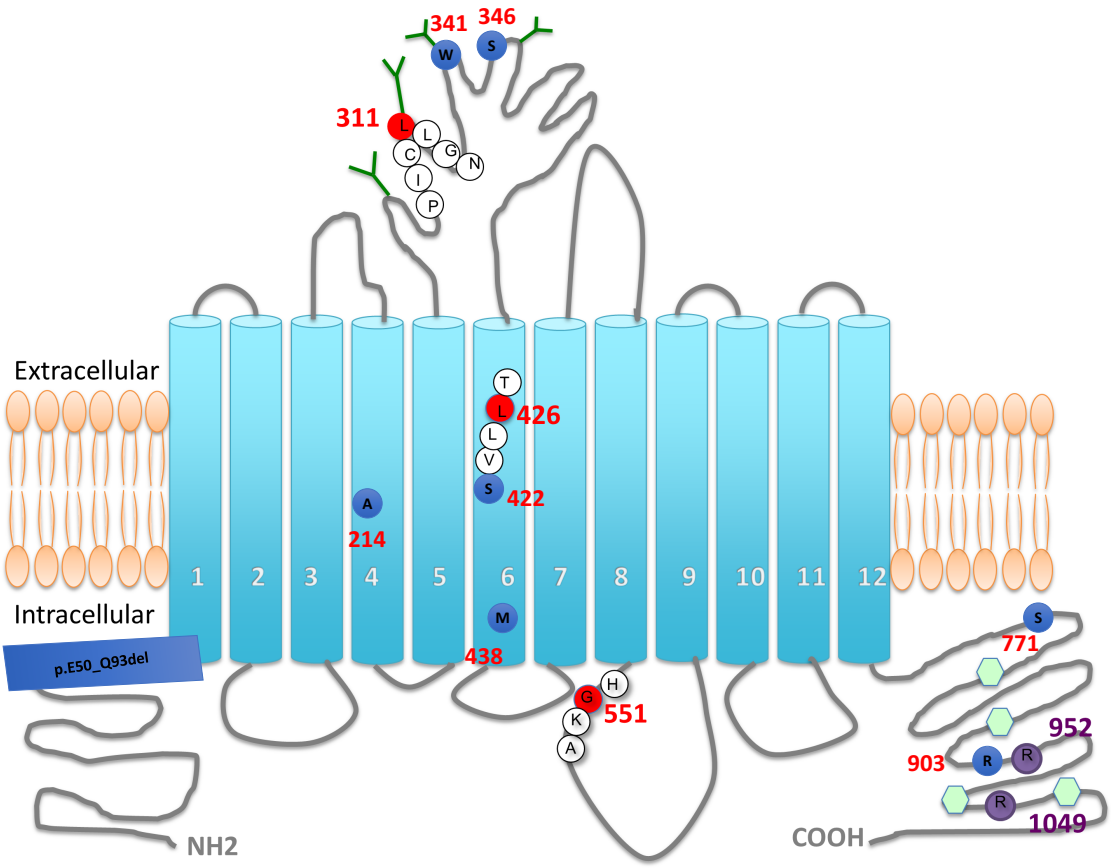

Figure 5-16 Schematic representation of KCC2 structure with location of mutations from this study and recently published studies. Mutations from this study are depicted in red circles, those identified from subsequent studies in blue circles and C-terminus "susceptibility" variants in purple circles. All variants are annotated according to ENST00000454036.2. Adapted from McTague *et al* Nat Commun. 2015 Sep 3;6:803.

	Mutation	EC diagnosis	Inheritance	Seizure Onset	Sz at onset	Peak Sz frequency	Ictal EEG (age)	MRI (age)	Other features	Effective treatments	Best developmental stage attained	Seizure outcome
1	c.279 + 1G > C A191V c.572C > T E50_Q93del	EIMFS	Recessive (parents carriers) unaffected sib het for c.279 + 1G > C	D1	Clonic seizures, apnoeas, facial flushing	9w	Migrating ictal focus (2m)	Thin CC, FL and TL atrophy and DM (2m and 13m)	Post-natal microcephaly Hypotonia	High-dose PB and KBR AZM for apnoeas	Some head control and rolling (4y8m)	SF 1y4m to 3y4m-currently daily tonic sz (4y8m)
2	c.279 + 1G > C A191V c.572C > T E50_Q93del	EIMFS	Recessive (parents carriers) unaffected sib het for c.279 + 1G > C	D3	Tonic seizures, ED	8w	Migrating ictal focus (2m)	Thin CC, FL atrophy, DM, arachnoid cyst L posterior fossa (5m)	Post-natal microcephaly Hypotonia	KBr, high-dose PB, SVA	No head control or rolling	SF 3 to 11 months; clonic migrating and tonic seizures 11m till current age (3y1m)
3	c.967T > C S323P c.1243A > G M415V	EIMFS	Recessive (parents carriers)	1.5m	Apnoea, staring episodes	5m	Migrating ictal focus (6.5m	Mild atrophy (3m)	Post-natal microcephaly Hypotonia-improved with Sz control	KD, LEV	Regained abilities from 9m. At 23m can crawl, sit, grasp and vocalise.	SF from 20m on KD
4	c.953G > C	EOEE	Recessive	D1	Eye	6m	Early ictal	Subdural	-	None	Unable to sit	Ongoing

	W318S c.2242_2244del S748del		(parents carriers)		deviation, cyanosis, tonic-clonic seizures, asymmetric tonic seizures		EEG not available. Later interictal EEG sharp waves over L central and frontal and slow background.	hygroma, bilateral hippocampal atrophy with increased FLAIR signal, mild cerebellar atrophy, DM of TL (10y and 20y). Progressive cerebellar atrophy (20y).			or speak (20 y)	seizures
5	c.1196C>T R880L c.2639G>T S399L	EIMFS	Recessive (one inherited allele, one *de novo* allele)	4m	GTCS and apnoeas evolving to refractory focal with ED and tonic Sz	6m	Migrating ictal focus at 6m	FL and TL atrophy(6m) L HS (4y)	-	KBr	Walked at 4 years spoke single word 6 y	SF from 10 years

Table 5.9 Subsequently published cases of *SLC12A5*-epilepsy AZM acetazolamide, D day, DM delayed myelination, EC electroclinical ED eye deviation, FL frontal lobe, HS hippocampal sclerosis, KBR potassium bromide, L left, m months, PB phenobarbitone Sz seizure, SF seizure free, SVA sodium valproate, TL temporal lobe, w weeks y years.

Reports of these additional cases strongly support the notion that biallelic loss of function *SLC12A5* mutations lead to EIMFS. This is also supported by phenotypic and electrophysiological data from established animal models of KCC2 dysfunction. Complete knockout of *Slc12a5* in mice leads to neonatal lethality due to respiratory insufficiency caused by abnormal central pattern generator function (Hübner et al. 2001). Patch clamping of spinal cord motoneurons in *Slc12a5*$^{-/-}$ mice revealed an abnormal excitatory effect of GABA and glycine, which was not seen in the wild type mice. In another murine model, the homozygous knock-outs retain approximately 5% KCC2 function and survive beyond the neonatal period (Woo et al. 2002). These animals display frequent spontaneous seizures and abnormal excitability in hippocampal slices. It subsequently became clear that the mice survived for the first few weeks of post-natal life due to expression of KCC2a, the immature transcript which was not affected by the targeted disruption of the first exon of *Slc12a5b* (Uvarov et al. 2007). The generation of a hypomorphic allele producing approximately 20-30% of Kcc2 protein levels resulted in a viable murine model but phenotypic information, other than a description of abnormal EEG activity, is limited (Vilen et al. 2001). Mice with one null and one hypomorphic allele, resulting in overall 15-20% of normal KCC2 protein production have also been generated (Tornberg et al. 2005). These mice showed normal locomotor function and coordination but increased susceptibility to induced seizures and abnormal cognitive function. The epileptic phenotype is also evident in a *Drosophila melanogaster kcc* mutant model (Hekmat-Scafe et al. 2006). Null mutations in *Kazachoc*, the drosophila ortholog of *SLC12A5*, leads to lethality, whilst partial loss of function causes increased seizure susceptibility mediated by GABA-A dysfunction.

Further evidence for the role of KCC2 in epileptogenesis comes from acute slice electrophysiology work in rodent studies, where application of specific KCC2 inhibitors promotes the development of continuous seizure-like activity (Sivakumaran et al. 2015; Kelley et al. 2016). Recently, it was shown that focal knockdown of KCC2 in the cortex using injection of AAV2-Cre-GFP in a floxed-*Slc12a5* mouse model is sufficient to induce seizures (MacKenzie et al. 2016). In hippocampal slices from patients with temporal lobe epilepsy, interictal activity was attributable to GABA-A depolarising transmission, which was subsequently linked to downregulation of KCC2 (Cohen et al. 2002). Subsequent studies have confirmed decreased KCC2 expression in brain tumours and peri-tumoural tissue, particularly gliomatous lesions (Pallud et al. 2014; Campbell et al. 2015). Although there is strong evidence for down-regulation of KCC2 in epileptogenic tissue such as gliomas, it has

been unclear whether this represents a primary event in epileptogenesis or a response to seizures. A recent elegant study dissected this temporal relationship and found in a rodent seizure model that KCC2 down-regulation and loss of function occurs prior to the emergence of synchronous bursting and therefore appears to play a more primary role in epileptogenesis (Chen et al. 2017).

KCC2 dysfunction has been widely implicated in a variety of other neurological disorders including spinal cord injury, trauma and neuropathic pain (Kaila et al. 2014) where downregulation of KCC2 leads to increased intra-neuronal chloride concentration and a depolarizing shift in the reversal potential of GABA. The resultant excessive levels of excitation are thought to contribute to the excitotoxic damage seen following trauma or hypoxic injury. KCC2 also postulated to play an important role in other neurodevelopmental disorders. The identification of significantly reduced levels of KCC2 with low KCC2/NKCC1 ratios in Rett syndrome implicated KCC2 dysfunction in disease pathogenesis (Duarte et al. 2013). Subsequent studies in *MECP2*-Rett patient neurons derived from induced pluripotent stem cells showed a significant deficit in KCC2 expression and a delayed GABA functional switch from excitation to inhibition (Tang et al. 2016).

There is therefore strong evidence for the physiological role of KCC2 in normal neurodevelopment. KCC2 dysfunction is associated with epileptogenesis and other neurodevelopmental defects. The mechanism by which loss of function of KCC2 leads to epilepsy in my EIMFS patients remains to be fully elucidated. However, decreased cell surface expression appears to be a potential disease mechanism for some if not all KCC2-EIMFS patients. The regulation of KCC2 expression is complex and includes both BDNF and activity-dependent up-regulation in addition to many other putative transcription factors (Medina et al. 2014). The cytoplasmic terminus is critical for membrane trafficking (Zhao et al. 2008). However, one of the most important mechanisms for regulation of KCC2 expression is phosphorylation of key residues such as serine 940 in the cytoplasmic terminus, which increases plasmalemmal KCC2. Other mechanisms by which a loss of KCC2 function might occur may be altered oligomerization, abnormal interaction with other chloride co-transporters or perturbation of the function of other transporters, leading to dysregulated ion binding. KCC2 plays a significant role at excitatory neurons, in synapse formation and dendritic branching (Chamma et al. 2012). This is clearly evident in animal models (see above), where abnormal dendritic branching can be rescued by KCC2 over-expression. Abnormalities of dendrite morphology or altered branching appear to be

common to many neurodevelopmental disorders including Down syndrome, autistic spectrum disorder and Fragile X syndrome (Kulkarni & Firestein 2012). It is now well established that dendritic spine formation and maintenance contribute to synaptic plasticity and memory formation after learning (Moser et al. 1994; Parajuli et al. 2017). Therefore, although this area requires further study, it may provide a link to the post-natal microcephaly, cerebral atrophy and observed neurodevelopmental and cognitive issues noted in KCC2-EIMFS.

There are many non-specific modulators of KCC2 including the loop diuretics frusemide and bumetanide which are weak KCC2 antagonists with significant antagonist activity against NKCC1. Bumetanide as a therapy for neonatal seizures has not lived up to the promise of early animal studies, largely due to lack of efficacy and serious adverse reactions including ototoxicity (Pressler et al. 2015). Development of more bioavailable lipophilic prodrugs of bumetanide may overcome some of these issues (Erker et al. 2016). There has been a great deal of interest in identifying a specific KCC2 modulator as KCC2 down-regulation is implicated in a range of severe intractable conditions such as neuropathic pain as well as representing a possible anti-epileptic target in more common acquired epilepsies as discussed above (Moore et al. 2017; Puskarjov, Kahle, et al. 2014; Löscher et al. 2013). There has also been interest in KCC2 as a drug target for hypoxic injury such as following stroke (Martín-Aragón Baudel et al. 2017). Gagnon *et al* used a high throughput chloride flux assay in NG-108 (modified neuroblastoma/glioma) cells to screen for KCC2 modulators for neuropathic pain(Gagnon et al. 2013). Further experiments led to identification of CLP257, a unique compound which lowered intracellular chloride and appeared to reverse KCC2 hypofunction in mature rat spinal neurons treated with BDNF (which down-regulates KCC2) by increasing cell surface expression. However, another group was unable to reproduce the effects of CLP257 on intracellular chloride or to show KCC2 expression in NG-108 cells, suggesting the action of CLP257 in animal models may occur via other receptors such as $GABA_A$ or MAO1 (Cardarelli et al. 2017; Gagnon et al. 2017). It therefore remains to be seen whether CLP257 will develop into a useful KCC2 agonist. The CLP257 story also highlights the issue of setting the level of KCC2 expression in model systems used to screen for novel KCC2 modulators. Further possible approaches to KCC2 modulation are likely to exploit the major regulatory pathways of phosphorylation/dephosphorylation of key residues such as serine 940 by kinases such as protein kinase C (Lee et al. 2007). N-ethylmaleimide (NEM) is a KCC2 agonist which has been used in animal work for many

years (Payne 1997) and is an alkylating agent thought to modify cysteine residues of a range of proteins including KCC2. Recently it was shown to act via dephosphorylation of the threonine 1007 residue via the WNK/SPAK pathway, leading to increased KCC2 cell surface expression in neurons and altered chloride extrusion capacity (Conway et al. 2017). NEM itself is unlikely to be a viable treatment as it is an alkylating agent with non-specific effects across other cation co-transporters including NKCC1, but development of a specific KCC2 activator which works via phosphorylation shows promise. Other possible drug targets include a number of G-protein coupled receptors including metabotropic glutamate receptors and zinc receptors which are known to activate phospholipase B, leading to protein kinase C activation and serine 940 phosphorylation (Mahadevan & Woodin 2016).

In conclusion, I have shown in this chapter that biallelic mutations of *SLC12A5* result in a severe early onset epilepsy and developmental delay as revealed by this study and further validated by subsequently published cases. Heterozygous C-terminus variants may represent susceptibility alleles for epilepsy and other neurodevelopmental disorders but their true role in epilepsy susceptibility requires further investigation and validation. A significant impact on transporter function for the mutations identified in this study has been demonstrated with a range of functional assays. Protein homology modelling predicts a significant impact of the compound heterozygous mutations on substrate binding. In addition, mutations lead to reduced cell surface expression in both immunoblotting and confocal studies. Reduced glycosylation revealed by biotinylation studies indicates altered post-translational processing and the presence of less mature protein at the cell surface. Electrophysiology experiments demonstrated an impact on chloride reversal potential and the assessment of the transporter under the stress of a chloride load. Lastly, a knockout zebrafish model displayed abnormal movements on the touch response test. All these complementary data point to a loss of transporter function, which I suggest leads to an increase in intraneuronal chloride, altering the polarity and strength of GABAergic inhibition on the brain and leading to epilepsy and developmental delay. In addition, the impact of these mutations on excitatory synapse formation and dendritic spine morphology warrants further investigation. For *SLC12A5*-EIMFS, the severe epileptic encephalopathy is likely due to disruption of both KCC2-driven neuronal inhibition and KCC2-mediated brain and neuronal network development. In addition to shedding light on a pathogenic mechanism in EIMFS, the identification of *SLC12A5* mutations also supports the long-standing notion that KCC2 dysfunction plays an integral role in epileptogenesis and

neurological disorders. While *SLC12A5* mutations represent a rare cause of epilepsy, further research is likely to have impact in more common epilepsies and many neurological disorders with significant morbidity. This will require the development of disease models which can act as platforms for drug discovery. Although there are current murine Slc12a5 knockout models which exhibit seizures, they have severely limited survival, with neonatal lethality in loss of both the immature (KCC2a) and mature (KCC2b) isoforms of KCC2 and survival until just P18-21 in selective KCC2b knockout (Woo et al. 2002; Hübner et al. 2001; Vilen et al. 2001). A model system where the disease-causing mutation is expressed in the native genetic milieu, such as a patient–derived induced pluripotent stem (IPSC) cell model, may overcome these difficulties of genetic background and mutation dosing. This would be complemented by the development of knock-in mouse models which are not currently available. IPSC models have provided valuable insights in several severe epilepsies such as Dravet syndrome and STXBP1-encephalopathy (Barral & Kurian 2016; Sun et al. 2016). In addition, establishment of a neuronal disease model would provide an ideal future platform for compound screening and drug discovery. Furthermore, this model would be ideal for the development and assessment of novel therapies such as new small molecules or gene therapy, whether mutation-specific RNA manipulation strategies or emerging genome editing techniques, or cell-based therapies (Kullmann et al. 2014; Maljevic et al. 2017).

Chapter 6 Conclusion and future perspectives: the heterogenous genetic landscape of epilepsy of infancy with migrating focal seizures

6.1 Molecular genetic investigation of the EIMFS cohort

In my PhD, I have studied the phenotype and investigated the underlying genetic aetiology in a cohort of 34 patients with the electroclinical syndrome of EIMFS. My clinical work has delineated both typical and atypical clinical features. During the molecular genetic investigation of this cohort (29 patients), I identified mutations in a previously reported disease gene, *KCNT1*, in ten patients, and found mutations in a novel gene, *SLC12A5*, in two patients.

The remaining 17 patients have undergone molecular genetic investigation by a variety of methods including diagnostic multiple gene NGS panel and research-based whole exome sequencing (**Table 6.1**). A genetic aetiology was identified in 4 of these 17 cases. Overall in 16/29 (55%) patients with EIMFS where genetic testing was possible, a putative genetic aetiology was identified.

Heterozygous *de novo* mutations of *SCN2A* were identified in two patients, Patient 24 and Patient 31. In Patient 24, local diagnostic NGS multiple gene panel testing at St. Thomas' Hospital, London identified a novel heterozygous *de novo* variant in *SCN2A* (c.640T>C S214P). *In silico* tools were predictive of pathogenicity; Polyphen2 0.999 (damaging), Provean -4.88 (deleterious, range ≤-2.5), SIFT 0 (≤ 0.05). Additional clinical features in this patient included severe gastrointestinal dysmotility and a dystonic movement disorder. Patient 31 was investigated with the Great Ormond Street Regional Genetics NGS multiple gene panel, revealing a heterozygous *de novo* variant in *SCN2A*, c.2995 G>A, E999K. In silico tools also indicated possible pathogenicity; Polyphen2 0.973 (probably damaging), Provean -3.74, SIFT 0.001. This variant has previously been reported in two patients; in a patient with Ohtahara syndrome (Nakamura et al. 2013) and most recently a patient with non-specific EOEE with suppression-burst pattern (Wolff et al. 2017). *De novo* heterozygous *SCN2A* mutations have been reported in a wide range of epilepsies (**Table 1.2, Table 1.4**), including EIMFS (Wolff et al. 2017; Dhamija et al. 2013; Howell et al. 2015). Indeed,

mutations in *SCN2A* have been found to be the second commonest cause (after *KCNT1*) in some cohorts with variants identified in 7/27 EIMFS cases (Howell et al. 2015). *SCN2A* encodes the α2 subunit of the voltage gated sodium channel and variants associated with the early onset severe form of *SCN2A*-epilepsy, as opposed to other later-onset or self-limiting phenotypes, appear to be associated with a marked gain of function in electrophysiological studies (Ogiwara et al. 2009; Wolff et al. 2017). Interestingly, several of these patients, have been shown to respond well, and indeed become seizure free, when treated with anti-epileptic medications that act via sodium channel blockade such as Carbamazepine and Phenytoin (Howell et al. 2015; Wolff et al. 2017). This was also the case in Patient 31, who became seizure free with Carbamazepine and relapsed on withdrawal. Patient 24 unfortunately did not show any such response. Other phenotypic features of *SCN2A*-EIMFS include a dystonic movement disorder and severe gastrointestinal features such as vomiting or dysmotility, as evident in Patients 24 and 31. Notably, in published cases *SCN2A*-EIMFS appears to have a less severe neurodevelopmental profile compared to *KCNT1*-EIMFS, with 2/5 cases manifesting mild intellectual disability in a recent study (Wolff et al. 2017). These two patients had become seizure free at two and 10 months on treatment with vigabatrin and phenytoin, respectively. Unfortunately, both patients in this study showed severe neurodevelopmental impairment. While the reports of treatment response are encouraging, longitudinal studies are now required to investigate whether early use of sodium-channel blockers could improve both seizure and cognitive outcome in *SCN2A*-epilepsy.

A missense variant in *GABRB3* (c.372A>C, L124F) was identified by whole exome sequencing in Patient 7 and confirmed on Sanger sequencing to be *de novo*. The variant occurs at a highly conserved residue and *in silico* tools Polyphen2 (0.947, possibly damaging) and SIFT (Damaging 0.022) indicate possible pathogenicity although the Provean score is neutral (2.19, <-2.5). It is not present in 1000 Genomes, EVS, ExAC or gnomAD. Patient 7, as described in Chapter 1, had several features atypical for EIMFS including marked basal ganglia changes with bilateral putaminal atrophy on brain MR imaging (**Figure 3-4**). The same *GABRB3* variant was also recently identified in a patient with EOEE characterised by onset of focal, migrating seizures at 2.5 months (but not meeting the diagnostic criteria for EIMFS) and severe global atrophy (Møller et al. 2017), but without basal ganglia imaging abnormalities. Functional validation of the pathogenicity of this variant has not been performed to date. Heterozygous mutations of *GABRB3*, which

encodes the ß$_3$ subunit of the GABA$_A$ receptor, have been implicated in a wide spectrum of epilepsies, from severe epileptic encephalopathies including Dravet syndrome to febrile seizures (Allen et al. 2013; Myers et al. 2016; Trump et al. 2016; Møller et al. 2017; Warrier et al. 2013; Zhang et al. 2015; Le et al. 2017; Hamdan et al. 2014). Only a small number of mutations have been functionally characterised, but the majority result in a loss of function which is postulated to lead to a lack of GABAergic inhibition (Møller et al. 2017; Janve et al. 2016; Hirose 2014). Therefore, while the confirmation of the *GABRB3* variant identified in Patient 7 in another patient may strengthen the case for pathogenicity, further functional validation is required.

Following recruitment to the BPNSU study, Patient 12 was recruited to another whole exome sequencing study which identified a *de novo* novel heterozygous deletion in *SMC1A*, c.1114delG, resulting in a premature stop codon (pVal372*) (Gorman et al. 2017). The deleted nucleotide occupies a splice acceptor site and is predicted to result in non-sense mediated messenger RNA decay. *SMC1A* encodes the Structural Maintenance of Chromosome 1 protein, which forms part of a cohesin ring vital to the structural integrity of chromosomes during mitosis and meiosis. Missense variants and in-frame deletions of *SMC1A* account for approximately 5% of Cornelia du Lange syndrome, a multisystem disorder with features including facial dysmorphism, growth abnormalities, small hands and feet and cardiac anomalies ((Huisman et al. 2017). Recently, truncating mutations in *SMC1A* have emerged in females with epileptic encephalopathy characterised by treatment-resistant seizures with onset from the neonatal period to 3 years of age occurring in clusters, mild or no dysmorphic features and developmental delay (Lebrun et al. 2015; Huisman et al. 2017; Symonds et al. 2017; Goldstein et al. 2015; Jansen et al. 2016; Gorman et al. 2017). Therefore, although it is possible that *SMC1A* represents another disease gene for EIMFS, further cases are awaited to confirm this.

Analysis is currently ongoing for the remaining, unsolved cases (**Table 6.1**) and although many of the known EIMFS/EOEE genes have been excluded, it is likely that further genetic aetiologies will be elucidated.

EIMFS Cohort Patient No	Phenotype	Genetic Investigation					Diagnostic chromosomal microarray*	Diagnostic karyotype	Genetic cause identified?
		Sanger sequencing *KCNT1*	Sanger sequencng *SLC12A5*	NGS[1] Pilot Panel	NGS[2] Diagnostic Panel	WES			
1	EIMFS	+	-	-	-	+	-	N	*KCNT1*
2	EIMFS			No DNA					No DNA
3	EIMFS	+	-	-	-	+	-	N	*KCNT1*
4	EIMFS			No DNA					No DNA
5	EIMFS			No DNA					No DNA
6	EIMFS	+	-	+	-	-	N	-	*KCNT1*
7	EIMFS	+	-	+	-	+	N	-	*GABRB3*
8	EIMFS	+	+	+		-	N	-	WES analysis ongoing
9	EIMFS	+	-	+		+	N	-	WES analysis ongoing
10	EIMFS		-	No DNA					No DNA
11	EIMFS	+	+	-		-	N	-	Awaiting WES
12	EIMFS	+	+	+	-	-	-	N	*SMC1A*
13	EIMFS	+	-	+		+	N	-	WES analysis ongoing
14	EIMFS		-	Parents did not consent to further testing					No further testing

15	EIMFS	+	-	-	+	-	-	-	*KCNT1*
16	EIMFS	+	-	-	-	-	-	N	*KCNT1*
17	EIMFS	+	-	-	-	-	N	-	*KCNT1*
18	EIMFS	-	-	-	+	-	N	-	*KCNT1*
19	EIMFS	+	-	-	-	-	N	-	*KCNT1*
20	EIMFS	-	-	-	+	-	N	-	*KCNT1*
21	EIMFS	-	-	-	+	-	N	-	*KCNT1*
22	EIMFS	+	+	-	-	-	N	-	WES analysis ongoing
23	EIMFS	+	+	-	-	-	N	-	WES analysis ongoing
24	EIMFS	+	+	-	-	-	N	-	*SCN2A*
25	EIMFS	+	+	-	-	-	N	-	WES analysis ongoing
26	EIMFS	+	+	-	-	-	N	-	WES analysis ongoing
27	EIMFS	+	+	-	-	-	N	-	WES analysis ongoing
28	EIMFS	+	+	-	+	-	11.8 Mb heterozygous deletion Chr 20q11 copy number variant of uncertain significance	-	WES analysis ongoing
29	EIMFS	-	-	-	+	-	N	-	WES analysis ongoing
30	EIMFS	-	-	-	+	-	N	-	WES analysis

									ongoing
31	EIMFS	-	-	-	+	-	N		*SCN2A*
32	EIMFS	-	+	-	-	+	N		*SLC12A5*
33	EIMFS	-	+	-	-	-	N	-	*SLC12A5*
34	EIMFS	-	+	-	-	+	N	-	WES analysis ongoing

Table 6.1 Molecular Genetic Investigation of the EIMFS cohort. A variety of genetic techniques were used including Sanger sequencing of known and novel EIMFS genes, NGS panel and whole exome sequencing. Patients where a likely genetic cause has been identified are highlighted in green, those with a possible genetic aetiology requiring further validation in pale orange and those where further investigation is not possible in grey.

1. Pilot NGS panel included NGS sequencing and exon-level CNV analysis of *CDKL5*, *MECP2*, *ARX*, *ATRX*, *SLC9A6*, *SLC16A2*, *ADSL*, *CNTNAP2*, *NRXN1*, *PNKP*, *KIAA1279*, *UBE3A*, *EHMT1*, *FOXG1*, *MEF2C*, *SIP1*, *ZEB2*, *TCF4*, *STXBP1*, *SLC25A22*, *PCDH19*, *SCN1A*, *PLCB1*, *SPTAN1*, *KCNQ2*, *ARHGEF9*, *SCN2A*, *MAGI2* (Trump et al, 2016).

2. NGS diagnostic 45 gene panel included sequencing of *ADSL, ALG13, ARHGEF9, ARX, ATP1A3, ATRX, CDKL5, CHD2, CHRNA4, CHRNB2, CNTNAP2, EHMT1, FOXG1, GABRB3, GRIN2A, GRIN2B, KCNQ2, KCNT1, KIAA1279, LGI1, MAGI2, MBD5, MECP2, MEF2C, NRXN1, PCDH19, PLCB1, PNKP, POLG, PRRT2, SCN1A, SCN2A, SCN8A, SIP1 [ZEB2], SLC16A2, SLC25A22, SLC2A1 [GLUT1], SLC9A6, SPTAN1, STXBP1, SYNGAP1, TBC1D24, TCF4, UBE2A, UBE3A* (Trump et al, 2016*)*.

6.2 The complex genetic landscape of EIMFS

The first evidence of a genetic aetiology for EIMFS came in 2011 from the finding of *de novo* missense mutations in two patients (Carranza Rojo et al. 2011; Freilich et al. 2011). Since then, the genetic landscape has become increasingly complex, with a number of dominantly and recessively inherited genes identified in patients with EIMFS (**Table 6.2**).

Gene	Number of reported cases (including this study)	Mode of inheritance	Effect of mutation on protein function	Protein	Protein function
KCNT1	47	AD, usually *de novo*	Gain-of-function	Sodium activated potassium channel (K_{Na})	Outwardly rectifying potassium channel subunit, required for hyperpolarisation following repetitive firing Interaction with wider protein network including FMRP
SCN2A	15	AD, usually *de novo*	Likely to be gain-of-function	Type 2 voltage-gated sodium channel alpha subunit	Initiation and propagation of neuronal action potentials, located at axon initial segment
SCN1A	3	AD, usually *de novo*	Likely to be loss-of-function	Type 1 voltage-gated sodium channel alpha subunit	Initiation and propagation of neuronal action potentials, particularly in GABAergic interneurons
SCN8A	1	AD, usually *de novo*	Likely to be gain-of-function	Type 8 voltage-gated sodium channel alpha subunit	Initiation and propagation of neuronal action potentials, particularly in GABAergic interneurons; expressed later in post-natal development than *SCN2A*
SLC12A5	9	AR	Loss of function	Neuronal potassium chloride co-transporter	Determines strength and polarity of GABA signaling. Important in dendrite and excitatory synapse formation.
TBC1D24	2	AR	Loss-of-function	TBC domain containing RAB-specific GTPAse activating protein	Regulation of neurite growth and branching, morphological and functional maturation of neuronal circuits
SLC25A22	2	AR	Loss-of-function	Mitochondrial glutamate transporter	Catalyses the co-transport of glutamate with H^+ or exchanges glutamate for OH^-

PLCB1	1	AR	Loss-of-function	Phospholipase C-beta type 1	Catalyzes the generation of inositol 1,4,5-trisphosphate (IP3) and diacylglycerol (DAG) from phosphatidylinositol 4,5-bisphosphate (IP2), important in the intracellular transduction of many extracellular signals
QARS	2	AR	Loss-of-function	Amino-acyl tRNA synthetase	Ensure translational fidelity by matching of tRNA with correct amino acids Loss of function leads to impaired neuronal survival

Table 6.2 Genes implicated in EIMFS. AD autosomal dominant AR autosomal recessive.

6.3 What does a clinical diagnosis of EIMFS mean in the new-era of genomic medicine?

Given the disparate genetic aetiologies now identified, can EIMFS still be considered as one disorder, or does it merely reflect the age-related manifestation of a range of different insults, both genetic and metabolic, to cerebral function? These concepts are not necessarily mutually exclusive. Firstly, the question of whether all patients reported in the literature have the same disorder is related to the quality of the phenotypic data that is published, which is variable. There is also very likely to be reporting bias, where EIMFS patients with interesting genetic diagnoses are published as opposed to gene-negative patients. This may have been skewing the literature in EIMFS in recent years. However, despite this the patients do seem to share a specific ictal EEG signature which is consistently seen across different genetic aetiologies, while other clinical features may vary slightly, such as the increased presence of movement disorders in *KCNT1*-EIMFS. Selioutski et al performed sequential EEGs in two patients with EIMFS, one with a *KCNT1* and one with a *SCN2A* mutation and showed that they both had delayed maturation of normal EEG patterns, with delayed development of a normal continuous EEG. Furthermore, they demonstrated that the characteristic migrating foci could only be seen when the EEG became continuous at 70-100 postnatal days, perhaps explaining the time lag between onset of clinical seizures and the characteristic EEG abnormality (Selioutski et al. 2015). This shared EEG maturational abnormality is further evidence of the shared EEG phenotype between these different aetiologies.

Why do the seizures migrate in EIMFS and not in other EEs such as Dravet syndrome? I postulate that this may be a reflection of an abnormal functional or anatomical network specific to EIMFS and resulting from the underlying genetic abnormality. As a result of an abnormal neuronal network, ictal spread may not occur as it would in a more normal

system. In fact, the seizures may not be migratory but, rather, unable to migrate. Neuronal networks potentially represent a final common pathway for convergent aetiologies and have been investigated using EEG coupled with functional MRI in several epileptic encephalopathies, including West syndrome. In patients with West syndrome of both structural and "cryptogenic" causes, a "fingerprint" network of brain activation associated with hypsarrhythmia could be discerned (Siniatchkin & Capovilla 2013; Siniatchkin et al. 2007). This is an area that requires further research by analysing network properties in EIMFS of diverse genetic aetiologies using a source analysis method such as dynamic imaging of coherent source analysis (DICS), which has the advantage of using EEG data alone rather than requiring functional MRI data which might be technically challenging in infants (Japaridze et al. 2015).

If EIMFS does represent a discrete phenotype, how do these different aetiologies converge? It is clear is that mutations in a number of important synaptic proteins can lead to EIMFS but in reality the synapse is dynamic and complex with these proteins working in concert, not isolation. For example, voltage gated sodium channels allow influx of sodium, which activates KCNT1 channels. Therefore it is possible that a gain of SCN2A function leads to increased KCNT1 activation, hence the resultant similar phenotype. It is notable that many EIMFS genes, such as *SLC12A5* and *KCNT1*, have potentially much wider effects beyond the immediate excitation-inhibition imbalance leading to seizures, such as effects on dendritic branching and excitatory synapse formation. The post-natal microcephaly and severe cognitive impact of EIMFS points to a significant effect of these genes on early brain development including synapse and network formation.

Therefore, I suggest that the electroclinical syndromic diagnosis of EIMFS still has merit. For the 30-50% of patients where we are currently unable to make a genetic diagnosis, it allows us to give families reasonable prognostic information regarding seizure control and the impact on neurodevelopment. It is possible that as further genetic causes are discovered, sub-groups with slightly differing outcomes will emerge.

The story of genetic discovery in EIMFS has implications for other rare EEs. Firstly, it highlights the importance of rigorous phenotyping and gathering a cohort of similar patients, as this is most likely to lead to genetic discovery, as was the case for *KCNT1* and *SLC12A5*. Secondly, although *de novo* dominant mutations remain important in the EEs, study of families with more than one affected child can lead to genetic discovery in both

consanguineous and outbred populations. This study also adds to the emerging evidence that transporters, in addition to channels, are important in the epileptic encephalopathies (Thevenon et al. 2014; Kodera et al. 2013; Leen et al. 2010; A. Poduri, Heinzen, et al. 2013). I hope that my further research into network abnormalities in EIMFS and the generation of better disease models will have relevance for other epileptic encephalopathies, in which there remain many unanswered questions.

6.4 Conclusion

The current era of genetic discovery makes this an exciting and rewarding time to be a clinician scientist in training in the field of epilepsy genetics. However, while diagnostics have improved immeasurably, for my patients and their families the daily realities of severe early onset epilepsy remain bleak. It is now vital that we harness the possibilities of the genomic age and translate them into therapies and interventions with real, tangible benefits for children and young people with severe epilepsy, who are the most deserving of recipients.

Chapter 7 References

Aaberg, K.M. et al., 2017. Incidence and Prevalence of Childhood Epilepsy: A Nationwide Cohort Study. *Pediatrics*.

Abdelnour, E. et al., 2018. Does age affect response to quinidine in patients with KCNT1 mutations? Report of three new cases and review of the literature. *Seizure*, 55, pp.1–3.

Absoud, M. et al., 2010. A novel ARX phenotype: Rapid neurodegeneration with Ohtahara syndrome and a dyskinetic movement disorder. *Developmental Medicine and Child Neurology*, 52(3), pp.305–307.

Adzhubei, I.A. et al., 2010. A method and server for predicting damaging missense mutations. *Nature Methods*, 7(4), pp.248–249.

Alazami, A.M. et al., 2014. NECAP1 loss of function leads to a severe infantile epileptic encephalopathy. *Journal of medical genetics*, pp.1–6.

Alix, J.J.P. et al., 2016. An introduction to neonatal EEG. *Paediatrics and Child Health*, pp.1–8.

Allen, A.S. et al., 2013. De novo mutations in epileptic encephalopathies. Nature, 501(7466), 217–21.

Allen, N.M. et al., 2015. Unexplained early onset epileptic encephalopathy: Exome screening and phenotype expansion. *Epilepsia*.

Appavu, B. et al., 2016. Electroclinical phenotypes and outcomes in TBC1D24-related epilepsy. *Epileptic disorders : international epilepsy journal with videotape*, 18(3), pp.324–8.

Arai-Ichinoi, N. et al., 2015. Genetic heterogeneity in 26 infants with a hypomyelinating

leukodystrophy. *Human genetics*, 135(1), pp.89–98.

Ashkenazy, H. et al., 2010. ConSurf 2010: calculating evolutionary conservation in sequence and structure of proteins and nucleic acids. *Nucleic acids research*, 38, pp.W529-33.

Barba, C. et al., 2016. Congenital disorders of glycosylation presenting as epileptic encephalopathy with migrating partial seizures in infancy. *Developmental Medicine and Child Neurology*, 58(10), pp.1085–1091.

Barcia, G. et al., 2012. De novo gain-of-function KCNT1 channel mutations cause malignant migrating partial seizures of infancy. *Nature Genetics*, 44(11), pp.1255–9.

Barral, S. & Kurian, M.A., 2016. Utility of Induced Pluripotent Stem Cells for the Study and Treatment of Genetic Diseases: Focus on Childhood Neurological Disorders. *Frontiers in molecular neuroscience*, 9(September), p.78.

Basel-Vanagaite, L. et al., 2013. Biallelic SZT2 mutations cause infantile encephalopathy with epilepsy and dysmorphic corpus callosum. *American Journal of Human Genetics*, 93(3), pp.524–529.

Bateman, A. et al., 2000. The Pfam protein families database. *Nucleic acids research*, 28(1), pp.263–266.

Bausch, A.E. et al., 2015. The sodium-activated potassium channel Slack is required for optimal cognitive flexibility in mice. *Learning & memory (Cold Spring Harbor, N.Y.)*, 22(7), pp.323–35.

Bearden, D. et al., 2014. Targeted treatment of migrating partial seizures of infancy with quinidine. *Annals of Neurology*, 76(3), pp.457–461.

Bedoyan, J.K. et al., 2010. Duplication 16p11.2 in a child with infantile seizure disorder. *American Journal of Medical Genetics Part A*, 152A(6), p.n/a-n/a.

Ben-Ari, Y. et al., 2012. The GABA Excitatory/Inhibitory Shift in Brain Maturation and Neurological Disorders. *The Neuroscientist*, 18(5), pp.467–486.

Bender, A.C. et al., 2013. Focal Scn1a knockdown induces cognitive impairment without seizures. *Neurobiology of disease*, 54, pp.297–307.

Benkert, P., Biasini, M. & Schwede, T., 2011. Toward the estimation of the absolute quality of individual protein structure models. *Bioinformatics (Oxford, England)*, 27(3), pp.343–50.

Bennett, R.L. et al., 2002. Genetic Counseling and Screening of Consanguineous Couples and Their Offspring: Recommendations of the National Society of Genetic Counselors. *Journal of Genetic Counseling*, 11(2), pp.97–119.

Berg, A.T. et al., 2010. Revised terminology and concepts for organization of seizures and epilepsies: Report of the ILAE Commission on Classification and Terminology, 2005-2009. *Epilepsia*, 51(4), pp.676–685.

Bhattacharjee, A., Gan, L. & Kaczmarek, L.K., 2002. Localization of the Slack potassium channel in the rat central nervous system. *The Journal of comparative neurology*, 454(3), pp.241–54.

Biervert, C. & Steinlein, O.K., 1999. Structural and mutational analysis of KCNQ2, the major gene locus for benign familial neonatal convulsions. *Human Genetics*, 104(3), pp.234–240.

Blaesse, P. et al., 2009. Cation-Chloride Cotransporters and Neuronal Function. *Neuron*, 61(6), pp.820–838.

Blaesse, P. et al., 2006. Oligomerization of KCC2 correlates with development of inhibitory neurotransmission. *The Journal of neuroscience : the official journal of the Society for Neuroscience*, 26(41), pp.10407–10419.

Van Bogaert, P., 2013. Epileptic encephalopathy with continuous spike-waves during slow-wave sleep including Landau–Kleffner syndrome. In *Handbook of clinical neurology*. pp. 635–640.

Brown, M.R. et al., 2008. Amino-termini isoforms of the Slack K+ channel, regulated by

alternative promoters, differentially modulate rhythmic firing and adaptation. *The Journal of physiology*, 586(Pt 21), pp.5161–5179.

Brunklaus, A. et al., 2013. The clinical utility of an SCN1A genetic diagnosis in infantile-onset epilepsy. *Developmental Medicine and Child Neurology*, 55(2), pp.154–161.

Buiting, K., Williams, C. & Horsthemke, B., 2016. Angelman syndrome — insights into a rare neurogenetic disorder. *Nature Reviews Neurology*, 12(10), pp.584–593.

Campbell, S.L. et al., 2015. GABAergic disinhibition and impaired KCC2 cotransporter activity underlie tumor-associated epilepsy. *Glia*, 63(1), pp.23–36.

Capovilla, G. et al., 2013. The history of the concept of epileptic encephalopathy. *Epilepsia*, 54, pp.2–5.

Caraballo, R. et al., 2014. Epilepsy of infancy with migrating focal seizures: Six patients treated with bromide. *Seizure*, 23(10), pp.899–902.

Caraballo, R., Noli, D. & Cachia, P., 2015. Epilepsy of infancy with migrating focal seizures: Three patients treated with the ketogenic diet. *Epileptic Disorders*, 17(2), pp.194–197.

Caraballo, R.H. et al., 2016. Epileptic spasms in clusters and associated syndromes other than West syndrome : A study of 48 patients. *Epilepsy Research*, 123, pp.29–35.

Caraballo, R.H. et al., 2008. Migrating focal seizures in infancy: analysis of the electroclinical patterns in 17 patients. *Journal of child neurology*, 23(5), pp.497–506.

Cardarelli, R.A. et al., 2017. The small molecule CLP257 does not modify activity of the K+–Cl− co-transporter KCC2 but does potentiate GABAA receptor activity. *Nature Medicine*, 23(12), pp.1394–1396.

Carranza Rojo, D. et al., 2011. De novo SCN1A mutations in migrating partial seizures of infancy. *Neurology*, 77(4), pp.380–383.

Carvill, G.L. et al., 2014. GABRA1 and STXBP1: Novel genetic causes of Dravet syndrome. *Neurology*, 82(14), pp.1245–1253.

Carvill, G.L. et al., 2015. Mutations in the GABA Transporter SLC6A1 Cause Epilepsy with Myoclonic-Atonic Seizures. *The American Journal of Human Genetics*, 96(5), pp.808–815.

Carvill, G.L. et al., 2013. Targeted resequencing in epileptic encephalopathies identifies de novo mutations in CHD2 and SYNGAP1. *Nature genetics*, 45(7), pp.825–30.

Chamma, I. et al., 2012. Role of the neuronal K-Cl co-transporter KCC2 in inhibitory and excitatory neurotransmission. *Frontiers in Cellular Neuroscience*, 6(February), pp.1–15.

Chapman, K.E. et al., 2015. Seizing control of epileptic activity can improve outcome. *Epilepsia*, 56(10), pp.1482–1485.

Chen, H. et al., 2009. The N-terminal domain of Slack determines the formation and trafficking of Slick/Slack heteromeric sodium-activated potassium channels. *The Journal of neuroscience : the official journal of the Society for Neuroscience*, 29(17), pp.5654–65.

Chen, L. et al., 2017. KCC2 downregulation facilitates epileptic seizures. *Scientific Reports*, 7(1), p.156.

Chien, Y.H. et al., 2012. Dextromethorphan in the treatment of early myoclonic encephalopathy evolving into migrating partial seizures in infancy. *Journal of the Formosan Medical Association*, 111(5), pp.290–294.

Choi, Y. et al., 2012. Predicting the functional effect of amino acid substitutions and indels. A. G. de Brevern, ed. *PloS one*, 7(10), p.e46688.

Chong, P.F. et al., 2016. Ineffective Quinidine Therapy in Early-onset Epileptic Encephalopathy with KCNT1 Mutation. *Annals of neurology*.

Cilio, M.R. et al., 2009. Intravenous levetiracetam terminates refractory status epilepticus in two patients with migrating partial seizures in infancy. *Epilepsy Research*, 86(1), pp.66–71.

Claes, L. et al., 2001. De novo mutations in the sodium-channel gene SCN1A cause severe myoclonic epilepsy of infancy. *American journal of human genetics*, 68(6), pp.1327–1332.

Cohen, I. et al., 2002. On the Origin of Interictal Activity in Human Temporal Lobe Epilepsy in Vitro. *Science*, 298(5597), pp.1418–1421.

Consortium, E.E. et al., 2014. De Novo Mutations in Synaptic Transmission Genes Including DNM1 Cause Epileptic Encephalopathies. , pp.360–370.

Conway, L.C. et al., 2017. N-Ethylmaleimide increases KCC2 cotransporter activity by modulating transporter phosphorylation. *Journal of Biological Chemistry*, 292(52), pp.21253–21263.

Cooper, D.N. et al., 2013. Where genotype is not predictive of phenotype: towards an understanding of the molecular basis of reduced penetrance in human inherited disease. *Human genetics*, 132(10), pp.1077–130.

Coppola, G. et al., 1995. Migrating partial seizures in infancy: A malignant disorder with developmental arrest. *Epilepsia*, 36(10), pp.1017–1024.

Coppola, G. et al., 2006. Mutational scanning of potassium, sodium and chloride ion channels in malignant migrating partial seizures in infancy. *Brain and Development*, 28(2), pp.76–79.

Coppola, G. et al., 2007. Temporal lobe dual pathology in malignant migrating partial seizures in infancy. *Epileptic Disorders*, 9(2), pp.145–148.

Corry, P.C., 2014. Consanguinity and National/Community Disease Profiles Consanguinity and Prevalence Patterns of Inherited Disease in the UK Pakistani Community. *Hum Hered*, 77, pp.207–216.

Dedek, K. et al., 2003. Neonatal convulsions and epileptic encephalopathy in an Italian family with a missense mutation in the fifth transmembrane region of KCNQ2. *Epilepsy Research*, 54(1), pp.21–27.

Depienne, C. et al., 2010. Mechanisms for variable expressivity of inherited SCN1A mutations causing Dravet syndrome. *Journal of medical genetics*, 47(6), pp.404–410.

Depienne, C. et al., 2006. Parental mosaicism can cause recurrent transmission of SCN1A mutations associated with severe myoclonic epilepsy of infancy. *Human mutation*, 27(4), p.389.

Dhamija, R. et al., 2013. Novel de novo SCN2A mutation in a child with migrating focal seizures of infancy. *Pediatric Neurology*, 49(6), pp.486–488.

Djuric, M. et al., 2011. The efficacy of bromides, stiripentol and levetiracetam in two patients with malignant migrating partial seizures in infancy. *Epileptic Disorders*, 13(1), pp.22–26.

Don, R.H. et al., 1991. 'Touchdown' PCR to circumvent spurious priming during gene amplification. *Nucleic Acids Research*, 19(14), p.4008.

Doyle, D.A. et al., 1998. The structure of the potassium channel: molecular basis of K+ conduction and selectivity. *Science (New York, N.Y.)*, 280(5360), pp.69–77.

Dravet, C. et al., 2011. Severe myoclonic epilepsy in infancy (Dravet syndrome) 30 years later. *Epilepsia*, 52, pp.1–2.

Duarte, S.T. et al., 2013. Abnormal expression of cerebrospinal fluid cation chloride cotransporters in patients with Rett syndrome. M. D'Esposito, ed. *PloS one*, 8(7), p.e68851.

Dunbrack, R.L., 2002. Rotamer libraries in the 21st century. *Current opinion in structural biology*, 12(4), pp.431–40.

Duncan, R., 2001. Infantile spasms: the original description of Dr West. 1841. *Epileptic disorders*, 3(1), pp.47–8.

Ebrahimi-Fakhari, D. et al., 2015. The evolving spectrum of *PRRT2* -associated paroxysmal diseases. *Brain*, 138(12), pp.3476–3495.

Eddy, S.R., 2011. Accelerated Profile HMM Searches. *PLoS computational biology*, 7(10), p.e1002195.

Edvardson, S. et al., 2013. West syndrome caused by ST3Gal-III deficiency. *Epilepsia*, 54(2), pp.24–27.

Ehaideb, S. et al., 2017. Novel Compensatory Mechanisms Enable the Mutant KCNT1 Channels to Induce Seizures. *bioRxiv*, p.191171.

Elia, G., 2008. Biotinylation reagents for the study of cell surface proteins. *PROTEOMICS*, 8(19), pp.4012–4024.

Eling, P. et al., 2002. The mystery of the Doctor's son, or the riddle of West syndrome. *Neurology*, 58(6), pp.953–5.

Eltze, C.M. et al., 2013. A population-based study of newly diagnosed epilepsy in infants. *Epilepsia*, 54(3), pp.437–445.

Engel, J., 2001. ILAE Commission Report A Proposed Diagnostic Scheme for People with Epileptic Seizures and with Epilepsy : Report of the ILAE Task Force on Classification and Terminology De mo (V isi t htt p :/ / w lit me rg er . co m) (V isi t htt p :/ / w ww De fsp. *Epilepsia*, 42(6), pp.796–803.

Engel, J., 2006. Report of the ILAE Classification Core Group. *Epilepsia*, 47(9), pp.1558–1568.

Erker, T. et al., 2016. The bumetanide prodrug BUM5, but not bumetanide, potentiates the antiseizure effect of phenobarbital in adult epileptic mice. *Epilepsia*, 57(5), pp.698–705.

Escayg, A. et al., 2000. Mutations of SCN1A, encoding a neuronal sodium channel, in two families with GEFS+2. *Nature genetics*, 24(4), pp.343–5.

Eswar, N. et al., 2007. Comparative protein structure modeling using MODELLER. *Current protocols in protein science / editorial board, John E. Coligan ... [et al.]*, Chapter 2,

p.Unit 2.9.

Evely, K.M., Pryce, K.D. & Bhattacharjee, A., 2017. The Phe932Ile mutation in KCNT1 channels associated with severe epilepsy, delayed myelination and leukoencephalopathy produces a loss-of-function channel phenotype. *Neuroscience*, 351, pp.65–70.

Fasulo, L. et al., 2012. Migrating focal seizures during infancy: A case report and pathologic study. *Pediatric Neurology*, 46(3), pp.182–184.

De Filippo, M.R. et al., 2014. Lack of pathogenic mutations in six patients with MMPSI. *Epilepsy Research*, 108(2), pp.340–344.

Finn, R.D. et al., 2009. The Pfam protein families database. *Nucleic Acids Research*, 38(Database), pp.D211–D222.

Folbergrová, J. & Kunz, W.S., 2012. Mitochondrial dysfunction in epilepsy. *Mitochondrion*, 12(1), pp.35–40.

Freilich, E.R. et al., 2011. Novel SCN1A mutation in a proband with malignant migrating partial seizures of infancy. *Archives of neurology*, 68(5), pp.665–671.

Fridley, J. et al., 2013. Surgical treatment of pediatric epileptic encephalopathies. *Epilepsy research and treatment*, 2013, p.720841.

Fukuoka, M. et al., 2017. Quinidine therapy for West syndrome with KCNTI mutation: A case report. *Brain and Development*, 39(1), pp.80–83.

Fullston, T., 2011. The role of Aristaless related homeobox (ARX) gene mutations in intellectual disability. PhD, University of Adelaide, Australia.

Gagnon, M. et al., 2013. Chloride extrusion enhancers as novel therapeutics for neurological diseases. *Nature medicine*, 19(11), pp.1524–8.

Gagnon, M. et al., 2017. Reply to The small molecule CLP257 does not modify activity of the K+–Cl− co-transporter KCC2 but does potentiate GABAA receptor activity. *Nature*

Medicine, 23(12), pp.1396–1398.

Gaily, E. et al., 2016. Incidence and outcome of epilepsy syndromes with onset in the first year of life: A retrospective population-based study. *Epilepsia*, 57(10), pp.1594–1601.

Galanopoulou, A.S., 2013. Basic mechanisms of catastrophic epilepsy - Overview from animal models. *Brain and Development*, 35(8), pp.748–756.

Gilhuis, H.J., Schieving, J. & Zwarts, M.J., 2011. Malignant migrating partial seizures in a 4-month-old boy. *Epileptic Disorders*, 13(2), pp.185–187.

Glaser, F. et al., 2003. ConSurf: identification of functional regions in proteins by surface-mapping of phylogenetic information. *Bioinformatics (Oxford, England)*, 19(1), pp.163–4.

Gokben, S. et al., 2017. Targeted next generation sequencing: the diagnostic value in early-onset epileptic encephalopathy. *Acta Neurologica Belgica*, 117(1), pp.131–138.

Goldman, D.E., 1943. Potential, Impedance, and Rectification in membranes. *The Journal of general physiology*, 27(1), pp.37–60.

Goldstein, J.H.R. et al., 2015. Novel SMC1A frameshift mutations in children with developmental delay and epilepsy. *European Journal of Medical Genetics*, 58(10), pp.562–568.

Gorman, K.M. et al., 2017. Novel *SMC1A* variant and epilepsy of infancy with migrating focal seizures: Expansion of the phenotype. *Epilepsia*, 58(7), pp.1301–1302.

Gross-Tsur, V., Ben-Zeev, B., Shalev, R.S., 2004. Malignant Migrating Partial Seizures in Infancy. *Pediatric Neurology*, 31, pp.287–290.

Gururaj, S., Fleites, J. & Bhattacharjee, A., 2016. Slack sodium-activated potassium channel membrane expression requires p38 mitogen-activated protein kinase phosphorylation. *Neuropharmacology*, 103, pp.279–289.

Hahn, A., Heckel, M. & Neubauer, B. a., 2007. Pronounced microcephaly in a patient with

malignant migrating partial seizures in infancy. *Epileptic Disorders*, 9(1), pp.94–97.

Hamamy, H., 2012. Consanguineous marriages preconception consultation in primary health care settings. *Journal of Community Genetics*, 3(3), pp.185–192.

Hamdan, F.F. et al., 2014. De Novo Mutations in Moderate or Severe Intellectual Disability G. M. Cooper, ed. *PLoS Genetics*, 10(10), p.e1004772.

Hansen, N. et al., 2017. Mesial temporal lobe epilepsy associated with KCNT1 mutation. *Seizure*, 45, pp.181–183.

Hansen, N.F., 2016. Variant Calling From Next Generation Sequence Data. In *Methods in molecular biology (Clifton, N.J.)*. pp. 209–224.

Hartmann, A.-M. et al., 2010. Differences in the large extracellular loop between the K(+)-Cl(-) cotransporters KCC2 and KCC4. *The Journal of biological chemistry*, 285(31), pp.23994–4002.

Heather, J.M. & Chain, B., 2016. The sequence of sequencers: The history of sequencing DNA. *Genomics*, 107(1), pp.1–8.

Hekmat-Scafe, D.S. et al., 2006. Mutations in the K+/Cl- cotransporter gene kazachoc (kcc) increase seizure susceptibility in Drosophila. *The Journal of neuroscience : the official journal of the Society for Neuroscience*, 26(35), pp.8943–8954.

Heron, S.E. et al., 2012. Missense mutations in the sodium-gated potassium channel gene KCNT1 cause severe autosomal dominant nocturnal frontal lobe epilepsy. *Nature Genetics*, 44(11), pp.1188–1190.

Higurashi, N. et al., 2013. PCDH19-related female-limited epilepsy: Further details regarding early clinical features and therapeutic efficacy. *Epilepsy Research*, 106(1–2), pp.191–9.

Hildebrand, M.S. et al., 2016. A targeted resequencing gene panel for focal epilepsy. *Neurology*, 86(17), pp.1605–1612.

Hirose, S., 2014. *Mutant GABAA receptor subunits in genetic (idiopathic) epilepsy* 1st ed., Elsevier B.V.

Hite, R.K. et al., 2015. Cryo-electron microscopy structure of the Slo2.2 Na(+)-activated K(+) channel. *Nature*, 527(7577), pp.198–203.

Hmaimess, G. et al., 2006. Levetiracetam in a neonate with malignant migrating partial seizures. *Pediatric Neurology*, 34(1), pp.55–59.

Hoch, W., Betz, H. & Becker, C.M., 1989. Primary cultures of mouse spinal cord express the neonatal isoform of the inhibitory glycine receptor. *Neuron*, 3(3), pp.339–48.

Howell, K.B. et al., 2015. SCN2A encephalopathy: A major cause of epilepsy of infancy with migrating focal seizures. *Neurology*, in press(11), pp.958–66.

Howell, K.B., Harvey, A.S. & Archer, J.S., 2016. Epileptic encephalopathy: Use and misuse of a clinically and conceptually important concept. *Epilepsia*, 57(3), pp.343–347.

Hübner, C.A. et al., 2001. Disruption of KCC2 reveals an essential role of K-Cl cotransport already in early synaptic inhibition. *Neuron*, 30(2), pp.515–524.

Huisman, S. et al., 2017. Phenotypes and genotypes in individuals with *SMC1A* variants. *American Journal of Medical Genetics Part A*.

Humphrey, A. et al., 2014. Intellectual development before and after the onset of infantile spasms: A controlled prospective longitudinal study in tuberous sclerosis. *Epilepsia*, 55(1), pp.108–116.

Hunt, D. et al., 2014. Whole exome sequencing in family trios reveals *de novo* mutations in *PURA* as a cause of severe neurodevelopmental delay and learning disability. *Journal of Medical Genetics*, 51(12), pp.806–813.

Irahara, K. et al., 2011. Effects of acetazolamide on epileptic apnea in migrating partial seizures in infancy. *Epilepsy Research*, 96(1–2), pp.185–189.

Ishii, A. et al., 2013. A recurrent KCNT1 mutation in two sporadic cases with malignant

migrating partial seizures in infancy. *Gene*, 531(2), pp.467–471.

Iyer, R.S., Thanikasalam & Krishnan, M., 2014. Migrating partial seizures in infancy and 47XYY syndrome: Cause or coincidence? *Epilepsy and Behavior Case Reports*, 2(1), pp.43–45.

Jan, M.M., 2007. The value of seizure semiology in lateralizing and localizing partially originating seizures. *Neurosciences (Riyadh, Saudi Arabia)*, 12(3), pp.185–90.

Jansen, S. et al., 2016. *De novo* loss-of-function mutations in X-linked *SMC1A* cause severe ID and therapy-resistant epilepsy in females: expanding the phenotypic spectrum. *Clinical Genetics*, 90(5), pp.413–419.

Janve, V.S. et al., 2016. Epileptic encephalopathy de novo *GABRB* mutations impair γ-aminobutyric acid type A receptor function. *Annals of Neurology*, 79(5), pp.806–825.

Japaridze, N. et al., 2015. Neuronal Networks during Burst Suppression as Revealed by Source Analysis L. M. Ward, ed. *PLOS ONE*, 10(4), p.e0123807.

Jenkinson, E.M. et al., 2016. Mutations in SNORD118 cause the cerebral microangiopathy leukoencephalopathy with calcifications and cysts. *Nature Genetics*, 48(10), pp.1185–1192.

Jensen, M.A. et al., 2010. DMSO and Betaine Greatly Improve Amplification of GC-Rich Constructs in De Novo Synthesis S. Deb, ed. *PLoS ONE*, 5(6), p.e11024.

Jiang, Y. et al., 2002. Crystal structure and mechanism of a calcium-gated potassium channel. *Nature*, 417(6888), pp.515–22.

Jocic-Jakubi, B. & Lagae, L., 2008. Malignant migrating partial seizures in Aicardi syndrome. *Developmental Medicine and Child Neurology*, 50(10), pp.790–792.

Jóźwiak, S. et al., 2011. Antiepileptic treatment before the onset of seizures reduces epilepsy severity and risk of mental retardation in infants with tuberous sclerosis complex. *European Journal of Paediatric Neurology*, 15(5), pp.424–431.

Juang, J.-M.J. et al., 2014. Disease-Targeted Sequencing of Ion Channel Genes identifies de novo mutations in Patients with Non-Familial Brugada Syndrome. *Scientific Reports*, 4, p.6733.

Kaczmarek, L.K., 2013. Slack , Slick , and Sodium-Activated Potassium Channels. , 2013.

Kahle, K.T. et al., 2014. Genetically encoded impairment of neuronal KCC2 cotransporter function in human idiopathic generalized epilepsy. *EMBO reports*, 15(7), pp.766–74.

Kaila, K. et al., 2014. Cation-chloride cotransporters in neuronal development, plasticity and disease. *Nature Reviews Neuroscience*, 15(10), pp.637–654.

Karolchik, D. et al., 2004. The UCSC Table Browser data retrieval tool. *Nucleic acids research*, 32(Database issue), pp.D493-6.

Kato, M. et al., 2013. Clinical spectrum of early onset epileptic encephalopathies caused by KCNQ2 mutation. *Epilepsia*, 54(7), pp.1282–1287.

Kato, M. et al., 2004. Mutations of ARX Are Associated with Striking Pleiotropy and Consistent Genotype-Phenotype Correlation. *Human Mutation*, 23(2), pp.147–159.

Kato, M. et al., 2014. PIGA mutations cause early-onset epileptic encephalopathies and distinctive features. *Neurology*, 82(18), pp.1587–1596.

Kawasaki, Y. et al., 2017. Three Cases of KCNT1 Mutations: Malignant Migrating Partial Seizures in Infancy with Massive Systemic to Pulmonary Collateral Arteries. *Journal of Pediatrics*, pp.1–5.

Kelley, M.R. et al., 2016. Compromising KCC2 transporter activity enhances the development of continuous seizure activity. *Neuropharmacology*, 108, pp.103–110.

Kim, G.E. et al., 2014. Human Slack Potassium Channel Mutations Increase Positive Cooperativity between Individual Channels. *Cell Reports*, 9(5), pp.1661–1672.

Kim, G.E. & Kaczmarek, L.K., 2014. Emerging role of the KCNT1 Slack channel in intellectual disability. *Frontiers in Cellular Neuroscience*, 8(July), pp.1–12.

Kircher, M. et al., 2014. A general framework for estimating the relative pathogenicity of human genetic variants. *Nature genetics*, 46(3), pp.310–5.

Kitamura, K. et al., 2002. Mutation of ARX causes abnormal development of forebrain and testes in mice and X-linked lissencephaly with abnormal genitalia in humans. *Nature genetics*, 32(3), pp.359–369.

Kivity, S. et al., 2004. Long-term cognitive outcomes of a cohort of children with cryptogenic infantile spasms treated with high-dose adrenocorticotropic hormone. *Epilepsia*, 45(3), pp.255–62.

Klepper, J., 2012. GLUT1 deficiency syndrome in clinical practice. *Epilepsy Research*, 100(3), pp.272–277.

Koboldt, D.C. et al., 2009. VarScan: variant detection in massively parallel sequencing of individual and pooled samples. *Bioinformatics (Oxford, England)*, 25(17), pp.2283–5.

Koboldt, D.C. et al., 2012. VarScan 2: somatic mutation and copy number alteration discovery in cancer by exome sequencing. *Genome research*, 22(3), pp.568–76.

Kodera, H. et al., 2016. De novo *GABRA1* mutations in Ohtahara and West syndromes. *Epilepsia*, 57(4), pp.566–573.

Kodera, H. et al., 2013. De Novo Mutations in SLC35A2 Encoding a UDP-Galactose Transporter Cause Early-Onset Epileptic Encephalopathy. *Human Mutation*, 34(12), pp.1708–1714.

Korff, C.M., Brunklaus, A. & Zuberi, S.M., 2015. Epileptic activity is a surrogate for an underlying etiology and stopping the activity has a limited impact on developmental outcome. *Epilepsia*, 56(10), pp.1477–1481.

Kozak, M., 1986. Point mutations define a sequence flanking the AUG initiator codon that modulates translation by eukaryotic ribosomes. *Cell*, 44(2), pp.283–92.

Krivov, G.G., Shapovalov, M. V. & Dunbrack, R.L., 2009. Improved prediction of protein

side-chain conformations with SCWRL4. *Proteins*, 77(4), pp.778–795.

Kulkarni, V.A. & Firestein, B.L., 2012. The dendritic tree and brain disorders. *Molecular and Cellular Neuroscience*, 50(1), pp.10–20.

Kullmann, D.M. et al., 2014. Gene therapy in epilepsy-is it time for clinical trials? *Nature reviews. Neurology*, 10(5), pp.300–4.

Kursan, S. et al., 2017. The neuronal K(+)Cl(-) co-transporter 2 (Slc12a5) modulates insulin secretion. *Scientific reports*, 7(1), p.1732.

Kwong, A.K.-Y. et al., 2015. Analysis of Mutations in 7 Genes Associated with Neuronal Excitability and Synaptic Transmission in a Cohort of Children with Non-Syndromic Infantile Epileptic Encephalopathy M. Schuelke, ed. *PLOS ONE*, 10(5), p.e0126446.

Lal, D. et al., 2014. *DEPDC5* mutations in genetic focal epilepsies of childhood. *Annals of Neurology*, 75(5), pp.788–792.

Lalani, S.R. et al., 2014. Mutations in PURA Cause Profound Neonatal Hypotonia, Seizures, and Encephalopathy in 5q31.3 Microdeletion Syndrome. *The American Journal of Human Genetics*, 95(5), pp.579–583.

Lander, E.S. et al., 2001. Initial sequencing and analysis of the human genome. *Nature*, 409(6822), pp.860–921.

Lander, E.S. & Botstein, D., 1987. Homozygosity mapping: a way to map human recessive traits with the DNA of inbred children. *Science (New York, N.Y.)*, 236(4808), pp.1567–70.

Landrum, M.J. et al., 2014. ClinVar: public archive of relationships among sequence variation and human phenotype. *Nucleic acids research*, 42(Database issue), pp.D980-5.

Larsen, J. et al., 2015. The phenotypic spectrum of SCN8A encephalopathy.

Le, S.V. et al., 2017. A mutation in *GABRB3* associated with Dravet syndrome. *American*

Journal of Medical Genetics Part A, 173(8), pp.2126–2131.

Lebrun, N. et al., 2015. Early-onset encephalopathy with epilepsy associated with a novel splice site mutation in *SMC1A*. *American Journal of Medical Genetics Part A*, 167(12), pp.3076–3081.

Lee, E.H. et al., 2012. A case of malignant migrating partial seizures in infancy as a continuum of infantile epileptic encephalopathy. *Brain and Development*, 34(9), pp.768–772.

Lee, H.H.C. et al., 2007. Direct protein kinase C-dependent phosphorylation regulates the cell surface stability and activity of the potassium chloride cotransporter KCC2. *Journal of Biological Chemistry*, 282(41), pp.29777–29784.

Leen, W.G. et al., 2010. Glucose transporter-1 deficiency syndrome: The expanding clinical and genetic spectrum of a treatable disorder. *Brain*, 133(3), pp.655–670.

Lemke, J.R. et al., 2014. GRIN2B mutations in west syndrome and intellectual disability with focal epilepsy. *Annals of Neurology*, 75(1), pp.147–154.

Lemke, J.R. et al., 2012. Targeted next generation sequencing as a diagnostic tool in epileptic disorders. *Epilepsia*, 53(8), pp.1387–1398.

Leniger, T. et al., 2003. A new Chrna4 mutation with low penetrance in nocturnal frontal lobe epilepsy. *Epilepsia*, 44(7), pp.981–5.

Li, H. et al., 2009. The Sequence Alignment/Map format and SAMtools. *Bioinformatics*, 25(16), pp.2078–2079.

Li, H. & Durbin, R., 2009. Fast and accurate short read alignment with Burrows-Wheeler transform. *Bioinformatics (Oxford, England)*, 25(14), pp.1754–60.

Lim, C.X. et al., 2016. KCNT1 mutations in seizure disorders: the phenotypic spectrum and functional effects. *Journal of medical genetics*.

Lipsker, D, Walther, S, Schulz, R, Nave, S, Cribier, B., 1998. Life-threatening vasculitis related

to quinidine occurring in a healthy volunteer during a clinical trial. *Eur J Clin Pharmacol*, 54, p.2052.

Liu, Z. et al., 2017. Identification of De Novo DNMT3A Mutations That Cause West Syndrome by Using Whole-Exome Sequencing. *Molecular Neurobiology*.

Lomize, M.A. et al., 2012. OPM database and PPM web server: resources for positioning of proteins in membranes. *Nucleic Acids Research*, 40(D1), pp.D370–D376.

Lorenz, T.C., 2012. Polymerase Chain Reaction: Basic Protocol Plus Troubleshooting and Optimization Strategies. *Journal of Visualized Experiments*, (63), p.e3998.

Löscher, W., Puskarjov, M. & Kaila, K., 2013. Cation-chloride cotransporters NKCC1 and KCC2 as potential targets for novel antiepileptic and antiepileptogenic treatments. *Neuropharmacology*, 69, pp.62–74.

Lund, C. et al., 2014. CHD2 mutations in Lennox-Gastaut syndrome. *Epilepsy and Behavior*, 33, pp.18–21.

MacKenzie, G. et al., 2016. Compromised GABAergic inhibition contributes to tumor-associated epilepsy. *Epilepsy Research*, 126, pp.185–196.

Magiorkinis, E., Sidiropoulou, K. & Diamantis, A., 2010. Hallmarks in the history of epilepsy: Epilepsy in antiquity. *Epilepsy and Behavior*, 17(1), pp.103–108.

Mahadevan, V. & Woodin, M.A., 2016. Regulation of neuronal chloride homeostasis by neuromodulators. *Journal of Physiology*, 594(10), pp.2593–2605.

Maljevic, S., Reid, C.A. & Petrou, S., 2017. Models for discovery of targeted therapy in genetic epileptic encephalopathies. *Journal of Neurochemistry*.

Mangan, K.P. et al., 2015. Modeling Neurological Disease with Human iPS Cell-Derived Neurons Containing a KCNT1 Mutation. *Biophysical Journal*, 108(2), p.588a.

Marini, C. et al., 2006. Mosaic SCN1A mutation in familial severe myoclonic epilepsy of infancy. *Epilepsia*, 47(10), pp.1737–40.

Marsh, E. et al., 2005. Migrating partial seizures in infancy: Expanding the phenotype of a rare seizure syndrome. *Epilepsia*, 46(4), pp.568–572.

Martín-Aragón Baudel, M.A.S., Poole, A. V. & Darlison, M.G., 2017. Chloride co-transporters as possible therapeutic targets for stroke. *Journal of Neurochemistry*, 140(2), pp.195–209.

Martin, H.C. et al., 2014. Clinical whole-genome sequencing in severe early-onset epilepsy reveals new genes and improves molecular diagnosis. *Human Molecular Genetics*, 23(12), pp.3200–3211.

Matsumoto, A. et al., 1981. Long-term prognosis after infantile spasms: a statistical study of prognostic factors in 200 cases. *Developmental medicine and child neurology*, 23(1), pp.51–65.

McLaren, W. et al., 2010. Deriving the consequences of genomic variants with the Ensembl API and SNP Effect Predictor. *Bioinformatics (Oxford, England)*, 26(16), pp.2069–70.

McTague, A. et al., 2013. Migrating partial seizures of infancy: Expansion of the electroclinical, radiological and pathological disease spectrum. *Brain*, 136(5), pp.1578–1591.

McTague, A. et al., 2015. The genetic landscape of the epileptic encephalopathies of infancy and childhood. *The Lancet. Neurology*.

Medina, I. et al., 2014. Current view on the functional regulation of the neuronal K(+)-Cl(-) cotransporter KCC2. *Frontiers in cellular neuroscience*, 8(February), p.27.

Mefford, H.C., 2015. Clinical Genetic Testing in Epilepsy. *Epilepsy currents*, 15(4), pp.197–201.

Mefford, H.C. et al., 2011. Rare copy number variants are an important cause of epileptic encephalopathies. *Annals of Neurology*, 70(6), pp.974–985.

Merdariu, D. et al., 2013. Malignant migrating partial seizures of infancy controlled by

stiripentol and clonazepam. *Brain and Development*, 35(2), pp.177–180.

Merner, N.D. et al., 2015. Regulatory domain or CpG site variation in SLC12A5, encoding the chloride transporter KCC2, in human autism and schizophrenia. *Frontiers in cellular neuroscience*, 9, p.386.

Miceli, F. et al., 2013. Genotype – phenotype correlations in neonatal epilepsies caused by mutations in the voltage sensor of K v 7 . 2 potassium channel subunits. , pp.1–6.

Michaud, J.L. et al., 2014. The genetic landscape of infantile spasms. *Human molecular genetics*, pp.1–34.

Mikati, M.A. et al., 2015. Quinidine in the treatment of KCNT1-positive epilepsies. *Annals of Neurology*, 78(6), pp.995–999.

Milh, M. et al., 2013. Novel Compound Heterozygous Mutations in TBC1D24 Cause Familial Malignant Migrating Partial Seizures of Infancy. *Human Mutation*, 34(6), pp.869–872.

Milligan, C.J. et al., 2014. KCNT1 gain of function in 2 epilepsy phenotypes is reversed by quinidine. *Annals of Neurology*, 75(4), pp.581–590.

Møller, R.S. et al., 2017. Mutations in *GABRB3*. *Neurology*, 88(5), pp.483–492.

Møller, R.S., Heron, S.E., et al., 2015. Mutations in *KCNT1* cause a spectrum of focal epilepsies. *Epilepsia*, p.n/a-n/a.

Møller, R.S., Dahl, H.A. & Helbig, I., 2015. The contribution of next generation sequencing to epilepsy genetics. *Expert Review of Molecular Diagnostics*, 15(12), pp.1531–1538.

Moore, Y.E. et al., 2017. Seizing Control of KCC2: A New Therapeutic Target for Epilepsy. *Trends in Neurosciences*, 40(9), pp.555–571.

Mori, T. et al., 2016. Usefulness of ketogenic diet in a girl with migrating partial seizures in infancy. *Brain and Development*, 38(6), pp.601–604.

Morimoto, M. et al., 2006. SCN1A mutation mosaicism in a family with severe myoclonic

epilepsy in infancy. *Epilepsia*, 47(10), pp.1732–6.

Moser, M.B., Trommald, M. & Andersen, P., 1994. An increase in dendritic spine density on hippocampal CA1 pyramidal cells following spatial learning in adult rats suggests the formation of new synapses. *Proceedings of the National Academy of Sciences of the United States of America*, 91(26), pp.12673–5.

Mullen, S.A. et al., 2011. Glucose Transporter 1 Deficiency as a Treatable Cause of Myoclonic Astatic Epilepsy. *Archives of Neurology*, 68(9), p.1152.

Mullen, S.A. et al., 2011. Glucose transporter 1 deficiency as a treatable cause of myoclonic astatic epilepsy. *Archives of neurology*, 68(9), pp.1152–1155.

Mullen, S.A. et al., 2017. Precision therapy for epilepsy due to *KCNT1* mutations. *Neurology*, p.10.1212/WNL.0000000000004769.

Mungall, C.J. et al., 2017. The Monarch Initiative: an integrative data and analytic platform connecting phenotypes to genotypes across species. *Nucleic acids research*, 45(D1), pp.D712–D722.

Myers, C.T. et al., 2016. De Novo Mutations in SLC1A2 and CACNA1A Are Important Causes of Epileptic Encephalopathies. *American Journal of Human Genetics*, 99(2), pp.287–298.

Myers, C.T. et al., 2016. De Novo Mutations in SLC1A2 and CACNA1A Are Important Causes of Epileptic Encephalopathies. *The American Journal of Human Genetics*, 99(2), pp.287–298.

Myers, C.T. & Mefford, H.C., 2016. *Genetic investigations of the epileptic encephalopathies: Recent advances* 1st ed., Elsevier B.V.

Nabatame, S. et al., 2010. Bromoderma in a patient with migrating partial seizures in infancy. *Epilepsy Research*, 91(2–3), pp.283–288.

Nabbout, R. et al., 2013. Encephalopathy in children with Dravet syndrome is not a pure

consequence of epilepsy. *Orphanet Journal of Rare Diseases*, 8(1), p.176.

Nakamura, K., Kato, M., et al., 2013. Clinical spectrum of SCN2A mutations expanding to Ohtahara syndrome. *Neurology*, 81(11), pp.992–998.

Nakamura, K., Kodera, H., et al., 2013. De novo mutations in GNAO1, encoding a gαo subunit of heterotrimeric g proteins, cause epileptic encephalopathy. *American Journal of Human Genetics*, 93(3), pp.496–505.

Nakashima, M. et al., 2016. WDR45 mutations in three male patients with West syndrome. *Journal of Human Genetics*, 61(7), pp.653–661.

Need, a. C. et al., 2012. Clinical application of exome sequencing in undiagnosed genetic conditions. *Journal of Medical Genetics*, 49(6), pp.353–361.

Ng, P.C. & Henikoff, S., 2001. Predicting Deleterious Amino Acid Substitutions. *Genome Research*, 11(5), pp.863–874.

Nordli, D.R., 2012. Epileptic Encephalopathies in Infants and Children. *Journal of Clinical Neurophysiology*, 29(5), pp.420–424.

Numis, a. L. et al., 2014. KCNQ2 encephalopathy: Delineation of the electroclinical phenotype and treatment response. *Neurology*, 82(4), pp.368–370.

O'Callaghan, F.J.K. et al., 2011. The effect of lead time to treatment and of age of onset on developmental outcome at 4 years in infantile spasms: Evidence from the United Kingdom Infantile Spasms Study. *Epilepsia*, 52(7), pp.1359–1364.

Ogiwara, I. et al., 2009. mutations of voltage-gated sodium channel alpha II gene SCN2A in intractable epilepsies. *Neurology*, 73, pp.1046–1053.

Ohba, C. et al., 2015. De novo *KCNT1* mutations in early-onset epileptic encephalopathy. *Epilepsia*, p.n/a-n/a.

Ohba, C. et al., 2014. Early onset epileptic encephalopathy caused by de novo SCN8A mutations. *Epilepsia*, 55(7), pp.994–1000.

Ohtahara, S., 1977. A study on the age dependent epileptic encephalopathy. *No Te Hattatsu*, 9(1), pp.2–21.

Ohtahara, S. & Yamatogi, Y., 2006a. Ohtahara syndrome: With special reference to its developmental aspects for differentiating from early myoclonic encephalopathy. *Epilepsy Research*, 70(SUPPL.1), pp.2–5.

Ohtahara, S. & Yamatogi, Y., 2006b. Ohtahara syndrome: With special reference to its developmental aspects for differentiating from early myoclonic encephalopathy. *Epilepsy Research*, 70, pp.58–67.

Okuda, K. et al., 2000. Successful control with bromide of two patients with malignant migrating partial seizures in infancy. *Brain and Development*, 22(1), pp.56–59.

Olivetti, P.R. & Noebels, J.L., 2012. Interneuron, interrupted: Molecular pathogenesis of ARX mutations and X-linked infantile spasms. *Current Opinion in Neurobiology*, 22(5), pp.859–865.

Orhan, G. et al., 2014. Dominant-negative effects of KCNQ2 mutations are associated with epileptic encephalopathy. *Annals of neurology*, 75(3), pp.382–94.

Osborne, J.P. et al., 2010. The underlying etiology of infantile spasms (West syndrome): Information from the United Kingdom Infantile Spasms Study (UKISS) on contemporary causes and their classification. *Epilepsia*, 51(10), pp.2168–2174.

Otsuka, M. et al., 2010. STXBP1 mutations cause not only Ohtahara syndrome but also West syndrome-Result of Japanese cohort study. *Epilepsia*, 51(12), pp.2449–2452.

Paciorkowski, A.R. et al., 2011. Copy number variants and infantile spasms: evidence for abnormalities in ventral forebrain development and pathways of synaptic function. *European Journal of Human Genetics*, 19(12), pp.1238–1245.

Pallud, J. et al., 2014. Cortical GABAergic excitation contributes to epileptic activities around human glioma. *Science Translational Medicine*, 6(244), pp.24489–24489.

Panayiotopoulos, C., 2005. *The Epilepsies: Seizures, Syndromes and Management.*, Oxfordshire (UK): Bladon Medical Publishing.

Parajuli, L.K., Tanaka, S. & Okabe, S., 2017. Insights into age-old questions of new dendritic spines: From form to function. *Brain Research Bulletin*, 129, pp.3–11.

Parrini, E. et al., 2017. Diagnostic Targeted Resequencing in 349 Patients with Drug-Resistant Pediatric Epilepsies Identifies Causative Mutations in 30 Different Genes. *Human Mutation*, 38(2), pp.216–225.

Payne, J.A., 1997. Functional characterization of the neuronal-specific K-Cl cotransporter: implications for [K+]o regulation. *The American journal of physiology*, 273(5 Pt 1), pp.C1516-25.

Payne, J. a., Stevenson, T.J. & Donaldson, L.F., 1996. Molecular characterization of a putative K-Cl cotransporter in rat brain: A neuronal-specific isoform. *Journal of Biological Chemistry*, 271(27), pp.16245–16252.

Petrou, S, Ugur, M, Drummond, RM, Singer, JJ, Walsh, JVJr, ., 1997. P2X7 purinoceptor expression in Xenopus oocytes is not sufficient to produce a pore-forming P2Z-like phenotype. *FEBS Lett*, 411, pp.339–345.

Pettersen, E.F. et al., 2004. UCSF Chimera--a visualization system for exploratory research and analysis. *Journal of computational chemistry*, 25(13), pp.1605–1612.

Pettit, R.E. & Fenichel, G.M., 1980. *Benign familial neonatal seizures.*,

Pippucci, T. et al., 2013. A Novel Null Homozygous Mutation Confirms CACNA2D2 as a Gene Mutated in Epileptic Encephalopathy K. Brusgaard, ed. *PLoS ONE*, 8(12), p.e82154.

Plouin, P. & Kaminska, A., 2013. Neonatal seizures. *Handbook of Clinical Neurology*, 111, pp.467–476.

Poduri, A., Chopra, S.S., et al., 2012. Homozygous PLCB1 deletion associated with malignant migrating partial seizures in infancy. *Epilepsia*, 53(8), pp.146–150.

Poduri, A. et al., 2013. SLC25A22 is a novel gene for migrating partial seizures in infancy. *Annals of Neurology*, 74(6), pp.873–882.

Poduri, A., Heinzen, E.L., et al., 2013. SLC25A22 is a novel gene for migrating partial seizures in infancy. *Annals of Neurology*, 74(6).

Poduri, A., Evrony, G.D., et al., 2012. Somatic activation of AKT3 causes hemispheric developmental brain malformations. *Neuron*, 74(1), pp.41–8.

Poduri, A., Evrony, G.D., et al., 2013. Somatic Mutation, Genomic Variation, and Neurological Disease. *Science*, 341(6141), pp.1237758–1237758.

Pressler, R.M. et al., 2015. Bumetanide for the treatment of seizures in newborn babies with hypoxic ischaemic encephalopathy (NEMO): an open-label, dose finding, and feasibility phase 1/2 trial. *The Lancet Neurology*, 14(5), pp.469–477.

Puskarjov, M., et al., 2014. A variant of KCC2 from patients with febrile seizures impairs neuronal Cl- extrusion and dendritic spine formation. *EMBO Reports*, 15(6), pp.723–729.

Puskarjov, M., et al., 2014. Pharmacotherapeutic targeting of cation-chloride cotransporters in neonatal seizures. *Epilepsia*, 55(6), pp.806–818.

Rahman, S., 2012. Mitochondrial disease and epilepsy. *Developmental medicine and child neurology*, 54(5), pp.397–406.

Ramm-Pettersen, A. et al., 2013. Good outcome in patients with early dietary treatment of GLUT-1 deficiency syndrome: Results from a retrospective Norwegian study. *Developmental Medicine and Child Neurology*, 55(5), pp.440–447.

Rees, M.I. et al., 2006. Mutations in the gene encoding GlyT2 (SLC6A5) define a presynaptic component of human startle disease. *Nature Genetics*, 38(7), pp.801–806.

Richards, S. et al., 2015. Standards and guidelines for the interpretation of sequence variants: a joint consensus recommendation of the American College of Medical

Genetics and Genomics and the Association for Molecular Pathology. *Genetics in Medicine*, 17(5), pp.405–423.

Rivera, C. et al., 1999. The K+/Cl- co-transporter KCC2 renders GABA hyperpolarizing during neuronal maturation. *Nature*, 397(6716), pp.251–255.

Rizzi, S., Knaus, H.-G. & Schwarzer, C., 2016. Differential distribution of the sodium-activated potassium channels slick and slack in mouse brain. *The Journal of comparative neurology*, 524(10), pp.2093–116.

Rizzo, F. et al., 2016a. Characterization of two de novo KCNT1 mutations in children with malignant migrating partial seizures in infancy. *Molecular and Cellular Neuroscience*, 72, pp.54–63.

Rizzo, F. et al., 2016b. Characterization of two de novoKCNT1 mutations in children with malignant migrating partial seizures in infancy. *Molecular and cellular neurosciences*, 72, pp.54–63.

Robinson, P.N. et al., 2008. The Human Phenotype Ontology: A Tool for Annotating and Analyzing Human Hereditary Disease. *The American Journal of Human Genetics*, 83(5), pp.610–615.

Romiguier, J. et al., 2010. Contrasting GC-content dynamics across 33 mammalian genomes: relationship with life-history traits and chromosome sizes. *Genome research*, 20(8), pp.1001–9.

Rosanoff, M.J. & Ottman, R., 2008. Penetrance of LGI1 mutations in autosomal dominant partial epilepsy with auditory features. *Neurology*, 71(8), pp.567–571.

Saade, D. & Joshi, C., 2015. Pure cannabidiol in the treatment of malignant migrating partial seizures in infancy: a case report. *Pediatric Neurology*, 52(5), pp.544–7.

Saito, T. et al., 2017. A *de novo* missense mutation in *SLC12A5* found in a compound heterozygote patient with epilepsy of infancy with migrating focal seizures. *Clinical Genetics*.

Saitsu, H. et al., 2012. CASK aberrations in male patients with Ohtahara syndrome and cerebellar hypoplasia. *Epilepsia*, 53(8), pp.1441–1449.

Saitsu, H. et al., 2008. De novo mutations in the gene encoding STXBP1 (MUNC18-1) cause early infantile epileptic encephalopathy. *Nature genetics*, 40(6), pp.782–788.

Saitsu, H. et al., 2016. Impaired neuronal KCC2 function by biallelic SLC12A5 mutations in migrating focal seizures and severe developmental delay. *Scientific reports*, 6(July), p.30072.

Sakuma, T. et al., 2013. Efficient TALEN construction and evaluation methods for human cell and animal applications. *Genes to cells : devoted to molecular & cellular mechanisms*, 18(4), pp.315–26.

Sali, A. & Blundell, T.L., 1993. Comparative protein modelling by satisfaction of spatial restraints. *Journal of Molecular Biology*, 234(3), pp.779–815.

Scheffer, I.E. et al., 2016. Classification of the epilepsies : New concepts for discussion and debate — Special report of the ILAE Classification Task Force of the Commission for Classification and Procedure for Ilae Position Papers Epilepsies Accepted and Ready The classification o. , pp.1–8.

Scheffer, I.E. et al., 2009. Dravet syndrome or genetic (generalized) epilepsy with febrile seizures plus? *Brain & development*, 31(5), pp.394–400.

Scheffer, I.E., 2014. Epilepsy genetics revolutionizes clinical practice. *Neuropediatrics*, 45(2), pp.70–74.

Scheffer, I.E. et al., 2017. ILAE classification of the epilepsies: Position paper of the ILAE Commission for Classification and Terminology. *Epilepsia*, 58(4), pp.512–521.

Segal, E. et al., 2014. An uncommon presentation of a MECP2 mutation: Malignant migrating partial epilepsy of infancy with cataracts and upper motor neuron deficits. *Epilepsy Currents*, 14, p.424.

Selioutski, O. et al., 2015. Characteristic Features of the Interictal EEG Background in 2 Patients with Malignant Migrating Partial Epilepsy in Infancy. *Journal of Clinical Neurophysiology*, 32(4), pp.e23–e29.

Shaffer, P.L. et al., 2009. Structure and mechanism of a Na+-independent amino acid transporter. *Science (New York, N.Y.)*, 325(5943), pp.1010–4.

Sharma, S. et al., 2011. Child neurology: Epilepsy of infancy with migrating focal seizures. *Neurology*, 77(4), pp.0–5.

Shen, J. et al., 2010. Mutations in PNKP cause microcephaly, seizures and defects in DNA repair. *Nature genetics*, 42(3), pp.245–249.

Shen, M.-Y. & Sali, A., 2006. Statistical potential for assessment and prediction of protein structures. *Protein science : a publication of the Protein Society*, 15(11), pp.2507–24.

Sheridan, E. et al., 2013. Risk factors for congenital anomaly in a multiethnic birth cohort: an analysis of the Born in Bradford study. *The Lancet*, 382(9901), pp.1350–1359.

Shimada, S. et al., 2014. A novel KCNT1 mutation in a Japanese patient with epilepsy of infancy with migrating focal seizures. *Human Genome Variation*, 1(October), p.14027.

Singh, N.A. et al., 1998. A novel potassium channel gene, KCNQ2, is mutated in an inherited epilepsy of newborns. *Nature genetics*, 18(1), pp.25–29.

Singh, R. et al., 2001. Severe myoclonic epilepsy of infancy: extended spectrum of GEFS+? *Epilepsia*, 42(7), pp.837–44.

Siniatchkin, M. et al., 2007. Different Neuronal Networks Are Associated with Spikes and Slow Activity in Hypsarrhythmia. *Epilepsia*, 0(0), p.070816162212002–???

Siniatchkin, M. & Capovilla, G., 2013. Functional neuroimaging in epileptic encephalopathies. *Epilepsia*, 54(SUPPL.8), pp.27–33.

Sippl, M.J., 1993. Boltzmann's principle, knowledge-based mean fields and protein folding. An approach to the computational determination of protein structures. *Journal of*

computer-aided molecular design, 7(4), pp.473–501.

Sivakumaran, S. et al., 2015. Selective Inhibition of KCC2 Leads to Hyperexcitability and Epileptiform Discharges in Hippocampal Slices and In Vivo. *Journal of Neuroscience*, 35(21), pp.8291–8296.

Söding, J., Biegert, A. & Lupas, A.N., 2005. The HHpred interactive server for protein homology detection and structure prediction. *Nucleic Acids Research*, 33(suppl 2), pp.W244–W248.

Spence, M.A. & Hodge, S.E., 2000. The 'Circular' Problems of Calculating Risk: Dealing with Consanguinity. *Journal of Genetic Counseling*, 9(3), pp.179–201.

Staley, K.J. & Proctor, W.R., 1999. Modulation of mammalian dendritic GABA(A) receptor function by the kinetics of Cl- and HCO3- transport. *The Journal of physiology*, 519(3), pp.693–712.

Stamberger, H. et al., 2016. *STXBP1* encephalopathy. *Neurology*, 86(10), pp.954–962.

Stödberg, T. et al., 2015. Mutations in SLC12A5 in epilepsy of infancy with migrating focal seizures. *Nature communications*, 6, p.8038. Material reproduced in this thesis under creative commons license http://creativecommons.org/licenses/by/4.0/.

Strien, J., Sanft, J. & Mall, G., 2013. Enhancement of PCR Amplification of Moderate GC-Containing and Highly GC-Rich DNA Sequences. *Molecular Biotechnology*, 54(3), pp.1048–1054.

Sun, Y. et al., 2016. A deleterious Na $_{v}$ 1.1 mutation selectively impairs telencephalic inhibitory neurons derived from Dravet Syndrome patients. *eLife*, 5.

Symonds, J.D. et al., 2017. Heterozygous truncation mutations of the *SMC1A* gene cause a severe early onset epilepsy with cluster seizures in females: Detailed phenotyping of 10 new cases. *Epilepsia*, 58(4), pp.565–575.

Tang, Q.-Y. et al., 2016. Epilepsy-Related Slack Channel Mutants Lead to Channel Over-Activity by Two Different Mechanisms. *Cell reports*, 14(1), pp.129–39.

Tang, X. et al., 2016. KCC2 rescues functional deficits in human neurons derived from patients with Rett syndrome. *Proceedings of the National Academy of Sciences*, 113(3), pp.751–756.

Tarailo-Graovac, M. et al., 2016. Exome Sequencing and the Management of Neurometabolic Disorders. *New England Journal of Medicine*, 374(23), pp.2246–2255.

Thevenon, J. et al., 2014. Mutations in SLC13A5 cause autosomal-recessive epileptic encephalopathy with seizure onset in the first days of Life. *American Journal of Human Genetics*, 95(1), pp.113–120.

Tornberg, J. et al., 2005. Behavioural phenotypes of hypomorphic KCC2-deficient mice. *European Journal of Neuroscience*, 21(5), pp.1327–1337.

Touma, M. et al., 2013. Whole genome sequencing identifies SCN2A mutation in monozygotic twins with Ohtahara syndrome and unique neuropathologic findings. *Epilepsia*, 54(5), pp.81–85.

Trump, N. et al., 2016. Improving diagnosis and broadening the phenotypes in early-onset seizure and severe developmental delay disorders through gene panel analysis. *Journal of Medical Genetics*, 53(5), pp.310–317.

Untergasser, A. et al., 2012. Primer3—new capabilities and interfaces. *Nucleic Acids Research*, 40(15), pp.e115–e115.

Ünver, O. et al., 2013. Potassium bromide for treatment of malignant migrating partial seizures in infancy. *Pediatric Neurology*, 49(5), pp.355–357.

Uvarov, P. et al., 2007. A novel N-terminal isoform of the neuron-specific K-Cl cotransporter KCC2. *Journal of Biological Chemistry*, 282(42), pp.30570–30576.

Vanderver, A. et al., 2014. Identification of a novel de novo p.Phe932Ile KCNT1 mutation in

a patient with leukoencephalopathy and severe epilepsy. *Pediatric Neurology*, 50(1), pp.112–114.

Vanhatalo, S. et al., 2005. Slow endogenous activity transients and developmental expression of K +-Cl- cotransporter 2 in the immature human cortex. *European Journal of Neuroscience*, 22(11), pp.2799–2804.

Vears, D.F. et al., 2015. 'It's good to know': Experiences of gene identification and result disclosure in familial epilepsies. *Epilepsy Research*, 112, pp.64–71.

Veeramah, K.R. et al., 2013. Exome sequencing reveals new causal mutations in children with epileptic encephalopathies. *Epilepsia*, 54(7), pp.1270–1281.

Vendrame, M. et al., 2011. Treatment of malignant migrating partial epilepsy of infancy with rufinamide: Report of five cases. *Epileptic Disorders*, 13(1), pp.18–21.

Veneselli, E. et al., 2001. Malignant migrating partial seizures in infancy. *Epilepsy research*, 46(1), pp.27–32.

Vilen, H. et al., 2001. Construction of gene-targeting vectors: A rapid Mu in vitro DNA transposition-based strategy generating null, potentially hypomorphic, and conditional alleles. *Transgenic Research*, 10(1), pp.69–80.

Wang, J. et al., 2017. Epilepsy-associated genes. *Seizure*, 44, pp.11–20.

Warrier, V., Baron-Cohen, S. & Chakrabarti, B., 2013. Genetic variation in GABRB3 is associated with Asperger syndrome and multiple endophenotypes relevant to autism. *Molecular autism*, 4(1), p.48.

Weckhuysen, S. et al., 2013. Extending the KCNQ2 encephalopathy spectrum: Clinical and neuroimaging findings in 17 patients. *Neurology*, 81(19), pp.1697–1703.

Weckhuysen, S. et al., 2012. KCNQ2 encephalopathy: Emerging phenotype of a neonatal epileptic encephalopathy. *Annals of Neurology*, 71(1), pp.15–25.

West, W.J., 1841. ON A PECULIAR FORM OF INFANTILE CONVULSIONS. *The Lancet*, 35(911),

pp.724–725.

Wilmshurst, J.M., Appleton, D.B. & Grattan-Smith, P.J., 2000. Migrating partial seizures in infancy: two new cases. *Journal of child neurology*, 15(11), pp.717–722.

Wolf, P., 2014. History of epilepsy: nosological concepts and classification. *Epileptic disorders : international epilepsy journal with videotape*, 16(3), pp.261–9.

Wolff, M. et al., 2017. Genetic and phenotypic heterogeneity suggest therapeutic implications in SCN2A-related disorders. *Brain*, 140(5), pp.1316–1336.

Woo, N.S. et al., 2002. Hyperexcitability and epilepsy associated with disruption of the mouse neuronal-specific K-Cl cotransporter gene. *Hippocampus*, 12(2), pp.258–268.

Woods, C.G. et al., 2004. A new method for autozygosity mapping using single nucleotide polymorphisms (SNPs) and EXCLUDEAR. *Journal of medical genetics*, 41(8), p.e101.

Yamamoto, T. et al., 2016. Challenges in detecting genomic copy number aberrations using next-generation sequencing data and the eXome Hidden Markov Model: a clinical exome-first diagnostic approach. *Human Genome Variation*, 3(June), p.16025.

Yang, B. et al., 2006. Pharmacological activation and inhibition of Slack (Slo2.2) channels. *Neuropharmacology*, 51(4), pp.896–906.

Yang, Y. et al., 2013. Clinical Whole-Exome Sequencing for the Diagnosis of Mendelian Disorders. *New England Journal of Medicine*, 369(16), pp.1502–1511.

Ye, S., Li, Y. & Jiang, Y., 2010. Novel insights into K+ selectivity from high-resolution structures of an open K+ channel pore. *Nature structural & molecular biology*, 17(8), pp.1019–23.

Yu, F.H. et al., 2006. Reduced sodium current in GABAergic interneurons in a mouse model of severe myoclonic epilepsy in infancy. *Nature neuroscience*, 9(9), pp.1142–1149.

Yu, L. et al., 2005. Nuclear magnetic resonance structural studies of a potassium channel-charybdotoxin complex. *Biochemistry*, 44(48), pp.15834–41.

Yuan, P. et al., 2010. Structure of the Human BK Channel Ca2+-Activation Apparatus at 3.0 Å Resolution. *Science*, 329(5988), pp.182–186.

Zerem, A. et al., 2016. The molecular and phenotypic spectrum of *IQSEC2* -related epilepsy. *Epilepsia*, 57(11), pp.1858–1869.

Zhang, Q. et al., 2017. Gene mutation analysis of 175 Chinese patients with early-onset epileptic encephalopathy. *Clinical Genetics*, 91(5), pp.717–724.

Zhang, X. et al., 2014. Mutations in QARS, encoding glutaminyl-trna synthetase, cause progressive microcephaly, cerebral-cerebellar atrophy, and intractable seizures. *American Journal of Human Genetics*, 94(4), pp.547–558.

Zhang, Y. et al., 2015. Gene Mutation Analysis in 253 Chinese Children with Unexplained Epilepsy and Intellectual/Developmental Disabilities M. S. Shapiro, ed. *PLOS ONE*, 10(11), p.e0141782.

Zhao, B. et al., 2008. Identification of a novel di-leucine motif mediating K+/Cl− cotransporter KCC2 constitutive endocytosis. *Cellular Signalling*, 20(10), pp.1769–1779.

Zuberi, S.M. et al., 2011. Genotype-phenotype associations in SCN1A-related epilepsies. *Neurology*, 76(7), pp.594–600.

Chapter 8 Appendix

8.1 BPNSU study: Migrating Partial Seizures in Infancy – Research Proforma

Notifying consultant: Tertiary Centre:

First part of child's post code (up to 4 letters/figures):

Date of birth: Sex: Male / Female

Ethnic Group:

Age when MPSI considered most likely diagnosis:

Current age (give date of death if deceased):

Birth details:

Weight: …….

Gestation: …….

Type of delivery: Normal vaginal / Assisted vaginal / Elective LSCS / Emergency LSCS

Perinatal difficulties: resuscitation / Ventilation / Feeding difficulties

Occipitofrontal circumference (OFC) at birth

Mum's age

Dad's age

Mum's pregnancy history – Gravida ….. Para….

Any miscarriages, terminations or still births?

Ages of other siblings

Do any of the siblings have any neurological or other health problems?

If yes, give details

Any other important family history?

If yes, give details

Age at presentation with epilepsy …….

Describe seizures at presentation:

Semiology of each seizure type & date first noticed

1.

2.

3.

4.

Frequency of seizures: Awake ……. Asleep……

Do seizures occur in clusters?

Has the child had episodes of convulsive status epilepticus? Y / N

Give number of episodes here ……

Has child had episodes of non-convulsive status epilepticus? Y / N

Give number of episodes here ……

Has the child had episode of complex partial status epilepticus? Y / N

Give number of episodes here ……

Were autonomic features present? Give details

Rash:

Epiphora (production of tears):

Pupillary changes:

Salivation:

Other:

Examination findings at presentation

Any abnormal physical or neurological findings?

Any dysmorphic features?

If yes, give details here

Did the child as a baby have a ‘coarse’ facial appearance? Y / N

Investigations

How many EEGs has child had? .....

Was the first EEG normal? Y / N

Has the child had an ictal EEG? Y / N

If yes, were seizures captured from at least 2 different ‘foci’? Y / N

Please attach copies of EEG reports with this form

Has the child had a CT scan? Y / N (Give ages when performed)

Has the child had an MRI scan? Y / N (Give ages when performed)

Has the child had MR spectroscopy performed? Y / N (Give ages when performed)

Please attach copies of MRI or CT results with this form

Please fill in the table below regarding possible investigation list – and please give levels of any tests results if possible:

Please list any other investigations in table as well (space at the bottom)

Chromosomes	
Skin chromosomes	
Any other cytogenetic tests	
Ammonia	
Plasma lactate	
Plasma amino acids	
Liver function tests	
Acyl carnitine/carnitine profile	
Biotinidase	
Copper and caeruloplasmin	
White cell enzymes	
Very long chain fatty acids	
Sialated transferrins	
Urine amino and organic acids	
Urinary sulfites	
Mucopolysaccharide screen	
CSF lactate	
CSF fasting blood/glucose ratio	
CSF amino acids	
CSF neurotransmitters **Investigation table MPSI Continued.**	
TORCH screen	
MECP2 analysis	
CDKL5 mutation	
SCN1A mutation	
MERFF or MELAS	
Mitochondrial genome sequencing	
Any other molecular genetic tests (please describe)	
Muscle biopsy	
Liver biopsy	
PDH fibroblast activity	
Others, give details	

Please fill in table below regarding possible treatments the child has received:

Please list any other treatments tried at the bottom of the table

	Length of treatment	Max dose m/Kg	Reason for withdrawal	List drugs given in combination with this treatment
Pyridoxine				
Pyridoxal phosphate				
Biotin				
Folinic acid				
Carbamazepine				
Oxcarbamazine				
Phenytoin				
Phenobarbitone				
Sodium valproate				
Stiripentol				
Clobazam				
Clonazepam				
Nitrazepam				
Vigabatrin				
Levetiracetam				
Topiramate				
Lamotrigine				
Bromide Salts				
Zonisamide				
Gabapentin				
	Length of treatment	Max dose m/Kg	Reason for withdrawal	List drugs given in combination with this treatment
Ketogenic Diet (KD)				
Course(s) of prednisolone				

Course(s) of other steroid (give details)				
Course(s) of Immunoglobulin				
Vagal Nerve Stimulator				
Trial without medication				
Others				

Please list the treatment or combination of treatments used to produce the 'best' periods of seizure control

How old was the child during this period? ……

Which rescue medications, if any, have you found to be useful?

Course of condition:

What was the maximum number of seizures per day recorded?

How old was the child at this time?

Did seizure frequency decrease with time? Y / N

Please give details

Has child lost developmental milestones? Y / N

When did this happen?

Give details of developmental progress:

Please attach any relevant developmental assessments

Milestone	Age achieved	Age lost skill	Age regained skill
Social smile			
Visually alert			
Good head control			
Rolling over			
Sits with support			
Sits without support			
Pull to stand			
Crawling			
Cruising			
Walks with support			
Walks independently			
Makes babbling speech			
Recognisable single words			
Puts 2 words together			
Talks in sentences			
Waves bye bye			
Claps hands			
Feeds with fingers			
Feeds with spoon			
Toilet trained			

Did child develop any focal neurological signs? Y / N

Give details here including age first noticed

Give details of occipitofrontal circumference:

Birth	
Age	
Age	
Age	
Age	

If permission has been given for medical photographs to be used for research by parents, please send a photo of the child either as a print or via email as an attachment to Rachel Kneen or Amy McTague. Thanks for your help in filling out this form.

8.2 Web- based resources

1000 Genomes http://browser.1000genomes.org/index.html

Exome Aggregation Consortium (ExAC) http://exac.broadinstitute.org/

Genome Aggregation Consortium (gnomAD) http://gnomad.broadinstitute.org/

Exome Variant Server http://evs.gs.washington.edu/EVS/

Polyphen2 http://genetics.bwh.harvard.edu/pph2/,

SIFT/Provean http://provean.jcvi.org/genome_submit_2.php)

Ensembl http://www.ensembl.org/index.html

OMIM https://www.omim.org/

ClinVar https://www.ncbi.nlm.nih.gov/clinvar/

8.3 Single nucleotide polymorphism(SNP) arrays

Illumina CytoSNP12 arrays were performed by the local UCL Genomics Service in both parents, affected and unaffected children from Family 1 (Chapter 5). All processing was carried out in accordance with the Infinium HD Ultra Assay protocol (Rev B, 2010, Illumina Inc, San Diego, USA). The whole genome of 300ng of high quality genomic DNA was amplified overnight (37^0C, 20-24 hours), subsequently fragmented (37^0C for 1 hour and 15mins in hybridisation oven), precipitated and resuspended in hybridisation buffer. Samples were denatured and loaded onto the chips using a liquid handling robot (Freedom Evo, Tecan Ltd, Switzerland). Hybridisation took place overnight (16-20 hours) at 48°C. The probes on the chip were extended by a single hapten-labelled dideoxynucleotide (ddNTP) base complementary to the hybridised DNA. ddATP and ddTTP bases were labelled with

DNP (2,4-Dinitrophenol), ddCTP and ddGTP were labelled with Biotin. The DNA sample was then stripped off the chip using formamide. The staining procedure involved signal amplification by multi-layer immunohistochemical staining. The haptens were detected simultaneously by Streptavidin and an anti-DNP primary antibody conjugated to green and red fluorophores respectively (STM reagent, Illumina). They were then counterstained with biotinylated anti-streptavidin and a DNP-labelled secondary antibody to the anti-DNP primary antibody (ATM reagent, Illumina) to amplify the fluorescent signals. The last layer of stain was the STM, containing the fluorophores to allow signal detection. Finally the stained chips were coated to protect the dyes, and scanned using the iScan scanner with autoloader (Illumina Inc, San Diego, USA). Data was initially analysed using the Illumina Genomestudio software. This generates genotypes, and copy number and loss of heterozygosity data (cnvPartition v3.1.6, Illumina). Quality control checks were performed to assess the data quality. Samples were assessed for their call rate which should be >98% and >99% average across the batch. Specially designed control probes were also checked.

8.4 Great Ormond Street NGS multiple gene EIEE panel: methods

Custom TSCA method: a custom SureSelect library was created using Illumina's Design Studio tool (http://designstudio.illumina.com/truseqca/project). Briefly, genomic coordinates of 48 genes were uploaded to Design Studio to create the targeted panel. Libraries were made following the TruSeq Custom Amplicon Kit protocol (Illumina Technologies) and sequenced in-house on an Illumina MiSeq.

Sure Select method: a custom SureSelect library was created using Agilent's SureDesign tool (https://earray.chem.agilent.com/suredesign/). Briefly, genomic coordinates of either 45 (3 patients) or 66 (1 patient) genes were uploaded to SureDesign to create the targeted panel. Libraries were made following the SureSelectXT Custom Capture protocol (Agilent Technologies) and sequenced in-house on an Illumina MiSeq. For both panel designs sequence data were analysed using an in-house pipeline. Regions of interest were defined in BED file format by uploading HGNC genes names to the UCSC table browser (Karolchik et al. 2004). Sequence reads in FASTQ format were aligned to the reference human genome (hg19) using BWA (0.6.1-r104) and default settings (Li & Durbin 2009). Variant calling was performed across the entire region of interest using VarScan2 (v2.3.7) with the following settings: minimum 30X coverage, minimum 5 alternate reads, minimum phred-like base-quality of 20) (Koboldt et al. 2012; Koboldt et al. 2009). Variant calls in VCF format were

then annotated using Ensembl Variant Effect Predictor (v73) and the output parsed using an in-house script, converting the annotated VCF file into Excel format for subsequent variant filtering and prioritization (McLaren et al. 2010). For each case, coverage was assessed across the coding exons of the target genes and their intron-exon boundaries (+6bp and -12bp) and expressed as the percentage of bases covered at ≥30X.

8.5 Whole exome sequencing (WES) methods

8.5.1 WES at Institute of Neurology, London

Automated library construction was undertaken using an Agilent Bravo liquid handling workstation. TruSeq chemistry (Illumina Inc., San Diego, CA) was used to prepare single indexed, paired-end libraries from 2μg of genomic DNA that were subsequently enriched according to standard protocols supplied by Illumina (Illumina Inc., San Diego, CA). The enriched DNA libraries were sequenced, 2 x 101 bases on a HiSeq 1000 sequencing system (Illumina, Inc., San Diego, CA). The sequencing data was mapped to the human reference assembly, hg19 (GRCh37; downloaded from the UCSC genome browser) by Novoalign Software (Hansen 2016). After removal of PCR duplicates (Picard) and reads without a unique mapping location, variants were extracted using the Maq model in SAMtools (Li et al. 2009) and filtered by the following criteria: consensus quality $\geq$30, SNP quality $\geq$30 and root mean square mapping quality $\geq$30. These variants were further filtered by Annovar (Hansen 2016) against dbSNP build 135 (UCSC genome browser), 1000 Genomes and Exome Variant Server and intronic and non-coding variants were excluded.

8.5.2 WES at Duke University, USA

DNA was sheared for paired-end Illumina library preparation then enriched for target capture according to the manufacturer's instructions. Enriched libraries were sequenced using the HiSeq platform. Variants were called on each sample individually and filtering was applied for quality variables. Calls were merged, then annotated with allele frequencies from 1000 Genomes and Exome Variant Server (EVS) and with dbSNP132 unique rs identification numbers, if available. SIFT and PolyPhen scores for missense mutations were also included. All variants with a mean allele frequency of >0.01 in 1000 Genomes or EVS were excluded.

8.5.3 WES at Karolinska Institute, Sweden

Exome sequencing was undertaken for the parents and the affected siblings in Family 2 and bioinformatic analysis was performed using the Mutation Identification Pipeline v.1.5.6 http://mip-api.readthedocs.org/en/latest/index.html. Approximately 50 gigabases (Gb) of sequencing data was produced, generating an average 90-190 fold coverage of the exome within the family. The exome was sufficiently covered at 95.8% of the bases according to our cut-off limits (10x read depth) and 135,851 variants were called. 86% (116,691 variants) were single nucleotide variants (SNV) and 14% (19,160 variants) were indels. All variants were scored and ranked

8.6 Homology modelling methods

8.6.1 Homology modelling of mutations in KCNT1

HMMscan (Eddy 2011) against Pfam (database of sequence-based domain families) identified two domains in the sequence of human KCNT1 (isoform 1), (i) Ion channel (PF07885, at position 278-346) and (ii) calcium-activated BK potassium channel alpha-subunit family (PF03493, at position 495-598) (Bateman et al. 2000; Finn et al. 2009). Of the five novel mutations identified it was possible to model two; F346L (in the ion channel domain) and F502V in the gating ring containing RCK1 and RCK2 domains. HHPred was used for template-based structure prediction for the individual domains (Söding et al. 2005).

MODELLER-9v14 was used for homology modelling (Sali & Blundell 1993). For the modelling of the region possessing ion channel domain (residues 270-353), 20 models were built and assessed using DOPE (Discrete Optimized Protein Energy) score (Shen & Sali 2006). The best scoring model was then selected and examined for its quality using QMEAN (Benkert et al. 2011) . The side chain conformations for the selected model were further refined using a method based on backbone-dependent rotamer library – SCWRL4 (Krivov et al. 2009). The model of the gating region (residues 372-1044) was almost identical to the EM model except only seven and six residue substitutions in RCK1 and RCK2, respectively. This model has coordinates for both RCK1 and RCK2 domains but is missing a 163 amino acid linker (residues 633-796). A dimer model was generated by structure superimposition of individual models on the template dimer. This model was further subjected to 1000 steps (steepest descent) of energy minimization to reduce steric clashes and optimize the

positioning of side chains. Mutations were inserted into the respective models (F502V in gating region and F346L in ion channel) using the *swapaa* command in Chimera (Pettersen et al. 2004) with Dunbrack rotamer library and the rotamer was selected based on lowest clashes, highest number of H-bonds and highest probability.

Modelling of F346L: For F346L, the final homology model of the four-subunit ion-channel domain (in open conformation) was of reasonable quality with QMEAN Z-score of -3.97. The spatial position of the membrane is predicted using the PPM2.0 server (Lomize et al. 2012). The potassium-bound structure (open form) of calcium-gated potassium channel MthK from *Methanothermobacter thermaautotrophicus* (PDB ID: 1LNQ) was used as a template for modelling the ion channel domain (residues 270-353) (Jiang et al. 2002) . This template structure was identified upon sensitive sequence-based profile-profile comparison method-HHPred (Söding et al. 2005). The probability score (significance of the alignment) of 99% and 50% sequence similarity asserted the homologous relationship between the selected template and human KCNT1 ion channel domain. Further to model the tetramer of the ion channel domain, the biological assembly from the Protein Data Bank (PDB: 3LDC) was used (Ye et al. 2010). We also modeled the closed form of the ion-channel domain using the structure of potassium channel from *Streptomyces lividans* (PDBID: 2A9H), which shares 20% identity (31% similarity) with the KCNT1 ion-channel domain (Yu et al. 2005).

Modelling of mutation F502V: F502V is a conserved residue among homologs (CONSURF) (Glaser et al. 2003). The residue stretch (372-1044) which lies in the KCNT1 gating region (373-1174) was modelled using an almost identical (95%) recent cryo-EM structure of Slo2.2 channel from *Gallus gallus* in a closed form (without calcium) (PDB ID: 5A6F) (Hite et al. 2015). This appeared to be a suitable model (QMEAN aZ-Score = -1.82). Human KCNT1 gating region and the cryo-EM model share a sequence identity of ~95%. A template dimer was built from the cryoEM model by fitting a second copy (5A6F) in the EM density map (EMD: 3063), using the *fit_in_map* tool in Chimera based on which a model of the dimer of KCNT1 gating ring was generated (Pettersen et al. 2004).

8.6.2 Protein homology methods for mutations of *SLC12A5*:

Fold recognition of KCC2 was performed with HHPRED (Söding et al. 2005). The crystal structure of the *Methanocaldococcus jannaschii* ApcT Transporter (PDB: 3GIA; 2.35Å

resolution) was identified as the best template for residues 115-682 (TM middle domain), (HHPred e-value: 2.4×10^{-36}). The HHpred alignment was used as preliminary pairwise sequence alignment for homology modelling. The extended loop region between TM5 and TM6 (residues 303-407) could not be accurately modelled due to lack of sequence identity and was therefore removed. A preliminary homology model of KCC2 middle domain was calculated using MODELLER-9v10 (Eswar et al. 2007). The ConSurf web server (Ashkenazy et al. 2010) with default parameters, was used to evaluate the evolutionary conservation and improve the quality of the alignment accordingly. This alignment was then used to create 1000 homology models that were further assessed with the DOPE statistical potential score(Shen & Sali 2006). The model based on the lowest score (Normalized DOPE z-score: -0.464) was selected. Additional evaluation using the ProSA web server showed that the model quality (Z-score = -2.63) fell within a range typically found for native proteins of similar size(Sippl 1993). Next, selected non-synonymous substitutions were modeled into the KCC2 homology model with the *swapaa* command in Chimera (Pettersen et al. 2004) using the Dunbrack backbone-dependent rotamer library (Dunbrack 2002) and taking into account the lowest clash score, highest number of H-bonds and highest rotamer probability.

8.7 Xenopus oocyte cell model for *KCNT1*: electrophysiology methods

Variants were introduced into a wild-type human *KCNT1* expression construct using QuikChange Lightning Site-Directed Mutagenesis Kit (Agilent Technologies) according to manufacturer instructions (Milligan et al. 2014). Construct fidelity was confirmed by DNA sequencing. cDNAs were transcribed *in vitro* (mMessage mMachine; Ambion, Austin, TX). Oocytes (Dumont stage V or VI) were surgically removed from *Xenopus laevis* frogs and prepared (Petrou, S, Ugur, M, Drummond, RM, Singer, JJ, Walsh, JVJr 1997). Oocytes were kept in ND96 solution and stored at 17°C. Fifty nanoliters (0.2 ng/nl) of capped cRNA was injected into each oocyte using the Roboocyte system (Multi Channel Systems, Reutlingen, Germany) and oocytes incubated at 17°C. Electrodes containing1.5M K-acetate and 0.5M KCl were used to impale oocytes that were held at −90mV and perfused with bath solution containing 96mM NaCl, 2mM KCl, 1.8mM CaCl2, 1mM MgCl2, and 5mM HEPES, pH 7.5. 2-electrode voltage clamp recording was performed after 14-24 hours of expression. Recording frequency was 1kHz, and temperature was maintained between 20 and 22°C. To record expressed membrane currents, oocytes were held at −90mV, and test depolarizations lasting for 600-milliseconds were applied in 10mV increments, from −80mV

to +80mV, at 5 second intervals. Contemporaneous measurement of wild type (WT) currents was performed with the same batch of oocytes injected with mutant channels to maintain an internal control of possible variability in expression from different batches of oocytes. Quinidine (Sigma, St Louis, MO) was dissolved in ethanol to a concentration of 300 μM and was perfused continuously to the oocytes for 1 minute, following with 5 minute incubation. Currents were recorded before and after the application of the compound. Peak currents were measured at the end of each sweep for all clones, however in many of the mutants, saturation of the amplifiers was observed at +80mV, due to large currents so current at +10mV was set as a comparison point across all mutants and WT. Representative current traces and current voltage relationship curves were obtained using recordings that did not saturate the amplifier at +80mV. AxoGraph (AxoGraph Scientific, Sydney, Australia) was used to analyse the electrophysiological data, which is presented as mean ± standard error of the mean. Student t test was used to test statistical significance, performed on Prism 6 (GraphPad Software, La Jolla, CA).

8.8 SLC12A5 Immunoblotting studies: methods

The full-length human wild-type KCC2 and the three mutant KCC2 sequences were cloned into the mammalian expression vector, pCMV-Myc. We amplified the sequences from the Origene KCC2 wild-type expression vector and the mutagenized vectors using the Platinum® Taq DNA Polymerase High Fidelity (Life Technologies), custom-designed cloning primers (available on request) and 94°C for 2 min followed by 30 cycles of 94°C for 30 sec, 55°C for 30 sec and 68°C for 3 min 30 sec. Then using the QIAquick Gel Extraction Kit (QIAGEN) purified PCR products and the pCMV-Myc plasmid were successively digested first with EcoRI and then with Acc65I (isoschizomer of KpnI) according to manufacturer's protocol. Following purification with the QIAquick Gel Extraction Kit the PCR products were ligated into the EcoRI and KpnI sites of the vector pCMV-Myc (which was kindly provided from Dr Paul Gissen) using T4 DNA ligase (Promega). For amplification of Myc-tagged KCC2 constructs we transformed NEB 10-beta competent E.coli cells (New England BioLabs) with the plasmids and subsequently isolated the plasmids with the QIAGEN Plasmid Maxi Kit (QIAGEN). All expression constructs were confirmed by Sanger sequencing of the entire coding region, to ensure that during PCR amplification no additional mutations had been introduced. LLC-PK cells (non-transfected LLC-PK1 cells kindly supplied by Dr. Roxanne A. Vaughan, University of North Dakota) were then transiently transfected with equal amounts of WT, L311H, L426P and G551D constructs. 24hrs later, surface proteins were

labeled with biotin and cells were lysed. Biotinylated fraction and total cell lysates were eluted with 8% Tris-glycine, separated on a SDS polyacrylamide gel, transferred to nitrocellulose membrane and blotted with anti-myc antibodies. Control beta-actin bands were observed in the total cell lysate but not in the biotinylation assay. Densitometric analysis with NIH Image J yielded Area-Under-Curve (AUC) for each Western blot band.. Two analyses were undertaken to determine the effect of mutations.

1. Calculation of cell-surface KCC2 relative to the total level of KCC2 and normalization with WT values. In this analysis both bands are taken together for both surface and total expression, assuming full and equal recovery through biotinylation steps in work-up.

$$\left(\frac{surface}{total}\right) = \frac{AUC\ (glyco+deglyc}{AUC\ (glyco+degly}$$

2. Calculation of the fraction of glycosylated state in the cell-surface (i), or total expression, (ii):

$$\left(\frac{glyco}{glyco+deglyco}\right)surface = \left(\frac{AUC\ (glyco)sur}{AUC(glyco+deglyc} \right. \quad \text{(i)}$$

$$\left(\frac{glyco}{glyco+deglyco}\right)total = \left(\frac{AUC\ (glyco)t}{AUC(glyco+degl} \right. \quad \text{(ii)}$$

8.9 SLC12A5 Immunostaining and confocal microscopy

HEK293 cells were transfected with pCAGGS-KCC2-FLAG (Chamma et al. 2012) (gift from S. Levi, Institut National de la Santé et de la Recherche Médicale, Paris, France), pCAGGS-KCC2-FLAG-L311H, pCAGGS-KCC2-FLAG L426P or pCAGGS-KCC2-FLAG G551D and HcRed NLS using FuGENE (Promega). After 24 hours, cells were fixed in 4% (w/v) paraformaldehyde in phosphate buffered saline (PBS) for 15 sec, washed with PBS, incubated with 50 mM NH_4Cl for 10 min, washed with PBS and blocked for 30 min in PBS supplemented with 2% (w/v) bovine serum albumin (BSA) and 10% (v/v) goat serum. Total KCC2-FLAG in cells was assessed by the addition of 1% (v/v) Triton X-100 to blocking media. Cells were incubated for 1 hour with rabbit anti-FLAG antibody (1:200; Sigma, catalogue number F7425) in PBS with 2% BSA, washed in PBS, incubated with AlexaFluor 488-conjugated goat anti-rabbit antibody (1:600; Invitrogen, catalogue number A-11008) in

PBS-BSA, washed with PBS and mounted on slides. Images were collected using a Zeiss LSM 710 confocal microscope using x63 objective.

8.10 *Slc12a5* Zebrafish models and behavioural analysis: methods

Zebrafish (*Danio rerio*, AB strain) obtained from the Zebrafish International Resource Center (Eugene, OR) were maintained at 28.5°C following established procedures. The experiments were performed in accordance with the approved guidelines of the Committee on Animal Use and Care at the National Institute of Genetics, Japan. Zebrafish have two KCC2 orthologs (KCC2a and KCC2b), due to an ancient gene duplication. TALENs for zebrafish KCC2a and KCC2b were designed to target the fourth exon of both *KCC2a* and *KCC2b* genes. To construct TALEN plasmid, TAL effector repeats were assembled in pFUS plasmid by BsaI (New England Labs) digestion and following T4 DNA ligase reaction were subsequently subcloned into pCS2+ vector using BsmBI (New England Labs) restriction sites (Sakuma et al. 2013). The TALEN constructs were linearized by NotI digestion and used for in vitro transcription. Capped RNAs were synthesized using mMESSAGEmMACHINE SP6 kit (Life Technologies) according to the manufacturer's instruction. TALEN RNAs (200 pg for each TALEN) were injected into 1-cell stage zebrafish embryos and gene disruption of KCC2a (8 bp deletion) and KCC2b (5 base deletion) was confirmed by sequencing the F1 fish. KCC2a-KCC2b double knockout larvae were obtained by crossing double heterozygous carrier fish. Genotyping was done using following primers and PCR products were separated by 15~20% polyacrylamide gel electrophoresis.

KCC2a (genotyping, forward): 5'-TGGGTGTGTACCTGCCC-3'

KCC2a (genotyping, reverse): 5'-CCTGAGGAATAGAATCACACCC-3'

KCC2b (genotyping, forward): 5'-CGTTTACCTACCATGTCTTCAAAACAT-3'

KCC2b (genotyping, reverse): 5'-CCAGGTCATCCTGAGGAACAAA-3'

At 2 days post fertilization (dpf), the embryonic behavior of the wild-type and KCC2a-KCC2b double knockout embryos (both male and female, 10 per group) were investigated by a tactile response assay in which mechanosensory stimulation was applied to the tail. The

response was recorded using a dissection microscope (MZ16, Leica) and a high-speed CCD camera (HAS-220, Ditect).